



Technische Universität München
Department Chemie
Lehrstuhl für Organische Chemie II

**A Dual Inhibitor Attenuates Biofilm Formation and Virulence in
Staphylococcus aureus
and
Manipulation of ClpP Activity**

Barbara Eyermann

Vollständiger Abdruck der von der Fakultät für Chemie der Technischen Universität München
zur Erlangung des akademischen Grades eines

Doktors der Naturwissenschaften (Dr. rer. nat.)

genehmigten Dissertation.

Vorsitzender: Prof. Dr. Michael Groll
Prüfer der Dissertation: 1. Prof. Dr. Stephan A. Sieber
2. apl. Prof. Dr. Wolfgang Eisenreich

Diese Dissertation wurde am 24.09.2019 bei der Technischen Universität München
eingereicht und durch die Fakultät für Chemie am 17.10.2019 angenommen.

Danksagung

Zuallererst möchte ich mich bei Prof. Dr. Stephan A. Sieber bedanken. Dafür, dass ich meine Promotion an seinem Lehrstuhl durchführen durfte, für die gute Betreuung, Unterstützung und Begeisterung in all den Jahren. Ich habe sehr vielseitige Einblicke in die organische Synthese aber vor allem auch in die Biochemie bekommen, wofür ich sehr dankbar bin. Außerdem möchte ich ihm danken, dass ich die Möglichkeit hatte, sämtliche Konferenzen zu besuchen und Weiterbildungen zu machen.

Ich danke den Mitgliedern meiner Prüfungskommission, für ihre Zeit und ihre Bemühungen bei der Bewertung dieser Arbeit. Außerdem Danke ich Volker, Ines, Anja, Thomas, Dora und Theresa für das Korrekturlesen dieser Arbeit. Danke für sehr aufmerksames Lesen, wirklich hilfreiche Kommentare und eure Zeit die ihr geopfert habt.

Ein weiterer Dank geht an meine Kooperationspartnerin aus dem Labor von Prof. Bill Wüst, Megan C. Jennings, für die unkomplizierte Zusammenarbeit. Ebenfalls danke ich meinem Kooperationspartner aus dem Labor von Prof. Iris Antes, Maximilian Meixner für die gute Zusammenarbeit. Ich danke Thomas, Ines und Angela für die super Zusammenarbeit in unseren Group Jobs.

Ein ganz besonderer Dank geht an Katja B., Katja G. und Mona. Vielen Dank für euren außerordentlichen Einsatz und dass ihr das Labor und die Massen am Laufen haltet. Ohne euch wären wir aufgeschmissen. An dieser Stelle möchte ich auch allen Auszubildenden danken, die nicht nur zu einem reibungslosen Laboralltag beigetragen haben, sondern manchmal auch bei Synthesen geholfen haben. Vielen Dank an Karolina, Jaqueline, Roland, Linda, Alina und Marie. Ein weiterer Dank geht an meine Forschungspraktikanten, Sebastian P., Lisa, Sophia, Patrick, Markus, Sebastian F. und Chiara, für euren Einsatz im Labor. Ein besonderer Dank geht ebenfalls an Christina. Vielen lieben Dank, dass du dich einfach immer um alles kümmerst!

Ein riesengroßer Dank geht an alle meine Laborkollegen, die ältere Generation genauso wie die Jüngere. Ich bin jeden Tag wirklich gerne in die Arbeit gegangen, und dazu habt ihr einen großen Beitrag geleistet. Vielen lieben Dank an Jonas, Dora, Caro, Kyu, Thomas, Patrick A., Angela, Pavel, Martin, Theresa, Volker, Anja, Till, Ines, Robert, Josef, Lisa, Patrick Z., Nina, Stephan H., Franziska, Mathias und Christian. Ich bin unglaublich froh euch alle als Kollegen gehabt haben zu dürfen, fühlt euch an der Stelle bitte alle gedrückt. Ein besonderer Dank geht an unser Labor B, an Mathias, Patrick und Thomas. Vielen lieben Dank für die super

Nachbarschaft all die Jahre, für zahlreiche Diskussionen und Ratschläge, aufheiternde Worte und dass ihr die Arbeit im Labor einfach einfacher gemacht habt. Außerdem bedanke ich mich auch für die Zeit außerhalb der Arbeit, sei es beim Fußball spielen, beim Fitness, beim Grillen oder einfach in der Kaffeeküche.

Danken möchte ich auch den Kollegen, die das Labor bereits verlassen haben, Max, Maria, Wolfgang, Jan, Johannes, Matthias, Weining, Annabelle, Megan, Vadim, Lena und Markus. Vielen Dank, dass ich so viel von euch lernen durfte!

Der allergrößte Dank geht an meine Familie, die mich zwar vielleicht nicht immer verstanden haben, aber immer für mich da waren und mich in allem unterstützt haben. Meine Mama Elisabeth, meinen Papa Franz, meinem Bruder Peter, meiner quasi Schwägerin Rebekka und meinen Ehemann Jörg. Ich hab euch so unglaublich lieb, vielen Lieben Dank für Alles. Außerdem Danke ich an dieser Stelle meiner „zweiten“ Familie, den Eyermännern. Ich habe mich von Anfang an wie ein Familienmitglied gefühlt und danke euch dafür und dafür dass auch ihr immer für uns da seid. Der allergrößte Dank geht an meinen Schatz, der mit mir durch Dick und Dünn gegangen ist, alles ertragen hat und meinen Tag immer ein bisschen besser gemacht hat. Vielen Dank für deine aufmunternden Worte, dass du mir immer zuhörst und für den ein oder anderen nötigen Drücker. Ich bin sehr froh dass ich euch alle habe.

Abstract

Staphylococcus aureus is a major bacterial pathogen that is able to cause life-threatening diseases. Essential for pathogenicity are for example secreted proteins like hemolysins and cell surface-associated proteins. Two stages of *S. aureus* life cycle, the adhesion and the invasion phase, are tightly controlled by a two component system. If one of the phases is up-regulated, the other one is consequently down-regulated. In a phenotypic screen, we identified compound **AV73** that did not only reduce *alpha*-hemolysin production in *S. aureus*, but also impeded *in vitro* biofilm formation. Major virulence factors and biofilm promoting proteins were found down-regulated in a quantitative proteomics experiment, where bacterial proteomes and extracellular protein levels were analyzed. To further elucidate the mode of action, affinity-based protein profiling (A/BPP) was used for target identification. Besides labeling experiments, competition experiments as well as labeling with a minimal photoprobe were performed to distinguish between target proteins and background binders. Although it was not possible to fully consolidate the mode of action, four main hits that all play interesting roles in virulence or biofilm formation were detected, namely membrane protein insertase YidC, iron compound ABC transporter, sortase Srt and diadenylate cyclase.

Caseinolytic protease P (ClpP) which assembles with ATPases like ClpX to form a protease complex plays a major role in *S. aureus* virulence. While inhibition of ClpP leads to a decrease in virulence, activation of ClpP has a bactericidal effect. Both topics were covered within this thesis. Inhibition was addressed among others with inhibitors **AV335** and **AV339**. Several biochemical assays were performed to elucidate the mode of action. Furthermore, none of the inhibitors showed down-regulation of any major virulence factors in a quantitative proteomics experiment on extracellular protein levels.

Acyldepsipeptides (ADEPs) were used for activation, as they are known ClpP activators and bind to hydrophobic pockets at the apical site of ClpP and therefore, mimic the binding of ClpX. With an A/BPP-approach, targets and putative off-targets were investigated. Further, labeling of ClpP independently of its oligomeric and activity state was illustrated, which until now was only possible with covalent inhibitors in its active state. Several ADEP fragments and derivatives were synthesized for structure activity relationship (SAR) studies to detect best positions for the required moieties for a photoprobe, a photoreactive group and an alkyne handle. With several probes in hand, labeling experiments were performed with ClpP and inactive ClpP mutants, which confirmed clear labeling of all ClpP conformations. ClpP and two other proteins were identified in each of three independent A/BPP experiments, while

different other proteins were enriched in one or more of these experiments. Besides ClpP, D-alanine aminotransferase and *N*-acetylmuramoyl-L-alanine amidase domain-containing protein were consistently enriched. To confirm any of those as real targets, further experiments, for example a competition experiment, are required.

Zusammenfassung

Staphylococcus aureus ist ein wichtiger bakterieller Krankheitserreger, der lebensbedrohliche Krankheiten verursachen kann. Sekretierte Proteine, die für die Invasion des Wirts wichtig sind, und oberflächen-assoziierte Proteine, die für die Biofilmbildung entscheidend sind, sind wesentlich für deren Pathogenität. Die zwei Phasen, die Adhäsions- und Invasionsphase, werden von einem zwei-Komponenten-System streng kontrolliert. Wenn eine der beiden Phasen verstärkt reguliert wird, wird die andere automatisch schwächer reguliert und umgekehrt. Das macht die in einer phänotypischen Untersuchung identifizierte Verbindung **AV73** umso interessanter. Diese reduziert nicht nur die Bildung von *alpha*-Hämolysin in *S. aureus*, sondern inhibiert auch die Biofilmbildung *in vitro*. In quantitativen Proteomik-Experimenten von bakteriellem Proteom und extrazellulären Proteinen, konnte eine abgeschwächte Regulierung von wichtigen Virulenzfaktoren und biofilmfördernden Proteinen beobachtet werden. Um die Zielproteine von **AV73** und dadurch die Art der Wirkungsweise herauszufinden, wurde affinitäts-basiertes Protein-Profilings (A/BPP) durchgeführt. Hierfür wurde zunächst eine Photosonde, **AV73-p**, synthetisiert. Um Hintergrundmarkierungen der Photosonde auszuschließen, wurden neben den Markierungs-Experimenten auch Kompetitions-Experimente und Markierungen mit einer minimalen Sonde durchgeführt. Auch wenn der vollständige Wirkungsmechanismus nicht aufgeklärt werden konnte, wurden vier Zielproteine detektiert, die eine wichtige Rolle in Virulenz und Biofilmbildung spielen.

Caseinolytische Protease P (ClpP) fügt sich mit einer ATPase wie ClpX zu einem Protease-Komplex zusammen und spielt eine wichtige Rolle in der Virulenz von *S. aureus*. Während die Inhibition von ClpP zu einem Rückgang der Virulenz führt, hat die Aktivierung von ClpP eine bakterientötende Wirkung. Beide Themen wurden in dieser Doktorarbeit behandelt. Die Inhibitoren **AV335** und **AV339** wurden aus einer Untersuchung für ClpXP-Inhibitoren identifiziert. Um deren Wirkungsmechanismus herauszufinden wurden verschiedene biochemische Assays durchgeführt, er konnte allerdings nicht vollständig aufgeklärt werden. Außerdem haben strukturell ähnliche Inhibitoren, die moderate bis gute Ergebnisse in einem Hämolyse-Assay gezeigt haben, in Proteomik-Experimenten von extrazellulären Proteinen keine Regulierung von Virulenzfaktoren von extrazellulären Proteinen gezeigt.

Acyldepsipeptide (ADEPs) sind Aktivatoren von ClpP und wurden zur Behandlung dieses Teils der Doktorarbeit verwendet. ADEPs binden in hydrophobe Taschen an der apikalen Oberfläche von ClpP, ahmen dadurch die Bindung von ClpX nach und aktivieren so ClpP. Um weitere Zielproteine von ADEPs zu finden, wurde die A/BPP-Methode angewendet.

Durch die Synthese mehrerer ADEP-Fragmente konnten Struktur-Aktivitäts-Beziehungen und somit die besten Stellen für die Einführung einer photolabilen Gruppe, sowie eines Alkyls, herausgefunden werden. Mit den hergestellten Photosonden wurden Markierungs-Experimente mit ClpP und zwei inaktiven ClpP-Mutanten durchgeführt. ADEPs sind die ersten Sonden, die ClpP auch in einem inaktiven konformationell unabhängigen Zustand markieren können. Bis jetzt war nur die Markierung in einem aktiven Zustand mit Inhibitoren wie β -Laktonen möglich. Außerdem wurden in drei unabhängigen Markierungs-Experimenten ClpP und zwei weitere Proteine angereichert. Um diese, oder weitere angereicherte Proteine, die nur in einem oder zwei der Experimente gefunden wurden, als wirkliche Zielproteine zu identifizieren, müssen weitere Experimente, wie beispielsweise Kompetitions-Experimente, durchgeführt werden.

Introductory Remarks

This doctoral thesis was completed between December 2016 and October 2019 under the supervision of Prof. Dr. Stephan A. Sieber at the Chair of Organic Chemistry II at the Technical University of Munich.

Parts of this thesis have been published in:

Hofbauer, B.*, Vomacka, J.*, Stahl, M., Korotkov, V.S., Jennings, M., Wuest, W., Sieber, S.A., "A dual inhibitor of *Staphylococcus aureus* virulence and biofilm attenuates expression of major toxins and adhesins", *Biochemistry* **2018**, 57, 11, 1814-1820.

* contributed equally

Eyermann, B., Meixner, M., Brötz-Oesterhelt, H., Antes, I., Sieber S.A., "Acyldepsipeptide probes facilitate specific detection of caseinolytic protease P independent of its oligomeric and activity state", *ChemBioChem*, accepted.

Contributions:

Chapter II V. Korotkov performed the synthesis of **AV73** and analogues, B. Eyermann synthesized **AV73-p**. J. Vomacka conducted hemolysis and biofilm assays (*S. aureus* NCTC8325) for **AV73**. B. Eyermann repeated those and performed the same assays for **AV73-p**. M. Jennings performed biofilm assays with both compounds in *S. aureus* strains SH1000, USA300-0114, ATCC33591 and ATCC6538. Whole proteome analysis was conducted by J. Vomacka, AfBPP experiments by B. Eyermann. GO-Analysis was performed by M. Stahl and J. Vomacka.

Chapter III ClpP mutants were prepared by M. Hackl and P. Allihn. ADEP photoprobes were synthesized and AfBPP experiments were performed by B. Eyermann.

Abstract	iii
Zusammenfassung	v
Introductory Remarks	vii
I. THEORETICAL BACKGROUND	1
1. The Pathogen <i>Staphylococcus aureus</i>	1
1.1. <i>S. aureus</i> Infections	1
1.2. Communication of <i>S. aureus</i> – Quorum Sensing	3
2. AfBPP for target identification	6
II. AV73 A DUAL INHIBITOR OF BIOFILM FORMATION AND VIRULENCE	9
1. Introduction	9
2. Results and Discussion	10
2.1. AV73 is active against Hemolysis	10
2.2. AV73 inhibits Biofilm Formation	13
2.3. Synthesis of a Photoprobe and its Bioactivity	16
2.4. AfBPP with AV73-p	18
3. Conclusions and Outlook	21
III. MANIPULATION OF CLPP ACTIVITY	22
1. Introduction	22
1.1. The ClpXP protease system	22
1.2. Inhibition of ClpP leads to a reduction of virulence	25
1.3. Activation of ClpP leads to cell death	26
1.4. Known ADEP-Syntheses	31
1.5. Activity of a first ADEP-photoprobe	32
1.6. Scope of this work	33
2. Inhibition of the ClpXP complex	34
2.1. Inhibitors and related compounds	34
2.2. Assays to elucidate the mechanism of ClpXP inhibition and SAR studies	36
2.2.1. Protease and GFP unfolding Assay	36
2.2.2. Peptidase and ATPase Assay	37

2.2.3.	FITC-Casein Assay.....	38
2.2.4.	Thermal Shift Assay.....	39
2.2.5.	Conclusion.....	40
2.3.	Consequences for <i>S. aureus</i> phenotype and its proteomic level.....	41
2.3.1.	Hemolysis Assay.....	41
2.3.2.	Secretome analysis.....	42
2.4.	Conclusion.....	44
3.	Synthesis and Activity of ADEP Fragments and Derivatives.....	45
3.1.	Overview and Synthesis of ADEP fragments.....	45
3.2.	Activity of ADEP fragments.....	48
3.3.	Solid-phase ADEP and ADEP-probes synthesis.....	50
3.4.	Activity of ADEP derivatives.....	53
3.5.	MIC values in <i>S. aureus</i>	54
3.6.	Modeling Analysis.....	55
4.	AβBPP with synthesized ADEP photoprobes.....	56
4.1.	Gel-based labeling.....	56
4.1.1.	Labeling of recombinant SaClpP and in <i>S. aureus</i> lysate.....	56
4.1.2.	In situ labeling in <i>S. aureus</i>	58
4.1.3.	Labeling of ClpP in different conformational states.....	60
4.2.	MS-based labeling.....	61
4.2.1.	Labeling Challenge.....	61
4.2.2.	Optimized Conditions.....	65
5.	Conclusions and Outlook.....	69
IV	EXPERIMENTAL PART.....	72
1.	Organic Chemistry.....	72
1.1.	General material and methods.....	72
1.2.	Synthesis for Chapter II.....	74
1.3.	Synthesis for Chapter III.....	80
1.3.1.	General procedures for the synthesis of ADEP fragments.....	80
1.3.2.	Synthesis of ADEP fragments.....	81
1.3.3.	Synthesized amino acid derivatives for ADEP synthesis.....	95
1.3.4.	General procedures for solid phase peptide synthesis and cyclization.....	101
1.3.5.	Synthesized peptides by solid phase peptide synthesis and cyclization.....	103

2. Biochemical Procedures	107
2.1. General material and methods	107
2.1.1. Buffers and Solutions.....	107
2.1.2. Bacterial strains and media	108
2.1.3. Cultivation methods of bacteria	109
2.1.4. Determination of MIC values.....	109
2.1.5. BCA Assay	110
2.1.6. SDS-PAGE	110
2.2. Biochemical methods for Chapter II.....	111
2.2.1. Hemolysis Assay in Solution	111
2.2.2. Biofilm Assay.....	111
2.2.3. Whole proteome analysis	112
2.2.4. Gel-based AfBPP in <i>S. aureus</i>	115
2.2.5. Gel-free AfBPP in <i>S. aureus</i> (biofilm conditions)	116
2.2.6. MTT Assay.....	120
2.3. Biochemical methods for Chapter III.....	121
2.3.1. Protein expression and purification	121
2.3.2. Biochemical Assays	122
2.3.3. Labeling of recombinant ClpP, wt and mutants	125
2.3.4. Hemolytic Assay on agar plate	125
2.3.5. Secretome Analysis.....	125
2.3.6. Gel-based AfBPP in <i>S. aureus</i> lysate	128
2.3.7. Western Blot Analysis.....	128
2.3.8. Gel-based AfBPP in <i>S. aureus</i> intact cells.....	129
2.3.9. Gel-free AfBPP in <i>S. aureus</i> intact cells.....	130
 BIBLIOGRAPHY.....	 134
 LIST OF ABBREVIATIONS	 145
 APPENDIX	 150
1. Additional Figures (Chapter II, III)	150
2. Stained Gels (Chapter III)	154
3. Tables	156
4. NMR Spectra	162
 PERMISSIONS.....	 179

I. Theoretical Background

1. The Pathogen *Staphylococcus aureus*

1.1. *S. aureus* Infections

Staphylococcus aureus is a gram-positive bacterium, which colonizes the human skin, nares and gastrointestinal tract usually without causing any symptoms.^[1] In the USA, around 20% of the adults and 45% to 70% of the children carry *S. aureus* in their nares permanently. Additionally, 30% of the population carry *S. aureus* colonies temporarily.^[2,3] Although colonization is usually harmless to the host, colonized individuals carry a higher risk for developing *S. aureus* infections.^[1,3]

Diversity of *S. aureus*

S. aureus bacteria are master of diversity: They are able to cause acute and chronic illnesses,^[4] their infections can reach from mild diseases up to life-threatening conditions^[5] and they are able to colonise a wide range of host tissues.^[3] Superficial surfaces, for example the skin, can be affected as well as deeper tissues like the gastrointestinal tract, the heart and bones.^[3] Conditions caused by *S. aureus* include bacteremia, sepsis, toxic shock syndrome, wound infections, pneumonia, endocarditis and also catheter-related infections.^[4,6-8]

Numerous virulence factors are required to cause such a broad diversity of diseases in many different body sites.^[1,8,9] Essential for pathogenicity are for example secreted proteins like hemolysins, enterotoxins and cell surface-associated proteins.^[10,11] An important part of *S. aureus* virulence is its ability to form biofilms.^[12-14] Whereas biofilm formation is not required for a persistent infection, biofilm eradication is difficult and usually requires surgical intervention.^[15]

Life cycle of *S. aureus*

S. aureus life cycle consists of two parts: the adhesion phase in the beginning of an infection and the invasion phase when a certain amount of bacteria has accumulated.^[4,16] Cell surface proteins are synthesized in the adhesion phase, while in the invasion phase, where a certain amount of bacteria is already present, exoproteins are synthesized.^[11] Transition between these two phases is regulated *via* an intercellular communication process, called quorum sensing (QS),^[4,16] and will be discussed in further detail (see chapter 1.2.).

MRSA

Since methicillin was introduced in 1960,^[17] methicillin-resistant *S. aureus* (MRSA) was detected soon after and is one key pathogen responsible for healthcare associated infections difficult to treat.^[18,19] Although not relevant for this topic, it is noteworthy that MRSA already emerged in the mid 1940s, even before the first therapeutic use of methicillin.^[20] In the US, MRSA is responsible for over 12,000 fatalities per year,^[21] making it a key pathogen, not only in clinics. Also community-associated MRSA (CA-MRSA) increased significantly over the past years.^[22,23] Moving from the US to Europe, statistics of Wales show that MRSA deaths are at a comparable level with non-resistant *S. aureus* strains. A closer look reveals 2006 as the year with most *S. aureus* and MRSA deaths, with decreasing numbers since.^[25] These numbers can be explained by improvements including enhanced surveillance, adherence to clinical protocols, hand hygiene and environmental cleaning.^[26] Although the mean prevalence of MRSA is decreasing in Europe, Norway, for instance, records a significant increase in the annual number of registered people notified with MRSA.^[27] An overview of MRSA abundance for european countries is illustrated in figure 1.

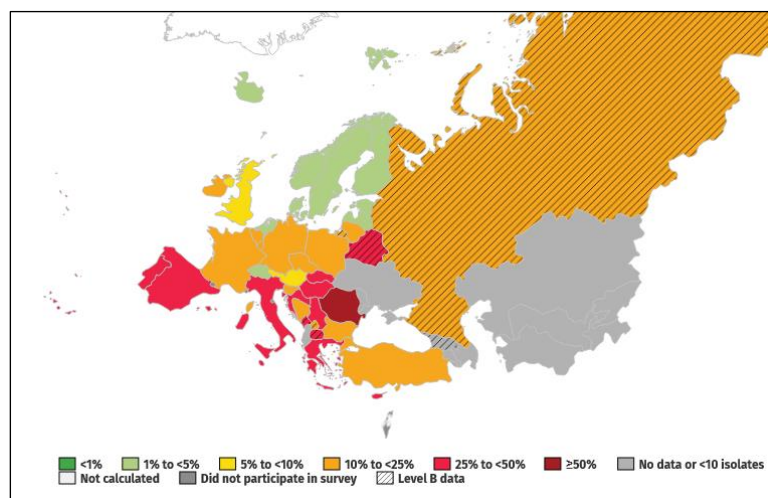


Figure 1. Percentage of invasive isolates of *Staphylococcus aureus* with resistance to methicillin (MRSA). Data are for 2015 to 2016 and were obtained from the World Health Organization.^[24]

MRSA prevalence is also high or even rising in the United States, Canada, Latin American countries, Australia and India.^[28] Clearly, MRSA and also non-resistant *S. aureus* still represent an important field of research.

Steps against MRSA and *S. aureus* virulence

There are different methods to combat MRSA and *S. aureus*, for example, looking for new targets.^[29] One approach is the use of natural products to combat MRSA. Here, one strategy is to use the synergism between natural antimicrobials and conventional antibiotics.^[19,30] For example, *Albano et al.* investigated the antibacterial properties of phenolic compounds found in essential oils. Eugenol for instance shows an excellent bactericidal activity against a broad range of organisms like *E. coli*, *P. aeruginosa* and *L. monocytogenes*.^[19,31,32] Its mechanism of action can be explained by the disruption of bacterial cytoplasmic membrane.^[19,33] In combination with antibacterial drugs like gentamicin, vancomycin and linezolid, it illustrates a synergistic effect. All in all, they found around ten synergistic interactions against MRSA strains, of which four combinations look promising and were confirmed by time kill curves.^[19]

Lee et al. showed, that extracts from the plant *M. oleifera* efficiently inhibit *S. aureus* biofilm formation.^[34] Among others, the following fatty acids were present: palmitoleic acid, oleic acid, linoleic acid and linolenic acid.^[34] At the same time, *cis*-11-eicosenoic acid significantly decreased hemolysis of red blood cells. Their results indicate, that a supercritical carbon dioxide fluid extract of *M. oleifera* and its unsaturated fatty acids are potentially useful for controlling biofilm formation and virulence of *S. aureus*.^[34]

Another strategy to combat *S. aureus* is to use other bacteria in combination. *Dunyach-Remy* and co-workers investigated the interaction of *S. aureus* with *H. kunzii*, which are low or non-virulent bacteria.^[35] They found that *H. kunzii* significantly reduce *S. aureus* virulence in nematodes.^[35] Furthermore, they observed a down-regulation of virulence factors after co-infection with *H. kunzii*. Keeping this in mind, factors produced by *H. kunzii* represent an interesting field for research.^[35]

1.2. Communication of *S. aureus* – Quorum Sensing

The accessory gene regulatory (*agr*) system was identified by *Recsei et al.* in 1986,^[3,36] and represents a communication tool of *S. aureus*. It is a two-component system and is activated by the autoinducing peptide AIP.^[11]

On the one hand, the *agr* system is responsible for the suppression of cell surface proteins, for example protein A and fibronectin binding proteins. On the other hand, it upregulates virulence factors, like leukocidin, hyaluronate lyase, *alpha*-, *beta*-, *gamma*- and *delta*-hemolysins, PSMs, lipases, proteases, nucleases and toxic shock syndrome toxins. All in all, around 100 virulence genes are upregulated by *agr* mediated quorum sensing.^[37,38]

The *agr* system functions complementary to the global regulator *sar* (*staphylococcal* accessory response) in controlling biofilm development.^[15,38] In the initial stages, *sarA* enhances the expression of adhesins, inhibits nucleases and proteases and therefore induces the attachment of cells and early biofilm formation.^[38] After biofilms have gained a significant population, *agr* expression is induced, which leads to an upregulation of virulence factors and a supporting of biofilm dispersal.^[15,38]

The two-component system is mediated by the autoinducing peptide (AIP), which is continuously produced by *S. aureus* cells. The *agr* locus is autoactivated when cell density reaches a certain threshold.^[38-41] After AIP binding to AgrC, a phospho-relay to AgrA is induced. Phosphorylated AgrA binds the *agr* locus, that consists of two promoters P2 and P3, which encode RNAII and RNAIII, respectively (Figure 2).^[3,4]

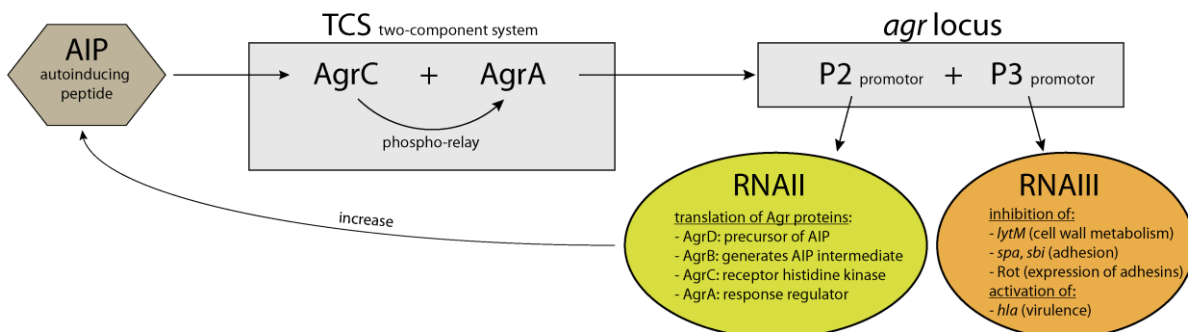


Figure 2. Simplified overview of quorum sensing. AIP activates the two-component system and AgrA binds to the promoters. The P2 promoter encodes RNAII, which leads to translation of Agr proteins and therefore more AIP and a higher activation. When more AIP is present, the P3 promoter encodes RNAIII, which inhibits proteins for the adhesion phase and activates the production of virulence factors.^[4]

At lower AIP levels, RNAII positively regulates the production of Agr proteins, which in turn leads to further AIP production and a higher stimulation of the whole process. When a lot of AIP has accumulated, RNAIII, which is highly connected to virulence, is encoded as well.^[4]

RNAIII positively regulates the expression of toxins and exo-enzymes for the lysis of immune cells. At the same time, high RNAIII concentrations lead to a down-regulation of Rot, being

responsible for the production of adhesins and immune evasion proteins.^[4] Therefore exhibiting a dual effect on virulence promotion.

By the production of σ -B, the sigB operon represents an additional level of control. σ -B is responsible for the upregulation of factors, that are necessary for the beginning of biofilm formation, e.g. clumping factor, fibronectin binding protein A or coagulase.^[15,42,43] Thus, sigB supports the bacteria in the adhesion phase of their life cycle.

2. AfBPP for target identification

Whereas activity based profiling (ABPP) is utilized to decipher targets of covalently binding compounds, often natural products, affinity based protein profiling (AfBPP), is applied for the identification of proteinogenic interaction partners of compounds with a non-covalent binding mode.^[44–46]

General concept of AfBPP

For affinity based protein profiling, a photoprobe with an attached bioorthogonal handle and a photoreactive group is needed.^[45,46] Scope of the probe design is to implement these modifications with minimal changes in bioactivity, while binding to the same target. Whereas the photoreactive group is needed for covalent linkage to the protein, the bioorthogonal handle is used for the attachment of a linker. Commonly used bioorthogonal reactions are for example the *Staudinger* ligation,^[47–49] copper or strain promoted 1,3-dipolar cycloadditions^[50–52] and inverse-electron-demand Diels-Alder reactions.^[47,53] Apart from a bioorthogonal handle, the linker is either equipped with a fluorescence tag, a biotin moiety or both and can be used for visualisation.

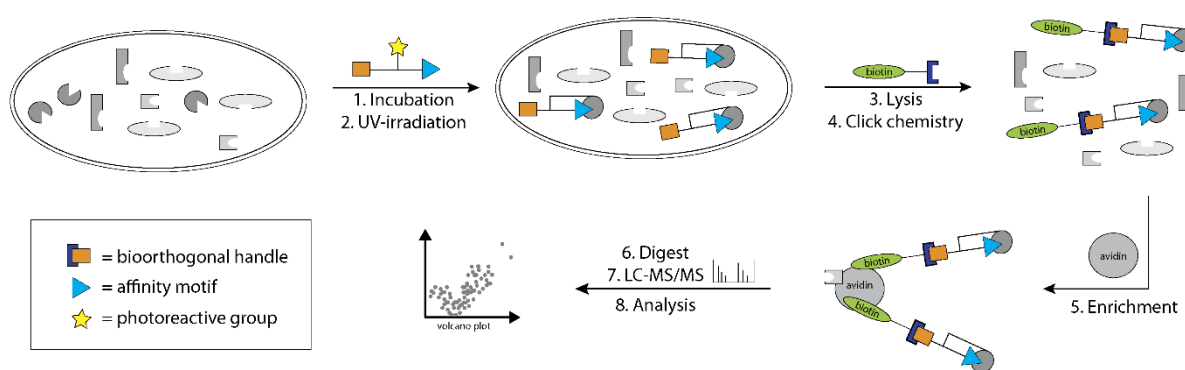


Figure 3. Shown is the general concept of MS-based AfBPP in intact cells.

Particularly, eukaryotic cells or bacteria are incubated with a photoprobe and irradiated to establish covalent linkage between the probe and the target protein. After lysis, a visualisation or enrichment tag is attached to the alkyne handle *via* a copper promoted cycloaddition, commonly known as click reaction^[54] (Figure 3). While rhodamine azide is often used for fluorescent visualisation, biotin azide is utilized for enrichment and quantification *via* MS/MS. A trifunctional linker^[55] with an attached fluorescence tag and a biotin azide moiety can be used for fluorescent visualisation after enrichment. Enrichment of labeled proteins can be achieved with biotin beads, utilizing the strong biotin-avidin affinity.^[56] Tryptic peptides

are measured, quantified and analyzed *via* statistical methods to find out the target proteins (Figure 3).

Photoreactive Groups

Photoreactive groups can be divided in three main groups, diazirines, aryl azides and benzophenones, each having their own advantages and disadvantages (Figure 4).^[57]

The selection of a photoreactive group depends on the structure of the original compound. Since bioactivity needs to be retained, some moieties might be more suitable than others. One disadvantage of benzophenones is the structural demanding size, potentially leading to a loss in bioactivity.^[58,59] Furthermore, benzophenones often need longer irradiation periods, leading to elevated unspecific labeling. On the other hand, irradiation can be performed at a wavelength above 300 nm, so that no proteins are damaged. Further advantages of benzophenones are, that they are synthetically easily accessible and inert to solvents.^[59–61] Aryl azides are easily accessible as well.^[58,59] Since they are often introduced in an already existing phenylring, the modification is minor and therefore likely to maintain bioactivity. Disadvantages of aryl azides are that they require a shorter wavelength for activation, which leads to protein damage, and that their photoaffinity yield is lower than that for carbenes.^[59,61] Advantages of the very popular diazirines are, that they can be irradiated at longer wavelengths, they are small in their size and they have a high crosslinking activity.^[62] In the past, these advantages lead to a steady increase in the use of diazirines as photoreactive groups.^[63,64]

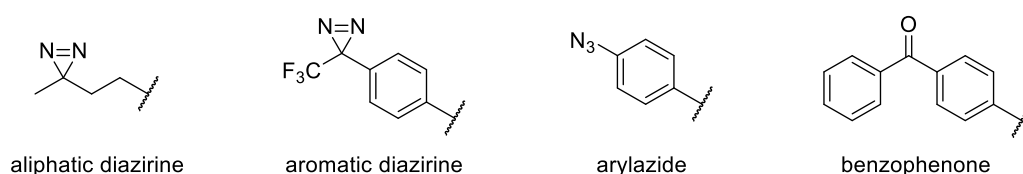


Figure 4. Structures of commonly used photoreactive moieties, an aliphatic and aromatic diazirine, an arylazide and a benzophenone.

After irradiation at a specific wavelength, highly reactive triplet ketyl diradicals, nitrenes or carbenes are formed. They instantly react with anything nearby and form a covalent crosslink between probe and protein.^[57]

Background Binding

A disadvantage of the application of photocrosslinkers is unspecific background binding. Since the whole amount of photocrosslinker will not solely be present at the target protein, other proteins that are nearby will be crosslinked as well. These drawbacks are usually met by

the application of two strategies: first, labeling with minimal photocrosslinker probes to exclude labeled proteins as targets, second performing competition experiments with the original compound to find out real targets. *Kleiner et al.* showed a whole proteome inventory of different background binders in two human cell lines, which can be referred to when labeling in eukaryotic cells.^[62] They tested four different minimal diazirine structures, one aryl azide and one benzophenone probe. Additionally, *Kleiner* tested three different diazirin background binders in *S.aureus* labeling, which can serve as a reference.^[64]

II. AV73 a Dual Inhibitor of Biofilm Formation and Virulence

1. Introduction

As illustrated before, *S. aureus* is able to switch between an adhesion and an invasion phase, which is tightly regulated by QS. These states can also be called defensive and offensive, respectively. RNAIII is encoded by the *agr* system after its activation and is responsible for the positive and negative regulation of virulence factors and Rot, respectively. While virulence factors are required for the offensive state, Rot is responsible for the production of adhesins and immune evasion proteins, which are necessary in the defensive phase of *S. aureus* life cycle.^[4] This special system comprising RNAIII and Rot is also called Double Selector Switch (DSS) and defines a double layered switch which involves transcriptional and post-transcriptional regulations.^[65] Regarding this whole system, exclusively favouring defensive or offensive phase, it might be hard to find a compound against both, virulence and biofilm formation. If one side is down-regulated, the other side will consequently be upregulated. This is what makes **AV73**, a compound that was identified upon the improvement of a known antivirulent compound, so interesting.

2. Results and Discussion

2.1. AV73 is active against Hemolysis

Hydroxyamide fatty acids were recently identified as inhibitors of Hla expression. The most potent antivirulent compound **AV59** did not reveal any *in vitro* resistance development and was effective in an abscess mouse model.^[66] Based on this compound, 35 derivatives with diverse structural features were synthesized and screened in a hemolysis assay. Three compounds **AV73**, **AV212** and **AV213** showed strong inhibition of hemolysis (Appendix: Figure A1). Due to its easy accessibility, **AV73** was chosen for further evaluations (Figure 5A). A hemolysis assay was performed using sheep erythrocytes and a hemolysis reduction of 80% with 50 μM **AV73** could be observed (Figure 5B). An EC_{50} of 30 μM (± 1.2 μM) was obtained for **AV73** in a concentration dependent hemolysis assay (Figure 5C).

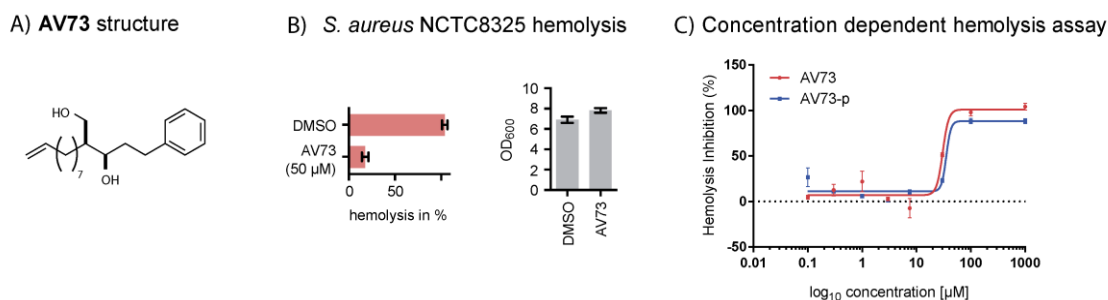


Figure 5. A) Structure of **AV73**. B) Hemolysis assay of **AV73** at 50 μM and DMSO in *S. aureus*. The assay was performed with a suspension of sheep erythrocytes in PBS, added to bacterial supernatants. The time resolved decrease in OD_{600} was measured. C) A concentration dependent hemolysis assay of **AV73** and **AV73-p** in *S. aureus* in three biological replicates.

To confirm these results and exclude any direct interactions of **AV73** with hemolysin or erythrocytes, additional experiments were performed. With a hemolysis assay using *S. aureus* secretome with different compound concentrations, it was shown that **AV73** does not directly affect Hla function (Figure 6A). In a different hemolysis assay, **AV73** did not cause direct lysis of erythrocytes either (Figure 6B).

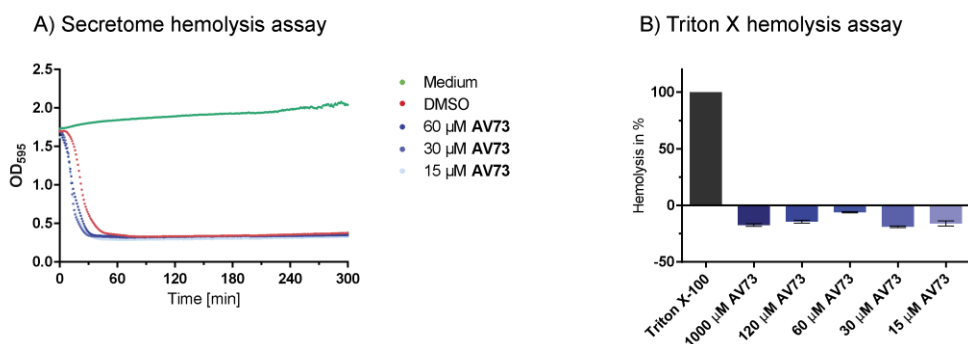


Figure 6. A) Hemolysis assay performed in three biological replicates (each in triplicates). *S. aureus* secretome was incubated with different **AV73** concentrations. Medium was used as a negative control (no hemolysis) and DMSO as a positive control. OD_{595} represents the intact erythrocytes. B) Direct hemolysis detection of **AV73**. **AV73** does not induce hemolysis at concentrations up to 1000 μM . The experiment was performed in two biological replicates with three technical replicates each. Triton X-100 was used as a positive control.

Whole Proteome Analysis

A quantitative full-proteome analysis was performed to get a deeper insight in the mode of action. Compound treated and untreated bacteria were grown under hemolysis conditions, lysed, digested and peptides were modified with either light or heavy dimethyl isotopes.^[67] After the samples were pooled, peptides were analyzed *via* tandem mass spectrometry (LC-MS/MS) and ratios of heavy to light peptides were determined and visualized in a volcano plot (Figure 7).

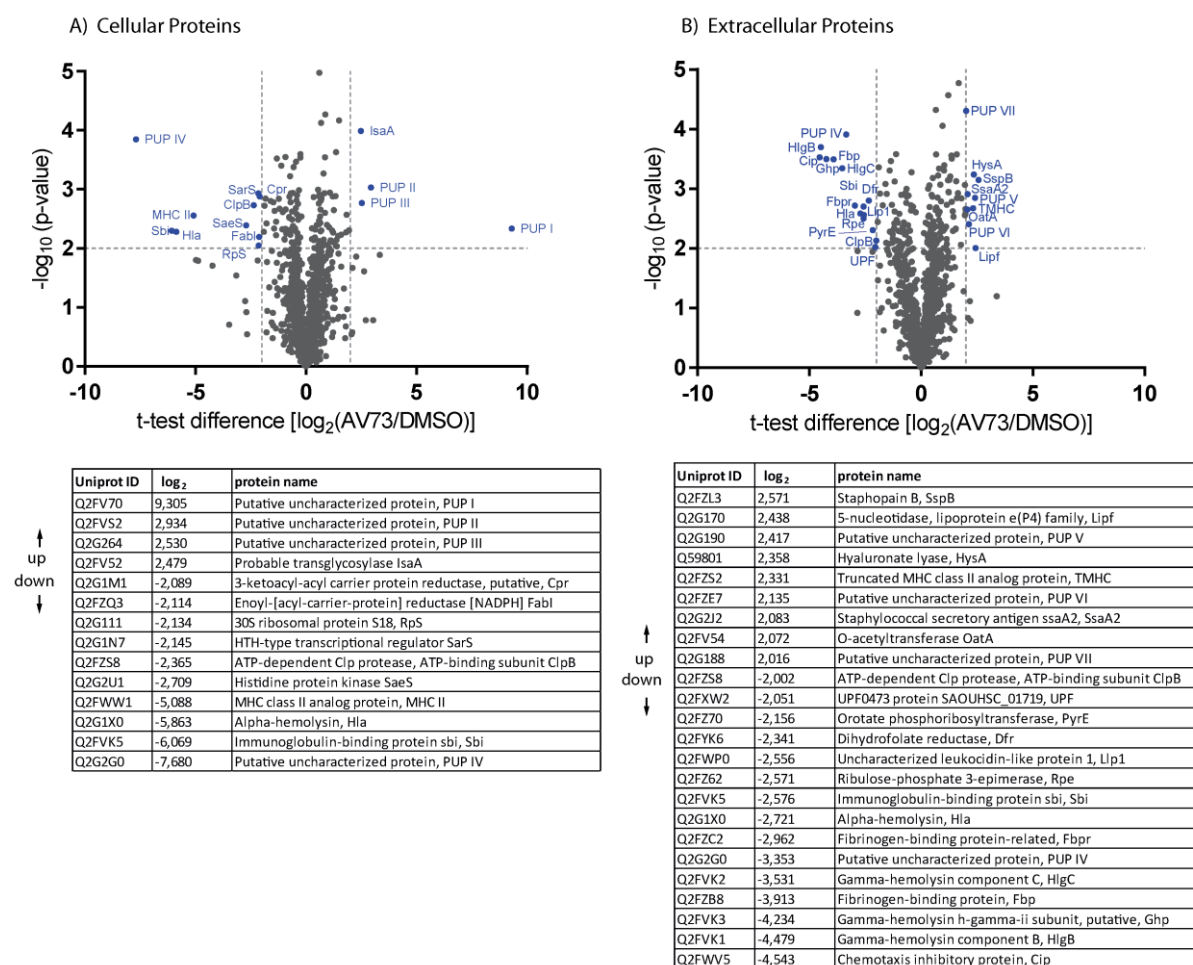


Figure 7. A) Whole proteome analysis of cellular proteins, performed under hemolysis conditions in four biological replicates. Most regulated proteins are marked and sorted in decreasing t-test difference order. Cut off lines were set at a minimum log₂ fold-change of 2 and a minimum $-\log_{10}$ (p-value) of 2. B) Whole proteome analysis of extracellular proteins was performed in four biological replicates. Most regulated proteins are again listed. Cut off lines were set at a minimum log₂ fold-change of 2 and a minimum $-\log_{10}$ (p-value) of 2.

As expected, a global down-regulation of virulence can be observed after AV73 treatment (Figure 7A). Confirming the results of the phenotypic screen, one of the most down-regulated proteins was Hla, the toxin responsible for erythrocyte lysis. Other known effectors contributing to *S. aureus* virulence were reduced in expression as well, namely transcriptional regulator SarS and histidine protein kinase SaeS. Initiated by RNAIII, SarS functions as

transcription regulator and plays an important role in virulence factor expression.^[37] Since Hla expression is repressed by SarS,^[37] it is likely to be up-regulated when SarS is down-regulated. This gives a hint, that down-regulation of Hla is achieved differently. Furthermore, SarS expression is repressed by *sarA* and *agr*,^[37] which makes sense according to the quorum sensing theory. Since bacteria were grown under hemolysis growth conditions, an activated *agr* system is implied and thereby SarS down-regulation. As elucidated in the introductory part, bacteria can switch between the adhesion phase and the invasion phase, whereas the latter is represented by hemolysis growth conditions, where the *agr* system is thought to be active.^[4] The transmembrane histidine kinase SaeS is part of the regulative two-component system SaeRS, with SaeR as response regulator.^[21,68] This TCS acts as an activator of toxin production, together with the global regulators *agr* and *sarA*. The *sae* locus is also responsible for Hla expression in the absence of *agr* and *sarA*.^[21,69] Furthermore, Sae is known to be essential for bacterial virulence in animal models.^[21,68]

Since proteins relevant for virulence are often secreted, the supernatant of **AV73** treated and untreated cells was analyzed (Figure 7B). Additionally to Hla, *gamma*-hemolysin and fibrinogen-binding protein were down-regulated among other virulence factors. While fibrinogen binding proteins play an important role in cell adhesion,^[70] *gamma*-hemolysin builds similar pores to *alpha*-hemolysin and forms a protein family together with leukocidins.^[71] Since both play essential roles in *S. aureus* virulence, its down-regulation is reasonable.

Furthermore, down-regulation of pathogenesis and cytolysis was confirmed by a more detailed analysis based on gene ontology (GO, Appendix: Table A1).

2.2. **AV73** inhibits Biofilm Formation

Interestingly, **AV73** is not only active against hemolysis, but it also inhibits biofilm formation, which will be discussed in the following section.

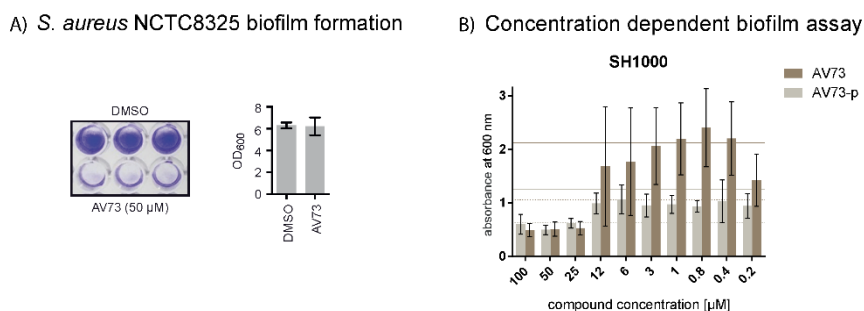


Figure 8. A) Biofilm assay of **AV73** at 50 μM and DMSO in *S. aureus* NCTC8325. Biofilm was grown under static conditions in 96-well plates and was stained with crystal violet. Bacterial growth with and without **AV73** was determined by OD₆₀₀ measurements. B) Concentration dependent biofilm assay of **AV73** and **AV73-p** in *S. aureus* SH1000. Solid line represents the DMSO control, the dashed line is half the OD₆₀₀ of the DMSO control. The experiment was performed in three biological replicates. MBIC₅₀ (**AV73**) < 25 μM, MBIC₅₀ (**AV73-p**) < 30 μM.

A concentration of 50 μM **AV73** is enough to fully prevent biofilm formation (Figure 8A). Using the biofilm forming reference *S. aureus* strain SH1000, an MBIC₅₀ of 25 μM could be obtained in a concentration dependent experiment (Figure 8B). Additionally, further *S. aureus* strains were tested, where **AV73** appeared to be effective against MRSA stain USA300 with an MBIC₅₀ of 50 μM (Figure 9A).

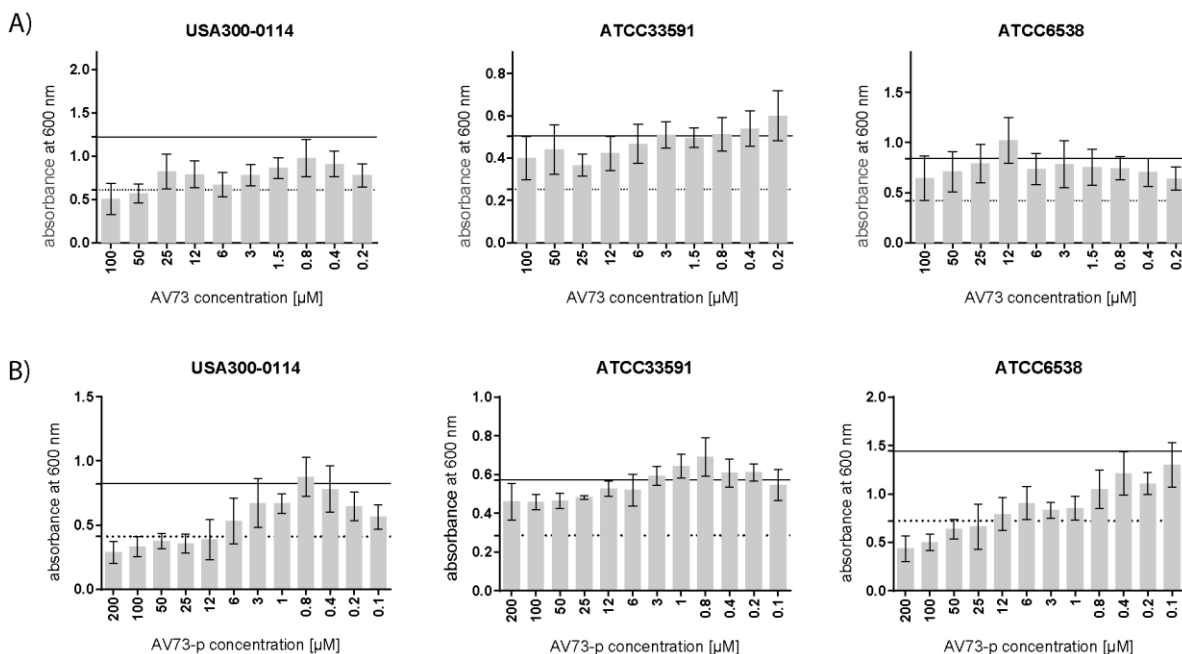


Figure 9. Biofilm assay with A) **AV73** and B) **AV73-p** in *S. aureus* strains USA300-0114, ATCC33591 and ATCC6538. Experiments were performed in three biological replicates. The solid line represents the DMSO control and the dashed line shows half the OD₆₀₀ of the DMSO control.

Whole Proteome Analysis

To get a deeper insight into the mode of action, again a whole proteome analysis was performed with bacteria grown under biofilm growth conditions. Samples were again lyzed, digested, dimethyl-labeled,^[67] pooled, measured and analyzed. Resulting volcano plots are shown in figure 10.

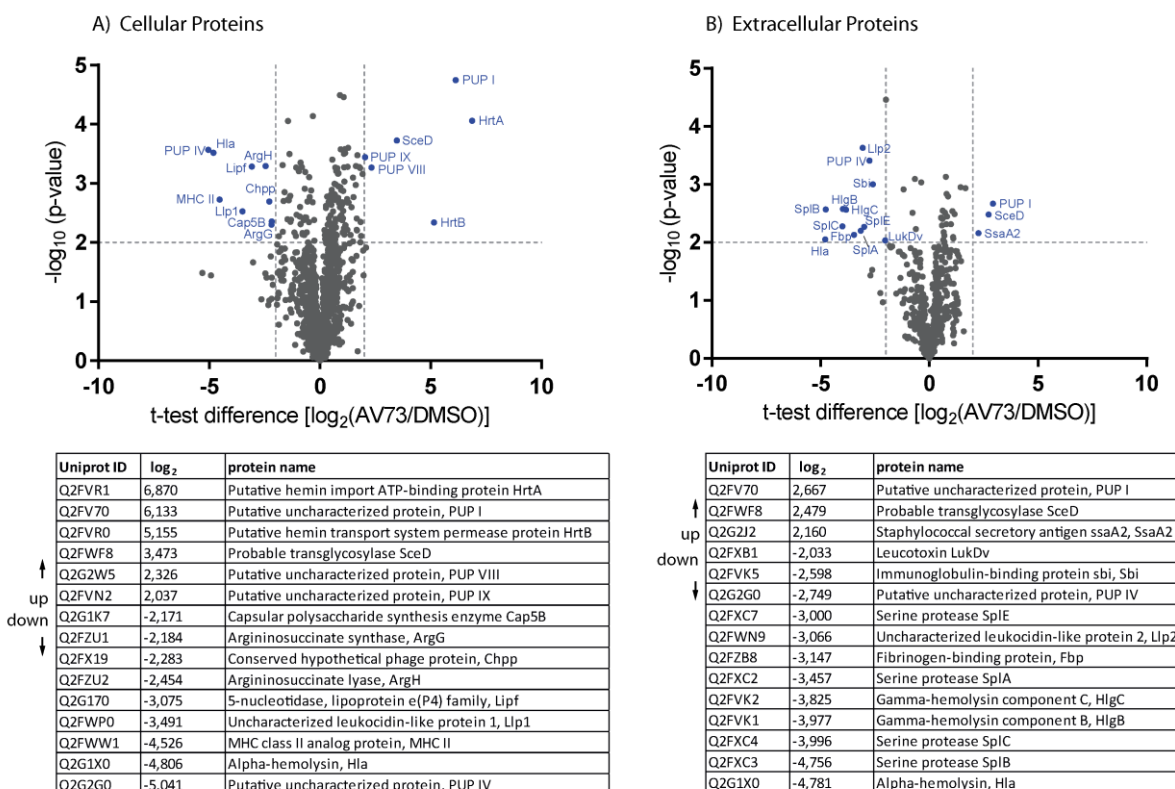


Figure 10. A) Whole proteome analysis of cellular proteins performed under biofilm growth conditions in four biological replicates. Most significantly regulated proteins are marked and listed by decreasing t-test difference. Cut off lines were set at a minimum log₂ fold-change of 2 and a minimum $-\log_{10}$ (p-value) of 2. B) Whole proteome analysis of extracellular proteins performed in four biological replicates. Most significantly regulated proteins are listed. Cut off lines were set at a minimum log₂ fold-change of 2 and a minimum $-\log_{10}$ (p-value) of 2.

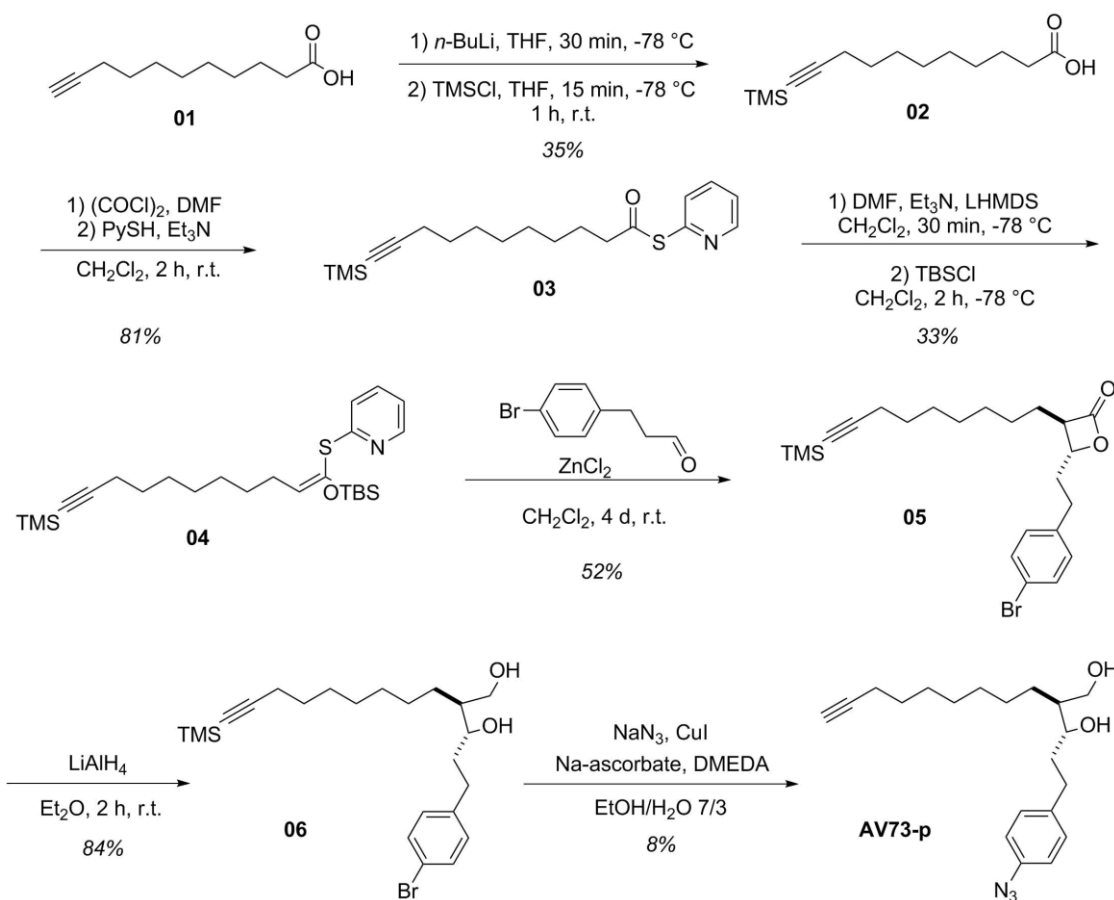
As was already the case in the analysis under hemolytic conditions, α -hemolysin is down-regulated significantly. Furthermore, leukocidin like proteins as well as capsular polysaccharide synthesis (CPS) enzyme were among the down-regulated proteins. Since capsular polysaccharide is an important virulence factor in the establishment of *S. aureus* infection,^[37] the down-regulation of its synthase upon **AV73**-treatment is not surprising. Leukocidins are part of the superfamily of β -barrel pore-forming toxins, like γ - and α -hemolysins, and play an important role in virulence.^[71] All together, a global down-regulation of virulence can be observed in the whole proteome analysis.

In the secretome again, α - and γ -hemolysin are down-regulated. Additionally, fibrinogen-binding protein and several SplA-F proteases are reduced in expression. Both play an

important role in biofilm formation. Whereas fibrinogen-binding protein is responsible for cell adhesion,^[70] serine proteases splA-F function in the exact opposite way.^[72] SplA-F are expressed upon induction of the *agr* system, which leads to the detachment of biofilm.^[72,73] When SplA-F are down-regulated, this should lead to an increased biofilm formation, which could be explained by the specific biofilm growth conditions. The down-regulation of fibrinogen-binding protein could be explained by **AV73**-treatment. Furthermore, GO enrichment analysis again confirmed cytolysis as down-regulated annotation (Appendix: Table A2).

2.3. Synthesis of a Photoprobe and its Bioactivity

Since the parent compound **AV73** already bears a phenyl ring and an alkene moiety, the design for the photoprobe is very clear from the beginning. By the attachment of an azide at the phenyl ring in *para*-position, an aryl azide is introduced as a photoreactive group. An alkyne handle is used as a biorthogonal handle and can be introduced instead of the terminal alkene in **AV73**. These minor structural changes might not have an impact on the compound's bioactivity.



Scheme 1. Synthetic route for the photoprobe **AV73-p**.

The six-step synthesis was initiated with a TMS-protection of the terminal alkyne of the starting material, undec-10-ynoic acid. After thioester formation a ketene acetal was synthesized. The lactone was synthesized in a tandem *Mukaiyama* aldol-lactonization with the corresponding aldehyde.^[74] After the reduction to the related diol, the azide was introduced and the alkyne deprotected simultaneously,^[75] to obtain photoprobe **AV73-p**.

Having the probe in hand, we first validated its bioactivity regarding hemolysis and biofilm formation. As already shown in several figures (Figure 5C, Figure 8B, Figure 9B) above, with

an IC_{50} of 30 μ M (**AV73**: 25 μ M) and an $MBIC_{50}$ of 35 μ M (**AV73**: 30 μ M), **AV73-p** largely retained antihemolytic and antibiofilm activities, respectively.

2.4. A/BPP with AV73-p

To define some experimental parameters like the required compound concentration of 60 μM , A/BPP was first performed gel-based in an analytical manner, using rhodamine azide as visualisation tag (Appendix: Figure A2 A).

Since the whole MS/MS-based workflow was already explained in the introductory part, here just a short summary with specific parameters. *S. aureus* was grown under biofilm growth conditions, incubated at a concentration of 60 μM AV73-p for one hour, irradiated for about 15 min, lyzed and clicked to biotin azide. After enrichment with avidin beads, digestion, and MS/MS measurement, the obtained data were quantified label-free and analyzed statistically (Figure 11).^[76]

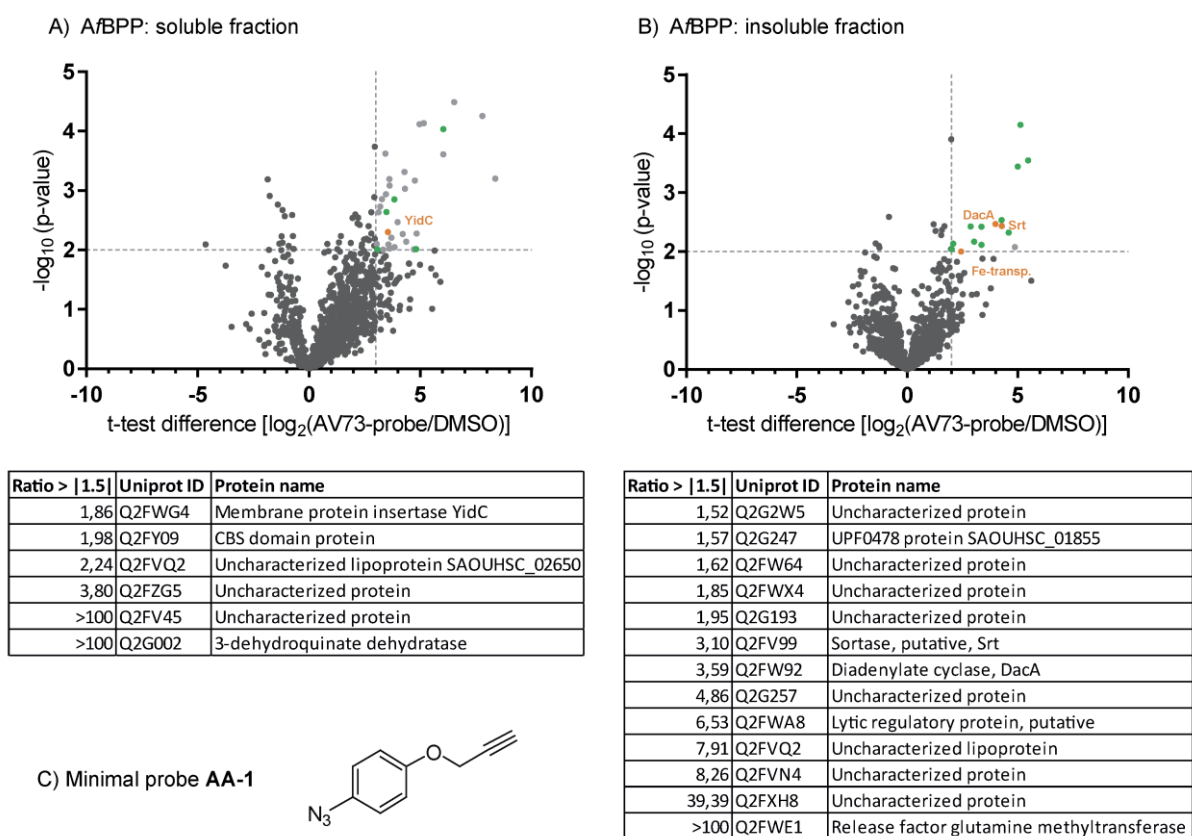


Figure 11. A) A/BPP volcano plot of AV73-p against DMSO in the soluble fraction. The experiment was performed in four biological replicates. Cut off lines were set at a minimum of \log_2 fold-change of 3 and a minimum $-\log_{10}$ (p-value) of 2. Proteins depicted in grey are found equally enriched in the background volcano plot (Appendix: Figure A3 A, B). Green marked proteins are found less enriched in the background volcano plot, as shown in the tables below. The orange marked protein is referred to in the text. B) Volcano plot of AV73-p against DMSO in the insoluble fraction. The experiment was performed in four biological replicates. Cut off lines were set at a minimum of \log_2 fold-change of 2 and a minimum $-\log_{10}$ (p-value) of 2. Color code same as in A). C) shows the structure of the minimal aryl azide photoprobe AA-1.^[62]

To further evaluate the data, additional control experiments were performed. On the one hand, a competition experiment with AV73 and AV73-p was conducted (Appendix: Figure A3 C,

D). Here, several proteins were lesser enriched than without competitor and are therefore more likely to be targets. On the other hand a minimal aryl azide photoprobe was used to differentiate background binding from possible targets (Figure 11C, Appendix: Table A6, 7).^[62] Only proteins with a \log_2 ratio greater than 1.5 in the **AV73-p** volcano plot in comparison to the background plot are considered as targets (Appendix: Figure A3 A, B).

Considering the background binding, the volcano plots of the soluble and insoluble fraction revealed six and 13 enriched proteins, respectively. Taking the competition experiment into account and looking deeper into the function of the proteins, four of them might be promising targets: the membrane protein insertase YidC, the putative iron compound ABC transporter, sortase SrtA-type enzyme and diadenylate cyclase.

Membrane protein insertase YidC plays an important role in inserting a diverse set of proteins into the lipid bilayer of bacteria.^[77,78] Whereas no direct evidence for its role in biofilm formation and virulence is given, a previous study showed that yidC1 and yidC2 contribute to *Streptococcus mutans* biofilm formation.^[79] Elimination of yidC2 in *S. mutans* resulted in a stress sensitive phenotype and impaired biofilm formation.^[79,80]

The iron compound ABC transporter lacks firm characterisation. Nevertheless, the whole proteome data support the importance of iron transport upon compound treatment. Two hemin im- and transporters are up-regulated after treatment with **AV73** (Figure 10A). Furthermore, iron is known to be essential for *S. aureus* biofilm formation,^[81] which fits, since bacteria were grown under biofilm growth conditions.

Numerous virulence proteins are covalently attached to the bacterial cell wall by sortase SrtA.^[82-84] Whereas the recognition of an LPXTG motif is necessary for proper attachment, SrtA additionally cleaves its substrates after threonine in C-terminal motifs. Furthermore, active sortase is required for the attachment of *S. aureus* to eukaryotic cells and thereby for pathogenesis.^[82,85,86] Mutants lacking sortase fail to display surface proteins, and have problems in the establishment of infections.^[82,84,85] Interestingly, virulence- and biofilm-associated proteins containing the LPXTG motif were identified in the treated proteome (Appendix: Table A3).

Diadenylate cyclase (DAC) is highly expressed during biofilm growth in *S. aureus* and is responsible for c-di-AMP synthesis. Cyclic-di-AMP represents an important transmitter in virulence regulation, which fits to the observed phenotype.^[87,88] *Gries et al.* detected a novel extracellular role of c-di-AMP. In particular, c-di-AMP-release during biofilm growth leads to

polarization of macrophages towards an anti-inflammatory state, and therefore contributing to biofilm persistence.^[88] Since the DAC gene has been shown to be essential in *S. aureus* and other gram-positive bacteria, it constitutes an interesting target for new drugs, which could be found by screening for DAC inhibitors. *Sintim* and co-workers found hydroxybenzylidene compounds as inhibitors, showing antibacterial and antibiofilm activities.^[87] Furthermore, cyclic-di-AMP also plays an important role in the pathogen *S. mutans*, where it regulates biofilm formation.^[89]

3. Conclusions and Outlook

All in all, compound **AV73** is active against virulence and inhibits biofilm formation, which was shown in different assays. Whole proteome data of cellular and extracellular proteins simultaneously showed a strong down-regulation of virulence and biofilm related proteins, including Hla and fibrinogen-binding protein. This is the case for experiments performed under hemolysis as well as biofilm growth conditions, and was further confirmed by gene ontology analysis.

To further elucidate the mode of action, an **AV73** photoprobe, **AV73-p**, was synthesized and applied in an affinity based protein profiling workflow. Additionally, two control experiments, a competition experiment and labeling with a minimal photoprobe to exclude background binding, were performed. Parallel binding to proteins associated with pathogenesis and matching the antivirulent and antibiofilm phenotype, was observed. Although this study cannot fully consolidate the mode of action, four main hits were detected, each playing an interesting part in virulence or biofilm formation, namely membrane protein insertase YidC, iron compound ABC transporter, sortase SrtA and diadenylate cyclase. To further clarify their roles in *S. aureus* virulence, further investigations are required.

Since **AV73** is active against both, virulence and biofilm formation, its mechanism probably goes beyond the DSS and the whole *agr* system. Its $IC_{50}/MBIC_{50}$ values are moderate and in need of improvement. Nevertheless, given the simple structure and the low toxicity (Appendix: Figure A2 B), an application in coatings might be possible or at least worth further investigation.

III. Manipulation of ClpP Activity

1. Introduction

1.1. The ClpXP protease system

Proteases and the importance of ClpP

A cell commonly produces extracellular and intracellular proteases. While extracellular proteases are monomeric with high substrate specificity and often synthesized inactive to protect the cell before they are secreted, intracellular proteases are multimeric complexes with little substrate specificity. Activity and substrate selection are tightly regulated in this case.^[90,91] Examples are Lon, HslUV (ClpQP), ClpXP and FtsH,^[90] which are all energy dependent proteases. A major portion of protein degradation is carried out by those kinds of proteases.^[92] They play an important role in the cleavage of damaged or short lived proteins, and consist of two parts, a proteolytic active core and an ATP-dependent subunit.^[11,90]

The caseinolytic protease P, ClpP, represents the proteolytic core of the ClpXP protease complex. Its major physiological role is to maintain cellular homeostasis by controlling degradation of short lived regulatory as well as misfolded and damaged proteins. Since this also includes proteins that are involved in regulating stress response and virulence factor production, ClpP plays an important role in pathogenicity of bacteria.^[93]

Function of the ClpXP complex^[94]

ClpP is a highly conserved serine protease, which assembles as a tetradecamer with an internal chamber formed by two back-to-back stacked heptameric rings (Figure 12). ClpP on its own can only act as a peptidase and degrade peptides up to six amino acids.^[92,93] For its proteolytic activity, an ATPase associated with diverse cellular activities (AAA+ family) is required. These ATPases form hexamers and can occur differently in various bacteria. Usually ClpA and ClpX are found in gram-negative and ClpC and ClpX in gram-positive

bacteria.^[90] Amongst other contacts, they bind to the surface of ClpP into hydrophobic pockets that are formed between two adjacent monomers, called the H pockets (Figure 12A). Upon binding, ClpP undergoes a structural reorientation and is kept in an active state. ATPases recognize, unfold and translocate the proteins, which can then be hydrolyzed in the internal chamber, by the 14 proteolytic active sites of ClpP.

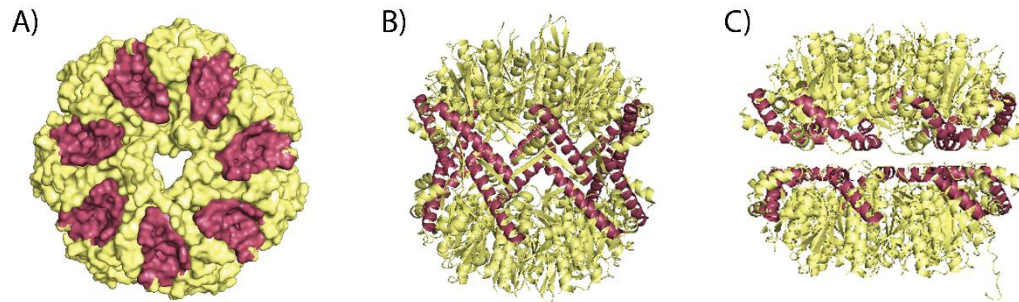


Figure 12. Structure of *Sα*ClpP tetradecamer in A) top and B) and C) side view. A) Hydrophobic pockets are marked in red. B) shows the active extended state, C) the inactive compressed form. In B) and C) the central helix, the “handle region” is marked in red. (PDB: 3sta)

Structural features of ClpP and ClpATPases

A ClpP monomer can be divided into three structural parts: the N-terminal region, which is located at the pore of the heptamer, the head region in the middle and the handle region which interacts with a second ClpP heptamer.^[95] ClpP is known to be present in three states, the active extended, the inactive compressed, and the intermediate compact state (Figure 12B, C).^[93,96] It possesses a unique region called the “handle region”, which is utilized for upper and lower heptameric ring contacts and plays an important role in conformational switches.^[97] However, the overall ClpP structure is very similar in all states. It is suggested that ClpP undergoes a cycle whereas in one step proteins are degraded in the active state, and in another step the hydrolyzed peptide fragments are released through equatorial pores in the compressed state.^[98–100]

Another striking aspect is the symmetry mismatch that occurs when ClpP as a heptameric ring and ClpX as a hexameric ring stack together. The binding of the two proteins occurs in two ways. The IGF-motifs of ClpX bind into the hydrophobic pockets on the surface of ClpP, whereas only two to three loops are bound at the same time.^[101–103] Additionally, ClpX pore-2-loops, are in contact with the N-terminal loops of ClpP, which are flexible in appearing in up or down conformation to compensate the symmetry mismatch.^[104]

The ClpP protease system is broadly conserved throughout bacteria and mammalian cells, where the ClpXP complex is localized in mitochondria.^[105] Typically, ClpP assembles as

homocomplex, though *M. tuberculosis* and *L. monocytogenes*, express two different forms of ClpP, ClpP1 and ClpP2, that can form a heterocomplex.^[106-108]

Key role of ClpP under stress conditions

As already mentioned, the ClpXP protease complex plays an important role under stress conditions, where proteins unfold or form aggregates.^[11,109,110] In this case, cells increase the production of chaperones and proteases, which degrade the misfolded proteins. Under such stress conditions ClpP plays a major role in the degradation of non-native proteins.^[11] The production of ClpP is clearly increased by heat shock and other stress conditions, which also indicates an important role in these situations.^[11,111] In particular, a $\Delta clpP$ mutant is more sensitive to growth under stress conditions, where misfolded proteins accumulate, than the wild type.^[11]

***S. aureus* ClpPs connection to virulence**

Frees et al. found out that both, ClpP and ClpX, are required for virulence in a mouse model. Mice were inoculated with *S. aureus* wild type and either a ClpP or a ClpX mutant. While an infection was caused by the wild type, almost no bacteria were detected with a ClpP or a ClpX mutant. Moreover, the amount of extracellular proteins and toxins is reduced in the mutant strains, which is in accordance with the results of the mouse model.^[11]

In the theoretical section, the living cycle of *S. aureus* was explained and it was shown that they are either in a biofilm promoting state, or in a toxin production phase.^[38] Due to the strict controlling system by quorum sensing, it is unlikely that one compound is able to reduce virulence and biofilm formation at the same time. This can also be shown on the example of ClpP. In a $\Delta clpP$ mutant strain, proteins that enhance biofilm formation e.g. adhesins, fibrinogen-binding proteins and elastin-binding proteins, are up-regulated. At the same time, virulence effectors are down-regulated.^[6] Currently, there are no approved antimicrobial agents targeting bacterial proteases, which makes them an important subject of ongoing research.^[90]

1.2. Inhibition of ClpP leads to a reduction of virulence

As mentioned before, ClpP plays an important role for the virulence of various pathogens. For instance, *L. monocytogenes* and *S. aureus* carrying a deletion of the *clpP* gene display attenuated virulence and are less infectious in murine abscess models.^[11,112,113] Upon chemical inhibition, the same phenotype can be observed,^[113] which shows that it is indeed possible to “disarm” pathogens.

Addressing this, β -lactones have been reported by *Böttcher* and *Sieber* to be the first selective inhibitors of ClpP (Figure 13).^[114] The 4-membered lactone ring is attacked by the catalytic serine, resulting in a covalent intermediate, blocking the active centre irreversibly. Preventing their application in therapeutics, the main drawback of β -lactones is that they are rapidly hydrolyzed in human plasma.^[113,115] Lactam, carbamate and ester moieties fail to inhibit ClpP. Heading for more stable moieties, a HTS was performed by *Hackl et al.* and phenyl esters were discovered as ClpP inhibitors. Structure-activity-optimization resulted in compounds that display superior protease inhibition, target selectivity and plasma half-life compared to β -lactones (Figure 13).^[113]

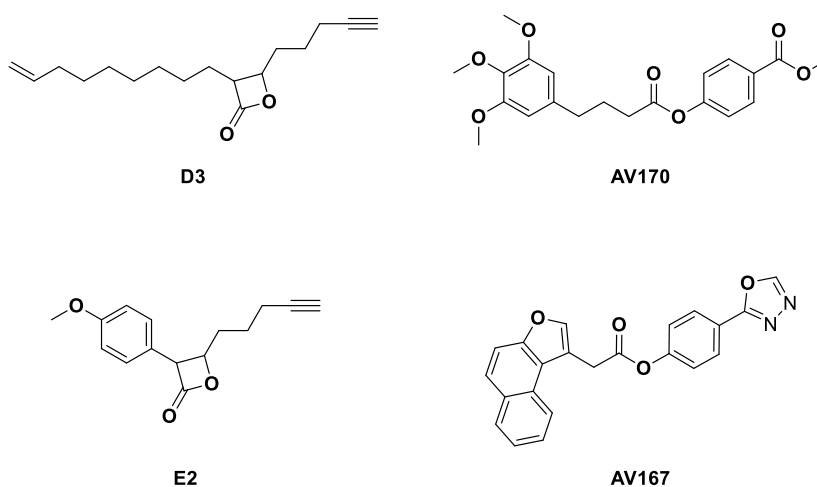


Figure 13. Structure of ClpP inhibitors, β -lactones **D3** and **E2** and phenyl esters **AV170** and **AV167**.

As bacteria are not killed upon ClpP inhibition, the selection pressure is missing, which leads to a decreased risk of resistance development. However, the downside of these phenyl esters is their poor stability, which therefore makes them subject of further optimization.^[113]

1.3. Activation of ClpP leads to cell death

Another method to manipulate ClpP activity is exactly the opposite, not the inhibition, but the activation of ClpP. This can be achieved by acyldepsipeptides (ADEPs). They show antibacterial activity in several strains and act *via* an entirely new mechanism, namely by activating ClpP.^[116] Taken together, most antibiotics have four proven targets: cell-wall biosynthesis, protein synthesis, DNA replication and repair, and cytoplasmic membrane function.^[117,118] Due to the rising antibiotics resistance crisis it is even more important to develop antibiotics addressing new targets.

Isolation and structure of natural ADEPs

The natural products A54556A (ADEP1) and B were first isolated in 1982 from *Streptomyces hawaiiensis*, from a mixture of eight depsipeptidic factors.^[119,120] Enopeptin A and B were isolated in 1991 from *Streptomyces* sp. RK-1051 (Figure 14).^[120,121] Altogether, ADEPs consist of a macrocyclic lactone core composed of five *S*-configured amino acids and a lipophilic acylated phenylalanine side chain. Ongoing structural optimization of the natural isolates led to the development of many different ADEP derivatives, some of them will be discussed later.^[120]

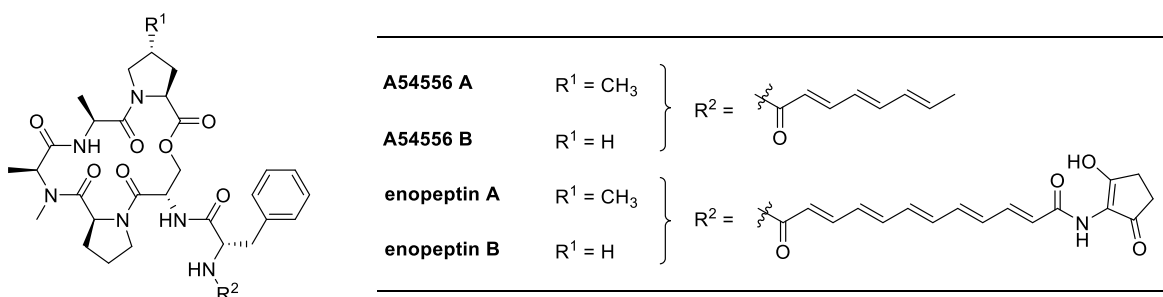


Figure 14. Structure of natural depsipeptide antibiotics.

Among others, ADEPs are active against gram-positive methicillin-resistant *S. aureus*, vancomycin-resistant *enterococci*, penicillin-resistant *S. pneumonia* and against gram-negative *N. meningitides* and *Neisseria gonorrhoeae*.^[90,116,122] Covering this broad range of bacterial species, there is a deep interest in further investigation.

Binding of ADEPs

ADEPs bind to the same hydrophobic pockets as ATPases like ClpX, mimicking the IGF loop of the chaperone. As a consequence, the N-terminal region is structurally reorganized and ClpP “opens its gate” for larger polypeptides (Figure 15).^[123,124] Usually, the axial pore formed by the N-terminal region of ClpP is narrow, to prevent uncontrolled proteolysis of the

ClpXP complex. Moreover, upon ADEP binding the rigidity of the equatorial region is increased and catalysis is stimulated.^[94,125] This allosteric effect additionally leads to an over-activation, which promotes the degradation of larger peptides or nascent proteins.^[94,126] Amongst others, one crucial substrate is the cell proliferation protein FtsZ. Upon FtsZ degradation, cells are not able to differentiate anymore, which leads to inhibition of cell division and thereby to cell death.^[94,127]

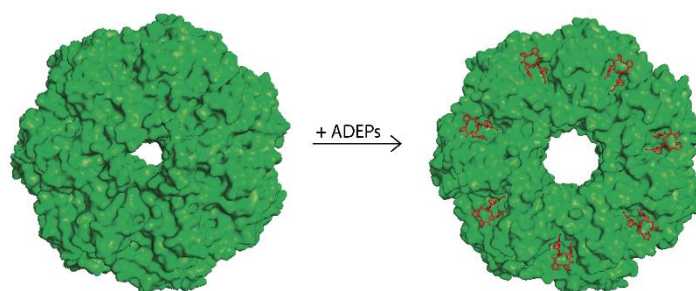


Figure 15. Top view of the structure of ClpP before (left) and after (right) the binding of ADEPs, which leads to an enlargement of the pore. (PDB left: 3sta, right: 5vz2)

The H pocket

H pockets are hydrophobic pockets, formed between two adjacent ClpP monomers at the apical surface of ClpP. As mentioned above, ATPases mediate interaction with these H pockets *via* their IGF-motifs. The phenyl moiety and the aliphatic side chain of ADEPs mimic this binding of the IGF loop. Crystal structures show a clear overlap of the phenylalanine moiety of ADEP1 with the phenylalanine located in the IGF loop.^[94,101,128] In *SaClpP* Tyr63 plays an important role in ADEP binding, by stabilizing it with two hydrogen bonds and one hydrophobic interaction. In ADEP-bound structures, the Tyr63 is rotated by 90° (Figure 16). This twist initiates activation of ClpP. In *SaClpP*, a mutation of Tyr63 to alanine leads to a rotated peptide backbone, due to a lower energy barrier. This mutation enables the degradation of casein and FtsZ of ClpP alone, which emphasizes a key role of this tyrosine in the hydrophobic pocket in activity regulation.^[93,129]

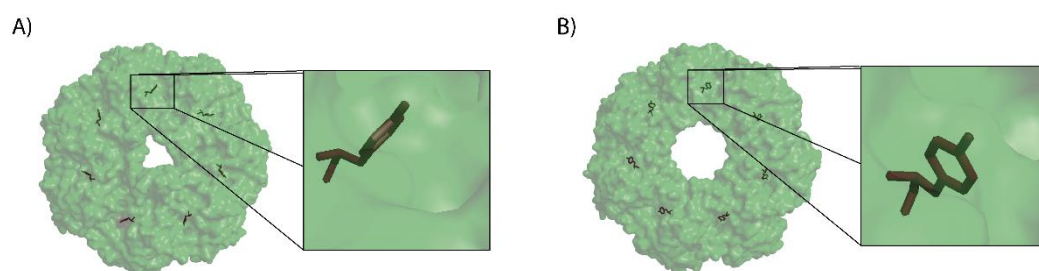


Figure 16. Structure of *SaClpP* with marked Tyr63, in A) without the binding of ADEPs and in B) rotated by 90° upon ADEP-binding. (PDB: A) 3sta, B) 5vz2)

The H pocket is also referred to as a „master switch“, which is not only connected to the N-terminal, but also to the handle region.^[94] “Filling” the H pocket leads to a stabilization of the handle in an active extended conformation, accelerated substrate turnover by catalytic sites, widened axial pores and an overall more stable and structurally less flexible complex. ADEPs can therefore be described as sterical locks which fix ClpP in the active extended form.^[94,124,128]

Activation and Inhibition by ADEPs

The described activation behaviour can be observed in different bacterial species like *B. subtilis*, *Streptococcus* and *Enterococcus*,^[116,130] whereas *mycobacteria* make an exception. Here, ADEPs inhibit ClpXP function by occupying the ATPase binding pocket, instead of leading to a conformational activation of ClpP.^[93,131] ADEPs have a higher affinity to ClpP than ATPases do, a single molecule is sufficient to displace a whole ATPase hexamer.^[94,126] In contrast to other bacteria, the cell division protein FtsZ is not degraded in *mycobacteria*. In this case, ADEPs kill the bacteria by preventing the interaction between ClpP1P2 and ATPases.^[93] Hence, the binding pocket seems to be occupied by both, activators and also inhibitors.

Optimization of ADEPs

Antibacterial activity is limited for natural ADEPs *in vitro*, and totally gone when moving to *in vivo* experiments.^[90,120] They seem to have pharmacologically unfavourable properties, like poor water solubility, chemical instability and rapid systemic clearance.^[90] Particularly, the chemical stability is limited by the lactone core, which is readily hydrolyzed in basic and acidic aqueous medium, the serine hydroxyl group, which eliminates under non-aqueous basic conditions, and the conjugated triene, which is sensitive to temperature and light.^[120]

Hence, *Hinzen et al.* went for structure activity relationship (SAR) studies. From the start, optimization was focused on parts of the molecule that are not directly involved in the binding to ClpP. Namely that were *N*-methylalanine, the northern proline and the aryl or alkyl chain. Moreover, they refer to a principle in medicinal chemistry, which is to increase potency by reducing the entropy disadvantage during the binding. That is why rigidification of the lactone core was also part of their investigations.^[120] In the end, they came up with ADEP4, which was the structure showing best potency and stability (Figure 17). Even treatment of lethal *S. aureus* infections in mice showed a therapeutic effect superior to a marketed antibiotic. The crucial elements they adopted were the pipercolate, the 3,5-difluoro-phenylalanine and the unsaturated tail.^[120]

Further optimizations were implemented by *Arvanitis et al.*, who designed ADEP B315 with 4-methylpipercolate and an *allo*-threonine (Figure 17). The compound has effective MICs in *S. aureus*, *S. pneumoniae* and *E. faecalis*.^[132,133] Additionally, ADEP B315 was effective in mice models with methicillin-sensitive and -resistant *S. aureus* strains. In the MRSA strain it even showed an effect, where vancomycin at the same dose was ineffective.^[133]

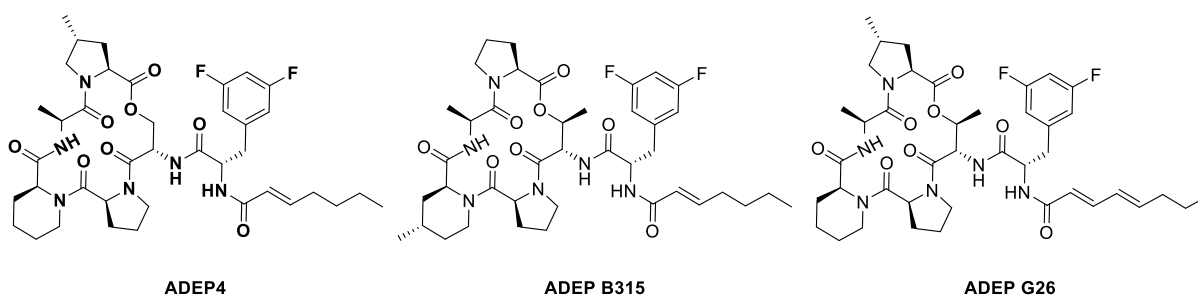


Figure 17. Structures of optimized ADEPs: ADEP4^[134], ADEP B315^[132] and ADEP G26^[122].

Goodreid et al. further improved ADEPs also for gram-negative bacteria. Most gram-negative bacteria are resistant to ADEPs, due to cellular efflux mechanisms or limited membrane penetration. Their optimized ADEP, here stated ADEP G26, shows potent antibacterial activity against the two gram-negative strains, *N. meningitides* and *N. gonorrhoeae* (Figure 17). Additionally, it shows activity against an *E. coli* strain with an outer membrane defect. Hence, a combined strategy with compounds known to compromise the outer membrane seems promising. Moreover, the compound G26 reveals improved activity in several gram-positive bacteria. Its structure contains the methylated northern proline, pipercolate, *allo*-threonine and octadienoic acid in the side chain (Figure 17). Stability studies showed the diene to be much more stable at ambient conditions than the original triene of the natural products.^[122]

In total, all optimized compounds show strong activity for various bacterial strains, although there is no variant which tackles all pathogenic strains at once. However, to address different problems with diverse optimized compounds seems to be a good strategy.

Resistance development and combination treatment

Resistance to ADEPs was found by selecting for colonies which grew on ADEP-containing agar plates. *Brötz-Oesterhelt et al.* found that resistance is mediated by the loss of ClpP activity, at least in bacteria where ClpP is not essential.^[116,130] This is achieved by mutations diminishing the function of the protein complex. Additionally, ADEPs are susceptible for efflux pumps, which plays a major role in for instance *M. tuberculosis*, but could be handled with efflux-pump inhibitors.^[116,125,130,135] In *M. tuberculosis* ClpP2 is essential and therefore resistance development by mutations is not possible, emphasizing ClpP2 as a good target for

drug development. In these bacteria ClpP2 is an essential protein, which excludes the above described resistance mechanism. Since this path is then impossible for the bacteria, it might be a good drug target.^[130] In the case of *M. tuberculosis*, where ClpP assembles as heterocomplex, ADEPs only bind to one heptameric ring, but appear to open the pores of both rings. In the heterocomplex, ClpP2 is directly stabilized, ClpP1 indirectly.^[136]

Interestingly, no cross-resistance to marketed antibiotics was found for ADEP4.^[116,137] ADEP4 not only kills persisters surviving ciprofloxacin treatment, it is also active against stationary phase *S. aureus*, where conventional antibiotics are inactive. In combination with other antibiotics, especially with rifampicin, ADEPs show a great efficacy spectrum.^[137] These two antibiotics together are even able to completely eradicate *S. aureus* biofilms *in vitro* and in a chronic infection mouse model, revealing a promising strategy for therapeutics.^[137]

Fragments of ADEPs and other natural product activators

Carney *et al.* found out, that fragments of ADEPs are necessary and sufficient to activate ClpP. The smallest fragment they describe (here stated **PAK4**) only consists of the side chain of an ADEP, which lies deep inside the hydrophobic pocket (Figure 18). The whole macrocyclic core is located on top of the pocket, taking over stabilization. They found that the peptidolactone core alone displays no activity.^[138]

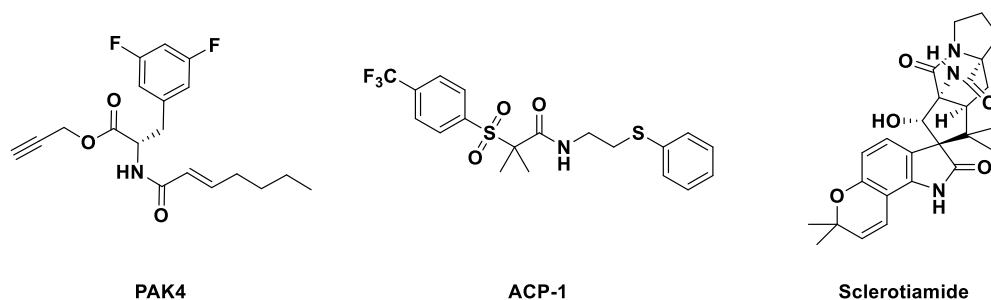


Figure 18. Structures of ClpP activators: ADEP fragment **PAK4**, ACP-1 and the natural activator sclerotiamide.

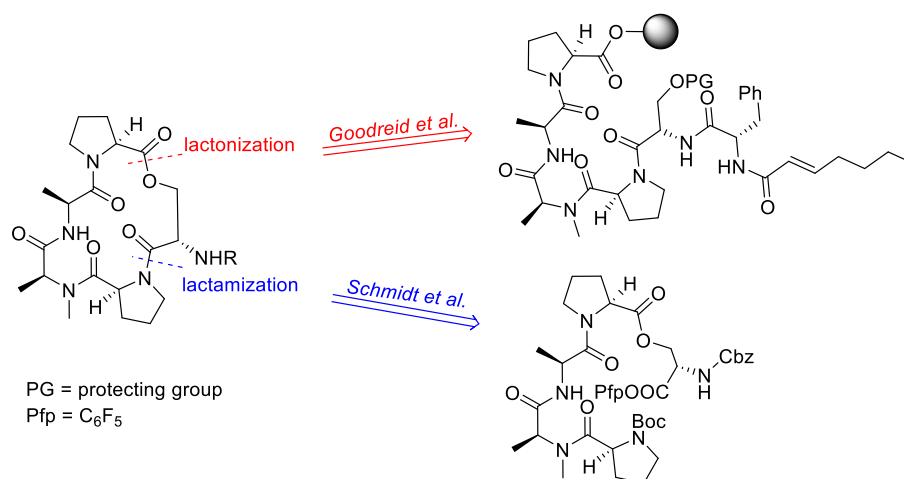
Using a high throughput screen (HTS) against commercially available compound libraries, Leung *et al.* identified several compounds that were able to activate ClpP. They called them activators of self-compartmentalizing proteases (ACPs). ACP-1 represents their optimized compound and shows good drug-like characteristics, with a ClpP activation comparable to ADEPs.^[93,139,140] Weaker ACPs not only bind to the H pocket, but also to the C pocket, which is located rather on the equatorial side of ClpP.^[93,139] Ye *et al.* claim, that this pocket could be used as an allosteric site to develop novel ClpP activators.^[93]

A HTS of fungal and bacterial secondary metabolites was performed by *Lavey et al.* and sclerotiamide could be identified as first non-ADEP natural product activator, with modest potency compared to ADEPs and ACPs.^[93,141] Thus, optimization of the natural product is required for further applications.

Taken together, a manifold of compounds besides ADEPs have been developed in order to manipulate ClpP activity. However, as ClpP displays a promising antibacterial target, further research for the development of more potent compounds is of urgent need.

1.4. Known ADEP-Syntheses

By now, two different approaches for ADEP-synthesis are known. On the one hand, *Schmidt et al.* established a method, which closes the ring with a lactamisation, followed by couplings to build up the side chain. Here, peptide fragments are synthesized in solution beforehand.^[142] On the other hand, *Goodreid et al.* published a synthesis for a peptide, built up using solid-phase peptide chemistry. The ring-closure is achieved *via* lactonization. Both methods will be illustrated in the following (Scheme 2).^[143]



Scheme 2. Two different approaches for ADEP synthesis. Lactonization of a pentapeptide, synthesized by solid-phase peptide chemistry, described by *Goodreid et al.* in 2015 and lactamisation of a heptapeptide synthesized by solution phase chemistry, described by *Schmidt et al.* in 1997.^[142,143]

In 1997, *Schmidt et al.* described the first ADEP synthesis, of enopeptin B^[142] and *Hinzen et al.* used the same method for the synthesis of different ADEP derivatives in 2006.^[120] In general, a tripeptide is coupled to a didepsipeptide, and the resulting pentadepsipeptide is cyclized with *Schmidt's* cyclization method, which was published in 1982.^[120,142,144] The cyclization of the activated acid as pentafluorophenylester takes place in a two-phase system consisting of aqueous NaHCO₃ and chloroform.^[142,144] After cyclization the Z group is

deprotected, a Boc-protected phenylalanine moiety is coupled, deprotected and coupled to the final acid.^[120,142] The same procedure with little adaptations was used by *Goodreid et al.* and *Carney et al.* in 2014.^[138,145]

The newer approach, introduced by *Goodreid et al.* in 2015, included three major changes: First, the peptide was synthesized *via* SPPS, second, the whole peptide chain was synthesized before the cyclization, and third, the cyclization involved the formation of a lactone.^[143] Since the yields of the lactam cyclization were rather low, this was an advantage in comparison to former methods. Cyclization and formation of the lactone is achieved by MNBA, DMAP and a Lanthanide (III) triflate catalyst. Furthermore, SPPS is a straightforward method to synthesize the desired peptide.

1.5. Activity of a first ADEP-photoprobe

For deeper investigations of ADEPs and ClpP a first ADEP photoprobe was synthesized previously, based on the ADEP7 structure (Figure 19).^[146] The synthesis was built on solution phase synthesis with lactam formation as cyclization method.^[142] Instead of 2-*E*-heptenoic acid, which is incorporated in ADEP7, a minimalist photoprobe, equipped with a diazirine moiety and an alkyne handle, was introduced to form the respective photoprobe **ADEP7-p** (Figure 19).^[146]

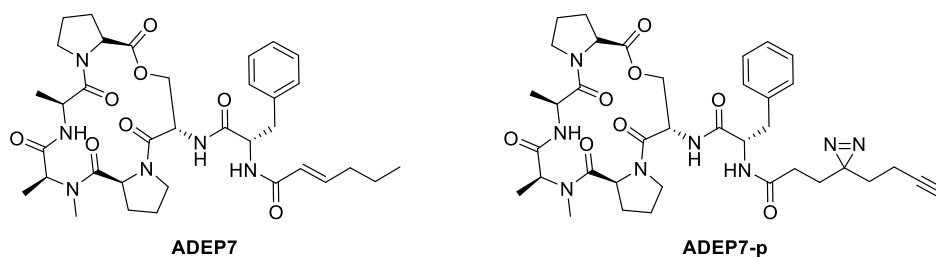


Figure 19. Structures of ADEP7 and the ADEP photoprobe **ADEP7-p**.

In order to monitor bioactivity of the ADEP photoprobe, a ClpP activation assay was performed. However, no activation of ClpP could be observed, probably caused by the incorporation of the diazirine and alkyne moieties.^[146] As a bioactive ADEP photoprobe will enable a huge number of experimental set ups, further optimization is of urgent need.

1.6. Scope of this work

As described above, caseinolytic protease P is a valuable target for compounds with antibiotic and antiviral effects, by activating and inhibiting ClpP.

The activation of ClpP constitutes an important issue and represents the main part in this part of the thesis. It was addressed by the investigation of ADEPs and their interaction with ClpP. Based on structure activity relationship studies and bioassays, a corresponding optimized photoprobe, equipped with a photoreactive group and a biorthogonal handle for the attachment of a linker, was designed and synthesized. Gel- and MS-based A/BPP experiments were performed and revealed ClpP as a target. Besides the investigation of off-targets, one goal was the labeling of ClpP in an inactive state, which was not possible before (Figure 20).

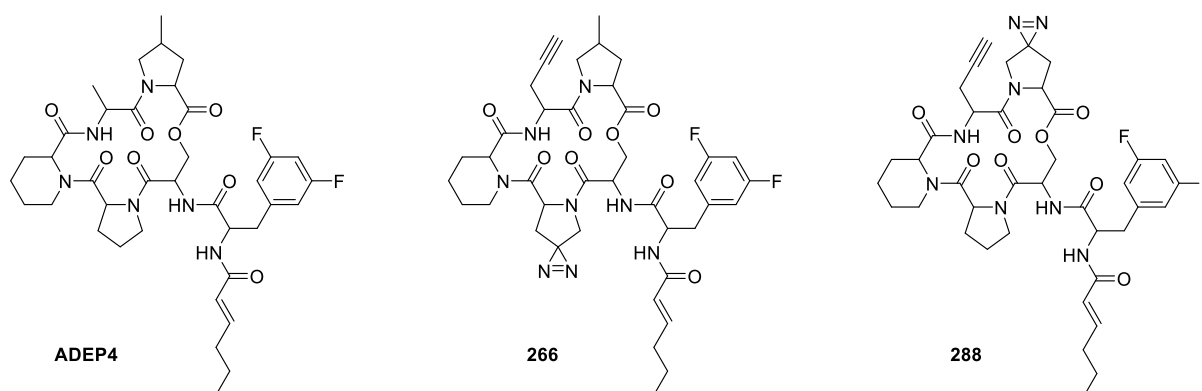


Figure 20. Structures of ADEP4 and two ADEP-photoprobes **266** and **288**.

Although the focus mainly lies on bactericidal compounds, the inhibition of the ClpXP complex was addressed as well. Inhibition of the ClpXP complex is attractive, since virulence of pathogens can be “switched off”.^[92,113,146,147] For this reason, two ClpXP inhibitor compounds were investigated regarding their activity and their phenotypic effect. In addition, the goal was to design and synthesize a photoreactive probe. ClpP and off-targets should be revealed with the application of an A/BPP workflow. The two ClpXP inhibitors are shown in figure 21 and originate from a HTS that was performed by *Fetzer et al.*^[149]

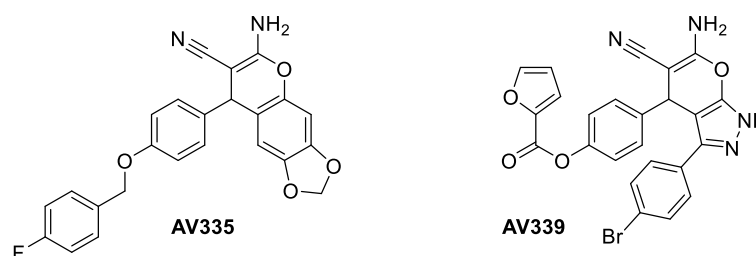


Figure 21. Structures of ClpXP inhibitors **AV335** and **AV339**.

2. Inhibition of the ClpXP complex

In this part of the thesis anti-virulence shall be covered by the investigation of ClpXP inhibition. As mentioned above, this might be an elegant way to overcome, or at least delay, resistance development.

2.1. Inhibitors and related compounds

A high throughput screen was performed to select for ClpXP inhibitors by *Fetzer et al.*,^[149] which was done *via* a protease assay, where GFP as substrate was detected *via* fluorescence. Two inhibitors **AV334** and **AV336**^[149] were published showing a disruption of the ClpX chaperone complex (Figure 22). Two further non-covalent inhibitors, **AV335** and **AV339**, exhibited interesting results and are dealt with in this thesis (Figure 22). Since the two compounds have some structural similarities, this was the basis for structure activity relationship studies, to make out the best modification site for the attachment of a photolabile moiety and an alkyne handle for *A/BPP* experiments. Furthermore, the mechanism of inhibition, or the place of the event should be elucidated.

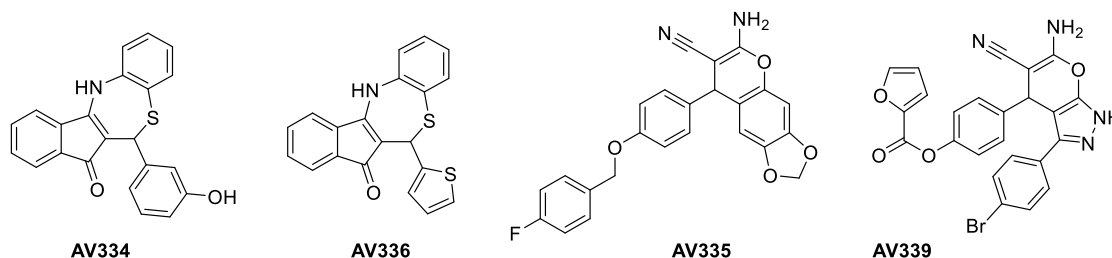


Figure 22. Structures of published ClpXP inhibitors **AV334** and **AV336** and inhibitors **AV335** and **AV339**.

Structurally similar compounds for SAR studies were obtained by *ChemDiv* (Figure 23) and biochemical assays were performed, which will be explained in more detail later (Chapter 2.2.). Several modifications at different positions of compound **AV335** were chosen to find out the importance of these parts of the molecule for ClpXP inhibition.

Compounds **CD8**, **CD9**, **CD11** with different substituents at the phenyl ring should reveal if the position or the substituent itself are important for the ability of ClpXP inhibition. While the parent compound **AV335** bears a fluorine in *para*-position, **CD8** has a fluorine in *meta*- and **CD9** and **CD11** a chlorine in *para*-position. If modifications are tolerated, an aryl azide could be introduced as photoreactive group in these positions.

Compounds lacking the phenyl ring (**CD1** to **C5**) were utilized to elucidate if the phenyl ring is an essential part of the molecule. Here, compounds **CD7** and **CD10** were of special interest,

because they not only lack the phenyl ring, but also bear an alkyne handle, which could be used for click chemistry and enrichment in an A/BPP experiment. Interestingly, compounds **CD4**, **CD6** and **CD7** bear an ether moiety and compound **CD3** an ester moiety at the phenyl ring. At those positions the introduction of a minimal photocrosslinker, equipped with a diazine and an alkyne handle might be possible.

If the alcohol in compounds **CD2** or **CD11** would be accepted, the introduction of a minimal photocrosslinker might be possible there too. The same applies to the amine in **CD1**, which could be used as an introductory position.

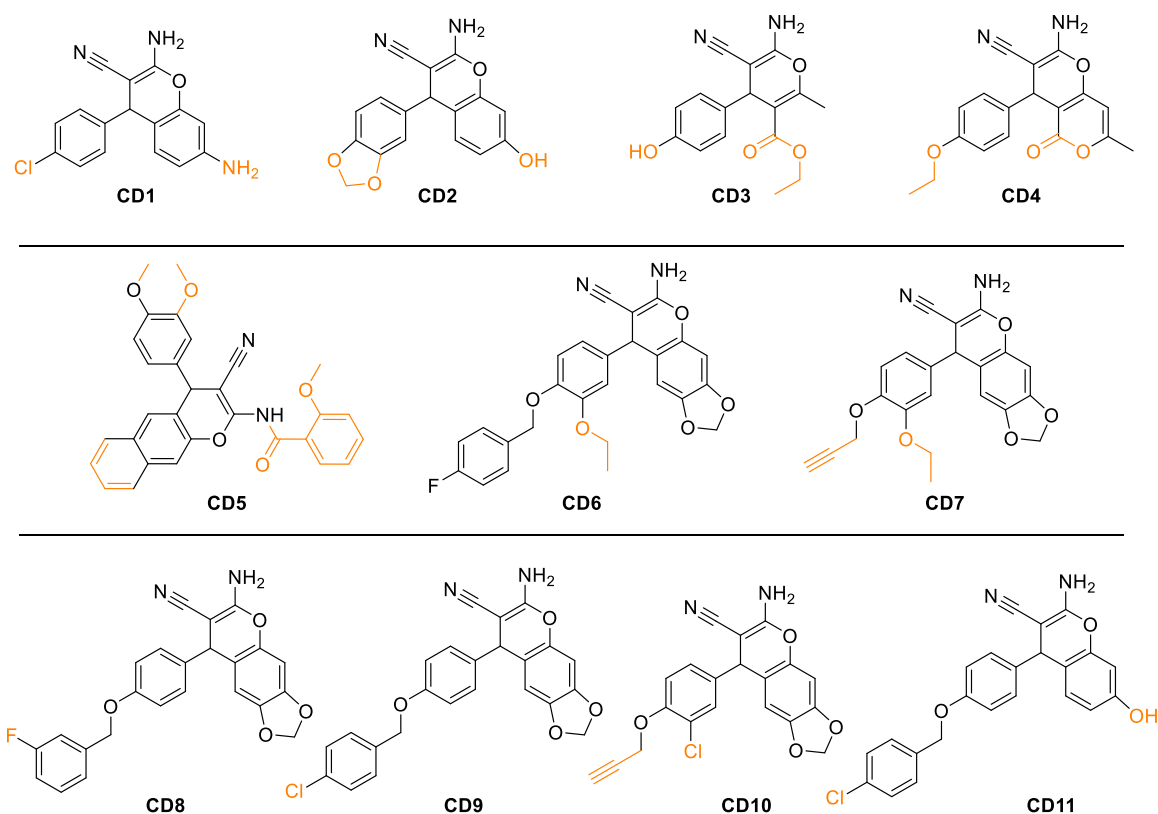


Figure 23. Structures of structurally similar compounds **CD1** to **CD11**. Parts of the molecules that differ to the parent compound **AV335** are marked in orange.

2.2. Assays to elucidate the mechanism of ClpXP inhibition and SAR studies

Studies to elucidate the mode of action were performed and structurally similar compounds **CD1** to **11** were used to simultaneously determine SAR studies for the design of a photoprobe.

2.2.1. *Protease and GFP unfolding Assay*

Before evaluating the mode of action, the modified compounds were tested for their inhibitory effect on the ClpXP complex, through a protease assay. Here, GFP equipped with a SsrA-tag was used as a substrate and protease activity was monitored *via* the fluorescence upon GFP unfolding. As depicted in figure 24A, it can be concluded that compounds **CD3** to **CD7** display no ClpXP inhibition. Compounds **CD1** and **CD2** show inhibition with IC_{50} values around 35 μ M. Strong inhibition with IC_{50} values of 0.7 μ M to 3.0 μ M emerge in compounds **CD8** to **CD11**. **AV335** and **AV339** were included as positive controls and showed IC_{50} values between 0.9 μ M and 3.0 μ M.

A possible mechanism for ClpXP inhibition could be the disruption of the protease complex. Therefore, a protease assay with an inactive ClpP mutant, S98A, was performed. In this case, fluorescence is only detected, if the complex is intact and GFP is unfolded (Figure 24B).

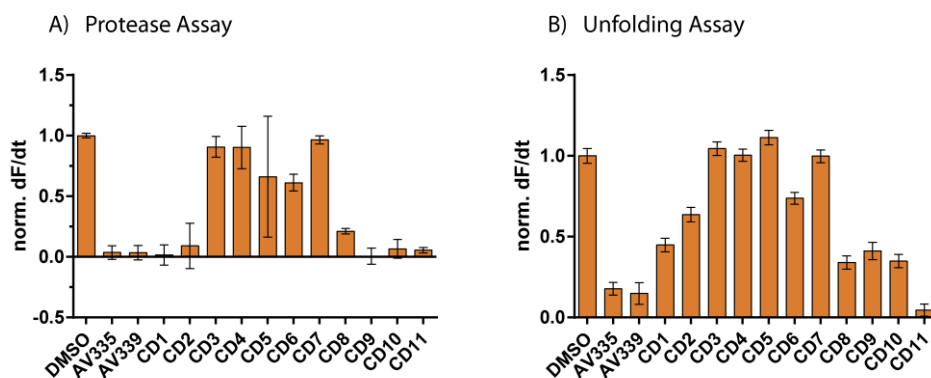


Figure 24. A) Protease activity assay and B) GFP-unfolding assay using SsrA-tagged GFP as substrate. For B) an inactive ClpP mutant (S98A) was used. All values were normalized to the DMSO control, which shows full protease and unfolding activity. Compounds were tested at concentrations of 100 μ M.

The results of the GFP unfolding assay for compounds **CD3** to **CD7** confirm the protease assay results, since no disruption of the complex was detected. For **AV335**, **AV336** and **CD11**, a disorder of the complex is likely, but for all other compounds (**CD1-2**, **CD8-10**) the assay did not give a clear result. For these compounds, fluorescence is around half as high as with the negative control, which might be a hint to complex disruption. Only the inhibited

protease activity can be reliably concluded and the suspected reason could be a disrupted ClpXP complex, but it cannot be confirmed.

2.2.2. Peptidase and ATPase Assay

Since it is not clear if the whole ClpXP complex is disrupted or if only one of the two proteins is inhibited, this needed to be examined. To get further information about the inhibited protein, peptidase and ATPase assays were performed to check for inhibition of ClpP and ClpX respectively.

For validation of the peptidase activity of ClpP, AMC substrate was used for detection *via* fluorescence. **AV170**, a phenyl ester that is known to inhibit ClpP activity,^[113] was used as a positive control at a final concentration of 1 μ M. All other compounds were tested at a concentration of 100 μ M (Figure 25A). Almost no compound shows inhibition on peptidase activity, apart from **CD11**, which shows a similar effect as the positive control.

To investigate ClpX activity, two different ATPase assays were performed. The first assay was an enzyme coupled assay, where the readout of ATPase activity was performed indirectly over NADH/H⁺.^[150] In the second assay, a malachite green assay, a complex that was directly formed with the ATP released phosphate was detected.^[149]

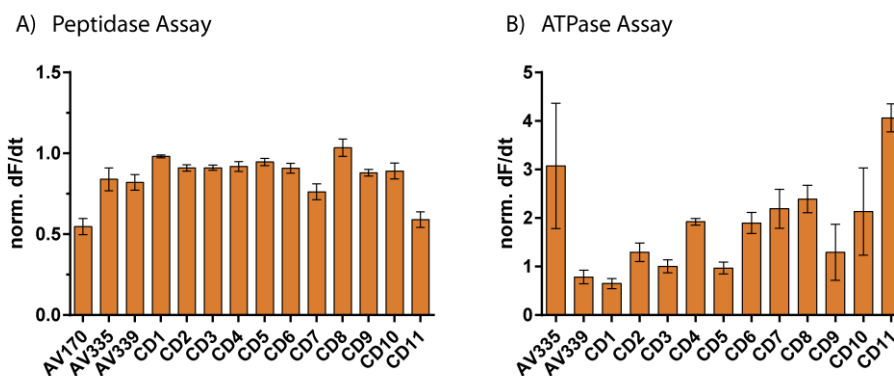


Figure 25. A) ClpP assay to check for peptidase inhibition upon treatment with the depicted compounds. Compounds were tested at 100 μ M, **AV170** was used as a positive control at a concentration of 1 μ M. All values were normalized to the DMSO control which was determined to an activity of one. B) ATPase assay, to check for the inhibition of ClpX. Compounds were tested at a concentration of 100 μ M. All values were normalized to the DMSO control which was determined to an activity of one. A+B) Activity was determined out of the initial slopes.

The enzyme coupled ATPase assay did not show any clear results (Figure 25B). Many of the compounds even seem to activate ClpX, especially **AV335** and **CD11**. It must be pointed out that in this assay a lot of enzymes are involved, increasing error probability. Therefore, a second assay, where the ATP released phosphate is directly detected, was performed. The malachite green assay showed around 30% and 50% inhibition of compounds **AV335** and

AV339 respectively (Appendix Figure A4). On the one hand, these results are more reliable due to the explained direct phosphate detection. On the other hand, these stand at least for compound **AV335** in direct contrast to the enzyme coupled ATPase assay. Therefore, the results cannot be considered definite or reliable.

2.2.3. FITC-Casein Assay

As the disruption of the complex might play a role as depicted above, it might be possible that the inhibitors bind to the same pockets, as activators do. ADEPs bind to hydrophobic pockets at the apical site of ClpP, which mimic the binding of ClpX, and thereby, activate ClpP.^[124,151] If this hydrophobic pocket would be occupied with inhibitor, ClpX would not be able to bind anymore and the complex would be disrupted. Furthermore, activation of the ClpP peptidase might be possible as well. Hence, a ClpP activity assay was performed using FITC-casein as substrate, where its degradation can be detected *via* fluorescence.

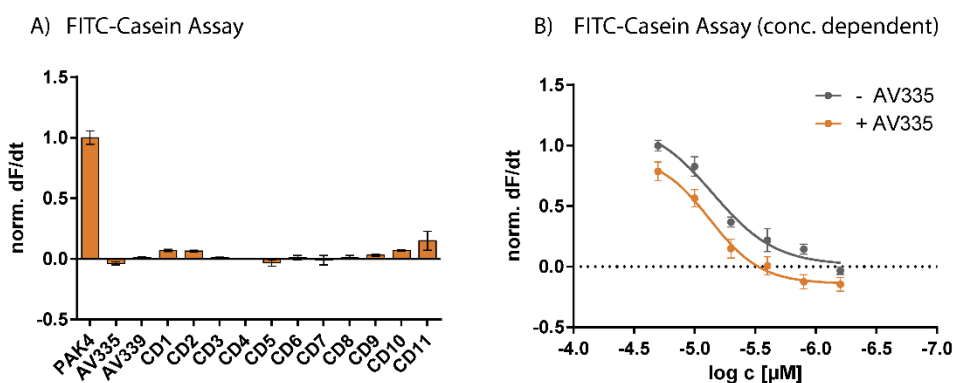


Figure 26. FITC-casein assay A) with different compounds at a concentration of 100 μM and B) concentration dependent with activator **PAK4** with and without inhibitor **AV335**.

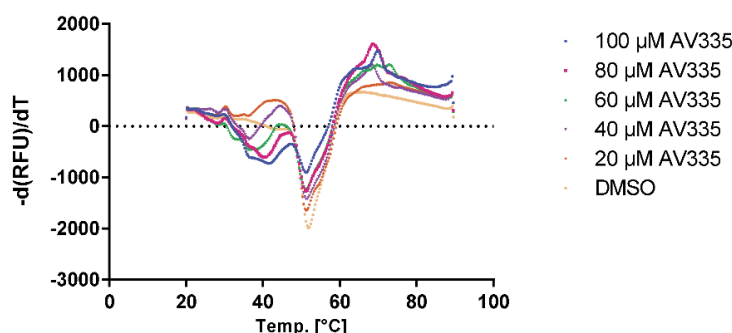
The ClpP activity assay revealed that none of the inhibitors have any activating effect on ClpP at a concentration of 100 μM. Here **PAK4**, an ADEP fragment which is known to activate ClpP, was used as a positive control (Figure 26A).^[138] An interaction of the inhibitor might still take place at the hydrophobic pockets, but without triggering activation. To check this, dose down experiments with **PAK4** in presence and absence of inhibitor **AV335** were performed. Once again, activity of ClpP was readout through a FITC-casein. A competition of inhibitors with **PAK4** would give a hint that both compounds interact with the same pocket. Looking at the concentration dependent FITC-casein assay, a slight shift can be seen upon **AV335** addition. This would fit with the positive result of the GFP unfolding assay, where a disruption of the complex is assumed.

2.2.4. Thermal Shift Assay

To further elucidate which protein is involved in the inhibition process, thermal shift assays (TSA) with both proteins, ClpP and ClpX, were performed. When interacting with a protein, a compound might have a stabilizing or destabilizing effect, which leads to a shift in the melting point of the protein and can be detected in this kind of assay.^[152] Therefore, the fluorescence of Sypro Orange is used as readout, which can be detected upon melting of the protein.^[153–155]

As illustrated in figure 27, no significant shifts of the melting point can be detected for the incubation of ClpP with AV335 and AV339 in comparison to the negative control DMSO. This leads to the assumption that no inhibitor-protein interaction occurs, or is at least not strong enough for affecting the proteins melting point. For melting curves with ClpX, no clear melting points could be determined with or without the addition of a compound.

A) Thermal Shift Assay with ClpP and AV335



B) Thermal Shift Assay with ClpP and AV339

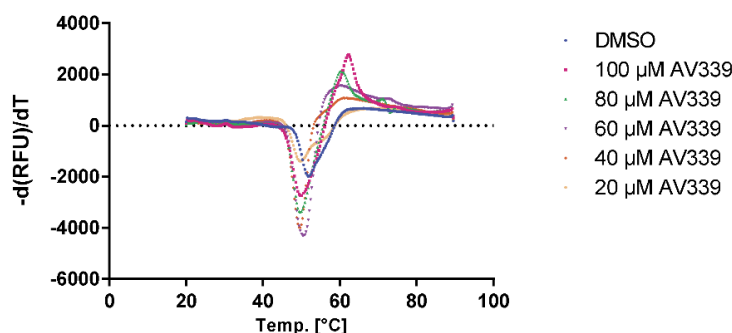


Figure 27. Thermal shift assays of ClpP with A) AV335 and B) AV339. Shown is the first derivative of the melting curve of the protein.

To sum up, TSAs did not help to reveal the inhibited protein. While the determination of the melting point of ClpX is problematic in general, ClpP did not show any shifts upon compound

treatment. This is a hint that the compound operates at the surface with only weak interactions, not affecting the melting point of ClpP.

2.2.5. Conclusion

To conclude, the inhibitors do not inhibit ClpP or ClpX on their own, neither in the peptidase assay nor in the ATPase assay. Moreover, the thermal shift assay did not give a clear hint for one solely inhibited protein. It is clear that some of the compounds (**AV335**, **339**, **CD1-2**, **CD8-11**) do inhibit the ClpXP complex. Although the mechanism is not elucidated yet, the disruption of the complex might play a role as indicated with the GFP unfolding assay.

2.3. Consequences for *S. aureus* phenotype and its proteomic level

It is well known that the inhibition of the ClpXP complex leads to a decrease in *S. aureus* virulence.^[149] As described before, compounds **AV335**, **AV339** and **CD8** to **CD11** show inhibition of ClpXP in a proteolytic assay. An alternative approach is to investigate their effects on the phenotype and on a proteomic level. For this, a hemolysis assay as well as a secretome analysis were performed.

2.3.1. Hemolysis Assay

To find out whether hemolysin production of *S. aureus* is down-regulated upon compound treatment, a blood agar hemolysis assay was performed. Compounds and bacterial suspension were placed onto defined slices of filter paper on the blood agar plates and **AV334**^[149] was utilized as a positive control (Figure 28). A reduction in hemolysin production of *S. aureus* can be observed when the blood on the agar plates is not affected and therefore no white area is visible around the filter paper.

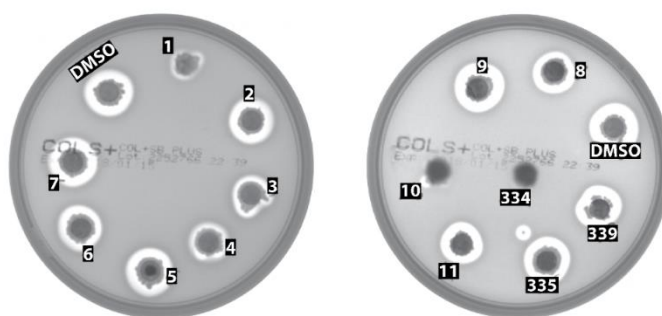


Figure 28. Hemolysis assay on blood agar plates. Compounds (100 mM stocks of **CD1** to **CD11**, **AV334** and **AV339** in DMSO, or DMSO) and bacterial suspension (*S. aureus*) was given on a filter paper on the agar plate. DMSO was used as negative, **AV334** as positive control. After 20 h at 37 °C the effect was be detected. The light area around the spots represents hemolytic activity.

As depicted in figure 28, most compounds did not inhibit *S. aureus* hemolysis production. Nevertheless, bacteria treated with **CD10** showed almost no hemolytic activity, comparable to the positive control with **AV334**. In contrast to the DMSO control, in the case of **CD1**, a really narrow white area can be observed around the bacteria. While **CD3** and **CD4** show medium activity, all other compounds show, like DMSO controls, no effect on hemolytic activity of *S. aureus*. With compounds **CD1** and **CD10** being the most promising regarding this assay, they were chosen for further secretome analysis experiments.

2.3.2. Secretome analysis

To clarify the phenotypic effect of compounds **CD1** and **CD10**, a secretome analysis of *S. aureus* NCTC8325 cells was performed. Cultures were grown with the respective compound at a concentration of 50 μ M for 20 h at 37 °C and were sterile filtered afterwards. The secretome was prepared for label free quantification and analyzed *via* MS/MS. Resulting volcano plots are shown in figure 29.

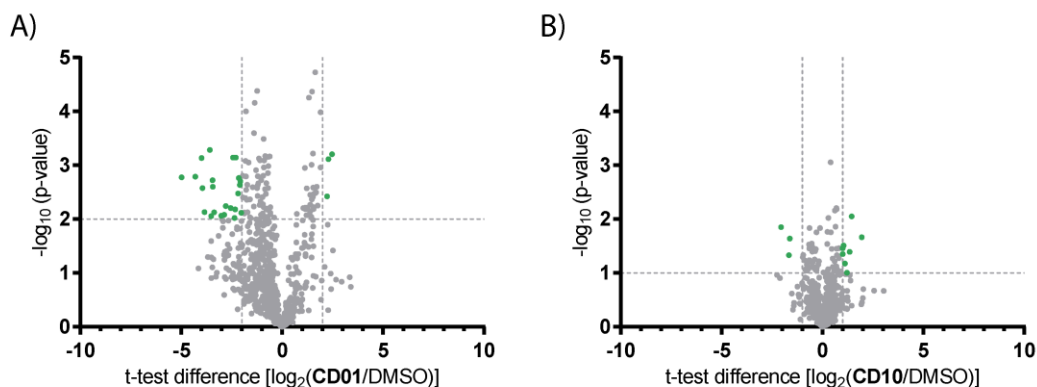


Figure 29. Secretome analysis of *S. aureus* with compounds A) **CD1** and B) **CD10** was performed in three biological replicates. Most regulated proteins are marked and sorted in decreasing t-test difference order (Appendix Table A4, 5). A) Cut off lines were set at a minimum \log_2 fold-change of 2 for and at a minimum $-\log_{10}$ (p-value) of 2. B) Due to the few protein regulation, cut off lines were set at a minimum \log_2 fold-change of 1 for and at a minimum $-\log_{10}$ (p-value) of 1.

In the volcano plot of compound **CD1**, a global down-regulation of proteins can be observed (Figure 29A). A closer look reveals that no major virulence factors e.g. Hla are present. Looking at the up-regulated section, two interesting proteins, surface protein G (SasG) and ESAT-6 secretion accessory factor EsaA, are found. Whereas SasG promotes adhesion of bacterial cells and cellular aggregation leading to biofilm formation,^[156,157] accessory factor EsaA is a virulence factor associated with pathogenesis and persistence in host tissues.^[158] This even indicates a more virulent pathogenic behaviour than without the treatment of **CD1**.

For compound **CD10** not many proteins are up- or down-regulated and are shown in the respective volcano plot (Figure 29B). One protein, truncated MHC class II analog protein is involved in pathogenesis,^[159] which unexpectedly is up-regulated. Regarding the two component regulation systems, this can either be a hint towards a down-regulation of another pathway or just the fact that **CD10** in this case has no visible effect on virulence.

Altogether one can say that almost no virulence or biofilm regulating proteins are up- or down-regulated, concluding that both compounds, **CD1** and **CD10**, failed the goal of ClpXP inhibition, the down-regulation of virulence. At least for compound **CD1** this result is in accordance with the hemolysis assay performed before (Chapter 2.3.1.). Since the result of the

hemolysis assay looked promising for **CD10**, it is not clear why the same result cannot be observed on a proteomic level. In comparison to compound **CD1** few proteins are regulated upon **CD10** treatment in general. It needs to be kept in mind that the hemolysis assay was performed with high compound concentrations of 100 mM. The exact concentration cannot be determined since it is given onto a filter paper in an agar plate, but it is clear that the secretome analysis was performed in a far lower range, 50 μ M in particular, which might be the reason for the opposing results. Although it might help to perform experiments with a higher compound concentration, this will not improve the compounds effect in general.

2.4. Conclusion

Several assays have been performed to reveal the mechanism of the ClpXP inhibition of compounds **AV334**, **AV339** and **CD1** to **CD11**, but it could not be fully elucidated. Some hints from the ATPase and the GFP unfolding assay point towards an inhibition of ClpX or an inhibition of the interaction of the two proteins respectively. The dose down FITC-casein assay, however, points towards an interaction with ClpP, which could take place at the surface of ClpP. This in turn might be a hint to the disruption of the complex. Unfortunately, none of these hints could be confirmed by other assays. Furthermore, the hemolysis assay determined to have an anti-hemolytic effect only in bacteria treated with **CD10** and slightly also **CD1**. These compounds were further tested in a secretome analysis, where no up- or down-regulations of important virulence factors could be observed. Another step could be to investigate the whole proteome or experiments could be repeated with far higher concentrations. However, this would not improve the effect of the compound itself.

3. Synthesis and Activity of ADEP Fragments and Derivatives

ADEPs activate ClpP and thereby have an antibacterial effect on *S. aureus*. To find ADEPs targets and off-targets and demonstrate labeling in inactive mutants, an appropriate photoprobe is needed for A/BPP experiments. First, ADEP fragments were generated to find beneficial positions for the introduction of a photoreactive group and an alkyne handle. Then a fragment photoprobe, as well as two ADEP photoprobes were designed and synthesized.

3.1. Overview and Synthesis of ADEP fragments

To figure out the best position for the introduction of the alkyne and the photoreactive moiety, an arylazide or a diazirine, several ADEP fragments were synthesized. As mentioned before, ADEP photoprobe **ADEP7-p** was not able to activate ClpP anymore (Figure 19). Since in this scaffold, the only alteration was made at the side chain, it is probably not available for modifications. Changes that could lead to deteriorated binding are the missing double bond, the length of the side chain, the additional alkyne and of course the additional diazirine moiety. These modifications should be addressed by the comparison of some known and also new designed ADEP fragments (Figure 30).

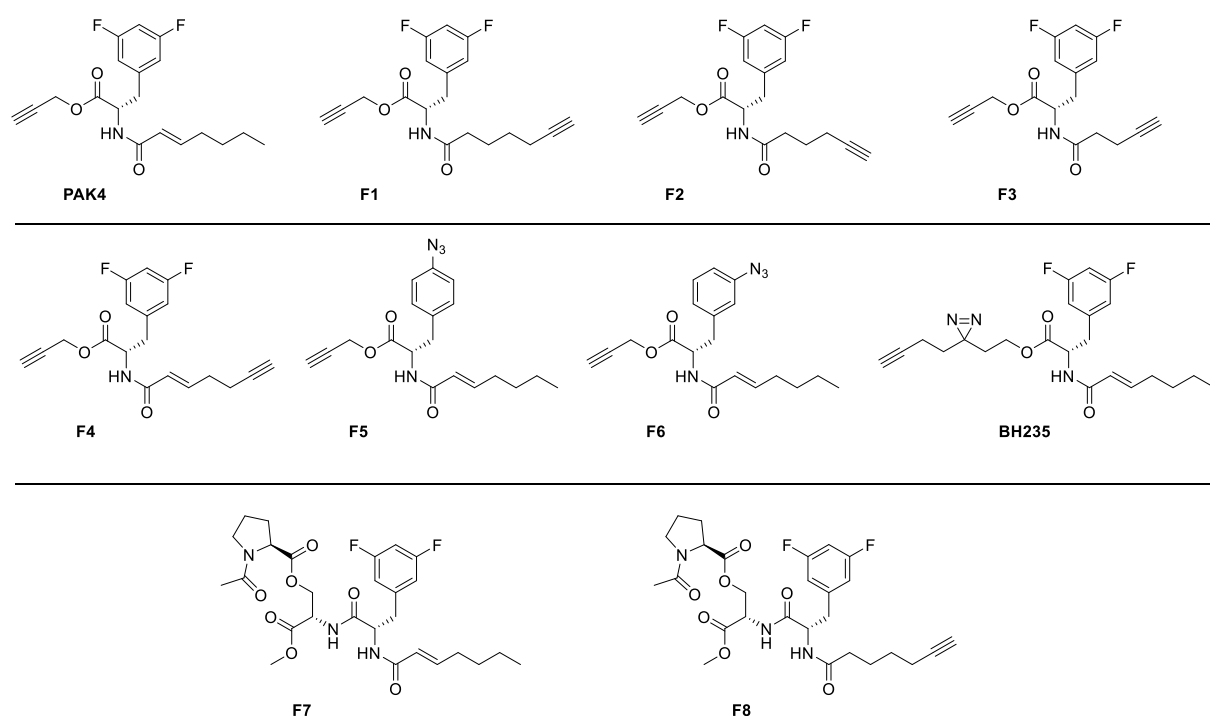
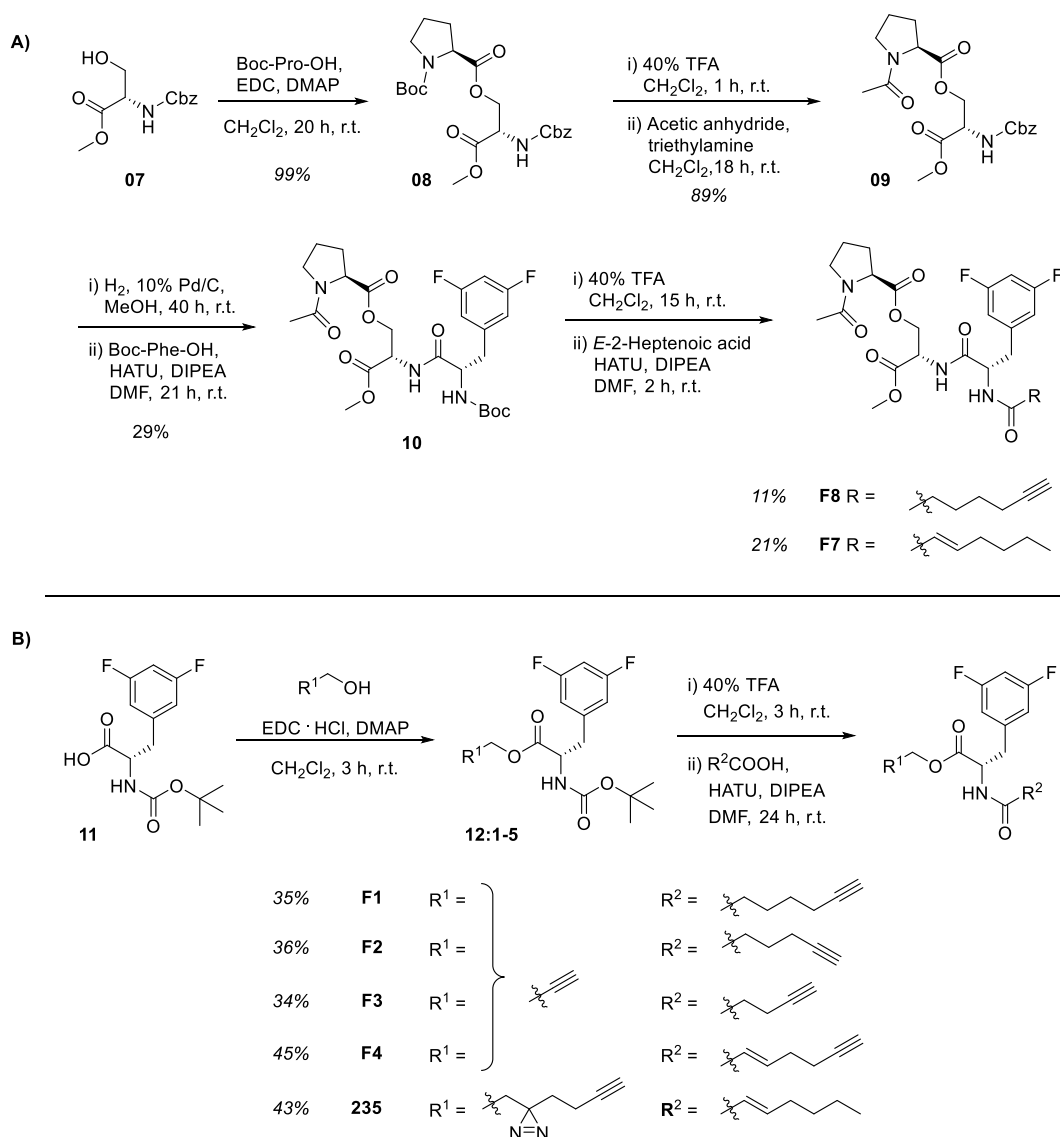


Figure 30. Overview of synthesized ADEP fragments. **PAK4** and **F7** were first synthesized by *Carney et al.* in 2014.^[138]

Literature known compounds **PAK4** and **F7** were chosen for comparison. While **PAK4** is a real minimal fragment, **F7** represents a bigger fragment.^[138] Fragment **F8**, based on **F7** was

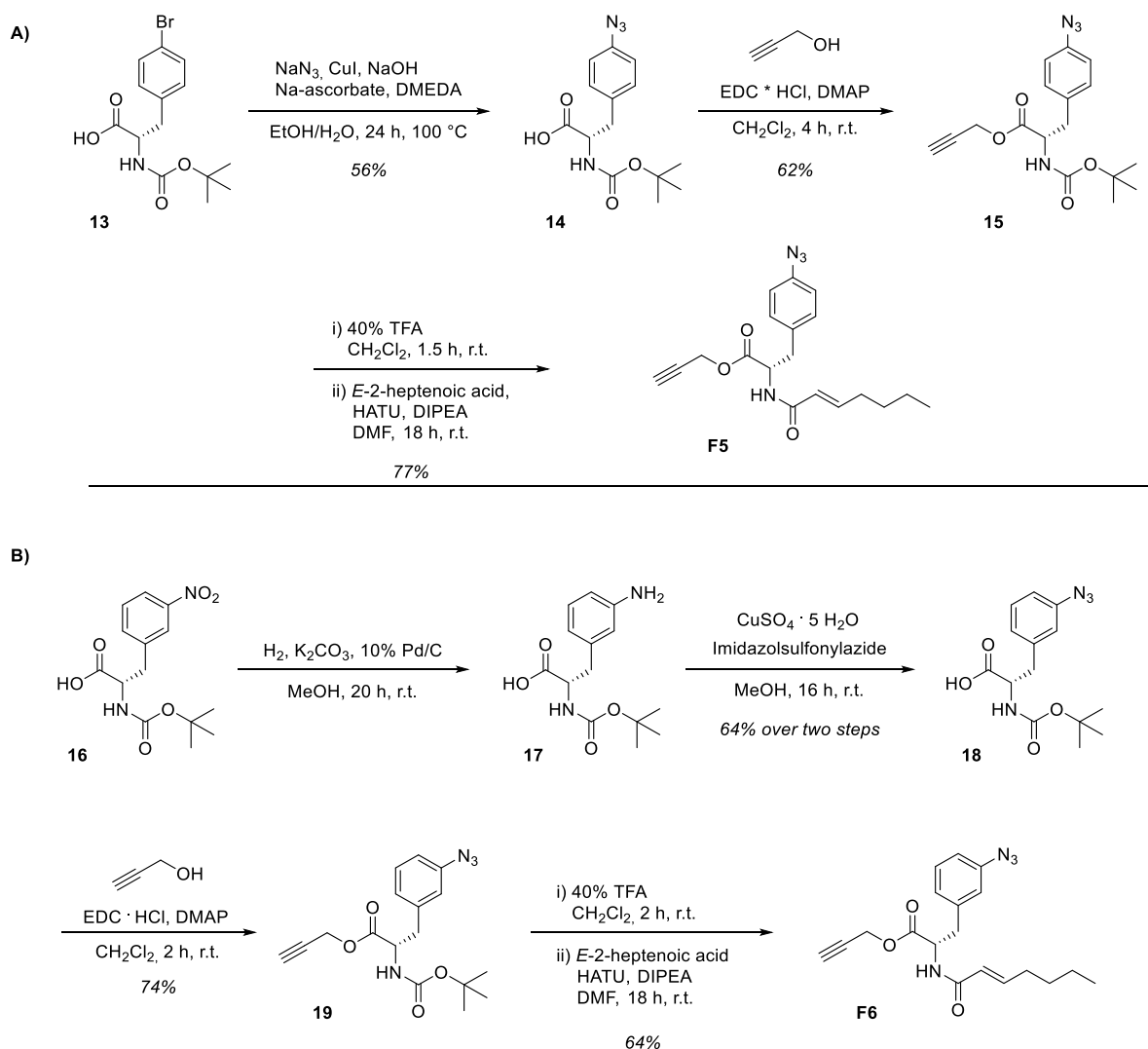
designed to show if the additional alkyne and the missing double bond constitute a problem. The length of the side chain, equipped with a terminal alkyne, was investigated with fragments **F1**, **F2** and **F3**. To further elucidate if the double bond is truly required for activity, fragment **F4** was designed, so that a direct comparison to compound **F1** was possible. Equipped with the double bond and an additional alkyne, they only differ in the double bond. A new position for the photoreactive moiety was found by the introduction of an arylazide at the phenylalanine, instead of the diazirine in the side chain. Both scaffolds with azide moieties in *para*- and *meta*-positions were designed for testing (**F5**, **F6**). An additional fragment, a small fragment ADEP photoprobe **BH235**, equipped with a diazirine moiety, was synthesized to have a small selection of probes (Figure 30).



Scheme 3. Synthetic routes for ADEP fragments A) **F7** and **F8** and B) fragments **F1**, **F2**, **F3**, **F4** and **BH235**.

Most of the fragments, **F1** to **F4** and **BH235**, were easily accessible *via* esterification followed by Boc-deprotection and amide coupling, as described by *Carney et al.* in 2014 (Scheme 3B).^[138] Reactions yielded between 34% and 45% of the respective product after three steps. Two bigger fragments, **F7** and **F8**, were synthesized *via* a four step synthetic route (Scheme 3A). Here, esterification as well as Boc-deprotection and following amidation worked with very good yields between 89% and 99%. Final steps gave moderate yields between 11% and 29%.^[138]

Aryl azides **F5** and **F6** were prepared starting from Boc-protected phenylalanine with bromide in *para*- and nitro group in *meta*-position, respectively. The introduction of an azide yielded in two possible photoprobes (Scheme 4). The azide in *para*-position was introduced according to a patent from 2014,^[160] the azide in *meta*-position was built up using imidazolsulfonylazide, which was synthesized beforehand.^[161,162] Yields in all reactions were moderate to good between 56% and 77%.



Having several ADEP fragments in hand, the next step was the evaluation of their activity, which will be described in the following chapter.

3.2. Activity of ADEP fragments

All of the known or new designed fragments were tested for their proteolytic activity on ClpP *via* monitoring of FITC-casein degradation. DMSO was used as a negative control, 20 μ M **PAK4** as a positive control. The activity of **PAK4** was defined as 100% and all other values were normalized to that. All compounds were tested at a concentration of 20 μ M (Figure 31).

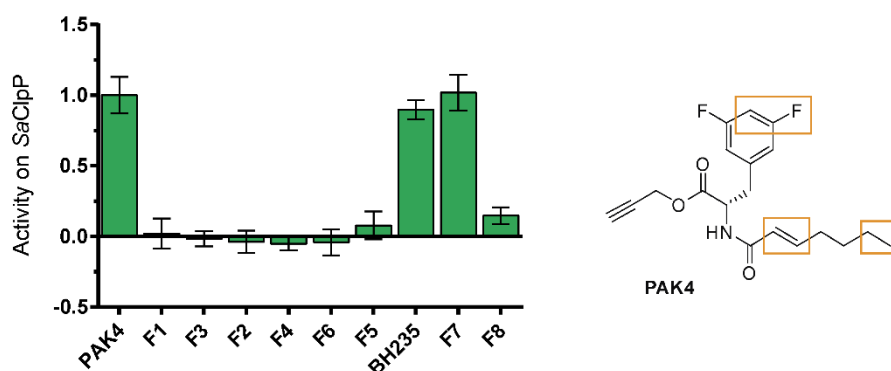


Figure 31. Results of a FITC-casein assay on the left and the structure of **PAK4** on the right with crucial structure elements that were addressed with fragment derivatives marked in orange. FITC-casein degradation was detected *via* fluorescence and all measurements were carried out in triplicates. Initial slopes over time were evaluated by a linear regression model.

As shown in figure 31, the known ADEP fragments **PAK4** and **F7** activate *SaClpP* as expected. The slight changes in the length of the side chain, represented by compounds **F1**, **F2** and **F3**, lead to a complete loss of activation. The same issue is observed with compound **F4**, which only differs in the additional alkyne to the known **PAK4** fragment. Furthermore, an aryl azide leads to the loss of activity as well, no matter if introduced in *para*- or in *meta*-position, shown with compounds **F5** and **F6** respectively. Comparison of **F7** and **F8** demonstrates the deteriorating effect of the additional alkyne on ClpP activation even with bigger fragments. These information serve well as restriction rule for the development of a whole ADEP derivative photo-probe. However, an active fragment-photoprobe **BH235** was synthesized by coupling a minimalist photocrosslinker to the western part of the **PAK4** molecule.

Regarding the results of the FITC-casein assay, modifications on the ADEP side chain are not feasible without diminution of activation ability. The missing alkene is no more accepted than the alkyne or the aryl azides, no matter in what position. This is the reason for the alkyne and the photoreactive group being integrated into the main ring of the ADEP. For the alkyne, a

propargylglycine was easily introduced instead of the alanine as a first trial. Two different approaches were followed for the introduction of the photoreactive group, a diazirine in this case.

The diazirine moiety shall be introduced within a photoproline. Since the ADEP core structure bears two prolines, which are referred to as northern and southern due to their positions, there are two possible sites for modification.

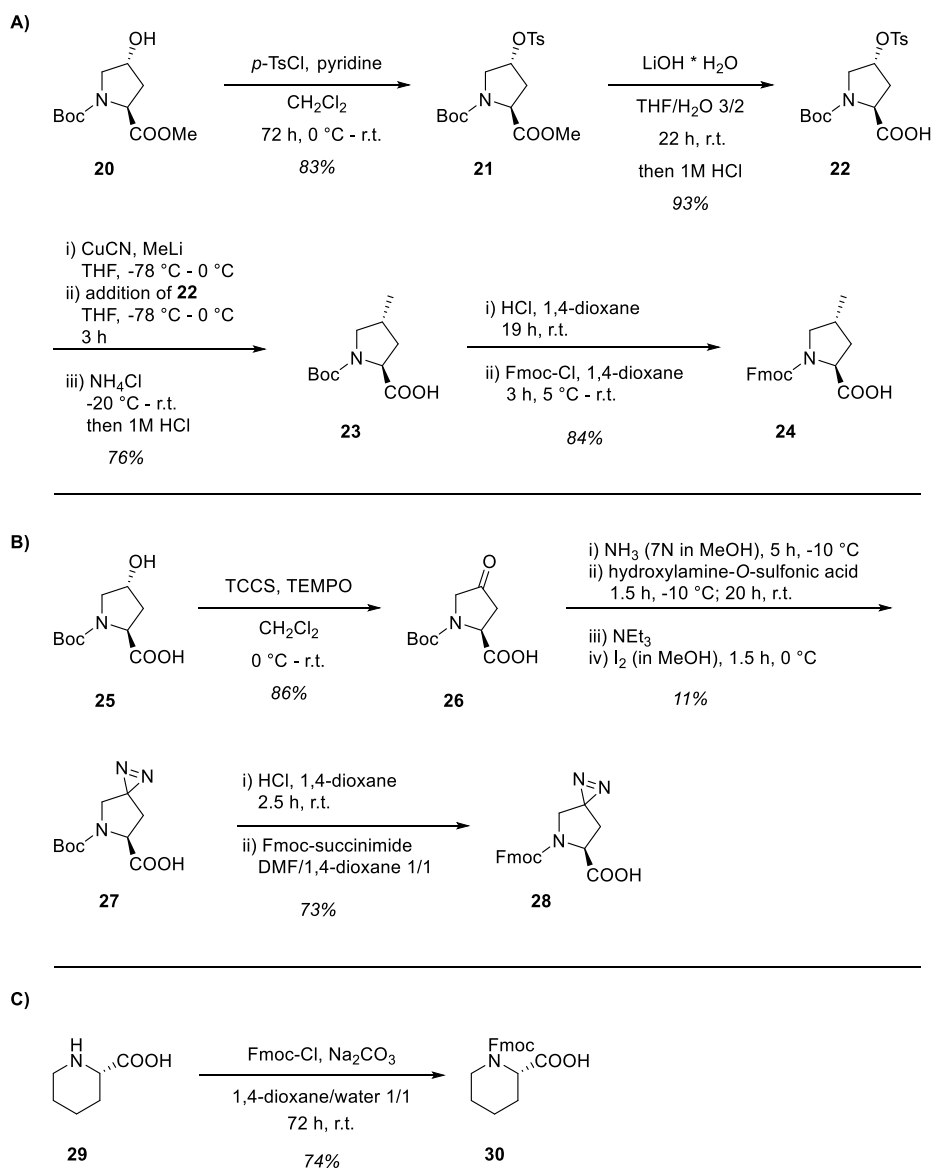
On the one hand, the aim is of course to maintain ADEP activation and therefore to make modifications where they will not affect the binding pocket. Since it is not directly interacting with the protein, the southern proline poses the perfect position. The drawback here is that during ADEPs' binding to ClpP, this proline seems to be mostly solvent exposed. This might become a problem, since the photoreactive group needs to crosslink with the protein.

On the other hand, the photoreactive group should be close to the protein, to be able to crosslink with the protein surface upon irradiation. Although it is known that the methyl group on the northern proline contributes to the activity of ADEPs,^[94,120] we attempted to incorporate the diazirine also in this position. With these two strategies, all contingencies were covered.

3.3. Solid-phase ADEP and ADEP-probes synthesis

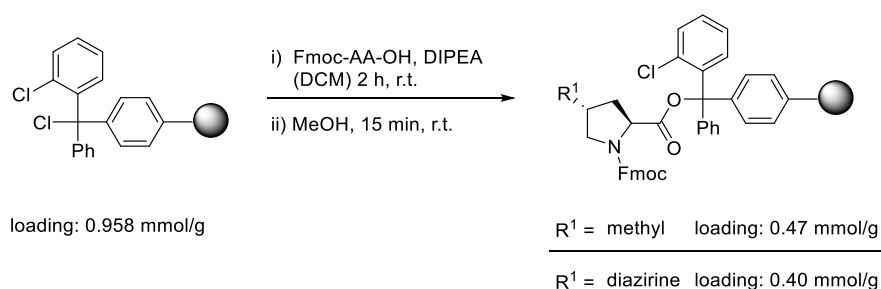
As mentioned in the introductory part, ADEPs can be synthesized *via* two main synthetic routes, solution phase chemistry and solid phase peptide synthesis (SPPS). Since SPPS seems to be more efficient and also simple to carry out, it was selected for further synthesis. Using this strategy, the cyclization of a synthesized heptapeptide was performed with a lactonization method.^[143]

Most of the Fmoc-protected amino acids were commercially available others were synthesized within this work. Methylated proline (**24**) and photoproline (**28**) were synthesized starting from hydroxylproline derivatives (**20**, **25**) and pipercolic acid (**29**) was Fmoc-protected (Scheme 5).



Scheme 5. Synthetic route of Fmoc-protected amino acid derivatives A) methylproline **24**, B) photoproline **28** and C) pipercolic acid **30**.

The synthesis of methylproline **24** was performed *via* a literature-known three-step synthetic route and is shown in Scheme 5.^[143] After tosylation of the acid- and amino-protected hydroxylproline (**20**), the methylester was reduced by LiOH and methylation was performed using *Gilman* reagent.^[163–165] Final steps were the deprotection of the Boc-group and the protection with Fmoc-chloride. All reactions worked with good yields between 76% and 93%. Photoproline **28** was synthesized according to *Robinson* and coworkers,^[166] only the oxidation step was carried out using TEMPO instead of *Jones reagent*. Whereas the introduction of the diazirine only showed a low yield of 11%, the other reactions worked well with yields of 86% and 73%.



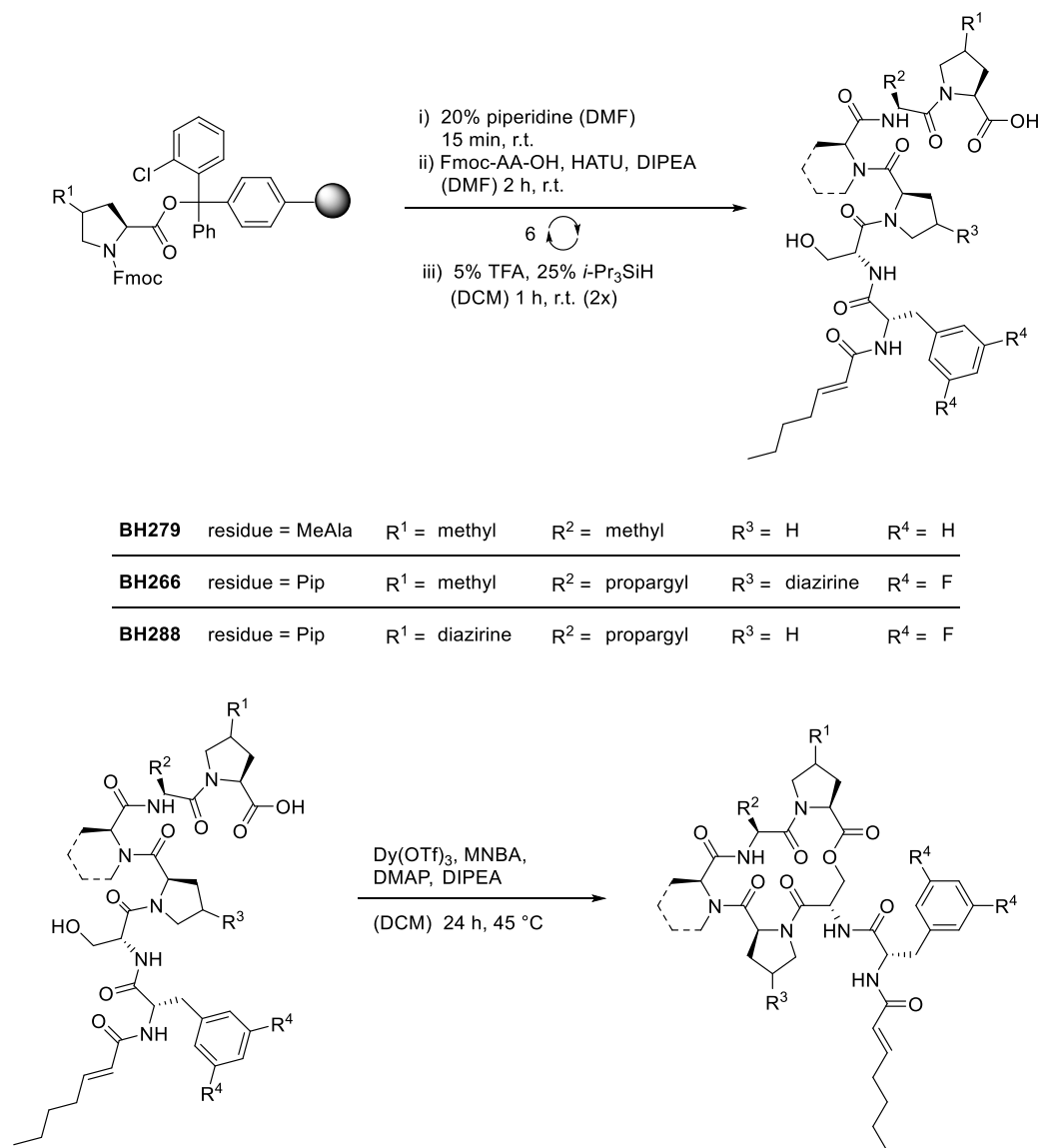
Scheme 6. Loading of the resin with either methylproline (**24**) or photoproline (**28**).

After the successful synthesis of all required amino acid derivatives, solid phase peptide chemistry was performed to generate the desired heptapeptide. The first amino acid was loaded onto the resin, followed by the coupling of five further amino acids and heptenoic acid. An overview of the used amino acids for different ADEP derivatives is shown in Table 1.

Table 1. Amino acid sequence for different ADEP derivatives. 2-*E*-heptenoic acid is abbreviated with acid.

ADEP derivative	AA linked to resin	AA in coupling order
BH279	Pro	Ala; Me-Ala; Pro; Ser; Phe; acid
BH266	Me-Pro (24)	Pra; Pip(30); Photo-Pro; Ser; F ₂ Phe; acid
BH288	Photo-Pro (28)	Pra; Pip(30); Pro; Ser; F ₂ Phe; acid

After the coupling, the obtained heptapeptide was directly used for the last step, the cyclization, which was performed according to the method of *Goodreid et al.*, published in 2015.^[143] The formation of the lactone was achieved with MNBA, DMAP, DIPEA and a lanthanide (III) triflate catalyst, Dy(OTf)₃. The cyclization was performed over 24 hours, by slowly adding heptapeptide to the reaction mixture (Scheme 7).



Scheme 7. Solid-phase peptide synthesis and cyclization of corresponding seco acids to build up ADEP derivatives.

Whereas the SPPS of **BH266** and **BH279** worked fine and had very good yields, the synthesis for **BH288** was challenging. Although comparable loadings were achieved, the reason for the tricky synthesis might be the photoproline, which in this case is directly linked to the resin. Incomplete coupling is improbable to be the reason since all couplings were controlled for completeness. The diazirine moiety might somehow get damaged due to its close proximity to the resin or during further coupling steps, which is rather unlikely since synthesis worked fine for probe **BH266**. Most cyclization reactions only worked with low yields. The identity of the synthesized derivatives was confirmed by HR-LC-MS. Having ADEP photoprobes in hand, their bioactivity will be discussed in the following.

3.4. Activity of ADEP derivatives

ADEP derivatives were tested for their proteolytic activity on ClpP, in the same manner as ADEP fragments before (Chapter 3.2.). Degradation of FITC-casein was monitored *via* fluorescence readout and thereof the activity was calculated.

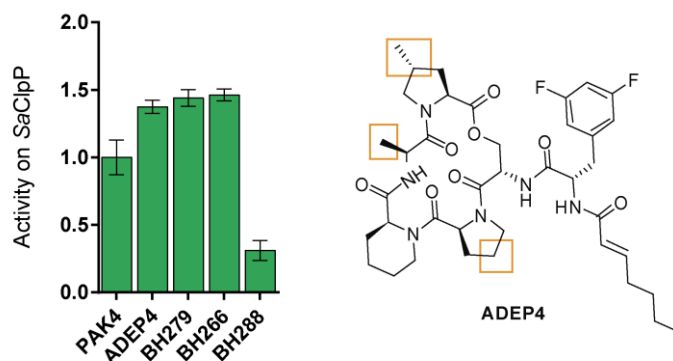


Figure 32. Left: Results of FITC-casein assay. Right: Structure of ADEP4 with critical structure elements marked in orange, which were addressed with synthesized derivatives. For better comparability, the activity of 20 μM **PAK4** was used as positive control and its activity defined as 100%. FITC-casein degradation was detected *via* fluorescence and all measurements were carried out in triplicates. Initial slopes over time were evaluated by a linear regression model.

ADEP derivatives **BH279** and **BH266** show comparable activation of *SaClpP* in comparison to the optimized ADEP4. **BH288** also activates ClpP, but to a far lower extent. It only shows about 25% of the other ADEPs' activity. One could argue that the diazirine on the northern proline, which is in the position of the methyl group in comparison to **BH266**, is a too major alteration. This was already a point when first designing the photoprobes and can clearly be seen in a crystal structure, which will be discussed further (Chapter 3.6.).^[167] As depicted in figure 32 compounds **BH266**, **BH279** and ADEP4 look like they would all activate ClpP equally. To get further information about the compounds activation ability, the experiment was performed with lower concentrations (Figure 33). As expected, the optimized compound, ADEP4, has the greatest effect and still activates ClpP at a concentration of 1 μM . **BH279** and **BH266** show no activation at 1 μM but still fully activate ClpP at 10 μM .

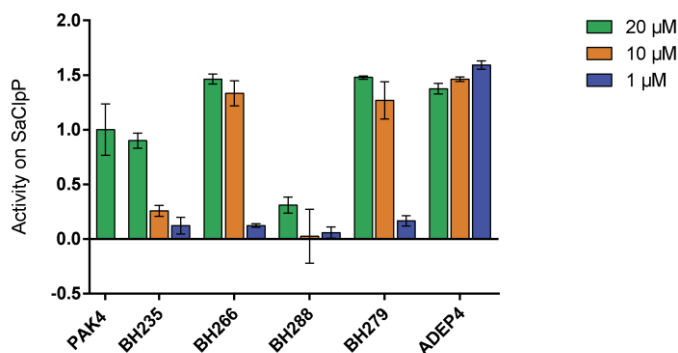


Figure 33. Results of FITC-casein assay with different concentrations. For better comparability, the activity of 20 μM **PAK4** was used as positive control and its activity defined as 100%. FITC-casein degradation was detected *via* fluorescence and all measurements were carried out in triplicates. Initial slopes over time were evaluated by a linear regression model.

3.5. MIC values in *S. aureus*

Selected compounds were chosen for MIC assays, where the minimal inhibitory concentration that is required for fully inhibiting growth of bacteria, was determined.

Table 2. Overview of MIC values of several ADEP fragments and derivatives.

Compound	MIC value \pm error		FITC-casein activity	Compound concentration
ADEP4	< 15 nM		150%	< 1 μ M
PAK4	20.0 μ M	\pm 6.12 μ M	100%	20 μ M
BH235	> 500 μ M		90%	20 μ M
BH279	4.35 μ M	\pm 2.33 μ M	150%	10 μ M
BH266	3.09 μ M	\pm 0.06 μ M	150%	10 μ M
BH288	> 50 μ M		30%	20 μ M

As expected, the optimized ADEP4 shows the lowest MIC value of <15 nM. The minor structural change of photoprobe **BH266** is already enough to lower the effect seriously to 3.09 μ M. Although the diazirine is largely solvent exposed, the additional alkyne must influence ClpP binding strongly. An even more drastic effect is observed with the diazirine in the **BH288** derivative. No MIC was detected for this compound up to 50 μ M. A similar effect can be observed looking at the values of **PAK4** and its corresponding photoprobe **BH235**. Whereas **PAK4** shows a MIC value of around 20 μ M, the modified compound has a MIC value of over 500 μ M (Table 2).

3.6. Modeling Analysis

Regarding the differences of MIC values and ClpP activation, the two ADEP-probes and their binding into the hydrophobic pocket will be described further. Looking at published crystal structures of ADEPs and ClpP, one can already see the problem of probe **BH288**. In probe **BH266** the diazirine is mainly solvent exposed, which is shown in white circles in figure 34 and probably leads to a weak cross-linking efficiency. The diazirine in probe **BH288** might clash with the protein surface, which is shown in the blue circles in figure 34. Since a drastic reduction in ClpP activation can be observed with **BH288**, the diazirine in the northern proline position must be the cause for that. This is further confirmed by the high MIC value of **BH288**. Still, these results were expected while designing the probes. However, the advantage of probe **BH288** is its better labeling capability.

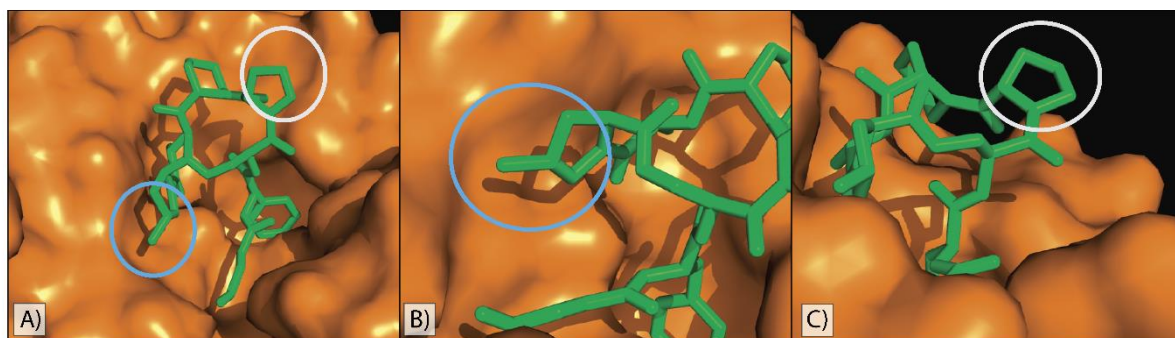


Figure 34. An ADEP derivative bound to ClpP is shown (PDB: 5vz2). ADEP is shown in stick representation and ClpP is illustrated as surface. The positions where the diazirine moiety was introduced, northern and southern proline, are marked with a blue and white circle, respectively. Different views on an ADEP derivative bound to ClpP are illustrated. In A) both proline residues are visible, in B) the northern and in C) the southern proline are focused.

4. AfBPP with synthesized ADEP photoprobes

4.1. Gel-based labeling

4.1.1. Labeling of recombinant SaClpP and in *S. aureus* lysate

After confirming the photoprobes activation on ClpP and the determination of their MIC values, labeling of recombinant protein was performed as a proof-of-concept. To elucidate if the probes are able to label ClpP, they were incubated together for an hour and irradiated with UV light for 14 min. A fluorescence tag was added *via* click chemistry and the readout was performed by SDS-PAGE (Figure 35).

In general, most experiments were first or exclusively performed with ADEP fragment probe **BH235**, due to its easy synthetic accessibility.

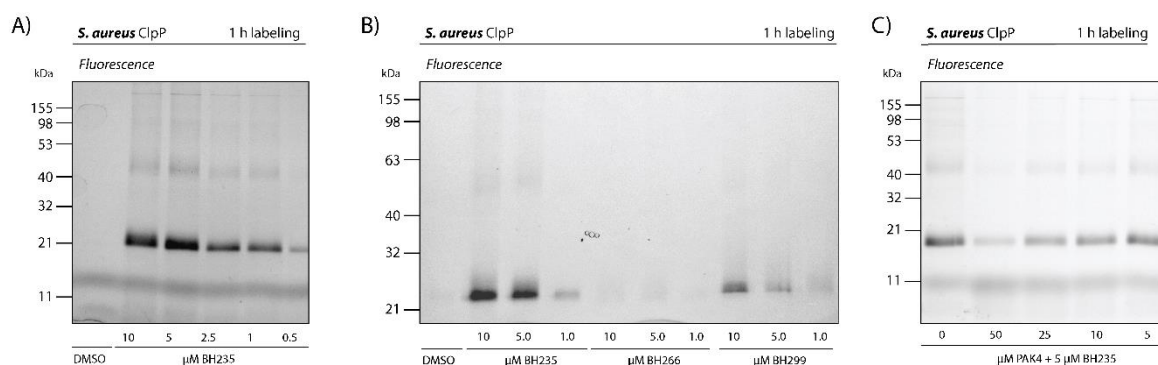


Figure 35. Gels of labeling experiments with recombinant ClpP. Gel A) shows concentration dependent labeling with compound **BH235**, gel B) the comparison of the different photoprobes **BH235**, **BH266** and **BH288** and gel C) a competition experiment with **BH235** and **PAK4** as competitor.

In figure 35, labeling experiments with recombinant ClpP are shown with different photoprobes and a competition experiment. The first step was to test if the probes are able to label ClpP at all. Satisfyingly, labeling with **BH235** could be shown in a concentration dependent manner from 10 μM to 0.5 μM (Figure 35A). Hence, the two more valuable ADEP photoprobes were tested as well. While photoprobe **BH266** only showed really weak labeling, the labeling of probe **BH288** was comparable to **BH235** (Figure 35B). A competition experiment was performed at a constant concentration of 5 μM of photoprobe **BH235** and a varying concentration of **PAK4** as competitor (Figure 35C). Both compounds were added to ClpP at the same time and show competitive effects. Best results were obtained with the highest competitor concentration tested, which corresponds to 100 times probe concentration. Further, labeling nicely shows a concentration dependent behaviour again.

To further approach the labeling in a cellular context, the next step was to move into bacteria. *S. aureus* were cultured until they reached an OD₆₀₀ between 5.5 and 6.5. After lysis they were incubated with the respective probe for one hour, irradiated with UV light and again a fluorescence tag was added *via* click chemistry. As for the recombinant protein, competition experiments were performed as well.

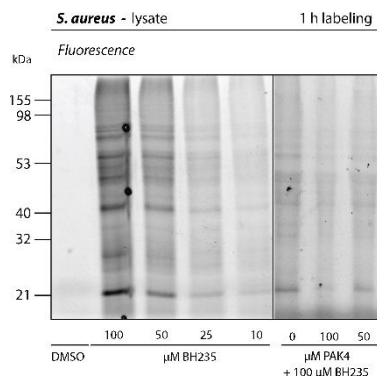


Figure 36. Labeling with fragment photoprobe **BH235** in *S. aureus* lysate and competition experiments with **PAK4**.

As already illustrated for the labeling of recombinant ClpP, concentration dependent labeling was shown in *S. aureus* lysate with probe **BH235** (Figure 36). While there is one strong band at the height of 21 kDa, which is likely to represent ClpP, there are further bands especially in the range of 40 kDa to 80 kDa. One must say that the whole labeling pattern is getting weaker with decreasing concentration, but is still visible at a concentration of 10 μM (Figure 36). For the competition experiment, **PAK4** was used in the same concentration as the photoprobe and still showed competitive effects (Figure 36).

4.1.2. *In situ* labeling in *S. aureus*

Since labeling in *S. aureus* lysate worked well, labeling of ClpP in intact *S. aureus* cells was tested next. For this, bacteria were grown until they reached stationary phase. After harvesting and washing, labeling was performed at $OD_{600} = 40$ in PBS. After irradiation with UV light at 365 nm for 14 min, lysis and click chemistry, readout was performed by SDS-PAGE.

As shown in the soluble and insoluble fraction in figure 37A and B respectively, a concentration dependent labeling with fragment photoprobe **BH235** was possible *in situ*. The band at around 21 kDa appears to be stronger in the membrane or insoluble fraction than in the soluble fraction. Whereas in the soluble fraction a clear band is only visible down to a concentration of 50 μ M, the insoluble fraction still illustrates strong labeling at 10 μ M. Regarding this, some experiments were only performed in the insoluble fraction.

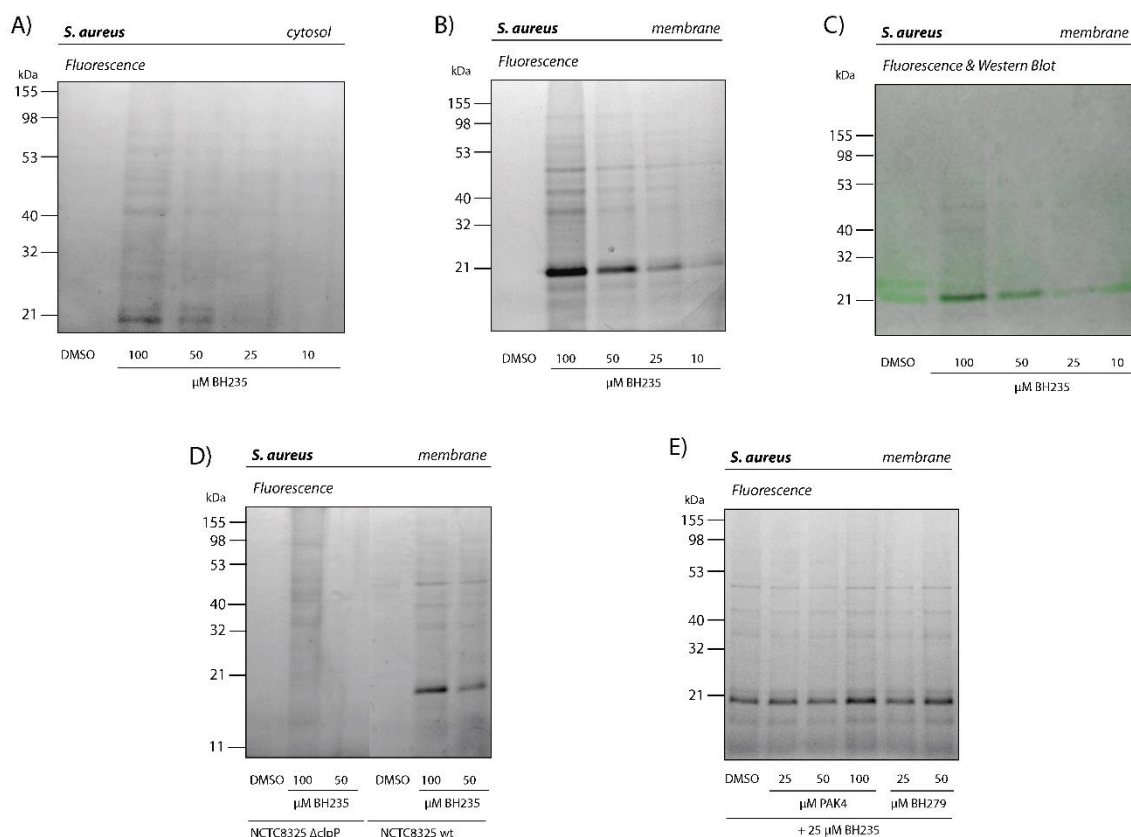


Figure 37. A) Soluble and B) insoluble fractions of labeling experiments in *S. aureus* NCTC8325. C) Overlay of western blot (green) with *Sa*ClpP antibody and fluorescence labeling. D) Labeling experiment in *S. aureus* NCTC8325 wt in comparison to a $\Delta clpP$ strain. E) Competition experiments with **PAK4** and **BH279** as competitors. All labeling experiments were performed with the **BH235** photoprobe.

Western blot analysis was performed to confirm that the band at around 21 kDa represents ClpP (Figure 37C). For that, a gel-based *A/BPP* experiment was performed as described earlier and the bands were blotted on a membrane. ClpP was made visible *via* a primary

SaClpP antibody and the chemiluminescence of an HRP complex, located on a secondary antibody. Photos of fluorescence and chemiluminescence (green) were overlaid, and ClpP could be identified as the band at 21 kDa. To further validate *SaClpP* as the target, and exclude an overlay of two proteins, labeling was performed in a $\Delta clpP$ *S. aureus* strain. Here again, the insoluble fraction was investigated. It was illustrated that the corresponding band, which was strongly labeled in the wild type, disappeared in the knockout strain, although background labeling is clearly visible at a concentration of 100 μ M (Figure 37D).

Additionally, a competition experiment was performed with ADEP fragment **PAK4** and derivative **BH279** but no competitive effects could be observed (Figure 37E). ADEP derivative **BH279** was included as competitor, since it illustrates better activation in the FITC-casein assay and is therefore considered a better competitor. Fragment probe **BH235** was used at a concentration of 25 μ M, while competitors had concentrations that were up to four times higher. Since no competition was visible, a higher amount of competitor might be required for *in situ* experiments.

Since the labeling experiment *in situ* could successfully be performed with the small photoprobe **BH235**, the more valuable ADEP photoprobes **BH266** and **BH288** were examined for *in situ* labeling in *S. aureus*.

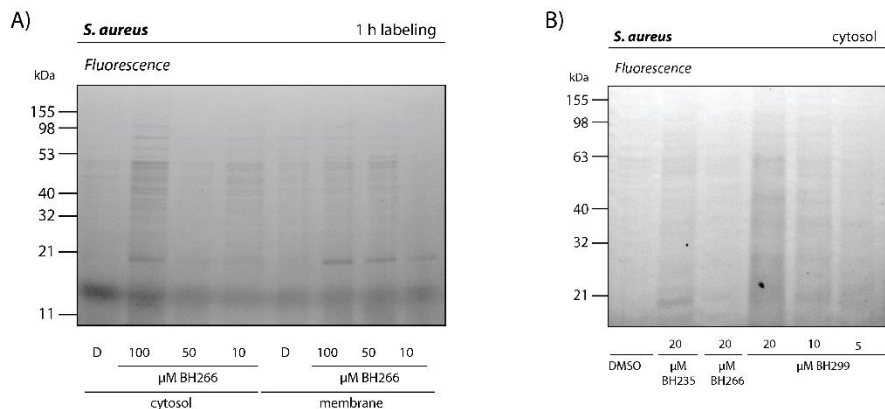


Figure 38. Labeling in *S. aureus* intact cells with photoprobes **BH266** and **BH288**. A) Soluble and insoluble fraction after labeling with **266**, B) soluble fraction of labeling with **235**, **266** and **288**.

The labeling with ADEP photoprobes **BH266** and **BH288** in *S. aureus* intact cells is shown in figure 38. Although the bands are weak, both probes show ClpP labeling and several additional bands that could represent ADEPs' off-targets.

4.1.3. Labeling of ClpP in different conformational states

It is commonly known that ClpP can be labeled with β -lactones or phenyl esters.^[113,114,168] Since these compounds address the catalytic active side, they are limited in labeling ClpP in non-active states, while with ADEP photoprobes, exactly this should be possible.

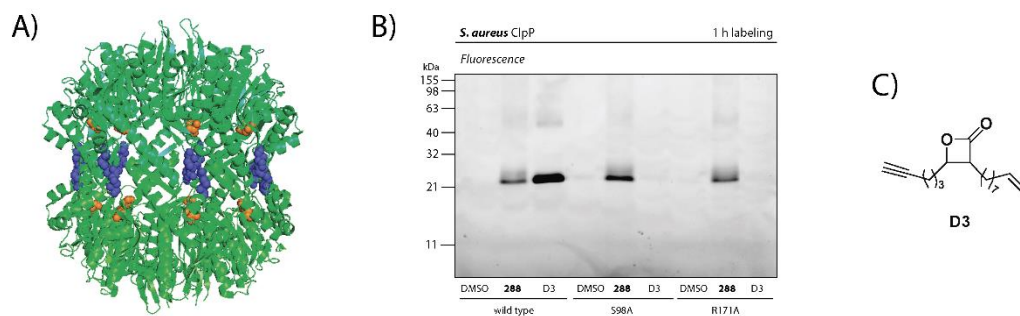


Figure 39. A) Side view of tetradecameric ClpP with marked mutated amino acids S98A (orange) and R171A (blue). (PDB: 3sta) B) Labeling of recombinant ClpP wt and mutants with **BH288** and **D3** as control. *Sa*ClpP was incubated with DMSO or compound for one hour, irradiated for 20 min and a click reaction was performed, as described in the experimental section. C) Structure of the β -lactone **D3**.

To prove this, an active site mutant, S98A, and a disrupted oligomerisation mutant, R171A, were labeled with an ADEP photoprobe, in comparison to the β -lactone **D3** (Figure 39). Labeling with the **D3** probe is slightly stronger than labeling with the photoprobe in the wild type. This can be explained by the covalent binding mode of the **D3** probe, in contrast to the ADEP photoprobe. Nevertheless, labeling of inactive mutants S98A and R171A is possible with **BH288**, which is not the case with **D3**.

The experiment clearly shows the ability to label ClpP independently of its activity and oligomeric state with ADEP photoprobes, in contrast to the so far limited β -lactones. This not only enables labeling of ClpP in an inactive state, the comparison between these two kind of probes might even be helpful to readout the activity state of ClpP in cells. This might also be an interesting approach regarding human ClpP, playing an important role in acute myeloid leukemia (AML).^[169]

4.2. MS-based labeling

4.2.1. Labeling Challenge

Although really clear labeling could be achieved in gel, MS-based identification of ClpP as a target was a challenge, which will be discussed in this section. An A/BPP workflow was conducted with a label free quantification method, as described in the introductory part.

First round of experiments

First experiments were carried out with conditions that lead to strong labeling in previous gel-based experiments. Probes **235** and **266** were utilized at concentrations of 25 μ M and 10 μ M respectively. For certain experiments, a trifunctional linker was used to visualize proteins *via* fluorescence after enrichment. Here, no enriched proteins were visible for probe **266** and the soluble fraction of probe **235**. Nevertheless, clear bands at 21 kDa were visible in the insoluble fraction for probe **235**, which would fit the size of *Sa*ClpP monomer. Even though, the target protein ClpP was not among the enriched proteins in any experiment (Table 3, Appendix: Figure A5 A).

Table 3. Overview of the first MS-based A/BPP experiments with fragmentation and ADEP photoprobe.

Compound	Concentration	Linker	Enrichment	Bands on Gel
BH235	25 μ M	biotin azide	no	-
BH235	25 μ M	TFL	no	yes
BH266	10 μ M	TFL	no	no

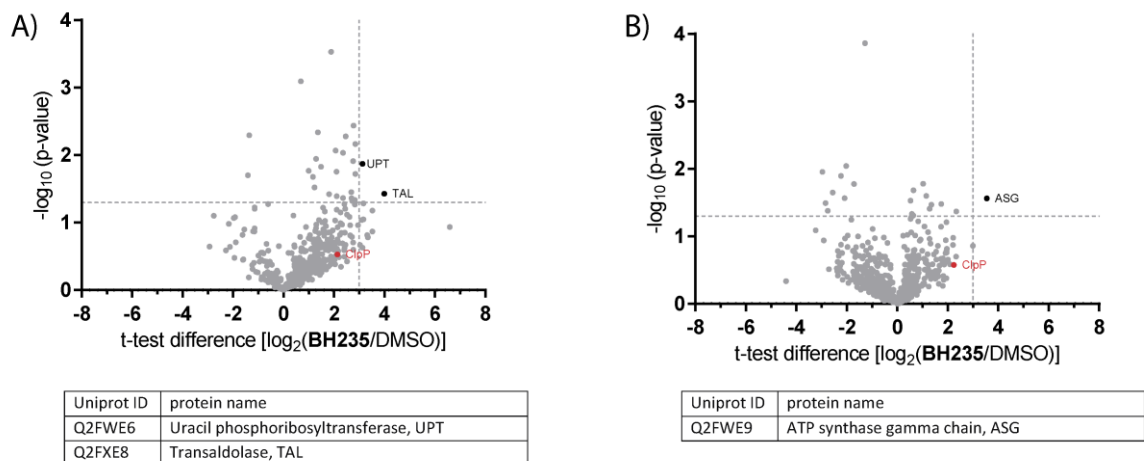


Figure 40. Volcano plots of A) soluble and B) insoluble fraction of MS-based labeling experiments with photoprobe **BH235** against DMSO with a trifunctional linker (Second entry in table 3). Experiments were performed in three biological replicates. Cut off lines were set at a minimum of \log_2 fold-change for enrichment of 3 and a minimum $-\log_{10}(p\text{-value})$ of 1.3. The red marked protein shows ClpP, proteins within the target area are listed.

Volcano plots of the AfBPP experiment with **BH235** are depicted in figure 40. Few proteins are enriched in the insoluble fraction, with solely one protein, ATP synthase gamma chain, meeting enrichment and significance criteria. In the soluble fraction an overall shift to the right is illustrated. The most enriched proteins are uracil phosphoribosyltransferase (UPT) and transaldolase (TAL). Interestingly both proteins were found among 105 *S. aureus* proteins in the surfactome of chronic phase infection, where *Lei et al.* identified biofilm matrix proteins directly from infected bone implants.^[170] Furthermore, they found leukocidins in the biofilm matrix, suggesting an active attack against the host immune system, despite their protection within the biofilm.^[170]

First optimizations

Since no enrichment of ClpP could be achieved, conditions needed to be optimized. In gel-based labeling, ClpP was observed in the insoluble fraction regularly. Since ClpP is a cytosolic protein, solubility issues might be brought about after irradiation. Crosslinks that are formed during irradiation or irradiation itself might lead to insolubility of the protein which leads to less protein amounts for labeling. To overcome this, different SDS concentrations during lysis and for resuspension of the insoluble fraction were tested gel-based. 0.2% and 0.4% SDS were determined as best concentrations, respectively (Appendix: Figure A6). For previous experiments no SDS was used during lysis and 0.2% SDS was used for resuspension of the insoluble fraction. Another point constitutes the solvent exposed diazirine of probe **266**. For this reason, longer irradiation times were tested, which only led to an increase in unspecific labeling (Appendix: Figure A5 B). To differentiate between possible targets and off-targets, competition experiments needed to be performed as well. Here, gel-based experiments have been conducted before and showed competition in *S. aureus* lysate (Figure 36).

Second round of experiments

Further labeling experiments were performed with optimized conditions using biotin azide as linker for enrichment. 0.2% and 0.4% SDS were used for lysis and resuspension respectively. Cells were irradiated for 14 min and photoprobes were used at a concentration of 20 μ M. However, ClpP could still not be enriched with these optimized conditions and no competition was observed for any protein target (Table 4).

Table 4. Overview of the second round of MS-based A/BPP experiments with a fragment and ADEP photoprobes.

Compound	Concentration	Linker	Enrichment	Competition
BH266	20 μ M	biotin azide	no	-
BH235	20 μ M	biotin azide	no	-
BH266	20 μ M	biotin azide	no	no

Volcano plots of A/BPP experiments with **BH266** are illustrated in figure 41. Besides two uncharacterised proteins in both fraction, Na(+)/H(+) antiporter subunit A1 and biotin_lipoyl_2 domain-containing protein are enriched in the soluble fraction. In general, only few proteins are enriched in both fractions.

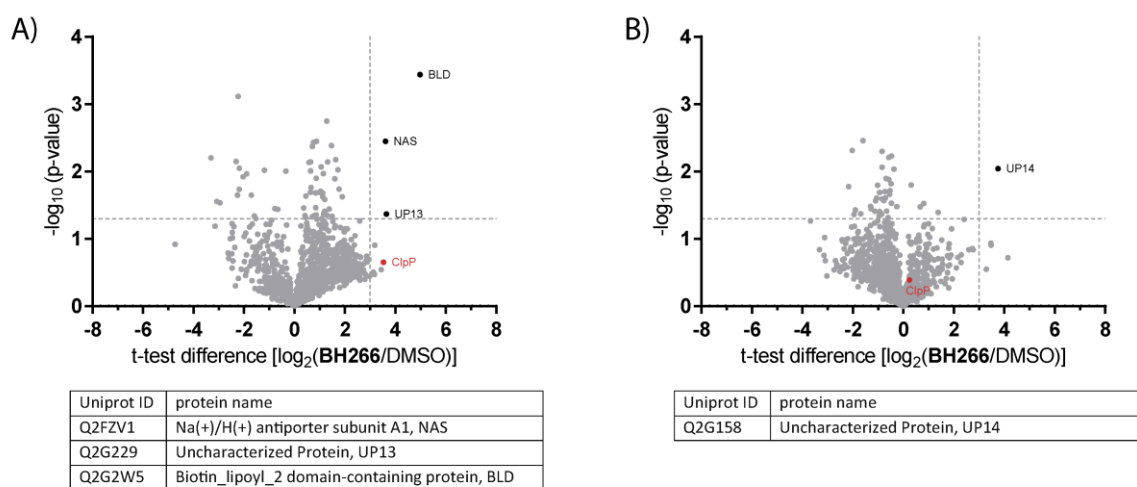


Figure 41. Volcano plots of A) soluble and B) insoluble fraction of MS-based labeling experiments with photoprobe **BH266** against DMSO. (First entry in table 4) Experiments were performed in three biological replicates. Cut off lines were set at a minimum of \log_2 fold-change for enrichment of 3 and a minimum $-\log_{10}(\text{p-value})$ of 1.3. The red marked protein shows ClpP, proteins within the target area are listed.

Further optimization

Since there was clear labeling in the gel, the click reaction seemed to work properly and did not pose a problem. Nevertheless, it was tested for optimization. A click reaction assay was performed which revealed BTTA and THPTA as far better ligands than TBTA, which was used before (Appendix: Figure A7 A). Because of this, all three ligands were tested in a gel-based labeling. All bands were in the same range of intensity, but the BTTA ligand seemed to be slightly better and was therefore chosen for some further experiments (Appendix Figure A7 B).

Third round of experiments

Here, the first experiment with probe **288**, which does not have the unfavourably directed diazirine, was performed at a concentration of 10 μ M with the trifunctional linker. Still, ClpP was not identified within the enriched proteins in the volcano plots of soluble or insoluble

fractions (Figure 42). Nevertheless, in the insoluble fraction two major toxins are enriched, namely *alpha*-hemolysin and *gamma*-hemolysin component C.^[171] Furthermore, *N*-acetylmuramoyl-L-alanine amidase sle1 (AM), which represents a vancomycin target,^[171] and AM domain-containing protein (AAD) are both enriched in the insoluble fraction. Interestingly, probable autolysin SsaALP (PAL), found in the soluble fraction, has weak lytic activity towards *S. aureus* cells and displays a high similarity to staphylococcal secretory antigen ssaA2 (SSA2), found in the insoluble fraction.^[172] SSA2 is associated with *S. aureus* pathogenicity, playing an important role in biofilm-associated infections.^[172,173] Additionally, UDP-*N*-acetylenol-pyruvoylglucosamine reductase (UPR), involved in bacterial cell wall biosynthesis,^[174] was found within the enriched proteins in the soluble fraction. Among others, 50S ribosomal protein L19 (RP3), putative lytic regulatory protein (LRP) and uncharacterised leukocidin-like protein (ULP) were enriched in the soluble fraction. Signal peptidase I (SP1) is considered a background binder, since it was also enriched with minimal diazirine probes.^[64]

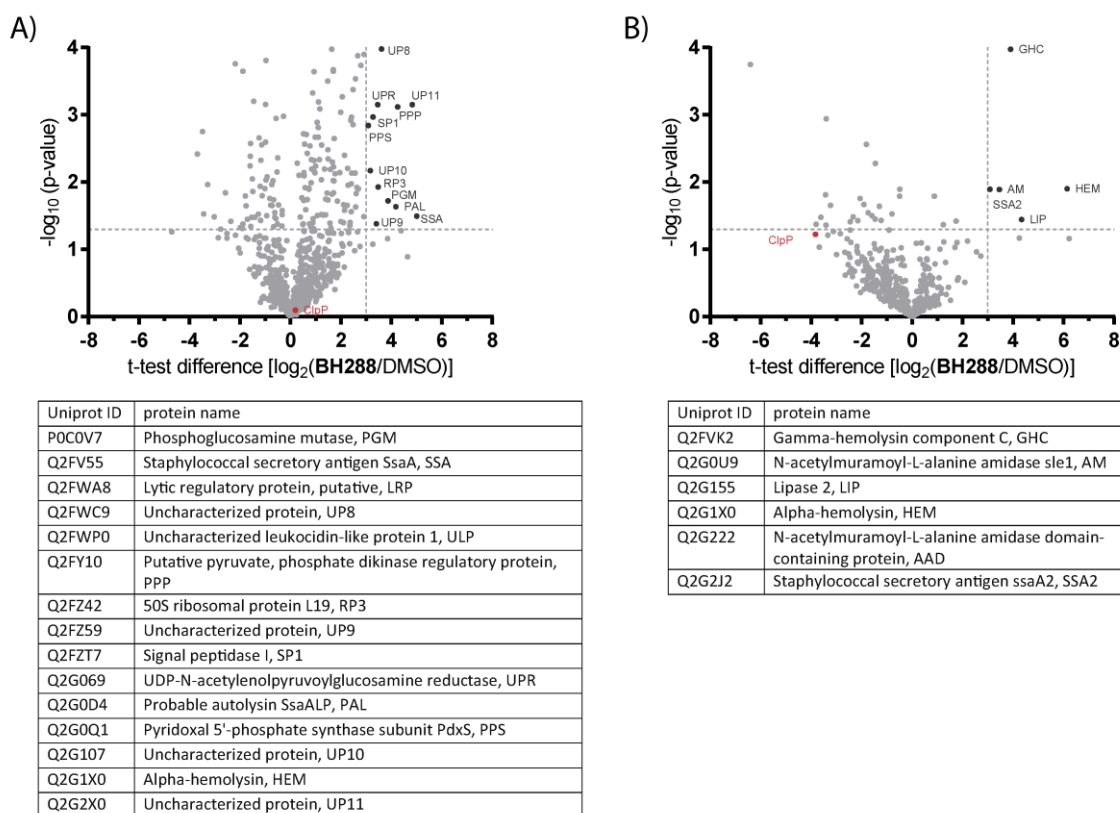


Figure 42. Volcano plots of A) soluble and B) insoluble fraction of MS-based labeling experiments with photoprobe **BH288** against DMSO. Experiments were performed in three biological replicates. Cut off lines were set at a minimum of \log_2 -change for enrichment of 3 and a minimum $-\log_{10}(\text{p-value})$ of 1.3. The red marked protein shows ClpP, proteins within the target area are listed.

Further optimization

Since the solubility of ClpP still seemed to be a problem, a different lysis condition was tested, using lysostaphin. Another advantage of this method is that separation of soluble and insoluble fraction is not necessary. Since all proteins present are together in one fraction evaluation is a lot easier. With separate fractions it is not clear how much protein appears in which fraction. Further, the ratio of protein amount in soluble and insoluble fraction might differ overall experiments. Even when looking at both fractions, it might be difficult to tell if a protein is enriched or not.

Fourth round of experiments

For this final round of experiments, only lysis conditions were optimized by the usage of lysostaphin and bacteria were grown in BHB instead of B medium as in experiments before. Satisfyingly, experiments with all photoprobes depicted a significant enrichment of ClpP and are discussed in the following.

Table 5. Overview of the fourth round of MS-based AfBPP experiments with a fragment and ADEP photoprobes.

Compound	Concentration	Linker	Enrichment	Bands on Gel
BH235	20 μ M	TFL	yes	yes
BH266	10 μ M	TFL	yes	yes
BH288	10 μ M	TFL	yes	yes

4.2.2. Optimized Conditions

Labeling was performed with all three photoprobes **235**, **266** and **288** with concentrations of 20 μ M, 10 μ M and 10 μ M, respectively. For enrichment, a trifunctional linker was used and proteins were visualized gel-based *via* fluorescence afterwards. For all three probes, bands were visible at 21 kDa, which fits ClpP (Appendix: Figure A8). Furthermore, MS-based AfBPP also revealed ClpP as enriched protein in all three volcano plots (Figure 43).

Interestingly, fragment probe **235** illustrated around 20 enriched proteins, while ADEP probes **266** and **288** show only around six enriched proteins. This could be an effect of the higher concentration that was used in the experiment with **235**, or perhaps it describes the impact of the more specific ADEP probes. On the one hand, specific labeling with whole ADEP probes **266** and **288** was expected. On the other hand, probe **288** did not show a low MIC value or activation of ClpP in the FITC-casein assay, making its selective labeling surprising. Nevertheless, it might be possible that **288** does not take the same position in the hydrophobic

pocket as **266**, since its diazirine moiety might clash with the protein surface. This clash might lead to a decreased activation of ClpP in the FITC-casein assay, and therefore to a lower MIC value, but still cause specific labeling.

Furthermore, besides ClpP, two proteins are enriched consistently in all three volcano plots. The three proteins that are enriched with probes **266** or **288** are all identified among the enriched proteins with probe **235**. Only one protein is solely enriched with probe **288** and several proteins with **235**. This also indicates that probes **266** and **288** partly cover different off-targets due to their unique structures. Altogether, these data give the results reliability. Some selected target proteins will be discussed in the following section.

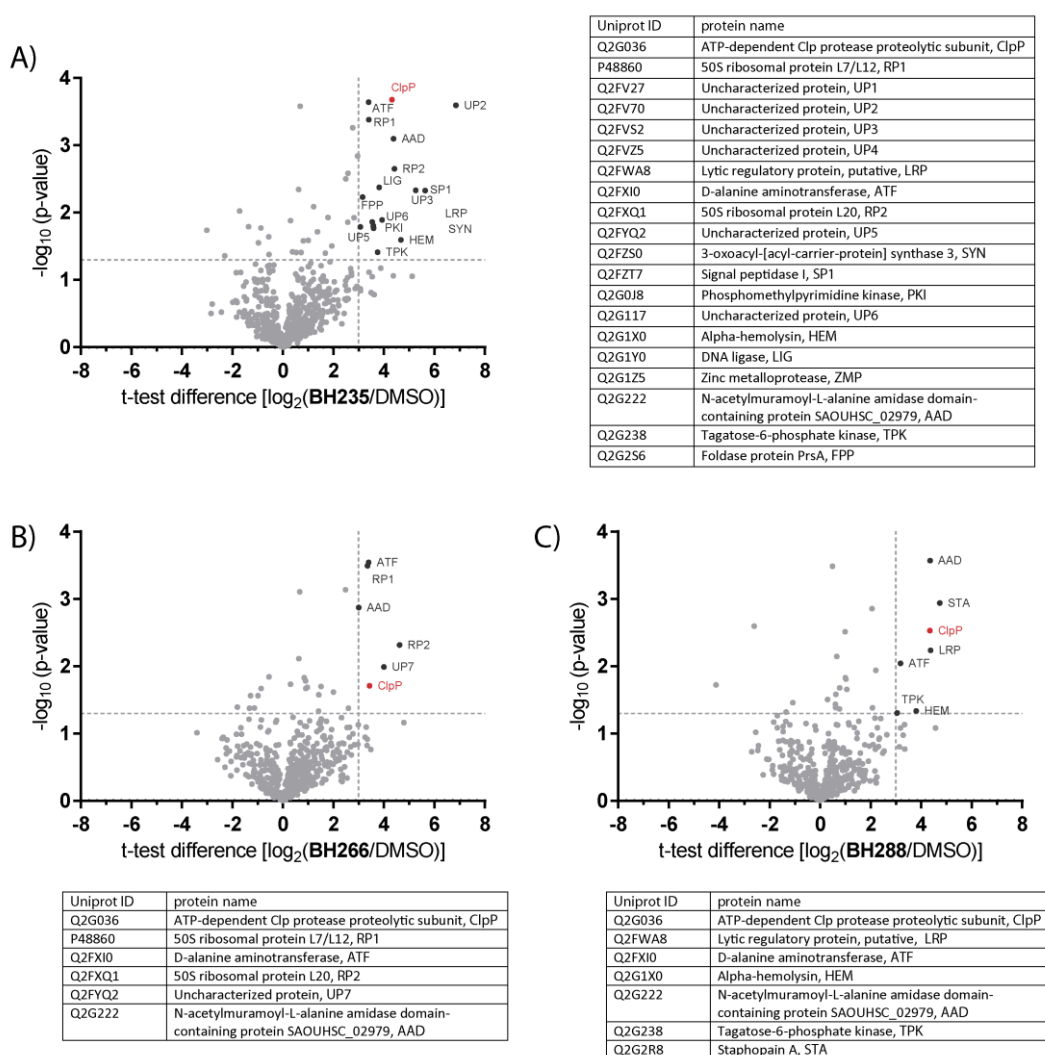


Figure 43. Volcano plots of MS-based labeling experiments with photoprobes A) **235**, B) **266** and C) **288** against DMSO. Experiments were performed in three biological replicates. Cut off lines were set at a minimum of \log_2 fold-change for enrichment of 3 and a minimum $-\log_{10}(p\text{-value})$ of 1.3. The red marked protein shows ClpP, proteins within the target area are listed.

As mentioned before, three proteins are constantly enriched in all three volcano plots, namely ClpP, D-alanine aminotransferase (ATF) and *N*-acetylmuramoyl-L-alanine amidase domain (AMD)-containing protein (AAD). Of course, ClpP was expected to be a target and functions as a positive control that adds up to the experiments reliability.

ATF has interesting interaction partners involved in bacterial cell wall formation, like D-ala-D-ala ligase.^[175] Furthermore, its interaction partner glutamate racemase provides glutamate that is required for cell wall biosynthesis and D-ala-D-ala carrier plays an indirect role in modulating the properties of the cell wall in gram-positive bacteria.^[175] All these interactions imply that ADEPs might have an indirect effect on the bacterial cell wall. Interestingly, ATF was found by *Artini et al.* to be impaired in an experiment with a natural compound which inhibits biofilm formation,^[176] making ATF an interesting off-target.

Interestingly, AMD is involved in several important cell functions, like secretion, cell division and cell adhesion. It is highly conserved among *S. aureus* clinical isolates and represents a vancomycin target.^[177] *Eirich et al.* found autolysin (Atl) to be a vancomycin target, which is a bifunctional enzyme whereas AMD represents one part.^[171,178] Here, we found that AMD containing protein might be an ADEP target as well, supported by the independent enrichment of AM and AAD in the insoluble fraction of an AfBPP experiment with **BH288**, where ClpP was not even enriched (Figure 42).

On the one hand, since photoprobe **266** showed a low MIC value, strong activation of ClpP in a FITC-casein assay and clear selective labeling, those targets are considered the most reliable. Other than an uncharacterized protein, two ribosomal proteins, 50S ribosomal protein L7/L12 (RP1) and L20 (RP2) were enriched with probes **266** and **235**. RP1 is known to play an important role for accurate translation, by contributing to the efficiency of a translational proofreading step.^[175,179] Matching these results, 50S ribosomal protein L19 (RP3) was enriched with probe **BH288** in an independent experiment (Figure 42A).

On the other hand, both photoprobes, **266** and **288**, might just cover different ADEP targets due to their unique structures. Enriched proteins with probes **288** and **235** are putative lytic regulatory protein, α -hemolysin and tagatose-6-phosphate kinase. Since α -hemolysin is a major toxin in *S. aureus*, it is interesting that it is found under the enriched proteins. Furthermore, staphopain A is enriched solely with probe **288**. Staphopain A is a protease secreted by *S. aureus* and represents an important immune evasion factor.^[180,181] It is also

known to inhibit biofilm formation and to disperse established biofilms. *Sonesson et al.* discussed that this might enable bacterial spread, but needs further investigation.^[180]

Most proteins have been enriched by using fragment probe **235**, most of which have already been discussed. Additionally, several uncharacterised proteins, as well as three background binders, were among the hits. Signal peptidase I (SP1) and zinc metalloprotease (ZMP) were enriched with minimal diazirine probes by *Kleiner*^[64] and an uncharacterised protein (UP1) with a minimal aryl azide probe in chapter II (Appendix Table A6). Further enriched proteins are 3-oxoacyl-[acyl-carrier-protein] synthase 3 (SYN) and phosphomethylpyrimidine kinase (PKI), foldase protein PrsA (FPP) which is required for the posttranslocational folding of exported proteins,^[182] and DNA ligase (LIG), which is the main protein responsible for DNA replication and essential for the repair of damaged DNA.^[183,184]

All in all, there are several interesting proteins within the enriched proteins, like ATF, AAD and ribosomal proteins, which play important roles in biofilm formation and translation. Additionally, several overlaps can be observed within independent experiments, where ClpP was not even enriched, meaning for instance AAD and *alpha*-hemolysin. To further elucidate if they are real ADEP targets, further investigations are needed. Here, the first step could be a competition experiment with ADEP4.

5. Conclusions and Outlook

Several ADEP fragments, derivatives and photoprobes equipped with an alkyne tag and a photolabile group were synthesized. Activity assays gave information about structure activity relationships, and revealed that changes are not accepted at the ADEP side chain. By the attachment of a minimal photocrosslinker to the western part of ADEP fragment **PAK4**, a small photoprobe **235** was obtained. This easily accessible compound could be used for first tests and the establishment of further experiments.

Furthermore, two ADEP photoprobes, **266** and **288** were synthesized *via* a lactonization method, published in 2015.^[143] The advantage of probe **266** is the retained activity in ClpP activation and comparable MIC to other ADEP derivatives. The drawback is the mostly solvent exposed photolabile group and thus weak labeling efficiency. For probe **288** exactly the opposite is the case, with strong labeling but weak activity on ClpP and no MIC with various concentrations tested.

Gel-based labeling experiments revealed that all three photoprobes are able to label recombinant ClpP in different intensities, whereas **266** showed the weakest and **288** and **235** comparable bands. Furthermore, ADEP photoprobes can label ClpP in no matter what activity or oligomeric state, in contrast to inhibitor probes that were used to label ClpP upon now. Since they bind to the active site, they only can detect ClpP in an active state. To show this, labeling of ClpP mutants S98A and R171A was performed successfully.

In further gel-based labeling experiments, ClpP was also detected when labeling in *S. aureus* lysate and intact cells was performed. To confirm that the strong band at 21 kDa really represents ClpP, western blot analysis and labeling in a $\Delta clpP$ strain were performed as controls. Both experiments revealed ClpP as a target.

Gel-free labeling experiments held many challenges. After numerous optimizations ClpP could be detected as enriched target by MS/MS measurements. While the small probe **235** showed many off-targets, the more specific probes **266** and **288** only showed around six proteins enriched. Altogether, three proteins including ClpP were enriched with all three photoprobes. Almost all other enriched proteins of one ADEP probe were also enriched with the fragment probe **235**. To prove the enriched proteins as ADEP targets, further investigations must be performed, starting for example with a competition experiment.

Since ADEPs have an antibiotic effect, off-targets in human cell lines would be attractive for deeper research as well. First experiments have been conducted within this thesis but are not shown and did not provide adequate results. Further optimization is required in this case.

IV Experimental Part

1. Organic Chemistry

1.1. General material and methods

Commercially available starting materials, reagents and dry solvents were obtained from *Sigma Aldrich*, *Acros Organics*, *TCI Europe*, *VWR*, *Fluorochem*, *Roth*, and *Alfa Aesar*, and were used without further purification. All air or water sensitive reactions were carried out under argon atmosphere in preheated reaction flasks. Anhydrous solvents and water-sensitive liquid chemicals were transferred using argon flushed syringes. Solvents removed under reduced pressure were evaporated at 40 °C.

The following cooling baths were used to maintain low temperatures as indicated in the experimental procedures: ice/water for 0 °C, ice/NaCl/water for -5 °C to -20 °C, dry ice/acetone for -78°C. For other temperatures between 0 °C and -60 °C, an isopropanol bath in combination with an Immersion Cooler HAAKE EK90 from *Thermo Scientific* was used. All temperatures were measured externally.

Analytical thin layer chromatography was recorded on TLC silica gel plates from *Merck*. For visualization, TLC plates were detected by UV light ($\lambda = 254 \text{ nm}$, 366 nm), or stained with the following solutions:

KMnO ₄	1% in 2% Na ₂ CO ₃ in water
Ninhydrin	0.3% in 3% acetic acid in <i>n</i> -butanol
PMA	10% in ethanol

Column chromatography was carried out using silica gel from *VWR* (40-63 μm). Purification by preparative high pressure liquid chromatography (HPLC) was performed using a *Waters* 2545 quaternary gradient module, a XBridge™ prep C18 column (5.0 μm , 30 × 150 mm, flow

rate = 50 mL/min) and a Waters 2998 PDA detector. Mobile phases were ACN (+ 0.1% TFA) and ddH₂O (+ 0.1% TFA).

Nuclear resonance spectra were measured on HD-300, HD-400 and AV-500 machines from *Bruker Bio Spin GmbH*. ¹H spectra were measured at a frequency of 300, 400 or 500 MHz, and ¹³C spectra at 75, 101 or 126 MHz. Chemical shifts (δ) are given in ppm values and are calibrated to the residual signal of the solvent peak:

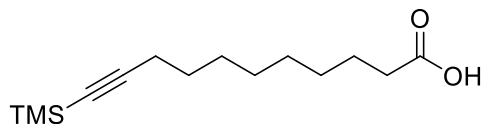
CDCl ₃	7.26 ppm	77.2 ppm
DMSO- <i>d</i> ₆	2.50 ppm	39.5 ppm
Methanol- <i>d</i> ₄	3.31 ppm	49.0 ppm
Acetone- <i>d</i> ₆	2.05 ppm	206 ppm

NMR spectra were processed by using *MestReNova7*. Peak multiplicities are designated by the following abbreviations: s, singlet; d, doublet; t, triplet; q, quartet; m, multiplet; dd, doublet of doublets; dt, doublet of triplets. Coupling constants *J* are given in Hz and the values were averaged and rounded.

High resolution mass spectra were measured on a LTQ-FT Ultra provided by *Thermo Fischer Scientific* using ESI or APCI. Non-high resolution mass spectra were measured on a LCQ-Fleet by *Thermo Fischer Scientific* using HESI or a MSQ-Plus by *Thermo Fischer Scientific* using ESI. Liquid chromatography mass spectra were recorded on all three instruments. MS data were processed using *Thermo Scientific Xcalibur 2.1*.

All final compounds were characterized by HR-MS and ¹H and ¹³C spectra. ADEP derivatives were characterized by HR-LC-MS data. Intermediates were confirmed by MS and ¹H spectra.

Compounds **CD01** to **CD11** were obtained from *Chem Div* (San Diego, USA). Several other compounds were synthesized by members of the *Sieber* research lab and kindly released for common usage. **AV73** and all compounds that were used for the hemolysis assay were published by *Hofbauer et al.* (Chapter II),^[185] the minimal aryl azide probe by *Kleiner et al.* (Chapter II).^[62] Compounds **AV335**, **AV339**, **AV334** and **AV336** were published by *Fetzer et al.* (Chapter III).^[149] β -lactone **D3** was synthesized as described by *Böttcher et al.*,^[147] phenyl ester **AV170**, as described by *Hack et al.*^[113] and ADEP fragment **PAK4** as described by *Carney et al.*^[138]. ADEP 4 was kindly provided by *Heike Brötz-Oesterhelt*.^[120] (Chapter III)

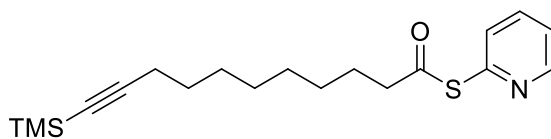
1.2. Synthesis for Chapter II**11-(trimethylsilyl)undec-10-ynoic acid (02)**

A solution of undec-10-ynoic acid (2.50 g, 13.7 mmol, 1.0 eq.) in THF (150 mL) was cooled to $-78\text{ }^{\circ}\text{C}$ and *n*-BuLi (13.2 mL, 32.9 mmol, 2.5 eq., 2.5 M in hexane) was added dropwise. After the solution was stirred for 30 min at the same temperature, freshly distilled TMSCl (5.00 mL, 856 mg/mL, 40.4 mmol, 3.0 eq.) was added. The reaction mixture was stirred for 15 min at $-78\text{ }^{\circ}\text{C}$ and 1 h at room temperature, before it was quenched with water (50 mL). After extraction with dichloromethane (DCM, 3×25 mL), the organic layer was dried over Na_2SO_4 and volatiles were removed under reduced pressure. The crude residue was purified by column chromatography (hexane/EtOAc 10/1 to 2/1 + 1% AcOH). Yield: 2.47 g (35%). $R_f = 0.26$ (hexane/EtOAc 5/1 + 1% AcOH).

$^1\text{H-NMR}$ (400 MHz, CDCl_3): δ (ppm) = 2.35 (t, $J = 7.5$ Hz, 2H), 2.21 (t, $J = 7.1$ Hz, 2H), 1.63 (*virt. p*, $J = 7.5$ Hz, 2H), 1.50 (dt, $J = 7.1$ Hz, 2H), 1.40–1.27 (m, 8H), 0.14 (s, 9H).

$^{13}\text{C-NMR}$ (101 MHz, CDCl_3): δ (ppm) = 179.9, 107.8, 84.5, 34.1, 29.2, 29.1, 29.0, 28.9, 28.7, 24.8, 20.0, 0.3.

HR-MS (ESI): m/z $[\text{M}+\text{H}]^+$ calcd for $\text{C}_{14}\text{H}_{26}\text{O}_2\text{Si}$: 255.1775, found 255.1774.

S-(pyridin-2-yl) 11-(trimethylsilyl)undec-10-ynethioate (03)

Acid **02** (2.40 g, 9.43 mmol, 1.0 eq.) was dissolved in DCM (30 mL), cooled to $0\text{ }^{\circ}\text{C}$ and DMF (3 drops) and oxalylchloride (1.21 mL, 14.2 mmol, 1.5 eq.) were added. The reaction mixture was stirred for 2 h at room temperature, and volatiles were removed under reduced pressure. 2-Thiopyridin (1.26 g, 11.3 mmol, 1.2 eq.) in DCM (30 mL) was added and the solution again cooled to $0\text{ }^{\circ}\text{C}$. NEt_3 (726 mg/mL, 2.62 mL, 18.9 mmol) was added and the reaction was quenched with 1 M HCl (aqueous, 30 mL) after 2 h. After washing with a saturated NaHCO_3 solution (aqueous, 3×25 mL), the organic layer was dried over Na_2SO_4 and

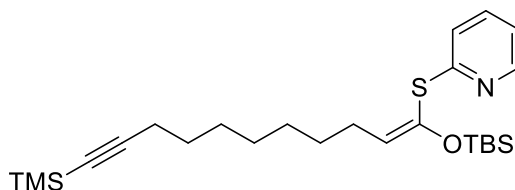
volatiles were removed under reduced pressure. The crude residue was purified by column chromatography (hexane/EtOAc 4/1 to 1/1). Yield: 2.65 g (81%). $R_f = 0.51$ (hexan/EtOAc 4/1).

$^1\text{H-NMR}$ (300 MHz, CDCl_3): δ (ppm) = 8.62 (ddd, $J = 5.0, 1.8, 0.9$ Hz, 1H), 7.79–7.70 (m, 1H), 7.62 (dt, $J = 8.0, 1.0$ Hz, 1H), 7.34–7.26 (m, 1H), 2.70 (t, $J = 7.5$ Hz, 2H), 2.20 (t, $J = 7.1$ Hz, 2H), 1.80–1.64 (m, 2H), 1.57–1.43 (m, 2H), 1.42–1.24 (m, 8H), 0.14 (s, 9H).

$^{13}\text{C-NMR}$ (75 MHz, CDCl_3): δ (ppm) = 196.6, 151.8, 150.4, 137.3, 130.3, 123.6, 107.8, 84.5, 44.4, 29.2, 29.0, 29.0, 28.8, 28.7, 25.5, 20.0, 0.3.

HR-MS (ESI): m/z $[\text{M}+\text{H}]^+$ calcd for $\text{C}_{19}\text{H}_{29}\text{NOSSi}$: 348.1812, found: 348.1812.

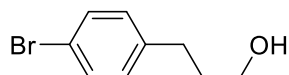
(Z)-2-((1-((tert-butyldimethylsilyl)oxy)-11-(trimethylsilyl)undec-1-en-10-yn-1-yl)thio)pyridine (04)



A solution of thioester **03** (2.65 g, 7.62 mmol, 1.0 eq.), DMF (1.15 mL, 15.0 mmol, 2.0 eq.) and NEt_3 (726 mg/mL, 2.05 mL, 14.8 mmol, 2.0 eq.) in DCM (30 mL) was cooled to -78°C and stirred for 10 min. After LHMDS (1 M in THF, 8.92 mL, 8.92 mmol, 1.2 eq.) was added and the mixture was stirred for 30 min, TBSCl (1.12 g, 7.41 mmol, 1.0 eq.) was added and the solution stirred for another 2 h at the same temperature, before it was warmed up to room temperature. The reaction was quenched with phosphate buffer (25 mM KH_2PO_4 , 40 mM $\text{Na}_2\text{HPO}_4 \cdot 2\text{H}_2\text{O}$, pH 7, 10 mL), the phases were separated and the organic layer was dried over MgSO_4 . Volatiles were removed under reduced pressure and the crude residue was purified by column chromatography (hexane/EtOAc 10/1 to 1/1). Yield: 1.48 g (33%). $R_f = 0.59$ (hexan/EtOAc 9/1).

$^1\text{H-NMR}$ (300 MHz, CDCl_3): δ (ppm) = 8.48–8.36 (m, 1H), 7.66–7.52 (m, 1H), 7.38–7.30 (m, 1H), 7.07–6.96 (m, 1H), 5.40 (t, $J = 7.3$ Hz, 1H), 2.27–2.11 (m, 4H), 1.64–1.44 (m, 4H), 1.44–1.24 (m, 6H), 0.87 (s, 9H), 0.14 (s, 9H), 0.08 (s, 6H).

HR-MS (ESI): m/z $[\text{M}+\text{H}]^+$ calcd for $\text{C}_{25}\text{H}_{43}\text{NOSSi}_2$: 462.2677, found 462.2678.

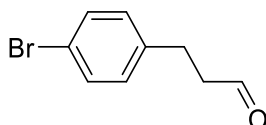
3-(4-bromophenyl)propan-1-ol (31)^[186]

3-(4-bromophenyl)propanoic acid (2.50 g, 10.9 mmol, 1.0 eq.) was dissolved in diethylether (90 mL) and cooled to 0 °C, then LiAlH₄ (620 mg, 16.4 mmol, 1.5 eq.) was added in small portions. The mixture was stirred for 10 min at 0 °C and for 2.5 h at room temperature. TLC was used as reaction control and the reaction was quenched at 0 °C with 1 M HCl (aqueous, 20 mL). After extraction with EtOAc (3×15 mL), the organic layer was dried over Na₂SO₄. Volatiles were removed under reduced pressure and a pure product was obtained. Yield: 1.14 g (quant.). *R*_f = 0.59 (hexane/EtOAc 9/1).

¹H-NMR (300 MHz, CDCl₃): δ (ppm) = 7.46–7.33 (m, 2H), 7.13–7.03 (m, 2H), 3.66 (t, *J* = 6.4 Hz, 2H), 2.77–2.60 (m, 2H), 1.95–1.77 (m, 2H).

¹³C-NMR (75 MHz, CDCl₃): δ (ppm) = 140.9, 131.6, 130.3, 119.7, 62.2, 34.1, 31.6.

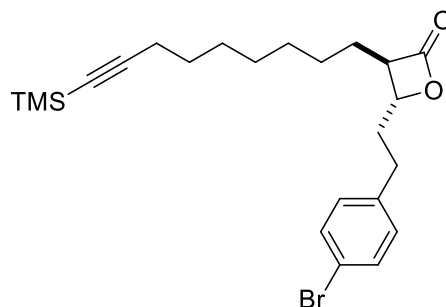
The spectral data are identical to those published in the literature.^[186]

3-(4-bromophenyl)propanal (32)^[187]

A solution of alcohol **31** (3.70 g, 17.2 mmol, 1.0 eq.) in DCM was cooled to 0 °C and NEt₃ (726 mg/mL, 11.9 mL, 86.0 mmol, 5.0 eq.), DMSO (15 mL) and SO₃·py (8.21 g, 51.6 mmol, 3.0 eq.) were added. The mixture was stirred for 35 min at 0 °C and was quenched with 1 M HCl (aqueous, 10 mL). Phases were separated and the aqueous phase was extracted with diethylether (3×10 mL). Combined organic layers were washed with saturated NaCl solution (aqueous, 10 mL) and dried over Na₂SO₄. Volatiles were removed under reduced pressure and a pure product was obtained. Yield: 548 mg (59%). *R*_f = 0.60 (hexane/EtOAc 3/1).

¹H-NMR (300 MHz, CDCl₃): δ (ppm) = 9.81 (t, *J* = 1.2 Hz, 1H), 7.41 (d, *J* = 8.4 Hz, 2H), 7.07 (dd, *J* = 8.0, 0.6 Hz, 2H), 2.99–2.83 (m, 2H), 2.85–2.72 (m, 2H).

The spectral data are identical to those published in the literature.^[188]

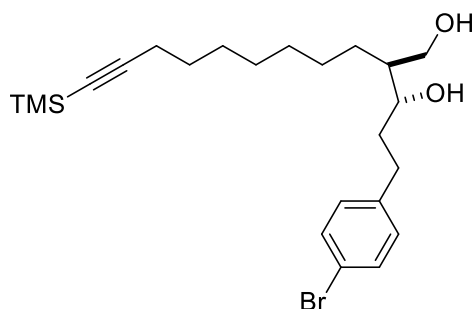
(3R,4R)-4-(4-bromophenethyl)-3-(9-(trimethylsilyl)non-8-yn-1-yl)oxetan-2-one (05)^[74]

Freshly melted ZnCl_2 (2.00 g) was suspended in DCM (10 mL) and aldehyde **32** (692 mg, 3.25 mmol, 1.0 eq., in 5 mL DCM) and ketene acetal **04** (1.50 g, 3.25 mmol, 1.0 eq., in 5 mL DCM) were added. The reaction mixture was stirred for 4 days at room temperature, before it was quenched with phosphate buffer (25 mM KH_2PO_4 , 40 mM $\text{Na}_2\text{HPO}_4 \cdot 2\text{H}_2\text{O}$, pH 7, 10 mL). The organic layer was separated and dried over Na_2SO_4 . Volatiles were removed under reduced pressure and the crude residue was purified by column chromatography (hexane/EtOAc 20/1 to 10/1). Yield: 752 mg (52%). $R_f = 0.33$ (hexane/EtOAc 18/1).

$^1\text{H-NMR}$ (400 MHz, CDCl_3): δ (ppm) = 7.43 (d, $J = 8.3$ Hz, 2H), 7.07 (d, $J = 8.3$ Hz, 2H), 4.19 (dt, $J = 8.5, 4.5$ Hz, 1H), 3.18 (ddd, $J = 8.4, 6.8, 3.9$ Hz, 1H), 2.77 (ddd, $J = 14.4, 9.2, 5.4$ Hz, 1H), 2.66 (ddd, $J = 14.1, 9.0, 7.4$ Hz, 1H), 2.21 (t, $J = 7.1$ Hz, 2H), 2.15–2.00 (m, 2H), 1.86–1.74 (m, 2H), 1.71–1.59 (m, 2H), 1.49 (q, $J = 7.3$ Hz, 2H), 1.46–1.18 (m, $J = 25.1, 5.6$ Hz, 6H), 0.14 (s, 9H).

$^{13}\text{C-NMR}$ (101 MHz, CDCl_3): δ (ppm) = 171.2, 139.3, 131.9, 130.2, 120.4, 107.7, 84.6, 76.8, 56.4, 36.2, 31.0, 29.3, 28.9, 28.8, 28.7, 27.9, 27.1, 20.0, 0.3.

HR-MS (ESI): m/z $[\text{M}+\text{H}]^+$ calcd for $\text{C}_{23}\text{H}_{33}\text{BrO}_2\text{Si}$: 449.1506, found: 449.1500.

(2S,3R)-5-(4-bromophenyl)-2-(9-(trimethylsilyl)non-8-yn-1-yl)pentane-1,3-diol (06)

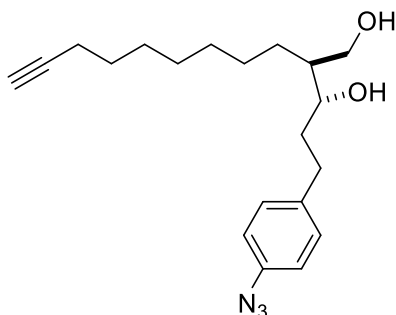
Lactone **05** (374 mg, 785 μmol , 1.0 eq.) was dissolved in diethylether (12 mL) and cooled to 0 °C before LiAlH_4 (63.0 mg, 1.57 mmol, 2.0 eq.) was added. The reaction was stirred for 2 h at r.t. and was quenched with saturated ammonium chloride solution (5 mL). After extraction with EtOAc (3 \times 5 mL), the organic layer was dried over Na_2SO_4 . Volatiles were removed under reduced pressure and the crude residue was purified by column chromatography (hexane/EtOAc 20/1 to 10/1). Yield: 316 mg (84%). R_f = 0.28 (hexane/EtOAc 5/1).

$^1\text{H-NMR}$ (300 MHz, CDCl_3): δ (ppm) = 7.40 (d, J = 8.3 Hz, 2H), 7.09 (d, J = 8.3 Hz, 2H), 3.94 (dd, J = 11.3, 2.92.4 Hz, 2H), 3.75–3.61 (m, 2H), 2.92–2.73 (m, 1H), 2.72–2.73 (m, 1H), 2.21 (t, J = 7.0 Hz, 2H), 1.91–1.74 (m, 4H), 1.49 (m, 2H), 1.42–1.31 (m, 4H), 1.33–1.20 (m, 6H), 0.14 (s, 9H).

$^{13}\text{C-NMR}$ (101 MHz, CDCl_3): δ (ppm) = 141.2, 131.6, 130.4, 119.7, 107.8, 84.5, 75.0, 64.3, 62.2, 60.6, 44.7, 37.5, 34.2, 31.8, 31.6, 29.9, 29.2, 28.9, 28.8, 28.7, 21.2, 20.0, 14.4, 0.4.

HR-MS (ESI): m/z $[\text{M}+\text{H}]^+$ calcd for $\text{C}_{23}\text{H}_{37}\text{BrO}_2\text{Si}$: 453.1819, found: 453.1820.

(2S,3R)-5-(4-azidophenyl)-2-(non-8-yn-1-yl)pentane-1,3-diol (AV73-p)^[75]



Bromide **06** (100 mg, 220 μmol , 1.0 eq.) was dissolved in degassed solvent (6 mL EtOH/ H_2O 7/3) and NaN_3 (28.7 mg, 441 μmol , 2.0 eq.), Na-ascorbate (2.18 mg, 11.0 μmol , 0.05 eq.), CuI (4.20 mg, 22.1 μmol , 0.1 eq.) and (1*S*,2*S*)- N^1,N^2 -dimethylcyclohexan-1,2-diamin (4.70 mg, 33.1 μmol , 0.2 eq.) were added. The reaction was heated to 100 °C and stirred for 5 h at this temperature. The reaction mixture was diluted in ethyl acetate (5 mL). After washing with 1 M HCl (aqueous, 4 mL) and half saturated NaHCO_3 solution (aqueous, 4 mL), the organic layer was dried over Na_2SO_4 . Volatiles were removed under reduced pressure and the crude residue was purified by reversed phase HPLC (ACN/ H_2O ; ACN 2% to 98%). Yield: 7.00 mg (8%).

¹H-NMR (500 MHz, CDCl₃): δ (ppm) = 7.22 (d, *J* = 8.4 Hz, 2H), 6.98 (d, *J* = 8.4 Hz, 2H), 3.97 (dd, *J* = 11.0, 2.9 Hz, 1H), 3.77–3.63 (m, 1H), 2.85 (ddd, *J* = 14.7, 9.3, 6.1 Hz, 1H), 2.73–2.65 (m, 1H), 2.20 (td, *J* = 7.1, 2.7 Hz, 2H), 1.96 (t, *J* = 2.7 Hz, 1H), 1.91–1.79 (m, 2H), 1.65–1.49 (m, 4H), 1.42 (d, *J* = 7.8 Hz, 4H), 1.33–1.28 (m, 6H).

¹³C-NMR (101 MHz, CDCl₃): δ (ppm) = 129.8, 119.1, 100.0, 84.9, 77.2, 75.0, 68.1, 64.1, 37.5, 31.6, 29.8, 29.0, 28.7, 28.6, 28.4, 27.2, 18.4.

HR-MS (ESI): *m/z* [M+H]⁺ calcd for C₂₀H₂₉N₃O₂: 344.2332, found: 344.2333.

1.3. Synthesis for Chapter III

1.3.1. *General procedures for the synthesis of ADEP fragments*

General procedure A: Synthesis of esters using EDC-HCl and DMAP.^[138,165]

EDC (1-Ethyl-3-(3-dimethylaminopropyl)carbodiimide)·HCl and DMAP (4-Dimethylaminopyridine) were added to a solution of the Boc-protected amino acid and the corresponding alcohol in dichloromethane (DCM). The reaction mixture was stirred at room temperature for several hours until TLC control showed complete consumption of the starting material. After the solvent has been removed under reduced pressure, the residue was taken up in ethyl acetate and was washed with 1 M HCl (aq., 3×), saturated NaHCO₃ (aq., 3×) and saturated NaCl solution (aq., 1×). The organic layer was dried over Na₂SO₄ and the solvent was removed under reduced pressure.

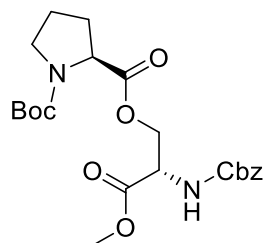
General procedure B: Deprotection of a Boc-group.^[138,165]

The Boc-protected amino acid was dissolved in 40% TFA in DCM and the reaction mixture was stirred for 1.5 h at room temperature. Argon was forced over the reaction to evaporate the solvent, which gave the crude product.

General procedure C: Synthesis of amides.^[138,165]

1-[Bis(dimethylamino)methylene]-1*H*-1,2,3-triazolo[4,5-*b*]pyridinium 3-oxid hexafluorophosphate (HATU) and *N,N*-Diisopropylethylamine (DIPEA) were added to the dissolved acid in dimethylformamide (DMF) and the reaction mixture was stirred for 15 min. Subsequently the amino acid in DMF was added and the reaction mixture was stirred until TLC control showed complete consumption of the starting material. Ethyl acetate (5 times the reaction volume) was added to the reaction mixture which was washed with 1 M HCl (aq., 3×), saturated NaHCO₃ solution (aq., 3×) and saturated NaCl solution (aq., 3×). The organic layer was dried over Na₂SO₄, the solvent was removed under reduced pressure and the crude product was purified by column chromatography (hexane/ethyl acetate).

1.3.2. Synthesis of ADEP fragments

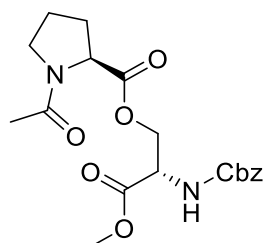
2-((S)-2-(((benzyloxy)carbonyl)amino)-3-methoxy-3-oxopropyl) 1-(tert-butyl) (S)-pyrrolidine-1,2-dicarboxylate (08)

Synthesized according to **general procedure A**, using methyl ((benzyloxy)carbonyl)-*L*-serinate (719 mg, 2.84 mmol, 1.0 eq.), *N*-(*tert*-Butoxycarbonyl)-*L*-proline (672 mg, 3.12 mmol, 1.1 eq.), EDC·HCl (816 mg, 4.26 mmol, 1.5 eq.) and DMAP (34.7 mg, 284 μ mol, 0.1 eq.) in 14 mL dichloromethane for 20 h. Washing steps were carried out with 5 mL aqueous solution each. 1.26 g (98%) of a pure colorless solid were obtained. R_f = 0.37 (hexane/ethyl acetate 1/1).

$^1\text{H-NMR}$ (400 MHz, CDCl_3 , note: mixture of rotamers 1/1): δ (ppm) = 7.40 – 7.30 (m, 10H), 5.95 (d, J = 8.4 Hz, 1H), 5.51 (d, J = 7.6 Hz, 1H), 5.18 – 5.06 (m, 4H), 4.69 – 4.57 (m, 3H), 4.52 – 4.37 (m, 3H), 4.28 (dd, J = 8.5, 4.0 Hz, 1H), 4.20 (dd, J = 8.6, 3.7 Hz, 1H), 3.77 (s, 6H), 3.57 – 3.33 (m, 4H), 2.25 – 2.09 (m, 2H), 1.89 (dtt, J = 19.4, 12.5, 5.7 Hz, 6H), 1.43 (s, 9H), 1.38 (s, 9H).

MS (ESI): m/z $[\text{M}+\text{H}]^+$ calcd for $\text{C}_{22}\text{H}_{30}\text{N}_2\text{O}_8$: 451, found: 451.

Analytical data are in accordance with those published in the literature.^[138]

(S)-2-(((benzyloxy)carbonyl)amino)-3-methoxy-3-oxopropyl acetyl-L-prolinate (09)

Deprotection was performed according to **general procedure B**, using amino acid derivative **08** (1.26 g, 2.80 mmol, 1.0 eq.) and trifluoroacetic acid (40% in DCM) for 1 h. The crude product was dissolved in 14 mL dichloromethane and 780 μ L (726 mg/mL, 5.59 mmol,

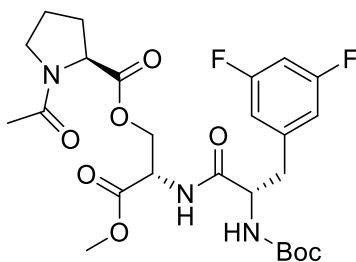
2.0 eq.) triethylamine and 530 μL (1.09 g/mL, 5.59 mmol, 2.0 eq.) acetic anhydride were added. The reaction mixture was stirred for 18 h and the solvent was removed under reduced pressure. The crude product was purified by column chromatography (ethyl acetate) and yielded 980 mg (89%) of a yellow oil. $R_f = 0.26$ (ethyl acetate).

$^1\text{H-NMR}$ (300 MHz, CDCl_3): δ (ppm) = 7.40 – 7.34 (m, 5H), 6.05 (d, $J = 7.7$ Hz, 1H), 5.14 (s, 2H), 4.71 – 4.58 (m, 2H), 4.47 – 4.34 (m, 2H), 3.77 (s, 3H), 3.61 – 3.45 (m, 2H), 2.25 – 2.12 (m, 1H), 2.08 (s, 3H), 2.01 – 1.93 (m, 3H).

MS (ESI): m/z $[\text{M}+\text{H}]^+$ calcd for $\text{C}_{19}\text{H}_{24}\text{N}_2\text{O}_7$: 393, found: 393.

Analytical data are in accordance with those published in the literature.^[138]

(S)-2-((S)-2-((tert-butoxycarbonyl)amino)-3-(3,5-difluorophenyl)propanamido)-3-methoxy-3-oxopropyl acetyl-L-prolinate (10)

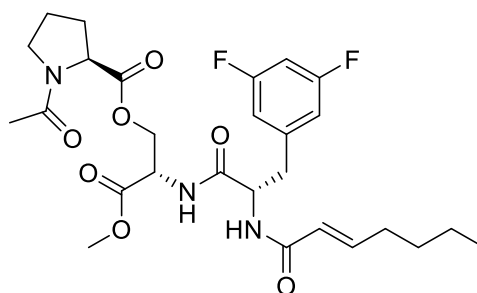


The protected amino acid **09** (980 mg, 2.50 mmol, 1.0 eq.) was dissolved in 18 mL methanol and added to Pd/C (10% on carbon, 325 mg) under argon atmosphere. 100 μL (2.50 mmol, 1.0 eq.) 1 M HCl was added, the reaction flask was flushed with hydrogen thrice and the reaction was stirred under hydrogen atmosphere for 40 h. Subsequently the reaction flask was flushed with argon and the reaction mixture was filtered through Celite[®] and the solvent was removed under reduced pressure. Part of the crude product (285 mg, 967 μmol , 1.0 eq.) was diluted in 3.4 mL DMF and *N*-Boc-difluorophenylalanine (320 mg, 1.06 mmol, 1.1 eq.), HATU (404 mg, 1.06 mmol, 1.1 eq.) and DIPEA (371 μL , 742 mg/mL, 2.13 mmol, 2.2 eq.) were added. The reaction mixture was stirred for 21 h, diluted with 40 mL ethyl acetate and washed with 1 M HCl (aq., 3 \times 15 mL), saturated NaHCO_3 solution (aq., 3 \times 15 mL) and saturated NaCl solution (aq., 15 mL). The organic layer was dried over Na_2SO_4 and the solvent was removed under reduced pressure. The crude product was purified by column chromatography (acetone/ethyl acetate 1/1) and yielded 96.0 mg (18%) of a yellow oil. $R_f = 0.46$ (acetone/ethyl acetate 1/1).

¹H-NMR (500 MHz, CDCl₃): δ (ppm) = 7.91 (d, *J* = 8.1 Hz, 1H), 6.77 – 6.64 (m, 3H), 5.71 (d, *J* = 8.6 Hz, 1H), 4.80 (dt, *J* = 7.9, 3.9 Hz, 1H), 4.65 – 4.52 (m, 3H), 4.38 (dd, *J* = 11.4, 3.9 Hz, 1H), 3.78 (s, 3H), 3.59 – 3.53 (m, 1H), 3.43 (td, *J* = 9.6, 6.9 Hz, 1H), 3.16 (dd, *J* = 13.8, 5.7 Hz, 1H), 3.03 (dd, *J* = 13.9, 7.4 Hz, 1H), 2.50 – 2.40 (m, 1H), 2.20 – 2.14 (m, 1H), 2.09 (s, 3H), 2.04 – 1.97 (m, 1H), 1.95 – 1.83 (m, 1H), 1.40 (s, 9H).

MS (ESI): *m/z* [M+H]⁺ calcd for C₂₅H₃₃F₂N₃O₈: 542, found: 542.

(S)-2-((S)-3-(3,5-difluorophenyl)-2-((E)-hept-2-enamido)propanamido)-3-methoxy-3-oxopropyl acetyl-L-prolinate (F7)



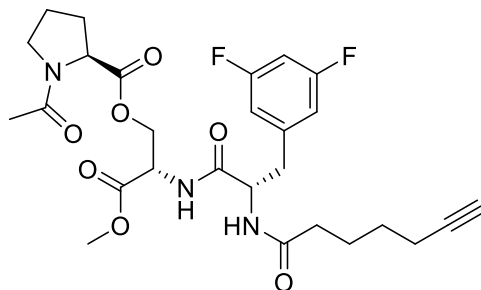
Deprotection was performed according to **general procedure B**, using 167 mg (310 μmol, 2.0 eq.) amino acid **10** and trifluoroacetic acid (1.0 mL, 40% in DCM) for 15 h. Hept-2-enoic acid (20 μL, 95.0 mg/mL, 186 μmol, 1.2 eq.) was dissolved in 0.9 mL DMF and 64.8 mg (170 μmol, 1.1 eq.) HATU and 30.0 μL (742 mg/mL, 170 μmol, 1.1 eq.) DIPEA were added. After the mixture has been stirred for 15 min, half of the deprotected crude product (123 mg, 155 μmol, 1.0 eq.) in 0.8 mL DMF was added to the reaction mixture. The reaction was stirred for 2 h at room temperature, diluted with 20 mL ethyl acetate and washed with 1 M HCl (aq., 3×10 mL), saturated NaHCO₃ solution (aq., 3×10 mL) and saturated NaCl solution (aq., 20 mL). The organic layer was dried over Na₂SO₄ and the solvent was removed under reduced pressure. The crude product was purified by column chromatography (hexane/ethyl acetate 1/2 to 1/4) and yielded 17.2 mg (21%) of the product. *R_f* = 0.10 (hexane/ethyl acetate 1/2).

¹H-NMR (300 MHz, CDCl₃): δ (ppm) = 7.67 (d, *J* = 8.1 Hz, 1H), 6.85 (dt, *J* = 15.3, 7.0 Hz, 1H), 6.74 – 6.63 (m, 3H), 5.88 – 5.81 (m, 1H), 4.94 (q, *J* = 6.6 Hz, 1H), 4.81 (dt, *J* = 8.1, 4.1 Hz, 1H), 4.57 – 4.50 (m, 2H), 4.39 (dd, *J* = 11.3, 3.9 Hz, 1H), 3.78 (s, 3H), 3.64 – 3.53 (m, 1H), 3.50 – 3.39 (m, 1H), 3.25 – 3.06 (m, 2H), 2.46 – 2.33 (m, 1H), 2.26 – 2.10 (m, 3H), 2.07 (s, 3H), 2.01 – 1.81 (m, 3H), 1.54 – 1.23 (m, 4H), 0.90 (t, *J* = 7.1 Hz, 3H).

HR-MS (ESI): *m/z* [M+H]⁺ calcd for C₂₇H₃₅F₂N₃O₇: 552.2516, found: 552.2514.

Analytical data are in accordance with those published in the literature.^[138]

(S)-2-((S)-3-(3,5-difluorophenyl)-2-(hept-6-ynamido)propanamido)-3-methoxy-3-oxopropyl acetyl-L-prolinate (F8)

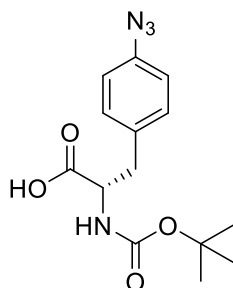


Deprotection was performed according to **general procedure B**, using 167 mg (310 μmol , 2.0 eq.) amino acid **10** and trifluoroacetic acid (1.0 mL, 40% in DCM) for 15 h. Hept-6-ynoic acid (20 μL , 99.7 mg/mL, 170 μmol , 1.1 eq.) was dissolved in 0.9 mL DMF and 64.8 mg (170 μmol , 1.1 eq.) HATU and 30.0 μL (742 mg/mL, 170 μmol , 1.1 eq.) DIPEA were added. After the mixture has been stirred for 15 min, half of the deprotected crude product (123 mg, 155 μmol , 1.0 eq.) in 0.76 mL DMF was added to the reaction mixture. The reaction was stirred for 2 h at room temperature, diluted with 20 mL ethyl acetate and washed with 1 M HCl (aq., 3 \times 20 mL), saturated NaHCO_3 solution (aq., 3 \times 20 mL) and saturated NaCl solution (aq., 20 mL). The organic layer was dried over Na_2SO_4 and the solvent was removed under reduced pressure. The crude product was purified by column chromatography (hexane/ethyl acetate 1/2 to 1/4) and yielded 9.20 mg (11%) of the product. $R_f = 0.10$ (hexane/ethyl acetate 1/2).

$^1\text{H-NMR}$ (400 MHz, CDCl_3): δ (ppm) = 7.52 (d, $J = 8.2$ Hz, 1H), 6.99 (d, $J = 5.1$ Hz, 1H), 6.76 – 6.64 (m, 3H), 4.92 – 4.75 (m, 2H), 4.59 – 4.49 (m, 2H), 4.49 – 4.37 (m, 1H), 3.79 (s, 3H), 3.67 – 3.59 (m, 1H), 3.55 – 3.45 (m, 1H), 3.24 – 3.04 (m, 4H), 2.29 – 2.16 (m, 4H), 2.13 (s, 3H), 2.07 – 1.97 (m, 2H), 1.94 (t, $J = 2.7$ Hz, 1H), 1.78 – 1.64 (m, 2H), 1.54 – 1.44 (m, 2H).

$^{13}\text{C NMR}$ (101 MHz, CDCl_3): δ (ppm) = 171.2, 170.7, 169.6, 112.5, 112.3, 102.6, 84.2, 77.4, 68.8, 64.2, 60.1, 53.1, 51.8, 48.7, 41.0, 37.4, 35.7, 28.2, 27.9, 25.1, 24.7, 18.3.

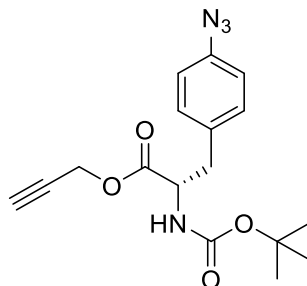
HR-MS (ESI): m/z $[\text{M}+\text{H}]^+$ calcd for $\text{C}_{27}\text{H}_{33}\text{F}_2\text{N}_3\text{O}_7$: 550.2359, found: 550.2355.

(S)-3-(4-azidophenyl)-2-((tert-butoxycarbonyl)amino)propanoic acid (14)^[75]

N-Boc-4-bromophenylalanine (**13**, 200 mg, 581 μmol , 1.0 eq.), CuI (11.1 mg, 58.0 μmol , 0.1 eq.), NaN_3 (113 mg, 1.74 mmol, 3.0 eq.), *N,N'*-Dimethylethylenediamine (DMEDA, 940 μL , 819 mg/mL, 87.0 μmol , 0.15 eq.), Na-ascorbate (115 mg, 581 μmol , 1.0 eq.) and NaOH (23.2 mg, 581 μmol , 1.0 eq.) were diluted in 5 mL ethanol/water (6/1) and heated to 100 °C. The reaction mixture was stirred for 24 h at 100 °C, diluted with 10 mL ethyl acetate and washed with 4 mL saturated NaCl solution. The aqueous phase was extracted with ethyl acetate (3 \times 3 mL), the combined organic layers were dried over Na_2SO_4 and the solvent was removed under reduced pressure. The crude product was purified by column chromatography (DCM/MeOH/acetic acid 94/5/1) and yielded 100 mg (56%) of the product.

¹H-NMR (300 MHz, CDCl_3): δ (ppm) = 7.29 – 7.12 (m, 2H), 7.03 – 6.92 (m, 2H), 4.92 (d, J = 8.1 Hz, 1H), 4.67 – 4.46 (m, 1H), 3.29 – 2.91 (m, 2H), 1.42 (s, 9H).

MS (ESI): m/z $[\text{M}+\text{H}]^+$ calcd for $\text{C}_{14}\text{H}_{18}\text{N}_4\text{O}_4$: 305, found: 306.

Prop-2-yn-1-yl (S)-3-(4-azidophenyl)-2-((tert-butoxycarbonyl)amino)propanoate (15)

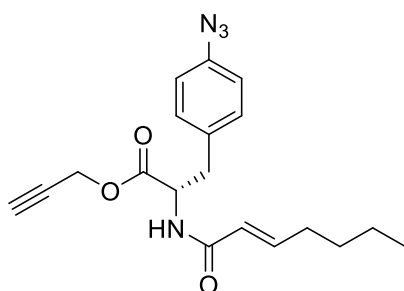
Amino acid derivative **15** was synthesized according to **general procedure A** using 100 mg (326 μmol , 1.0 eq.) amino acid **14**, 20.0 μL (948 mg/mL, 326 μmol , 1.0 eq.) propargyl alcohol, 75.0 mg (392 μmol , 1.2 eq.) EDC \cdot HCl and 2.00 mg (16.0 μmol , 0.1 eq.) DMAP in 4 mL DCM for 4 h. Washing steps were carried out with 3 mL aqueous solution each. After

column chromatography (hexane/ethyl acetate 4/1), 69.0 mg (62%) of a yellow oil were obtained.

¹H-NMR (500 MHz, CDCl₃): δ (ppm) = 7.15 (d, *J* = 8.4 Hz, 2H), 6.96 (d, *J* = 8.4 Hz, 2H), 4.94 (d, *J* = 6.6 Hz, 1H), 4.84 – 4.64 (m, 2H), 4.65 – 4.57 (m, 1H), 3.19 – 3.00 (m, 2H), 2.51 (t, *J* = 2.5 Hz, 1H), 1.42 (s, 9H).

MS (ESI): *m/z* [M-Boc+H]⁺ calcd for C₁₇H₂₀N₄O₄: 245, found: 245.

Prop-2-yn-1-yl (S,E)-3-(4-azidophenyl)-2-(hept-2-enamido)propanoate (F5)

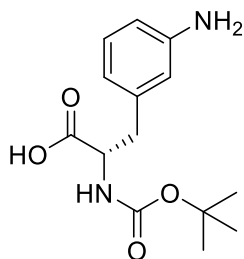


Deprotection was performed according to **general procedure B**, using 69.0 mg (203 μmol, 1.0 eq.) amino acid **15** and trifluoroacetic acid (2.0 mL, 40% in DCM) for 1.5 h. All of the crude product was used for the amide synthesis according to **general procedure C**, using 40.0 μL (960 mg/mL, 223 μmol, 1.1 eq.) *E*-2-heptenoic acid, 85.0 mg (223 μmol, 1.1 eq.) HATU and 40.0 μL (742 mg/mL, 223 μmol, 1.1 eq.) DIPEA in 2.5 mL DMF for 18 h. Washing steps were carried out with 3 mL aqueous solution each. 38.0 mg (77%) of the product was obtained after purification with column chromatography (hexane/ethyl acetate 1/1). No total pure product was obtained; impurities were subtracted out.

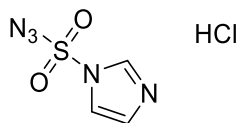
¹H-NMR (500 MHz, CDCl₃): δ (ppm) = 7.12 (d, *J* = 8.5 Hz, 2H), 6.95 (d, *J* = 8.5 Hz, 2H), 6.86 (dt, *J* = 15.3, 6.9 Hz, 1H), 5.76 (dt, *J* = 15.3, 1.5 Hz, 1H), 4.99 (dt, *J* = 7.7, 5.5 Hz, 1H), 4.89 – 4.62 (m, 2H), 3.18 (*virt.* qd, *J* = 14.0, 5.5 Hz, 2H), 2.53 (t, *J* = 2.5 Hz, 1H), 2.23 – 2.14 (m, 2H), 1.47 – 1.39 (m, 2H), 1.38 – 1.31 (m, 2H), 0.91 (t, *J* = 7.3 Hz, 3H).

¹³C-NMR (126 MHz, CDCl₃): δ (ppm) = 165.5, 158.1, 151.9, 146.6, 139.2, 132.4, 131.0, 129.7, 122.8, 119.3, 115.0, 77.4, 77.0, 75.8, 53.1, 53.0, 37.3, 30.4, 14.0.

HR-MS (ESI): *m/z* [M-Boc+H]⁺ calcd C₁₉H₂₂N₄O₃: 355.1765, found: 335.1766.

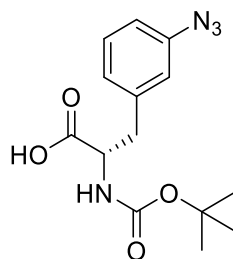
(S)-3-(3-aminophenyl)-2-((tert-butoxycarbonyl)amino)propanoic acid (17)^[161]

N-Boc-3-aminophenylalanine **16** (200 mg, 645 μmol , 1.0 eq.) was dissolved in 9 mL methanol and K_2CO_3 (107 mg, 773 μmol , 1.2 eq) and Pd/C (10% on carbon, 17.6 mg) were added under argon atmosphere. The reaction flask was flushed with hydrogen thrice and stirred for 20 h under hydrogen atmosphere. Subsequently the flask was flushed with argon, the reaction mixture was filtered through Celite[®] and the solvent was removed under reduced pressure. The crude product was used without further purification.

1H-imidazole-1-sulfonyl azide hydrogen chloride (Imidazolsulfonylazide 33)^[162]

Sulfonylchloride (3.23 mL, 1.67 g/mL, 40.0 mmol, 1.1 eq.) was added to a suspension of NaN_3 (2.60 g, 40.0 mmol, 1.1 eq.) in 40 mL acetonitrile at 0 °C under argon atmosphere. After the reaction was stirred for 18 h at room temperature, it was cooled to 0 °C and imidazole (2.59 g, 38.1 mmol, 1.0 eq.) was added in portions. The reaction mixture was stirred for 3.5 h at room temperature and 80 mL ethyl acetate were added. The organic layer was washed with water (80 mL) and saturated NaHCO_3 solution (80 mL) and was dried over Na_2SO_4 . 10 mL HCl (4 M in dioxane) were added and the mixture was cooled to 0 °C. The pure product was filtered off and washed with ethyl acetate. Yield with 20% ethyl acetate: 2.41 g.

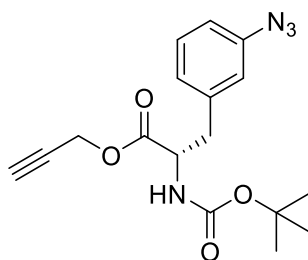
¹H-NMR (300 MHz, $\text{DMSO}-d_6$): δ (ppm) = 8.54 – 8.47 (m, 1H), 7.94 (*virt.* t, J = 1.6 Hz, 1H), 7.29 (dd, J = 1.8, 0.8 Hz, 1H).

(S)-3-(3-azidophenyl)-2-((tert-butoxycarbonyl)amino)propanoic acid (18)^[161]

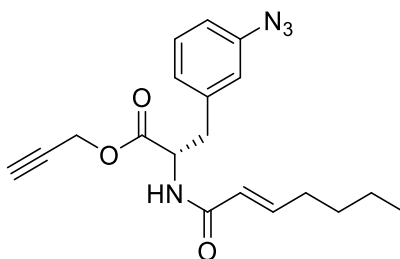
The crude amine **17** (205 mg, 645 μmol , 1.0 eq.) was dissolved in 5 mL methanol and imidazolsulfonylazide **33** (134 mg, 773 μmol , 1.2 eq.) and $\text{CuSO}_4 \cdot \text{H}_2\text{O}$ (1.61 mg, 6.45 μmol , 0.01 eq.) were added. The reaction mixture was stirred for 16 h at room temperature and the solvent was removed under reduced pressure. The residue was dissolved in water and acidified to pH 3 with 1 M HCl (aq.). The mixture was extracted with ethyl acetate (3 \times 3 mL), dried over Na_2SO_4 and the solvent was removed under reduced pressure. The crude product was purified by column chromatography (hexane/ethyl acetate 3/1 to 1/1 + 2% acetic acid) and yielded 127 mg (64%) of a colorless solid. $R_f = 0.06$ (hexane/ethyl acetate 3/1).

$^1\text{H-NMR}$ (300 MHz, CDCl_3): δ (ppm) = 7.06 – 6.77 (m, 4H), 5.01 – 4.77 (m, 1H), 4.67 – 4.50 (m, 1H), 3.31 – 2.98 (m, 2H), 1.43 (s, 9H).

MS (ESI): m/z $[\text{M-H}]^-$ calcd $\text{C}_{14}\text{H}_{18}\text{N}_4\text{O}_4$: 305, found: 305.

Prop-2-yn-1-yl (S)-3-(3-azidophenyl)-2-((tert-butoxycarbonyl)amino)propanoate (19)

Amino acid derivative **19** was synthesized according to **general procedure A** using 127 mg (415 μmol , 1.0 eq.) amino acid **18**, 240 μL (948 mg/mL, 415 μmol , 1.0 eq.) propargyl alcohol, 95.0 mg (498 μmol , 1.2 eq.) EDC \cdot HCl and 3.00 mg (20.0 μmol , 0.1 eq.) DMAP in 4 mL DCM for 2 h. Washing steps were carried out with 5 mL aqueous solution each. 106 mg (74%) of a yellow solid was obtained. The product was used for the next step without further purification.

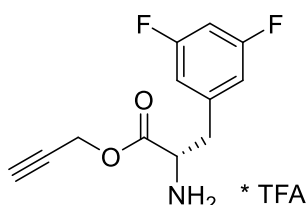
Prop-2-yn-1-yl (S,E)-3-(3-azidophenyl)-2-(hept-2-enamido)propanoate (F6)

Deprotection was performed according to **general procedure B**, using 106 mg (308 μmol , 1.0 eq.) amino acid **19** and trifluoroacetic acid (2.5 mL, 40% in DCM) for 2 h. All of the crude product was used for the amide synthesis according to **general procedure C**, using 50.0 μL (960 mg/mL, 339 μmol , 1.1 eq.) *E*-2-heptenoic acid, 130 mg (339 μmol , 1.1 eq.) HATU and 60.0 μL (742 mg/mL, 339 μmol , 1.1 eq.) DIPEA in 2.5 mL DMF for 18 h. Washing steps were carried out with 3 mL aqueous solution each. 70.0 mg (64%) of the product was obtained after purification with column chromatography (hexane/ ethyl acetate 5/1). No total pure product was obtained; impurities were subtracted out.

$^1\text{H-NMR}$ (300 MHz, CDCl_3): δ (ppm) = 7.51 – 7.42 (m, 4H), 6.79 (t, J = 1.7 Hz, 1H), 6.22 (dt, J = 15.8, 1.5 Hz, 2H), 5.86 (d, J = 7.6 Hz, 1H), 4.87 – 4.61 (m, 2H), 3.19 (qd, J = 13.9, 5.6 Hz, 2H), 2.54 (t, J = 2.5 Hz, 1H), 2.45 – 2.36 (m, 2H), 1.60 – 1.48 (m, 2H), 1.47 – 1.40 (m, 2H), 0.90 (t, J = 7.3 Hz, 3H).

$^{13}\text{C-NMR}$ (126 MHz, CDCl_3): δ (ppm) = 170.7, 165.4, 140.6, 140.3, 137.6, 129.9, 129.6, 120.8, 120.1, 77.3, 75.9, 52.9, 52.8, 37.5, 32.8, 31.8, 22.3, 13.8.

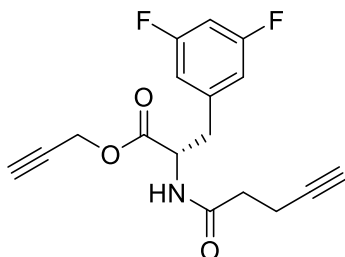
HR-MS (ESI): m/z $[\text{M}+\text{H}]^+$ calcd $\text{C}_{19}\text{H}_{22}\text{N}_4\text{O}_3$: 355.1765, found: 355.1765.

Prop-2-yn-1-yl (S)-2-((tert-butoxycarbonyl)amino)-3-(3,5-difluorophenyl)propanoate (37)

Amino acid derivative **37** was synthesized according to **general procedure A**, using 500 mg (**11**, 1.66 mmol, 1.0 eq.) *N*-Boc-3,5-difluoro-phenylalanine, 95.8 μL (948 mg/mL, 1.66 mmol, 1.0 eq.) propargyl alcohol, 309 mg (1.99 mmol, 1.2 eq.) EDC·HCl and 10.2 mg (83.1 μmol ,

0.1 eq.) DMAP in 20 mL DCM for 3 h. Washing steps were carried out with 10 mL aqueous solution each. The crude product (459 mg) was deprotected according to **general procedure B**, using trifluoroacetic acid (10 mL, 40% in DCM) for 1 h. The deprotected product was used for the next step without further purification.

Prop-2-yn-1-yl (S)-3-(3,5-difluorophenyl)-2-(pent-4-ynamido)propanoate (F3)



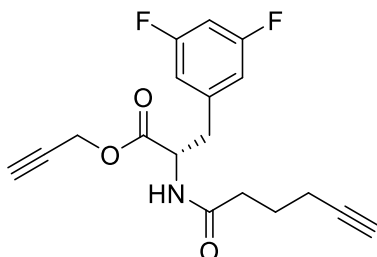
F3 was synthesized according to **general procedure C**, using 81.0 mg (338 μmol , 1.0 eq.) compound **37**, 36.5 mg (372 μmol , 1.1 eq.) 4-pentynoic acid, 142 mg (372 μmol , 1.1 eq.) HATU and 48.1 μL (742 mg/mL, 372 μmol , 2.2 eq.) DIPEA in 3 mL DMF for 24 h. Washing steps were carried out with 8 mL aqueous solution each. 36.9 mg (34% over three steps) of the product were obtained after purification with column chromatography (hexane/ethyl acetate 6/1). $R_f = 0.24$ (hexane/ethyl acetate 6/1 + 0.5% acetic acid).

$^1\text{H-NMR}$ (400 MHz, CDCl_3): δ (ppm) = 6.77 – 6.66 (m, 3H), 6.15 (d, $J = 7.4$ Hz, 1H), 4.94 (dt, $J = 7.4, 5.4$ Hz, 1H), 4.76 (*virt.* ddd, $J = 66.2, 15.5, 2.5$ Hz, 2H), 3.18 (*virt.* qd, $J = 13.9, 5.5$ Hz, 2H), 2.64 – 2.37 (m, 5H), 2.02 (t, $J = 2.6$ Hz, 1H).

$^{13}\text{C-NMR}$ (101 MHz, CDCl_3): δ (ppm) = 170.7, 170.4, 164.4, 161.9, 139.4, 112.8, 112.6, 103.0, 82.8, 76.7, 76.2, 69.9, 53.2, 53.0, 37.5, 35.3, 14.8.

HR-MS (ESI): m/z $[\text{M}+\text{H}]^+$ calcd $\text{C}_{17}\text{H}_{15}\text{F}_2\text{NO}_3$: 320.1093, found: 320.1092.

Prop-2-yn-1-yl (S)-3-(3,5-difluorophenyl)-2-(hex-5-ynamido)propanoate (F2)



Synthesized according to **general procedure C**, using 81.0 mg (338 μmol , 1.0 eq.) compound **37**, 41.7 mg (372 μmol , 1.1 eq.) 5-hexynoic acid, 142 mg (372 μmol , 1.1 eq.) HATU and 48.1 μL (742 mg/mL, 372 μmol , 2.2 eq.) DIPEA in 3 mL DMF for 24 h. Washing steps were

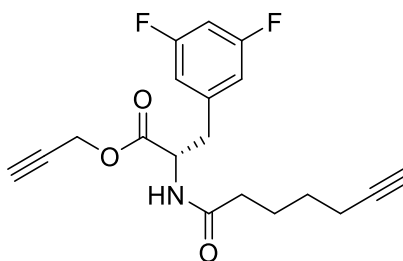
carried out with 8 mL aqueous solution each. 41.0 mg (36% over three steps) of the product was obtained after purification with column chromatography (hexane/ethyl acetate 5/1). $R_f = 0.21$ (hexane/ethyl acetate 5/1).

$^1\text{H-NMR}$ (400 MHz, CDCl_3): δ (ppm) = 6.75 – 6.64 (m, 3H), 5.96 (d, $J = 7.7$ Hz, 1H), 4.93 (dt, $J = 7.7, 5.6$ Hz, 1H), 4.75 (*virt.* ddd, $J = 65.5, 15.5, 3.5$ Hz, 2H), 3.23 – 3.10 (m, 2H), 2.55 (t, $J = 2.5$ Hz, 1H), 2.37 (t, $J = 7.3$ Hz, 2H), 2.29 – 2.22 (m, 2H), 1.99 (t, $J = 2.7$ Hz, 1H), 1.93 – 1.80 (m, 2H).

$^{13}\text{C-NMR}$ (101 MHz, CDCl_3): δ (ppm) = 172.0, 170.5, 164.3, 161.8, 139.5, 112.7, 112.5, 103.0, 83.3, 77.4, 76.1, 69.6, 53.2, 52.7, 37.6, 34.8, 24.0, 17.8.

HR-MS (ESI): m/z $[\text{M}+\text{H}]^+$ calcd $\text{C}_{18}\text{H}_{17}\text{F}_2\text{NO}_3$: 334.1249, found: 334.1249.

Prop-2-yn-1-yl (S)-3-(3,5-difluorophenyl)-2-(hept-6-ynamido)propanoate (F1)

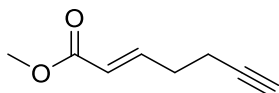


Synthesized according to **general procedure C**, using 21.0 mg (87.9 μmol , 1.0 eq.) compound **37**, 12.8 μL (997 mg/mL, 96.7 μmol , 1.1 eq.) 6-heptynoic acid, 35.2 mg (96.7 μmol , 1.1 eq.) HATU and 33.6 μL (742 mg/mL, 193 μmol , 2.2 eq.) DIPEA in 1.0 mL DMF for 24 h. Washing steps were carried out with 10 mL aqueous solution each. 16.4 mg (35% over three steps) of the product were obtained after purification with column chromatography (hexane/ethyl acetate 5/1). $R_f = 0.21$ (hexane/ethyl acetate 2/1).

$^1\text{H-NMR}$ (300 MHz, CDCl_3): δ (ppm) = 6.79 – 6.62 (m, 3H), 5.94 (d, $J = 7.7$ Hz, 1H), 5.01 – 4.91 (m, 1H), 4.78 (*virt.* ddd, $J = 65.9, 15.5, 2.5$ Hz, 2H), 3.26 – 3.11 (m, 2H), 2.58 (t, $J = 2.5$ Hz, 1H), 2.51 – 2.19 (m, 1H), 2.30 – 2.20 (m, 3H), 1.98 (t, $J = 2.7$ Hz, 1H), 1.83 – 1.73 (m, 2H), 1.62 – 1.53 (m, 2H).

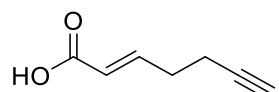
$^{13}\text{C-NMR}$ (126 MHz, CDCl_3): δ (ppm) = 172.3, 170.5, 163.9, 162.0, 139.4, 112.5, 102.5, 83.9, 76.0, 68.8, 53.0, 52.6, 37.5, 35.9, 27.8, 24.5, 18.2.

HR-MS (ESI): m/z $[\text{M}+\text{H}]^+$ calcd $\text{C}_{19}\text{H}_{19}\text{F}_2\text{NO}_3$: 348.1406, found: 348.1403.

Methyl (*E*)-hept-2-en-6-ynoate (34)^[189]

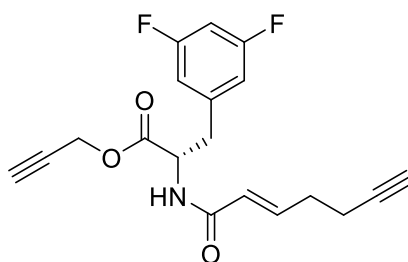
DMSO (4.05 mL, 1.10 g/mL, 57.1 μmol , 2.4 eq.) was added to a solution of oxalylchloride (2.45 mL, 1.48 g/mL, 28.5 μmol , 1.2 eq.) in 60 mL DCM at $-60\text{ }^\circ\text{C}$ and the mixture was stirred for 10 min. 2.21 mL (900 mg/mL, 23.8 μmol , 1.0 eq.) 4-pentyn-1-ol were added in 20 mL DCM and the mixture was again stirred for 15 min before 16.5 mL (726 mg/mL, 119 μmol , 5.0 eq.) triethylamine were added and the mixture was allowed to thaw to $0\text{ }^\circ\text{C}$. After 9.54 g (28.5 μmol , 1.2 eq.) $\text{Ph}_3\text{PCHO}_2\text{Me}$ were added, the reaction was stirred for 90 min at room temperature, before 100 mL water were added and the mixture was extracted with DCM (3 \times 25 mL). The organic layer was dried over Na_2SO_4 and the solvent was removed under reduced pressure. The crude product was purified by column chromatography (hexane/ethyl acetate 15/1 to 10/1) and yielded 2.05 g (62%) of a yellow oil. $R_f = 0.52$ (hexane/ethyl acetate 10/1).

¹H-NMR (300 MHz, CDCl_3): δ (ppm) = 6.98 (dt, $J = 15.7, 6.5$ Hz, 1H), 5.90 (dt, $J = 15.7, 1.5$ Hz, 1H), 3.73 (s, 3H), 2.48 – 2.39 (m, 2H), 2.39 – 2.31 (m, 2H), 2.00 (t, $J = 2.5$ Hz, 1H).

(*E*)-hept-2-en-6-ynoic acid (35)^[189]

NaOH (22.0 mL, 1 M aq. solution, 21.7 mmol, 1.5 eq.) was added to a solution of 2.00 g (14.5 mmol, 1.0 eq.) compound **34** in 20 mL tetrahydrofuran (THF) and the reaction mixture was stirred at $50\text{ }^\circ\text{C}$ for 1 h. Subsequently HCl (25 mL, 1 M aq. solution, 24.6 mmol, 1.7 eq.) was added and the mixture was extracted with ethyl acetate (2 \times 25 mL), the organic layer was dried over Na_2SO_4 and the solvent was removed under reduced pressure. The crude product was purified by column chromatography (hexane/ethyl acetate 5/1 + 1% acetic acid) and yielded 335 mg (20%) of a yellow oil. $R_f = 0.63$ (hexane/ethyl acetate 5/1 + 1% acetic acid).

¹H-NMR (300 MHz, CDCl_3): δ (ppm) = 7.10 (dt, $J = 15.7, 6.6$ Hz, 1H), 5.91 (dt, $J = 15.7, 1.6$ Hz, 1H), 2.53 – 2.43 (m, 2H), 2.43 – 2.34 (m, 2H), 2.01 (t, $J = 2.6$ Hz, 1H).

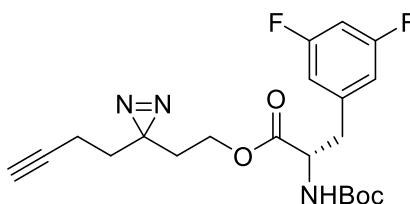
Prop-2-yn-1-yl (S,E)-3-(3,5-difluorophenyl)-2-(hept-2-en-6-ynamido)propanoate (F4)

ADEP fragment **F4** was synthesized according to **general procedure A**, using 200 mg (**11**, 664 μmol , 1.0 eq.) *N*-Boc-3,5-difluoro-phenylalanine, 40.0 μL (948 mg/mL, 664 μmol , 1.0 eq.) propargyl alcohol, 127 mg (664 μmol , 1.0 eq.) EDC·HCl and 8.10 mg (66.4 μmol , 0.1 eq.) DMAP in 3 mL DCM for 3 h. Washing steps were carried out with 2 mL aqueous solution each. All of the crude product was deprotected according to **general procedure B**, using trifluoroacetic acid (3.0 mL, 40% in DCM) for 1 h. All of the deprotected product was used for the amide synthesis according to **general procedure C**, using 82.3 mg (664 μmol , 1.0 eq.) compound **35**, 277 mg (729 μmol , 1.1 eq.) HATU and 250 μL (742 mg/mL, 1.46 mmol, 2.2 eq.) DIPEA in 3 mL DMF for 72 h. Washing steps were carried out with 4 mL aqueous solution each. 103 mg (45% over three steps) of the product were obtained after purification with column chromatography (hexane/ethyl acetate 2/1). $R_f = 0.42$ (hexane/ethyl acetate 2/1).

$^1\text{H-NMR}$ (300 MHz, CDCl_3): δ (ppm) = 6.89 (dt, $J = 15.4, 6.4$ Hz, 1H), 6.76 – 6.61 (m, 3H), 6.04 – 5.92 (m, 1H), 5.88 (dt, $J = 15.4, 1.5$ Hz, 1H), 4.99 (dt, $J = 7.6, 5.4$ Hz, 1H), 4.76 (*virt.* ddd, $J = 52.6, 15.9, 2.9$ Hz, 2H), 3.30 – 3.08 (m, 2H), 2.55 (t, $J = 2.5$ Hz, 1H), 2.47 – 2.29 (m, 4H), 2.00 (t, $J = 2.5$ Hz, 1H).

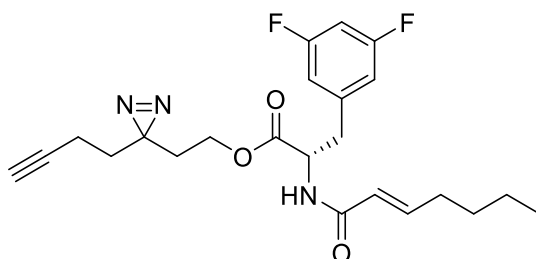
$^{13}\text{C-NMR}$ (75 MHz, CDCl_3): δ (ppm) = 170.5, 165.1, 143.7, 139.5, 124.0, 112.8, 112.5, 103.3, 103.0, 102.6, 82.8, 77.4, 76.2, 69.6, 53.2, 52.9, 37.6, 31.0, 17.7.

HR-MS (ESI): m/z $[\text{M}+\text{H}]^+$ calcd $\text{C}_{19}\text{H}_{17}\text{F}_2\text{NO}_3$: 346.1249, found: 346.1249.

2-(3-(but-3-yn-1-yl)-3H-diazirin-3-yl)ethyl(S)-2-((*tert*-butoxycarbonyl)amino)-3-(3,5-difluorophenyl)propanoate (12e)

Amino acid derivative **12e** was synthesized according to **general procedure A**, using 50.0 mg (166 μmol , 1.0 eq.) *N*-Boc-3,5-difluoro-phenylalanine, 22.9 mg (166 μmol , 1.0 eq.) minimal photocrosslinker **36** (2-(3-(but-3-yn-1-yl)-3H-diazirin-3-yl)ethan-1-ol), 38.2 mg (199 μmol , 1.2 eq.) EDC·HCl and 1.01 mg (8.30 μmol , 0.05 eq.) DMAP in 1.5 mL DCM for 2.5 h. Washing steps were carried out with 2 mL aqueous solution each. 63.3 mg of a yellow oil were obtained. The product was used for the next step without further purification.

2-(3-(but-3-yn-1-yl)-3H-diazirin-3-yl)ethyl(S,E)-3-(3,5-difluorophenyl)-2-(hept-2-enamido)propanoate (BH235)



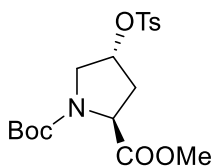
Synthesis was performed according to **general procedure B**, using 64.0 mg (152 μmol , 1.0 eq.) amino acid **12e** and trifluoroacetic acid (1.5 mL, 40% in DCM) for 1.5 h. All of the crude product was used for the amide synthesis according to **general procedure C**, using 21.0 μL (960 mg/mL, 154 μmol , 1.0 eq.) *E*-2-heptenoic acid, 64.0 mg (169 μmol , 1.1 eq.) HATU and 59.0 μL (742 mg/mL, 339 μmol , 2.2 eq.) DIPEA in 1.5 mL DMF for 24 h. Washing steps were carried out with 2 mL aqueous solution each. 28.6 mg (43%) of a light yellow solid were obtained after purification with column chromatography (hexane/ethyl acetate 5/1 to 3/1). $R_f = 0.76$ (hexane/ethyl acetate 3/2).

$^1\text{H-NMR}$ (500 MHz, CDCl_3): δ (ppm) = 6.88 (dt, $J = 15.3, 7.0$ Hz, 1H), 6.75 – 6.62 (m, 3H), 5.94 (d, $J = 7.6$ Hz, 1H), 5.81 (dt, $J = 15.3, 1.5$ Hz, 1H), 4.96 (dt, $J = 7.6, 5.8$ Hz, 1H), 4.06 (dt, $J = 11.4, 6.3$ Hz, 1H), 3.96 (dt, $J = 11.4, 6.3$ Hz, 1H), 3.22 (dd, $J = 13.9, 5.8$ Hz, 1H), 3.15 (dd, $J = 13.9, 5.8$ Hz, 1H), 2.20 (*virt. dq*, $J = 7.0, 1.5$ Hz, 2H), 2.03 – 1.98 (m, 3H), 1.79 (t, $J = 6.3$ Hz, 2H), 1.65 (td, $J = 7.4, 2.3$ Hz, 2H), 1.49 – 1.40 (m, 2H), 1.38 – 1.29 (m, 2H), 0.91 (t, $J = 7.3$ Hz, 3H).

$^{13}\text{C-NMR}$ (126 MHz, CDCl_3): δ (ppm) = 171.0, 165.6, 146.8, 122.7, 112.5, 112.3, 102.9, 82.6, 69.7, 60.6, 53.0, 37.7, 32.2, 32.1, 31.9, 30.4, 26.4, 22.4, 14.0, 13.4.

HR-MS (ESI): m/z $[\text{M}+\text{H}]^+$ calcd $\text{C}_{23}\text{H}_{27}\text{F}_2\text{N}_3\text{O}_3$: 432.2093, found: 432.2092.

1.3.3. Synthesized amino acid derivatives for ADEP synthesis

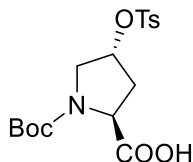
1-(*tert*-butyl) 2-methyl (2S,4R)-4-(tosyloxy)pyrrolidine-1,2-dicarboxylate (21)^[165]

N-Boc-*trans*-4-hydroxy-L-proline methyl ester (**20**, 5.00 g 20.4 mmol, 1.0 eq.) was dissolved in 18 mL dichloromethane and after the solution was cooled to 0 °C, 6.42 mL (982 mg/mL, 79.5 mmol, 3.9 eq.) pyridine was added slowly. 7.77 g (40.8 mmol, 2.0 eq.) *p*-TsCl were dissolved in 18 mL dichloromethane and added slowly to the reaction mixture. The mixture was allowed to warm up to room temperature and was stirred for 72 h. After TLC control, water was added, the phases were separated, the organic layer was dried over Na₂SO₄, and the solvent was removed under reduced pressure. The crude product was purified by column chromatography (hexane/ethyl acetate 2/1) and yielded 6.78 g (83%) of the colorless product. $R_f = 0.28$ (hexane/ethyl acetate 5/1).

¹H-NMR (300 MHz, CDCl₃, mixture of rotamers 3:2 ratio): δ (ppm) = 7.78 (d, $J = 7.8$ Hz, 2H), 7.36 (d, $J = 7.8$ Hz, 2H), 5.09 – 4.99 (m, 1H), 4.44 – 4.29 (m, 1H), 3.72 (s, 3H), 3.68 – 3.55 (m, 2H), 2.60 – 2.34 (m, 4H), 2.24 – 2.05 (m, 1H), 1.40 (2×s, 9H).

MS (ESI): m/z [M-Boc+H]⁺ calcd C₁₈H₂₅NO₇S: 300, found: 300.

Analytical data are in accordance with those published in the literature.^[165]

(2S,4R)-1-(*tert*-butoxycarbonyl)-4-(tosyloxy)pyrrolidine-2-carboxylic acid (22)^[165]

LiOH·H₂O (3.49 g, 83.2 mmol, 4.9 eq.) was added slowly to a solution of 6.78 g (16.9 mmol, 1.0 eq.) proline derivative **21** in 300 mL tetrahydrofuran/water (3/2). The reaction mixture was stirred for 20 h at room temperature. After reaction control, the mixture was brought to pH 2 with 1 M HCl (aq.) and extracted with ethyl acetate (3×150 mL). The organic layer was dried over Na₂SO₄ and the solvent was removed under reduced pressure. 6.01 g (15.6 mmol,

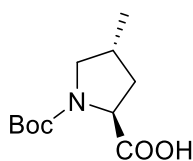
93%) of the pure product was obtained as yellow oil. $R_f=0.35$ (hexane/ethyl acetate 1/1+1%AcOH).

$^1\text{H-NMR}$ (300 MHz, CDCl_3 , mixture of rotamers 3:2 ratio): δ (ppm) = 7.79 (d, $J = 8.2$ Hz, 2H), 7.37 (d, $J = 8.2$ Hz, 2H), 5.08 – 4.96 (m, 1H), 4.52 – 4.30 (m, 1H), 3.82 – 3.47 (m, 2H), 2.68 – 2.13 (m, 5H), 1.43 (2×s, 9H).

MS (ESI): m/z $[\text{M-Boc+H}]^+$ calcd $\text{C}_{17}\text{H}_{23}\text{NO}_7\text{S}$: 286, found: 286.

Analytical data are in accordance with those published in the literature.^[165]

(2S,4R)-1-(tert-butoxycarbonyl)-4-methylpyrrolidine-2-carboxylic acid (23)^[165]

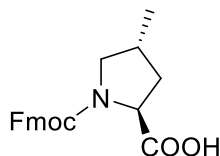


Methyl lithium (1.6 M in diethylether, 5.68 mL, 13.8 mmol, 5.3 eq.) was added to a solution of CuCN (627 mg, 7.01 mmol, 2.7 eq.) in 14 mL THF at -78 °C. The reaction mixture was warmed up and stirred for 15 min at 0 °C. Subsequently the reaction mixture was cooled to -78 °C again, and 1.00 g (2.55 mmol, 1.0 eq.) proline derivative **22** in 9.3 mL tetrahydrofuran was added slowly. The reaction mixture was warmed up to -20 °C quickly and was further allowed to warm up to 0 °C in 3 h. After the reaction mixture was cooled to -20 °C again, saturated NH_4Cl solution was added until no reaction could be observed anymore. The mixture was allowed to warm up to room temperature overnight. 30 mL 1 M HCl (aq.) was added, followed by 10 mL water. After the mixture was extracted with chloroform (3×55 mL), the organic layer was dried over Na_2SO_4 and the solvent was removed under reduced pressure. The crude product was purified by column chromatography (hexane/ethyl acetate 2/1) and yielded 454 mg (1.98 mmol, 76%) of the colorless product. $R_f=0.25$ (hexane/ethyl acetate 2/1).

$^1\text{H-NMR}$ (300 MHz, CDCl_3 , mixture of rotamers 1:1 ratio): δ (ppm) = 4.42 – 4.25 (m, 1H), 3.77 – 3.46 (m, 1H), 3.04 – 2.82 (m, 1H), 2.49 – 2.29 (m, 1H), 1.96 – 1.81 (m, 1H), 1.72 – 1.59 (m, 1H), 1.45 (2×s, 9H), 1.05 (2×s, 3H).

MS (ESI): m/z $[\text{M-Boc+H}]^+$ calcd $\text{C}_{11}\text{H}_{19}\text{NO}_4$: 130, found: 130.

Trans/cis ratio was determined to be 9/1 by $^1\text{H-NMR}$ of the corresponding HCl salt and comparison to published data. Analytical data are in accordance with those already published in the literature.^[165]

(2S,4R)-1-(((9H-fluoren-9-yl)methoxy)carbonyl)-4-methylpyrrolidine-2-carboxylic acid (24)^[143,165]

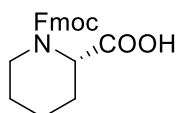
The Boc-protected amino acid derivative **23** (454 mg, 1.98 mmol, 1.0 eq.) was dissolved in 40 mL 4 M HCl in dioxane under argon atmosphere and the reaction mixture was stirred overnight at room temperature. After the solvent was removed under reduced pressure it was diluted in chloroform and the solvent was removed again thrice.

The crude product was diluted in 12 mL dioxane and 24 mL of an aqueous 10% Na₂CO₃ solution were added slowly and the reaction mixture was stirred for 5 min. After the mixture was cooled to -5 °C, Fmoc-Cl (493 mg, 1.90 mmol, 1.0 eq.) in 18 mL dioxane was added and stirred at room temperature for 3 h. Subsequently the reaction mixture was acidified to pH 2 with concentrated HCl, then 60 mL water were added. After the mixture was extracted with chloroform (3×70 mL), the organic layer was washed with saturated NaCl solution and dried over Na₂SO₄. The solvent was removed under reduced pressure and the crude product was purified by column chromatography (hexane/ethyl acetate 4/1 + 1% acetic acid) to yield 583 mg (84%) of the product.

¹H-NMR (300 MHz, CDCl₃): δ (ppm) = 7.82 – 7.69 (m, 2H), 7.65 – 7.50 (m, 2H), 7.47 – 7.27 (m, 4H), 4.56 – 4.21 (m, 4H), 3.86 – 3.44 (m, 1H), 3.06 – 2.91 (m, 1H), 2.53 – 2.09 (m, 2H), 2.03 – 1.65 (m, 1H), 1.12 – 0.98 (m, 3H).

MS (ESI): *m/z* [M+H]⁺ calcd C₂₁H₂₁NO₄: 352, found: 353.

Analytical data are in accordance with those published in the literature.^[143]

(S)-1-(((9H-fluoren-9-yl)methoxy)carbonyl)piperidine-2-carboxylic acid (30)^[190]

Fmoc-Cl (2.20 g, 8.52 mmol, 1.1 eq.) in 33 mL dioxane was added to a solution of 1.00 g (7.74 mmol, 1.0 eq.) pipercolic acid and 4.10 g (37.7 mmol, 5.0 eq.) Na₂CO₃ in 33 mL water and the reaction mixture was stirred for 72 h at room temperature. Subsequently 50 mL water

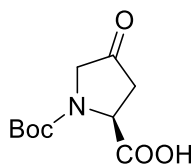
were added and the mixture was washed with diethylether (3×10 mL). The aqueous phase was acidified (pH 2, conc. HCl), extracted with ethyl acetate (3×15 mL) and the organic layer was washed with saturated NaCl solution (1×15 mL) and dried over Na₂SO₄. The solvent was removed under reduced pressure and the crude product was purified by column chromatography (hexane/ethyl acetate 1/1 + 1% acetic acid) to yield 2.01 g (74%) of the colorless product.

¹H-NMR (300 MHz, CDCl₃): δ (ppm) = 7.85 – 7.70 (m, 2H), 7.70 – 7.50 (m, 2H), 7.46 – 7.28 (m, 4H), 5.14 – 4.69 (m, 1H), 4.59 – 4.36 (m, 2H), 4.33 – 4.01 (m, 2H), 3.40 – 2.98 (m, 1H), 2.48 – 2.12 (m, 1H), 1.83 – 1.58 (m, 3H), 1.59 – 1.14 (m, 2H).

MS (ESI): *m/z* [M+H]⁺ calcd C₂₁H₂₁NO₄: 352, found: 352.

Analytical data are in accordance with those published in the literature.^[190]

(S)-1-(*tert*-butoxycarbonyl)-4-oxopyrrolidine-2-carboxylic acid (26)

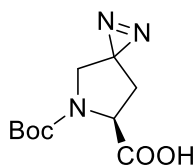


2.00 g (8.65 mmol, 1.0 eq.) Trichloroisocyanuric acid (TCCA) was added to 2.00 g (**23**, 8.65 mmol, 1.0 eq.) *N*-Boc-L-hydroxyproline in 40 mL DCM, the solution was cooled to 0 °C and 67.0 mg (432 μmol, 0.05 eq.) 2,2,6,6-Tetramethylpiperidinyloxy (TEMPO) was added and the reaction mixture was stirred for 30 min at 0 °C and 3 h at room temperature. Subsequently 20 mL water were added and the solvents removed under reduced pressure. The resulting slurry was taken up in 30 mL ethyl acetate, filtered through Celite[®] and the solution was acidified with 1 M HCl (aq.) to pH 4. The organic layer was washed with water (3×10 mL) and saturated NaCl solution (10 mL), dried over Na₂SO₄ and the solvent was removed under reduced pressure. 1.70 g (86%) of a light brown solid were obtained as pure product.

¹H-NMR (500 MHz, acetone-*d*₆, mixture of rotamers 5:4 ratio): δ (ppm) = 4.73 (t, *J* = 7.4 Hz, 1H), 3.95 – 3.66 (m, 2H), 3.13 (*virt.* td, *J* = 19.0, 10.4 Hz, 1H), 2.57 (*virt.* dd, *J* = 19.0, 7.4 Hz, 1H), 1.45 (2×s, 9H).

MS (ESI): *m/z* [M+ACN+Na]⁺ calcd C₁₀H₁₅NO₅: 293 found: 293.

Analytical data are in accordance with those published in the literature.^[166,191]

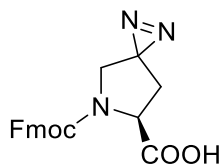
(S)-5-(*tert*-butoxycarbonyl)-1,2,5-triazaspiro[2.4]hept-1-ene-6-carboxylic acid (27)

9.35 mL (7 N in MeOH, 65.4 mmol, 15 eq.) NH_3 was added to a solution of 1.00 g (4.36 mmol, 1.0 eq.) ketone **26** in 3.5 mL MeOH under argon atmosphere at $-10\text{ }^\circ\text{C}$. After the reaction mixture was stirred at $-10\text{ }^\circ\text{C}$ for 5 h, 641 mg (5.67 mmol, 1.3 eq.) hydroxylamine-*O*-sulfonic acid in 4 mL MeOH were added at $-78\text{ }^\circ\text{C}$ and the reaction mixture was stirred for 1.5 h at $-10\text{ }^\circ\text{C}$. The mixture was allowed to warm up to room temperature, stirred for 16 h and filtered off and washed with methanol (10 mL). Subsequently 1.22 mL (726 mg/mL, 8.77 mmol, 2.0 eq.) NEt_3 was added and the reaction was cooled to $0\text{ }^\circ\text{C}$ before 1.44 g (5.67 mmol, 1.3 eq.) iodine (in 25 mL MeOH) was added, until a brown color remains. The reaction mixture was stirred for 2 h at $0\text{ }^\circ\text{C}$ before the solvent was removed under reduced pressure. The resulting slurry was taken up in 25 mL water, brought to pH 2 with 1 M HCl (aq.) and extracted with ethyl acetate (4×8 mL). The organic layer was washed with saturated NaCl solution (3×10 mL) and dried over Na_2SO_4 . The solvent was removed under reduced pressure and the crude product was purified by reversed phase HPLC (ACN/ H_2O ; ACN 2% to 98%) and yielded 166 mg (11%) of the pure product.

$^1\text{H-NMR}$ (500 MHz, CDCl_3 , mixture of rotamers 5:4 ratio): δ (ppm) = 4.74 – 4.51 (m, 1H), 3.27 – 3.01 (m, 2H), 2.44 – 2.23 (m, 1H), 1.87 – 1.61 (m, 1H), 1.51 – 1.41 (m, 9H).

HR-MS (ESI): m/z $[\text{M-H}]^-$ calcd $\text{C}_{10}\text{H}_{15}\text{N}_3\text{O}_4$: 240.0990, found: 240.0991.

Analytical data are in accordance with those published in the literature.^[166,191]

(S)-5-(((9H-fluoren-9-yl)methoxy)carbonyl)-1,2,5-triazaspiro[2.4]hept-1-ene-6-carboxylic acid (28)

0.66 mL conc. HCl was added to a solution of 280 mg (1.16 mmol, 1.0 eq.) diazirine **27** in 6 mL dioxane, the reaction mixture was stirred for 2 h and the solvent was removed under reduced pressure. The resulting slurry was taken up in 10 mL water and lyophilized overnight.

The brown oil was diluted in 5.6 mL of a 9% Na₂CO₃ aqueous solution and 353 mg (1.05 mmol, 0.9 eq.) Fmoc-succinimide in 1.2 mL DMF/dioxane (1/1) was added and the reaction stirred for 5 min. Subsequently 6.3 mL DMF/dioxane (1/1) were added and the mixture was stirred for 10 min before 25 mL water were added. After the mixture was washed with diethylether (20 mL) and ethyl acetate (20 mL), the aqueous layer was acidified with conc. HCl to pH 2. The aqueous phase was extracted with ethyl acetate (5×20 mL), dried over Na₂SO₄ and the solvent was removed under reduced pressure. The crude product was purified by reversed phase HPLC (ACN/H₂O; ACN 2% to 98%) and 331 mg (73%) pure product were obtained.

¹H-NMR (500 MHz, CDCl₃): δ (ppm) = 7.78 – 7.73 (m, 2H), 7.56 – 7.53 (m, 2H), 7.42 – 7.29 (m, 4H), 4.73 (dd, *J* = 9.9, 2.6 Hz, 1H), 4.56 – 4.41 (m, 2H), 4.31 – 4.16 (m, 1H), 3.33 – 3.21 (m, 1H), 3.17 – 3.06 (m, 1H), 2.44 – 2.33 (m, 1H), 1.76 (dd, *J* = 15.2, 2.6 Hz, 0.6H), 1.56 (dd, *J* = 15.2 Hz, 0.4H).

HR-MS (ESI): *m/z* [M+H]⁺ calcd C₂₀H₁₇N₃O₄: 364.1292, found: 364.1292.

Analytical data are in accordance with those published in the literature.^[166,191]

1.3.4. General procedures for solid phase peptide synthesis and cyclization

General Procedure D: Loading of the resin.

The weight of a syringe fitted with a frit was determined, the resin (2-chlorotriyl chloride resin, 100-200 mesh, loading: 0.958 mmol/g) was added, and the weight determined again. The amino acid was dissolved in 3 mL dichloromethane, 140 μ L DIPEA were added, the solution was filled into the syringe and was shaken for 4 h. Subsequently 0.5 mL methanol was added and the syringe was shaken for 15 min. Then the resin was washed with DCM (1 \times 5 mL), DMF (3 \times 5 mL), DCM (3 \times 5 mL) and MeOH (2 \times 5 mL), before it was dried for 3 h in a desiccator. The weight of the syringe with resin was determined again and the load of the resin was calculated with the following equation (1, m_1 =weight of unloaded resin, m_2 =weight of loaded resin).

$$n = \frac{(m_2 - m_1) * 1000}{(M_{AA} - M_{HCl}) * m_2} \quad (1)$$

General Procedure E: Deprotection of amino acids.

Before the first deprotection, the resin was shaken with 5 mL DMF for 20 min. For the deprotection, the resin was shaken with 5 mL 20% piperidine in DMF for 10 min, the same procedure was repeated with fresh solution for another 5 min. After that, the resin was washed with 5 mL DMF (3 \times 2 min).

General Procedure F: Coupling of amino acids.

HATU (154 mg, 410 μ mol) in DMF (2.0 mL) was added to the corresponding amino acid in DMF (2.0 mL), followed by DIPEA (198 μ L, 742 mg/mL, 1.14 mmol) in DMF (0.5 mL) and nitrogen was forced through the solution for 5 min. 2.5 mL DMF were added to the resin, followed by the amino acid mixture. The resin was shaken for 2 h and then washed with DMF (5 \times 5 mL). A chloranil test was performed after each coupling to check for completion of the reaction.

General Procedure G: Execution of the chloranil test.

A few resin beads were washed with DCM and given in a small reaction vessel. 200 μ L acetone or acetaldehyde were added for secondary or primary amines, respectively. After 50 μ L chloranil (saturated solution in toluol) was added, the mixture was shaken for 10 min. When the resin beads turned blue or green, the coupling step was repeated.

General Procedure H: Cleavage of the resin.

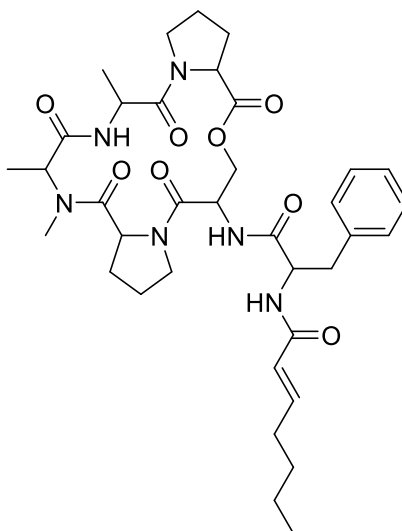
The resin was shaken with 7 mL DMF (2×5 min) and 7 mL methanol (3×5 min) and dried under high vacuum. Then, 1.5 mL triisopropylsilane and 0.3 mL TFA in 4 mL DCM were added and rinsed with 2 mL DCM. After the mixture was shaken for 1 h, the solution was given into a flask and the procedure was repeated. Nitrogen was flushed over the combined solutions overnight and the residue was taken up in chloroform, which was removed under reduced pressure three times. After the peptide was dried under high vacuum for 2.5 h, it was resuspended in 5 mL pentane/diethylether (1/1) in an ultrasonic bath and filtered subsequently. The pure peptide was dried under high vacuum again.

General Procedure I: Cyclization of the heptapeptide.

To a solution of MNBA (2-Methyl-6-nitrobenzoic anhydride) and DMAP in DCM, DIPEA was added, followed by Dy(OTf)₃ under argon atmosphere. The peptide in DCM was added to the refluxing mixture over 24 h and the solvent was removed under reduced pressure. The crude product was purified by reversed phase HPLC.

1.3.5. Synthesized peptides by solid phase peptide synthesis and cyclization

ADEP derivative BH279



518 mg 2-chlorotrityl chloride resin was loaded with Fmoc-proline (222 mg, 658 μmol) according to **general procedure D**, to obtain a loading of 766 $\mu\text{mol/g}$. Following amino acids were coupled to the resin using **general procedures E, F and G**: Fmoc-alanine (62.3 mg, 200 μmol), Fmoc-Me-alanine (97.6 mg, 300 μmol), Fmoc-proline (101 mg, 285 μmol), Fmoc-serine (103 mg, 284 μmol), Fmoc-phenylalanine (116 mg, 300 μmol) and *E*-2-heptenoic acid (40.5 μL , 950 mg/mL, 304 μmol). The heptapeptide was cleaved of the resin using **general procedure H** and the cyclization was performed according to **general procedure I**, using the resulting heptapeptide (60.0 mg, 84.2 μmol , 1.0 eq.), MNBA (86.9 mg, 253 μmol , 3.0 eq.), DIPEA (40.1 μL , 742 mg/mL, 236 μmol , 2.8 eq.), DMAP (61.7 mg, 505 μmol , 6.0 eq.) and $\text{Dy}(\text{OTf})_3$ (51.3 mg, 84.2 μmol , 1.0 eq.). The crude product was purified by reversed phase HPLC (ACN/ H_2O ; ACN 2% to 60%). Identity was determined *via* HR-LC-MS, NMR data are provided as additional information.

$^1\text{H-NMR}$ (500 MHz, CDCl_3): δ (ppm) = 8.56 (d, $J = 9.5$ Hz, 1H), 7.30 – 7.27 (m, 2H), 7.23 – 7.07 (m, 4H), 6.92 (dt, $J = 14.7, 7.1$ Hz, 1H), 6.67 (d, $J = 8.8$ Hz, 1H), 6.22 (d, $J = 15.4$ Hz, 1H), 5.16 (dd, $J = 8.4, 2.7$ Hz, 1H), 4.95 – 4.86 (m, 1H), 4.86 – 4.75 (m, 2H), 4.61 (q, $J = 7.5$ Hz, 1H), 4.51 (t, $J = 9.7$ Hz, 1H), 4.46 (d, $J = 8.4$ Hz, 1H), 3.78 – 3.69 (m, 1H), 3.66 – 3.48 (m, 3H), 3.36 – 3.27 (m, 1H), 2.97 (d, $J = 7.3$ Hz, 2H), 2.85 (s, 3H), 2.44 – 2.29 (m, 1H), 2.25 – 2.11 (m, 4H), 2.05 – 1.83 (m, 5H), 1.53 (d, $J = 6.9$ Hz, 3H), 1.47 – 1.20 (m, 7H), 0.89 (t, $J = 7.2$ Hz, 4H).

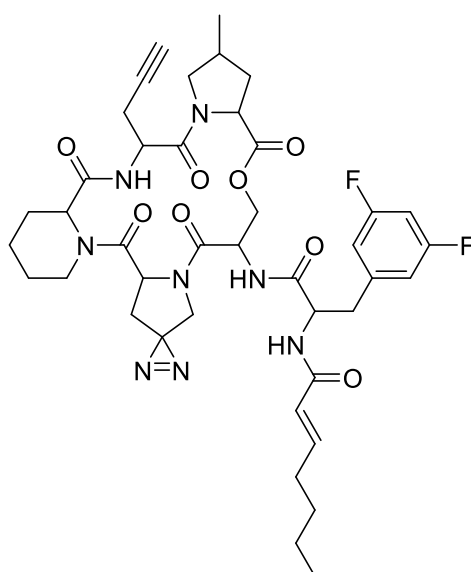
$^{13}\text{C-NMR}$ (126 MHz, CDCl_3): δ (ppm) = 172.8, 172.2, 171.4, 170.1, 170.1, 166.7, 164.8, 146.6, 136.1, 129.5, 128.8, 127.1, 123.2, 64.9, 59.3, 56.6, 56.4, 55.6, 51.2, 48.1, 47.2, 46.7, 38.9, 32.0, 31.1, 31.0, 30.7, 30.5, 23.3, 22.4, 21.3, 17.7, 15.8, 14.0.

HR-LC-MS (ESI): m/z $[\text{M}+\text{H}]^+$ calcd $\text{C}_{36}\text{H}_{50}\text{N}_6\text{O}_8$: 695.3763, found: 695.3761.

HPLC (2-60% ACN, 17 min): R_t =11.0-11.4 min.

Analytical data are in accordance with those published in the literature.^[143]

ADEP-Probe 266



503 mg 2-chlorotrityl chloride resin was loaded with Fmoc-proline derivative **24** (126 mg, 359 μmol) according to **general procedure D**, to get a loading of 473 $\mu\text{mol/g}$. Following amino acids were coupled to the resin using **general procedures E, F and G**: Fmoc-propargylglycine (158 mg, 473 μmol), Fmoc-pipecolic acid (**30**, 170 mg, 473 μmol), Fmoc-photoproline **28** (124 mg, 341 μmol), Fmoc-serine (154 mg, 473 μmol), Fmoc-3,5-difluorophenylalanine (129 mg, 306 μmol) and *E*-2-heptenoic acid (63.4 μL , 950 mg/mL, 473 μmol). The heptapeptide was cleaved of the resin using **general procedure H** and the cyclization was performed according to **general procedure I**, using the resulting heptapeptide (10.0 mg, 11.9 μmol , 1.0 eq.), MNBA (12.3 mg, 35.7 μmol , 3.0 eq.), DIPEA (5.68 μL , 742 mg/mL, 33.4 μmol , 2.8 eq.), DMAP (8.70 mg, 71.5 μmol , 6.0 eq.) and $\text{Dy}(\text{OTf})_3$ (7.30 mg, 11.9 μmol , 1.0 eq.). The crude product was purified by reversed phase HPLC (ACN/ H_2O ; ACN 2% to 60%). Yield: 8.34 mg (85%). Identity was determined *via* HR-LC-MS, NMR data are provided as additional information.

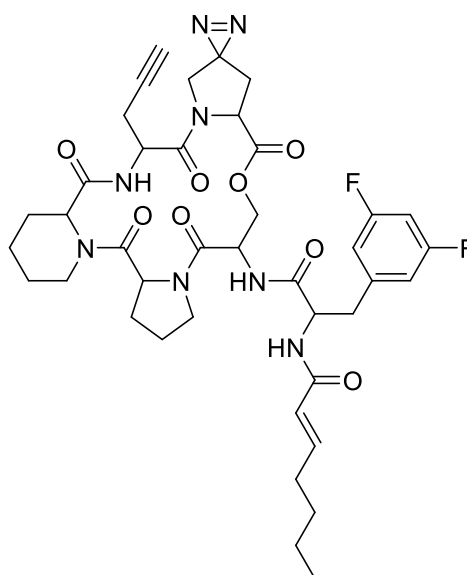
¹H-NMR (500 MHz, methanol-*d*₄): δ (ppm) = 8.53 (d, *J* = 9.7 Hz, 1H), 6.90 – 6.64 (m, 3H), 6.22 (dt, *J* = 15.3, 1.5 Hz, 1H), 5.50 (dd, *J* = 9.8, 2.1 Hz, 1H), 5.31 (ddd, *J* = 5.7, 4.4, 1.1 Hz, 2H), 5.21 – 5.06 (m, 1H), 4.96 (dd, *J* = 11.9, 1.8 Hz, 1H), 4.77 – 4.71 (m, 1H), 4.62 (dd, *J* = 7.9, 5.7 Hz, 1H), 4.59 – 4.49 (m, 2H), 4.07 (s, 1H), 3.76 – 3.39 (m, 2H), 3.23 – 2.70 (m, 2H), 2.63 (s, 2H), 2.42 – 2.12 (m, 5H), 2.09 – 1.89 (m, 4H), 1.73 – 1.52 (m, 4H), 1.51 – 1.39 (m, 3H), 1.21 – 1.12 (m, 1H), 1.07 – 0.97 (m, 2H), 0.97 – 0.78 (m, 13H).

¹³C-NMR (126 MHz, methanol-*d*₄): δ (ppm) = 177.9, 172.3, 170.8, 170.0, 168.2, 165.9, 145.3, 140.8, 129.4, 123.1, 121.1, 81.0, 71.2, 64.0, 59.8, 57.5, 56.1, 54.4, 51.0, 50.5, 45.9, 42.1, 41.6, 40.7, 39.7, 39.0, 37.8, 35.1, 33.2, 31.9, 31.7, 31.3, 30.9, 30.2, 29.4, 29.2, 29.1, 28.9, 28.8, 26.7, 25.5, 22.4, 21.8, 20.1, 12.8.

HR-LC-MS (ESI): *m/z* [M+H]⁺ calcd C₄₁H₅₀F₂N₈O₈: 821.3783, found: 821.3782.

HPLC (2-98% ACN, 17 min): Rt=10.2-11.3 min.

ADEP-Probe 288



559 mg 2-chlorotrityl chloride resin was loaded with Fmoc-photoproline **28** (110 mg, 303 μmol) according to **general procedure D**, to get a loading of 400 μmol/g. Following amino acids were coupled to the resin using **general procedures E, F and G**: Fmoc-propargylglycine (172 mg, 510 μmol), Fmoc-pipecolic acid (**30**, 181 mg, 510 μmol), Fmoc-proline (173 mg, 510 μmol), Fmoc-serine (177 mg, 510 μmol), Fmoc-3,5-difluorophenylalanine (218 mg, 510 μmol) and *E*-2-heptenoic acid (69.4 μL, 950 mg/mL, 510 μmol). The heptapeptide was cleaved of the resin using **general procedure H** and the cyclization

was performed according to **general procedure I**, using the resulting heptapeptide (50.0 mg, 60.6 μmol , 1.0 eq.), MNBA (62.6 mg, 182 μmol , 3.0 eq.), DIPEA (28.9 μL , 742 mg/mL, 170 μmol , 2.8 eq.), DMAP (44.4 mg, 364 μmol , 6.0 eq.) and Dy(OTf)₃ (37.0 mg, 60.6 μmol , 1.0 eq.). The crude product was purified by reversed phase HPLC (ACN/H₂O; ACN 2% to 98%). Yield: 3.05 mg (6%). Identity was determined *via* HR-LC-MS, NMR data are provided as additional information.

¹H-NMR (500 MHz, methanol-*d*₄): δ (ppm) = 8.64 (d, J = 9.7 Hz, 1H), 8.19 – 8.10 (m, 1H), 7.33 – 7.01 (m, 3H), 6.91 – 6.71 (m, 1H), 6.16 (d, J = 15.1 Hz, 1H), 5.44 – 5.26 (m, 1H), 4.73 (d, J = 8.9 Hz, 1H), 4.63 – 4.47 (m, 1H), 3.98 – 3.78 (m, 1H), 3.73 – 3.62 (m, 1H), 3.53 – 3.41 (m, 1H), 3.21 – 3.06 (m, 1H), 3.00 – 2.83 (m, 2H), 2.82 – 2.57 (m, 3H), 2.57 – 2.32 (m, 2H), 2.30 – 1.86 (m, 5H), 1.85 – 1.55 (m, 4H), 1.45 – 1.27 (m, 9H), 1.21 – 1.14 (m, 1H), 0.93 (t, J = 7.2 Hz, 3H).

¹³C-NMR (126 MHz, methanol-*d*₄): δ (ppm) = 172.0, 171.4, 170.9, 170.3, 168.1, 145.3, 123.1, 118.0, 117.0, 80.7, 71.3, 65.1, 58.1, 57.5, 57.1, 54.5, 51.2, 50.2, 48.7, 46.2, 40.7, 37.5, 33.0, 31.3, 30.6, 30.2, 30.0, 27.4, 27.3, 24.5, 22.6, 21.8, 21.6, 20.4, 12.8.

HR-MS (ESI): m/z [M+H]⁺ calcd C₄₀H₄₈F₂N₈O₈: 807.8636, found: 807.8636.

HPLC (2-98% ACN, 17 min): Rt=10.0-10.5 min.

2. Biochemical Procedures

2.1. General material and methods

2.1.1. *Buffers and Solutions*

In general, ddH₂O is used as a solvent if not defined differently.

General Buffers	Composition	
PBS (pH 7.4)	136.9 mM	NaCl
	10.1 mM	Na ₂ HPO ₄
	2.7 mM	KCl
	1.8 mM	KH ₂ PO ₄
HEPES (pH 7.5)	30 mM	HEPES
PZ-Buffer (pH 7.6)	25 mM	HEPES
	200 mM	KCl
	5 mM	MgCl ₂ ·6H ₂ O
	1 mM	DTT
	10% (v/v)	Glycerol

Buffers/Solutions for SDS-PAGE	Composition	
Laemmli Buffer (2×)	63 mM	Tris-HCl
	10% (v/v)	Glycerol
	2% (w/v)	SDS
	0.0025% (w/v)	Bromphenol blue
	5% (v/v)	β-Mercaptoethanol
SDS Running Buffer (10×, pH 8.3)	24.8 mM	Tris
	191.8 mM	Glycine
	3.5 mM	SDS
Coomassie Staining Solution	0.25% (w/v)	Coomassie Brilliant Blue R250
	9.2% (v/v)	Acetic acid
	45.4% (v/v)	Ethanol
Coomassie Destaining Solution	10% (v/v)	Acetic acid
	20% (v/v)	Ethanol

Buffers/Solutions for WB Analysis	Compositioin	
Blotting Buffer	48 mM	Trizma
	39 mM	Glycine
	0.04% (w/v)	SDS
	20% (v/v)	MeOH
PBS-T	0.5% (v/v)	Tween-20 in PBS
Ponceau Red	0.1 % (w/v)	Ponceau S
	5% (v/v)	Acetic acid

2.1.2. Bacterial strains and media

Commercially available *S. aureus* strains were obtained from the following suppliers: Institute Pasteur, France (NCTC8325); American Type Culture Collection (ATCC33591, ATCC6538). Strains SH1000 and USA300-0114 were obtained from Prof. Bettina Buttaro at the Lewis Katz School of Medicine at Temple University. The NCTC8325 Δ clpP strain was constructed as published by Fetzer *et al.*^[192]

Organism	Strain	Mutant / wt	Medium	Antibiotic
<i>S. aureus</i>	NCTC8325	wt	B / BHB	-
<i>S. aureus</i>	USA300	wt	B / BHB	-
<i>S. aureus</i>	NCTC8325	Δ clpP	BHB	Erythromycin
<i>E. coli</i>	BL21 (DE3)		LB	

Bacterial Medium	Composition	
LB medium	5.0 g/L	Yeast extracts
	10 g/L	Tryptic peptone
	5.0 g/L	NaCl
B medium	5.0 g/L	Yeast extracts
	10 g/L	Tryptic peptone
	5.0 g/L	NaCl
	1.0 g/L	K ₂ HPO ₄

BHB medium	17.5 g/L	Brain Heart Infusion
	2.5 g/L	Na ₂ HPO ₄
	2.0 g/L	Glucose
	5.0 g/L	Tryptic peptone
	5.0 g/L	NaCl

1000× Antibiotic Stock	Concentration	
Erythromycin	10 mg/mL	in EtOH
Ampicillin	100 mg/mL	in ddH ₂ O/EtOH 1/1

2.1.3. Cultivation methods of bacteria

For an overnight culture 5 mL of the respective medium and 5 µL of bacterial glycerol stock were shaken in a culture tube over night at 37 °C and 200 rpm. Day cultures were grown in 250 mL flasks with four baffles, with 50 mL medium and 1:100 inoculations with overnight culture. Bacterial glycerol stocks were prepared out of 600 µL overnight culture and 400 µL sterile glycerol and frozen at -80 °C. For growth curves, OD₆₀₀ measurements (*Eppendorf BioPhotometer*) were conducted every 30 to 60 minutes with 1:10 dilution of the bacterial suspension.

2.1.4. Determination of MIC values

The minimal inhibitory concentration (MIC) is defined as the concentration of a compound sufficient to fully inhibit visible growth of bacteria. The outer rows of a clear flat bottom 96-well plate were filled with 150 µL medium as sterile control without any bacteria or compound. 75 µL medium were provided in the remaining wells and 75 µL of DMSO or compound (1:200) in medium were added in the first column. For a dilution series, 75 µL were taken out of the first column and were diluted 1:1 with the medium in the second column, and so on. An overnight culture of the desired bacteria was diluted 1:5000 with medium and 75 µL were added to all inner wells. The bacteria were incubated for 18 h at 37 °C and 200 rpm. The MIC of the substances was defined as the lowest concentration at which no bacterial growth could be observed.

2.1.5. BCA Assay

A dilution series of bovine serum albumin (BSA, 400 µg/mL, 200 µg/mL, 100 µg/mL, 50 µg/mL, 25 µg/mL, 0 µg/mL) and protein samples were diluted with PBS (1:10) and 50 µL were pipetted in a 96-well plate (transparent, flat bottom) in triplicates. To each well 100 µL freshly prepared BCA mix (15 parts reagent 1 and one part reagent 2, Roti[®]-Quant universal, *Carl Roth*) were added. After 30 min at 37 °C the absorption at 492 nm was measured at a Tecan Infinite M200pro. Protein concentrations can be determined from the BSA calibration curve.

2.1.6. SDS-PAGE

After 100 µL 2× Laemmli sample buffer were added to each sample, samples were vortexed and analyzed *via* SDS PAGE: 12.5% or 15% agarose gel (PEQLAB *Biotechnologie GmbH*, PerfectBlue Dual Gel System, gels were prepared according to the manual), 2.5 h, 150 V, 8 µL fluorescent protein standard (BenchMark[™] Fluorescent Protein Standard, *Thermo Fischer Scientific*) and fluorescence imaging (*GE Healthcare*, ImageQuant LAS-4000).

2.2. Biochemical methods for Chapter II

2.2.1. *Hemolysis Assay in Solution*

This assay was performed by Dr. Jan Vomacka and Barbara Eyermann for **AV73** and by Barbara Eyermann for **AV73-p**.

50 μL of an overnight culture of *S. aureus* was grown in 5 mL B medium in a plastic culture tube until an OD_{600} between 0.38 and 0.59 was reached. Bacteria were serially diluted in B medium [1:9 (v/v) in three steps] to get a final concentration of 3.4×10^4 bacteria per mL according to previously recorded growth curves. To 990 μL of bacterial suspension was added 10 μL DMSO or compound (100 \times stock in DMSO, different concentrations) in a plastic culture tube, vortexed and grown for 20 h at 37 $^{\circ}\text{C}$ and 200 rpm with tightly closed lid. 800 μL were harvested in a 2 mL microcentrifuge tube at 6600 $\times g$ for 7 min at room temperature. 100 μL of the supernatant were transferred to a microtiter plate (in triplicates) and incubated with 50 μL of diluted sheep blood solution [10% (v/v) in PBS, heparinized sheep blood washed 5 \times with PBS, *Elocin-lab GmbH*] and measured in a 1 min interval at 600 nm at 37 $^{\circ}\text{C}$ with a Tecan Infinite M200pro. Incubation of 100 μL growth medium with 50 μL sheep blood solution was used as a negative, DMSO as a positive control.

2.2.2. *Biofilm Assay*

Biofilm assays for *S. aureus* strains SH1000, USA300-0114, ATCC33591 and ATCC6538 were conducted by Dr. Megan C. Jennings using procedure 2. Biofilm assays for strain NCTC8325 were performed by Dr. Jan Vomacka (**AV73**) and Barbara Eyermann (**AV73** and **AV73-p**) using procedure 1.

Procedure 1

50 μL of an overnight culture of *S. aureus* was grown in 5 mL BHB medium (1:100) in a plastic culture tube. Test compound in DMSO or DMSO control were added with a volume ratio of 1:100 and the cultures were grown under static conditions at 37 $^{\circ}\text{C}$ for 24 h in a 96-well plate with 100 μL culture per well. Bacterial culture was removed carefully with a multichannel pipette avoiding biofilm destruction. The biofilm was carefully washed with 200 μL ddH₂O. The 96-well plates were dried for 3 h at 37 $^{\circ}\text{C}$ under static conditions and then dried overnight at room temperature. Per well, 50 μL of a 1:5 dilution of 1% (w/v) crystal violet (dissolved in 25% ethanol in ddH₂O) in PBS were added and the plate was incubated for 10 min at room temperature. The crystal violet solution was removed, the

colored biofilm washed 2-4 times with ddH₂O and dissolved in 30% acetic acid in ddH₂O. After 1:10 dilution in 30% acetic acid in ddH₂O, the absorbance at 595 nm was measured with a TECAN Infinite M200pro.

Procedure 2

50 µL of an overnight culture of *S. aureus* was grown in 5 mL BHB medium in a plastic culture tube. After 1:100 dilution of the culture with fresh BHB medium, test compound in DMSO or DMSO control were added with a volume ratio of 1:100 and the cultures were grown under static conditions at 37 °C for 24 h in a 96-well plate with 100 µL culture per well. Plates were emptied by inverting and shaking, washed with 200 µL ddH₂O and dried for 3 h at 37 °C and overnight at room temperature. Per well 50 µL of 1% (w/v) crystal violet (25% in ethanol in ddH₂O) was added and incubated for 10 min at room temperature. Excess crystal violet was removed by submerging plates in fresh tap water until the run off was colorless. Plates were then inverted and dried at room temperature. Crystal violet was redissolved with 200 µL of 95% ethanol, 100 µL of which was then transferred to a fresh flat bottom 96-well plate for absorbance measurements at 595 nm.

2.2.3. Whole proteome analysis

The whole experiment was conducted by Dr. Jan Vomacka, data analysis was performed by Dr. Jan Vomacka and Barbara Eyermann.

Growth

Bacteria were cultured under defined growth conditions according to chapter 2.2.1. for 20 h or chapter 2.2.2. for 24 h. Cultures were collected in a 50 mL falcon tube and centrifuged at 6200×g for 5 min at 4 °C. 3 mL of the supernatant were precipitated with 12 mL cold acetone (−80 °C, MS grade). The remaining supernatant was disposed and the pellet was resuspended in PBS to get OD₆₀₀ = 40. 1 mL of this suspension was centrifuged (6200×g, 2 min, 4 °C), the supernatant was removed and the pellets were stored over night at −80 °C.

Lysis and Precipitation

Pellets were resuspended in 1 mL PBS (4 °C) and transferred to a 'Precellys Glass/Ceramic Kit SK38 2.0 mL' tube. Tubes were cooled on ice for 5 min and cells were lysed with the Precellys Homogeniser using three times lysis program 3 (5400 rpm, run number: 1, run time: 20 sec, pause: 5 sec). After each lysis run the tubes were cooled on ice for 5 min. The ball mill tubes were centrifuged (16200×g, 10 min, 4 °C), 800 µL of supernatant were transferred to 15 mL falcon tubes and 4 mL of cold acetone (−80 °C, MS grade) were added. Proteins

were precipitated over night at $-80\text{ }^{\circ}\text{C}$. The precipitated proteins were thawed on ice, pelletized ($16900\times g$, 15 min, $4\text{ }^{\circ}\text{C}$) and the supernatant was disposed. Falcon tubes were stored on ice during the following washing procedure: The proteins were washed two times with 1 mL cold methanol ($-80\text{ }^{\circ}\text{C}$). Resuspension was achieved by sonication (15 sec at 10% intensity) and proteins were pelletized *via* centrifugation ($16900\times g$, 10 min, $4\text{ }^{\circ}\text{C}$). Only MS grade water was used for the following procedures.

Reduction, Alkylation, Digest

After washing the pellet was resuspended in 200 μL denaturation buffer (7 M urea, 2 M thiourea in 20 mM, HEPES buffer, pH 7.5). Dithiothreitol (DTT, 1 M, 0.2 μL) was added, the tubes were mixed by vortexing shortly and incubated in a thermoshaker (450 rpm, 45 min, r.t.). Then 2-iodoacetamide (IAA, 550 mM, 2 μL) was added, the tubes were mixed by vortexing shortly and incubated in a thermoshaker (450 rpm, 30 min, r.t., in the dark). Remaining IAA was quenched by the addition of DTT (1 M, 0.28 μL). The tubes were shortly mixed by vortexing and incubated in a thermoshaker (450 rpm, 30 min, r.t.). LysC (0.5 $\mu\text{g}/\mu\text{L}$) was thawed on ice and 1 μL was added to each microcentrifuge tube, the tubes were shortly mixed by vortexing and incubated in a thermoshaker (450 rpm, 4 h, r.t., in the dark). TEAB (tetraethylammonium bromide) solution (600 μL , 50 mM in water) and then trypsin (1.5 μL , 0.5 $\mu\text{g}/\mu\text{L}$ in 50 mM acetic acid) were added to each tube with a short vortexing step after each addition. The microcentrifuge tubes were incubated in a thermoshaker (450 rpm, 13-15 h, $37\text{ }^{\circ}\text{C}$). The digest was stopped by adding 6 μL formic acid (FA) and vortexing.

Desalting and Labeling

50 mg SepPak C18 columns (*Waters*) were equilibrated by gravity flow with 1 mL acetonitrile, 1 mL elution buffer (80% ACN, 0.5% FA) and 3 mL aqueous 0.5% FA solution. Subsequently the samples were loaded by gravity flow, washed with 5 mL aqueous 0.5% FA solution and labeled with 5 mL of the respective dimethyl labeling solution. The following solutions were used: light (L): 30 mM NaBH_3CN , 0.2% CH_2O , 10 mM NaH_2PO_4 , 35 mM Na_2HPO_4 , pH 7.5; medium (M): 30 mM NaBH_3CN , 0.2% CD_2O , 10 mM NaH_2PO_4 , 35 mM Na_2HPO_4 , pH 7.5; heavy (H): 30 mM NaBD_3CN , 0.2% $^{13}\text{CD}_2\text{O}$, 10 mM NaH_2PO_4 , 35 mM Na_2HPO_4 , pH 7.5. Labeled peptides were eluted into new 2.0 mL Protein LoBind Eppendorf tubes, by the addition of 250 μL elution buffer by gravity flow followed by 250 μL elution buffer by vacuum flow until all liquid was eluted from the column. The eluates were lyophilized.

Before MS measurement the samples were dissolved in 30 μL 1% FA by pipetting up and down, vortexing and sonication for 15 min (brief centrifugation after each step). Differentially labeled samples were mixed. 0.45 μm centrifugal filter units (VWR) were equilibrated with two times 500 μL water, 500 μL 0.05 N NaOH and two times 500 μL 1% FA (centrifugation: 16200 \times g, 1 min, r.t.). Reconstituted samples were filtered through the equilibrated filters (centrifugation: 16200 \times g, 2 min, r.t.).

MS/MS-measurement

Samples were analyzed *via* HPLC-MS/MS using an UltiMate 3000 nano HPLC system (Dionex) equipped with Acclaim C18 PepMap100 75 μm ID \times 2 cm trap and Acclaim C18 PepMap RSLC, 75 μm ID \times 15 cm separation columns coupled to Thermo Fischer LTQ Orbitrap Fusion (*Thermo Fisher Scientific Inc.*). Samples were loaded on the trap and washed for 10 min with 0.1% FA (at 5 $\mu\text{L}/\text{min}$), then transferred to the analytical column and separated, using a 112 min gradient from 4% to 35% ACN, followed by 4 min at 80% ACN in 0.1% FA (at 200 nL/min flow rate). LTQ Orbitrap Fusion was operated in a 3 second top speed data dependent mode. Full scan acquisition was performed in the orbitrap at a resolution of 120000 and an ion target of 4e5 in a scan range of 300 – 1700 m/z. Monoisotopic precursor selection as well as dynamic exclusion for 60 sec were enabled. Precursors with charge states of 2 – 7 and intensities greater than 5e3 were selected for fragmentation. Isolation was performed in the quadrupole using a window of 1.6 m/z. Precursors were collected to a target of 1e2 for a maximum injection time of 250 ms with “inject ions for all available parallelizable time” enabled. Fragments were generated using higher-energy collisional dissociation (HCD) and detected in the ion trap at a rapid scan rate. Internal calibration was performed using the ion signal of fluoranthene cations (EASY-ETD/IC source).

The mass spectrometry proteomics data have been deposited to the ProteomeXchange Consortium *via* the PRIDE partner repository with the dataset identifier PXD008067.^[193]

Data Analysis

Peptide and protein identifications were performed using MaxQuant 1.5.3.8 software with Andromeda as search engine using following parameters: Carbamidomethylation of cysteines as fixed and oxidation of methionine as well as acetylation of N-termini as dynamic modifications, trypsin/P as the proteolytic enzyme, 4.5 ppm for precursor mass tolerance (main search ppm) and 0.5 Da for fragment mass tolerance (ITMS MS/MS tolerance). Searches were performed against the Uniprot database for *S. aureus* NCTC8325 (taxon

identifier: 93061, downloaded on 8.5.2014). Quantification was performed using dimethyl labeling with the following settings: light: DimethLys0, DimethNter0; medium: DimethLys4, DimethNter4 and heavy: DimethLys8, DimethNter8 with a maximum of four labeled amino acids. Variable modifications were included for quantification. The I = L, requantify and match between runs (default settings) options were used. Identification was done with at least two unique peptides and quantification only with unique peptides.

Statistical analysis was performed with Perseus 1.6.0.0. Dimethyl-labeling ratios were $\log_2(x)$ transformed and z-score normalized. The average values of technical replicates were calculated and $-\log_{10}(p\text{-values})$ were obtained by a two sided one sample *t*-test over four biological replicates. Putative contaminants, reverse peptides and peptides only identified by site were deleted, cut off lines were set at $-\log_{10}(p\text{-value})$ of 2 and a *t*-test difference of 2. *p*-values were corrected with the method of Benjamini and Hochberg.^[194]

Functional protein enrichment analyses were performed using the Database for Annotation, Visualisation and Integrated Discovery (DAVID).^[195,196] Uniprot accessions of at least 4-fold significantly depleted proteins in whole proteome studies were selected and compared to an internal reference protein set of *Staphylococcus aureus* and *Staphylococcus aureus* subsp. *aureus* NCTC 8325. *p*-values were corrected with the method of Benjamini and Hochberg.^[194]

2.2.4. Gel-based AfBPP in *S. aureus*

Growth, Labeling and Irradiation

Bacteria were cultured under hemolysis or biofilm conditions (chapter 2.2.1. and 2.2.2) without the addition of compound or DMSO. Cultures were collected in a 50 mL falcon tube and centrifuged at 6000×g for 4 min at 4 °C. The supernatant was disposed and the pellet was washed with PBS and then resuspended in PBS to get a suspension with OD₆₀₀ = 40. To 198 μL of this suspension in a microcentrifuge tube 2 μL of **AV73-p** (10, 6 and 3 mM in DMSO), a minimal photoprobe **AA-1** (0.3 mM in DMSO) or DMSO were added and the tube was briefly mixed by vortexing. After 30 min incubation at r.t. in the dark, the microcentrifuge tube was again mixed by vortexing and incubated for another 30 min at r.t. in the dark. The suspension was diluted with 800 μL PBS and transferred into a transparent 6-well plate and irradiated with UV light (280 – 315 nm, *Luzchem* LZC-UVB) under cooling for 30 min, while the 6-well plate was shaken after 15 min. The irradiated bacterial suspension was transferred to a 1.5 mL microcentrifuge tube and after centrifugation (6000×g, 10 min, 4 °C) the supernatant was removed and the pellets were stored over night at –80 °C.

Lysis and Click Reaction

Pellets were resuspended in 200 μ L PBS (4 °C) and transferred to Precellys Lysing Kits (0.5 mL, filled with 50 to 100 mg 0.5 mm glass beads). Tubes were cooled on ice for about 5 min and cells were lysed with the Precellys Homogeniser using three times lysis program 3 (5400 rpm, run number: 1, run time: 20 s, pause: 5 s). After each lysis step the tubes were cooled on ice for 5 min. The supernatant was transferred into a new 1.5 mL microcentrifuge tube and centrifuged at max. speed for 10 min at 4 °C to separate the soluble and insoluble fractions. The insoluble fraction was washed with 800 μ L PBS (4 °C) and resuspended in 200 μ L PBS (4 °C) by sonication (10 sec at 10% intensity). 86 μ L of each sample and each fraction was transferred to new 1.5 mL microcentrifuge tubes and treated with 10 μ L gel-based click reagent mix [2 μ L RhN₃ (5-TAMRA azide, (tetramethylrhodamine 5-carboxamido-(6-azido-hexanyl)), (life technologies, T10182); 5 mM in DMSO), 2 μ L fresh TCEP (50 mM in ddH₂O), 6 μ L TBTA ligand (1.67 mM in 80% *t*-BuOH and 20% DMSO)]. The final concentrations were: 104 μ M RhN₃, 1.04 mM TCEP and 104 μ M TBTA ligand. The lysates were mixed by vortexing and incubated for 1 h at r.t. in the dark. Samples were analyzed *via* SDS-PAGE (chapter 2.1.5.).

2.2.5. Gel-free AfBPP in *S. aureus* (biofilm conditions)

Growth

An overnight culture of *S. aureus* was grown in 5 mL BHB medium in a plastic culture tube. After 1:100 dilution of the culture with fresh BHB medium, the cultures were grown under static conditions at 37 °C for 24 h in a 96-well plate with 100 μ L culture per well. Bacterial culture was removed carefully with a multichannel pipette avoiding biofilm destruction. The biofilm was resuspended in PBS, was collected in a 50 mL falcon tube and centrifuged at 6200 \times g for 5 min at 4 °C. The supernatant was disposed and the pellet was resuspended in PBS to get OD₆₀₀ = 40. Around twelve 96-well plates are needed for 8 mL OD₆₀₀ = 40 suspension.

Labeling and Irradiation

1 mL of this suspension and 10 μ L of **AV73-p** (6 mM in DMSO), **AA-1** (6 mM in DMSO) or DMSO were mixed by vortexing. For the competition experiment 5 μ L **AV73** (36 mM in DMSO) and 10 μ L **AV73-p** (6 mM in DMSO) were added. After 30 min incubation at r.t. in the dark, the tubes were mixed by vortexing and incubated for another 30 min at r.t. in the dark. The suspension was transferred into culture dishes (5.5 cm diameter) and irradiated under cooling for 30 min with UV light (280 – 315 nm, *Luzchem* LZC-UVB), with shaking

after 15 min. The irradiated bacterial suspension was transferred to a 2 mL microcentrifuge tube. After centrifugation (6000×g, 10 min, 4 °C) the supernatant was removed and the pellets were washed twice with 1 mL PBS and then stored at –80 °C.

Lysis and Click Reaction

Pellets were resuspended in 1 mL PBS (4 °C) and transferred to 'Precellys Lysing Kit SK38 2.0 mL' tubes. The tubes were cooled on ice for 5 min and cells were lysed with the Precellys Homogeniser using three times lysis program 3 (5400 rpm, run number: 1, run time: 20 sec, pause: 5 sec). After each lysis run the tubes were cooled on ice for 5 min. 800 µL of the supernatant were transferred to new 1.5 mL microcentrifuge tubes and centrifuged at max. speed for 10 min at 4 °C to separate the soluble and insoluble fractions. The pellet was washed with 1 mL PBS and then resuspended in 1 mL PBS by sonication (10 sec, 10% intensity). Protein concentration was adjusted to 1.5 mg/mL after a BCA assay (chapter 2.1.5.). In a 15 mL falcon tube, 500 µL solution were treated with 43 µL gel-free click reagent mix [3 µL Biotin-PEG3-N₃ (*Jena Bioscience*, CLK-AZ104P4-100; 10 mM in DMSO), 10 µL TCEP (50 mM in ddH₂O), 30 µL TBTA ligand (1.667 mM in 80% *t*-BuOH and 20% DMSO)]. Resulting in final concentrations of: 233 µM Biotin-PEG3-N₃, 581 µM TCEP and 58.2 µM TBTA ligand. The lysates were mixed by vortexing and 10 µL CuSO₄ solution (50 mM in ddH₂O) were added to start the click reaction. The lysates were mixed by vortexing again and incubated for 1 h at r.t. in the dark. Subsequently the lysates were transferred to 15 mL reaction tubes and 4 mL of cold acetone (–80 °C, MS grade) were added. Proteins were precipitated over night at –20 °C.

Enrichment

The precipitated proteins were thawed on ice, pelletized (16900×g, 15 min, 4 °C) and the supernatant was disposed. Proteins were washed two times with 1 mL cold methanol (–80 °C). Resuspension was achieved by sonication (10 sec at 10% intensity) and proteins were pelletized *via* centrifugation (16900×g, 10 min, 4 °C). After the washing steps the supernatant was disposed and the pellet was resuspended in 500 µL 0.2% SDS in PBS at r.t. by sonication (10 sec at 10% intensity). 50 µL avidin-agarose beads (*Sigma-Aldrich*) were prepared by washing three times with 1 mL 0.2% (w/v) SDS in PBS. All centrifugation steps were conducted at 400×g for 2 min at room temperature. 500 µL protein solution was added to the washed avidin-agarose beads and incubated under continuous inverting (1 h, r.t.). Beads were washed three times with 1 mL 0.2% SDS in PBS and five times with 1 mL PBS.

Reduction, Alkylation and Digest

The beads were resuspended in 200 μL denaturation buffer (7 M urea, 2 M thiourea in 20 mM HEPES buffer, pH 7.5). TCEP (500 mM in ddH₂O, 2 μL) was added, the tubes were mixed by vortexing shortly and incubated in a thermoshaker (600 rpm, 60 min, 37 °C). Then 2-iodoacetamide (IAA, 500 mM in 50 mM TEAB solution in ddH₂O, 2 μL) was added, the tubes were mixed by vortexing shortly and incubated in a thermoshaker (600 rpm, 30 min, r.t., in the dark). Remaining IAA was quenched by the addition of DTT (1500 mM, 0.28 μL). The tubes were shortly mixed by vortexing and incubated in a thermoshaker (600 rpm, 30 min, r.t.). LysC (0.5 $\mu\text{g}/\mu\text{L}$) was thawed on ice and 1 μL was added to each microcentrifuge tube, the tubes were shortly mixed by vortexing and incubated in a thermoshaker (600 rpm, 2 h, r.t., in the dark). TEAB solution (600 μL , 50 mM in ddH₂O) and then trypsin (1.5 μL , 0.5 $\mu\text{g}/\mu\text{L}$ in 50 mM acetic acid) were added to each tube with a short vortexing step after each addition. The microcentrifuge tubes were incubated in a thermoshaker (600 rpm, 15 h, 37 °C). The digest was stopped by adding 10 μL FA and vortexing. After centrifugation (16616 \times g, 3 min, r.t.) the supernatant was transferred to a new Protein LoBind Eppendorf tube. TFA (500 μL , aqueous 0.1% solution) was added to the beads and after vortexing and centrifugation (16616 \times g, 1 min, r.t.) the supernatant was added to the supernatant collected before.

Desalting

50 mg SepPak C18 columns (*Waters*) were equilibrated by gravity flow with 1 mL acetonitrile, 1 mL elution buffer (80% ACN, 0.5% FA) and 3 mL aqueous 0.1% TFA solution. Subsequently the samples were loaded by gravity flow, washed with 3 mL aqueous 0.1% TFA solution and 0.5 mL aqueous 0.5% FA solution. Elution of proteins into new 2.0 mL Protein LoBind Eppendorf tubes was performed by the addition of 500 μL elution buffer by gravity flow followed by 250 μL elution buffer by vacuum flow until all liquid was eluted from the column. The eluates were lyophilized.

Before MS measurement the samples were dissolved in 20 μL aqueous 1% FA by pipetting up and down, vortexing and sonication for 15 min (brief centrifugation after each step). 0.22 μm centrifugal filter units (*VWR*) were equilibrated with 300 μL 1% FA (16616 \times g, 1 min, r.t.) and samples were filtered through the equilibrated filters (centrifugation: 16200 \times g, 2 min, r.t.).

MS/MS-measurement

Samples were analyzed *via* HPLC-MS/MS using an UltiMate 3000 nano HPLC system (*Dionex*) equipped with Acclaim C18 PepMap100 75 μm ID \times 2 cm trap and EASY-SPRAY

RSLC C18 50 cm × 75 μm separation columns coupled to Thermo Fischer LTQ Orbitrap Fusion (*Thermo Fisher Scientific Inc.*). Samples were loaded on the trap and washed for 7 min with 0.1% TFA (at 5 μL/min), then transferred to the analytical column and separated using a, 115 min gradient from 5% to 32% ACN followed by 10 min at 90% ACN in 0.1% FA (at 300 nL/min flow rate). LTQ Orbitrap Fusion was operated in a 3 second top speed data dependent mode. Full scan acquisition was performed in the orbitrap at a resolution of 120000 and an ion target of 2e5 in a scan range of 300–1500 m/z. Monoisotopic precursor selection as well as dynamic exclusion for 60 sec were enabled. Precursors with charge states of 2–7 and intensities greater than 5e3 were selected for fragmentation. Isolation was performed in the quadrupole using a window of 1.6 m/z. Peptide intensity threshold was set to 5e3 and automatic gain control was set to 1e4 with a maximum injection time of 50 ms with “inject ions for all available parallelizable time” enabled. Fragments were generated using higher-energy collisional dissociation (HCD) and detected in the ion trap at a rapid scan rate. Internal calibration was performed using the ion signal of fluoranthene cations (EASY-ETD/IC source).

The mass spectrometry proteomics data have been deposited to the ProteomeXchange Consortium *via* the PRIDE partner repository with the dataset identifier PXD008067.^[193]

Data Analysis

Peptide and protein identifications were performed using MaxQuant 1.6.0.1 software with Andromeda as search engine using following parameters: Carbamidomethylation of cysteines as fixed and oxidation of methionine as well as acetylation of N-termini as dynamic modifications, trypsin/P as the proteolytic enzyme, 4.5 ppm for precursor mass tolerance (main search ppm) and 0.5 Da for fragment mass tolerance (ITMS MS/MS tolerance). Searches were performed against the Uniprot database for *S. aureus* NCTC8325 (taxon identifier: 93061, downloaded on 26.06.2017). Quantification was performed using label-free quantification (LFQ). The match between runs (default settings) option was used. Identification was done with at least 2 unique peptides and quantification only with unique peptides.

Statistical analysis was performed with Perseus 1.6.0.0. LFQ ratios were $\log_2(x)$ transformed. $-\log_{10}(p\text{-values})$ were obtained by a two sample *t*-test over four biological replicates. Putative contaminants, reverse peptides and peptides only identified by site were deleted. Values were filtered for three in at least one group. Cut off lines were set at $-\log_{10}(p\text{-value})$ of 2 and at *t*-test difference of 3, for soluble fraction, and 2 for insoluble fraction. Due to the low

compound access in the competition experiment, the cut off for the t-test difference of the soluble fraction was set at 2. *p*-values were corrected by permutation based FDR > 0.5.

2.2.6. MTT Assay

Human liver cancer cells, HepG2, were cultivated in RPMI medium, supplemented with 10% (v/v) fetal bovine serum (FBS) and 2 mM L-glutamine. Cells were seeded in a transparent 96-well plate, 4000 cells per well (200 μ L/well) and grown overnight at 37 °C and 5% CO₂. The medium was removed and replaced by fresh medium with compound (1:1000) in DMSO, while DMSO was used as a negative control. After incubation for 20 h, 20 μ L 3-(4,5-dimethyl-2-thiazolyl)-2,5-diphenyl-2H-tetrazolium bromide solution (MTT, 5 mg/mL in PBS) was added to each well. Cells were incubated for 3 h, medium was removed and the formed formazan was resuspended in 200 μ L DMSO per well. Absorbance and a reference wavelength were determined by a Tecan Infinite[®] F200Pro at 570 nm and 630 nm, respectively. All experiments were performed in triplicates. Data were normalized with respect to the DMSO control (GraphPad Prism 6).

2.3. Biochemical methods for Chapter III

2.3.1. Protein expression and purification

Protein overexpression and purification of *SaClpP*, *SaClpP* mutants, *SaClpX* and GFP-*ssrA* were performed according to a published general procedure. ^[113,197,198] Overexpression and purification of *SaClpP* mutants were performed by Patrick Allihn and Dr. Mathias Hackl.

***SaClpP* and mutants.** The Gateway cloning system (*Life Technologies*) was utilized to clone a C-terminal STREP-II affinity tagged *SaClpP* construct into pET301 expression vectors. 1 L LB-medium was inoculated with 10 mL (1:100) overnight culture of the respective *E. coli* BL21(DE3) strain and grown in presence of ampicillin (100 µg/mL) at 37 °C at 200 rpm until OD₆₀₀ of 0.6 was reached, then IPTG (0.5 mM final concentration) was added and the bacteria were grown overnight at 30 °C and 200 rpm. After the bacteria were harvested (6000×g, 10 min, 4 °C) and washed with 25 mL PBS, the pellet was stored at –20 °C. Then, the pellet was thawed on ice, Strep-binding buffer (100 mM Tris/HCl, 150 mM NaCl, 1 mM EDTA, pH 8, filtered) was added up to 20 mL and the pellet was resuspended. After lysis, (*Bandelin* Sonoplus, twice: 7 min 30% intensity and 3 min 80% intensity on ice) the suspension was centrifuged (3800×g, 30 min, 4 °C) and the supernatant was loaded on a pre-equilibrated StrepTrap HP column (5 mL, *GE Healthcare*). After the column was washed with 40 mL binding buffer, elution was performed with 20 mL elution buffer (binding buffer + 2.5 mM desthiobiotin). Fractions containing protein were collected, concentrated and subjected to preparative size exclusion chromatography (HiLoad 16/60 Superdex 200 pg gelfiltration column, *GE Healthcare*). Fractions containing protein were collected, concentrated and stored at –80 °C.

***SaClpX*.** The Gateway cloning system (*Life Technologies*) was utilized to clone a N-terminal His6-tag and a TEV cleavage site construct into vector pET300. 1 L LB-medium was inoculated with 10 mL (1:100) overnight culture of the respective *E. coli* BL21(DE3) strain and grown in the presence of ampicillin (100 µg/mL) at 37 °C at 200 rpm until OD₆₀₀ of 0.6 was reached, then IPTG (0.5 mM final concentration) was added and the bacteria were grown for 4 h at 25 °C. After the bacteria were harvested (6000×g, 10 min, 4 °C) and washed with 25 mL PBS, the pellet was stored at –20 °C. The pellet was thawed on ice, lysis buffer (25 mM HEPES pH 7.5, 200 mM KCl, 5% glycerol, 1 mM DTT, 0.5 mM ATP, 5 mM MgCl₂) was added up to 20 mL and the pellet was resuspended. After lysis, (*Bandelin* Sonoplus, twice: 7 min 30% intensity and 3 min 80% intensity on ice) the suspension was

centrifuged (38000×g, 30 min, 4 °C) and the supernatant was loaded on a pre-equilibrated His Trap HP 5 mL column (*GE Healthcare*). After the column was washed with 50 mL washing buffer (25 mM HEPES pH 7.5, 200 mM KCl, 5% glycerol, 1 mM DTT, 0.5 mM ATP, 40 mM imidazole), elution was carried out with 20 mL elution buffer (25 mM HEPES pH 7.5, 200 mM KCl, 5% glycerol, 1 mM DTT, 0.5 mM ATP, 300 mM imidazole). Fractions containing protein were collected, followed by digestion with His₆-tagged TEV protease at 4 °C overnight. Cleavage was monitored by intact-protein mass spectrometry. A second affinity purification was carried out and flow-through containing protein were collected, concentrated and subjected to a Superdex 200 pg 16/60 column (*GE Healthcare*).

GFP-ssrA. The Gateway cloning system (*Life Technologies*) was utilized to clone a N-terminal STREP-II affinity tagged and a C-terminal SsrA (AANDENYALAA) tagged eGFP construct into pDEST007 expression vectors. 1 L LB-medium was inoculated with 10 mL (1:100) overnight culture of the respective *E. coli* KY2266 strain and grown in the presence of ampicillin (100 µg/mL) at 37 °C at 200 rpm until OD₆₀₀ of 0.6 was reached, then anhydrotetracycline (ATET, 0.2 mg/L) was added and the bacteria were grown for 4.5 h at 37 °C. After the bacteria were harvested (6000×g, 10 min, 4 °C) and washed with 25 mL PBS, the pellet was stored at -20 °C. Then, the pellet was thawed on ice, Strep-binding buffer (100 mM Tris/HCl, 150 mM NaCl, 1 mM EDTA, pH 8, filtered) was added up to 20 mL and the pellet was resuspended. After lysis (*Bandelin Sonoplus*, twice: 7 min 30% intensity and 3 min 80% intensity on ice), the suspension was centrifuged (38000×g, 30 min, 4 °C) and the supernatant was loaded on a pre-equilibrated StrepTrap HP column (5 mL, *GE Healthcare*). After the column was washed with 40 mL binding buffer, elution was performed with 20 mL elution buffer (binding buffer + 2.5 mM desthiobiotin). Fractions containing protein were collected, concentrated and stored at -80 °C.

2.3.2. Biochemical Assays

FITC Casein Assay^[126,199]

The aim of this assay was to determine the proteolytic activity of ClpP in the presence of different compounds. For the FITC-casein assay, 100 µL sample was prepared in a black 96-well plate, with a concentration of 1 µM *Sa*ClpP (monomer concentration) and different final concentrations of the compound (100× stock in DMSO, final concentrations: 100 µM, 20 µM, 10 µM, 1 µM). As a positive control **PAK4** was used with a concentration of 20 µM and DMSO as a negative control. All conditions were measured in triplicates. 1 µL DMSO or compound in DMSO was added to each well and 80 µL ClpP in PZ-buffer (1.25 µM) was

added. After incubation at 37 °C for 15 min, 20 µL substrate (2 mM FITC-casein, 10 mM casein, in PBS) was added to each sample and the 96-well plate was shaken carefully. After excitation at 485 nm, the fluorescence emission was measured on a Tecan Infinite® F200Pro at 535 nm. Initial slopes over time were evaluated by a linear regression model, and all values were normalized to the **PAK4** control, after subtraction of the DMSO control (Microsoft Excel and GraphPad Prism 6).

Peptidase Assay

The aim of this assay was to determine the inhibition of ClpP peptidase activity in the presence of different compounds, by monitoring the cleavage of fluorogenic Suc-Leu-Tyr-AMC (*Bachem*) substrate, as published by *Gersch et al.*^[200] 1 µL of DMSO or compound (100× stock in DMSO, final concentrations: 100 µM) were provided in a black flat bottom 96-well plate and 98 µL ClpP in PZ-buffer (1 µM final concentration) were added. As a positive control **AV170** was used at a concentration of 1 µM. After incubation for 15 min at 37 °C, 1 µL AMC substrate (20 mM in DMSO, final concentration: 200 µM) was added and fluorescence recorded for 90 min. (excitation: 380 nm, emission: 440 nm, Tecan Infinite® F200Pro) The initial slope of the signal over time was determined *via* a linear regression model (GraphPad Prism 6) and the DMSO control was defined as 100% activity.

Protease and GFP Unfolding Assay

Activity of the ClpXP complex was determined with a protease assay. In the presence of different compounds, degradation of GFP-SsrA was detected *via* fluorescence by a Tecan Infinite® F200Pro. For the GFP unfolding assay, an inactive ClpP mutant, S98A, was used. All conditions were measured in triplicates.

0.6 µL compound (100× stock in DMSO, final concentration: 100 µM) or DMSO were given in a white flat 96-well plate in triplicates and 59 µL enzyme buffer mix (2.8 µM ClpP, 2.4 µM ClpX in PZ-buffer; ATP regeneration mix: 4 mM ATP, 16 mM creatine phosphate, 20 U/mL creatine phosphokinase) were added and the mixture incubated for 15 min at 37 °C. 1 µL SsrA-GFP was added and after excitation at 485 nm fluorescence was measured at 535 nm for 3 h (Tecan Infinite® F200Pro). DMSO was used as positive control with an activity of 100%, while a control set up without ClpP was used as a negative control. The initial slope of the fluorescence signal over time was determined *via* linear regression (GraphPad Prism 6).

ATPase Assays

ClpX activity was determined by two different assays in the presence of different compounds and DMSO.

Enzyme coupled ATPase assay

In this enzyme coupled assay the decrease of NADH/H⁺, which is proportional to ATPase activity, is measured. To 1 μ L compound (100 \times stock in DMSO, final concentration: 100 μ M) or DMSO was added 89 μ L enzyme master mix (100 mM HEPES, pH 7.0, 200 mM KCl, 20 mM MgCl₂, 1 mM DTT, 1 mM NADH, 2 mM phosphoenolpyruvate, 50 U/mL lactate dehydrogenase, 50 U/mL pyruvate kinase, 5% (v/v) glycerol) containing ClpX (4 μ M final concentration) in a transparent flat 96-well plate. The mixture was incubated for 15 min at 37 °C and 10 μ L ATP (200 mM in ddH₂O) were added. Absorbance was measured at 340 nm for 2 h at a Tecan Infinite[®] F200Pro to monitor the amount of NADH/H⁺.

Malachite green assay

In this ATPase assay, the released phosphate is directly detected, which is formed by ATP hydrolysis and therefore represents ClpX activity. For a dye solution 36 mL malachite green (0.045% in H₂O), 12 mL ammonium molybdate (4.2% in 4 M HCl) and 1 mL Triton-X-100 (1% in H₂O) solutions were combined, incubated for 1 h, filtered through a 0.45 μ m filter and incubated for another hour at room temperature. In a reaction tube 2 μ L compound (100 \times stock in DMSO, final concentrations: 50 μ M) or DMSO and 200 μ L PZ-buffer containing 4 μ M ClpX were added and the mixture was incubated for 10 min at room temperature. 7.5 μ L ATP solution (100 mM in H₂O) was added and the tube vortexed to start the reaction. After defined time points (2, 5, 10 and 14 min) 50 μ L of the sample were given into a plastic cuvette filled with 800 μ L dye solution and 50 μ L PZ buffer. After the cuvette was inverted and the mixture had time to react for 1 min, 100 μ L citric acid (34% in H₂O) were added and the cuvette was inverted again. The absorbance was measured at 650 nm in triplicates. Data was analyzed by calculating the slope (GraphPad Prism 6) *via* linear regression. DMSO-treated samples were normalized to 100% activity and samples without ClpX were used as a negative control to account for potential autohydrolysis of ATP.

Thermal Shift Assay

To 197 μ L master mix (PZ buffer and 5 μ M final concentration ClpP or ClpX) in a reaction tube were added 1 μ L Sypro Orange (1:2000, in ddH₂O, *Sigma-Aldrich*) and 2 μ L compound (100 \times stock in DMSO, final concentrations: 100, 80, 60, 40, 20 μ M) or DMSO. 50 μ L of the mixture was given in a white 96-well PCR plate in triplicates. Fluorescence intensity was

measured at temperatures from 20 °C to 89.6 °C (0.3 °C steps) in a CFX96 Real-Time System (BioRad). Data were analyzed using Bio-Rad CFX Manager 3.0.

Click Reaction Assay

For the click reaction assay three conditions were tested, with the following reagents and concentrations: Condition 1: 100 μM TBTA, 52 mM TCEP; Condition 2: 500 μM BTTA, 2 mM sodium ascorbate; Condition 3: 500 μM THPTA, 2 mM NaAsc. For all experiments 10 μM probe (**BH235**), 20 μM coumarin-azide and 1 mM CuSO₄ were used. In a black 96-well plate were given all ingredients (1 μL probe, 2 μL coumarin-azide, 6 μL TBTA/17.5 μL BTTA or THPTA, 2 μL TCEP or sodium ascorbate) and PBS (304.5 μL or 308 μL) in triplicates, and then 7 μL CuSO₄ were added to each well. Fluorescence was detected by a Tecan Infinite[®] F200Pro.

2.3.3. Labeling of recombinant ClpP, wt and mutants

0.5 μL DMSO or compound (100× stock in DMSO, different concentrations) was added to a transparent 96-well plate and 44 μL SaClpP in PBS (final concentration 2 μM) were added. After incubation for one hour in the dark, the mixture was irradiated for 10 min at 365 nm (Philips TL-DBLB18W), 5 μL gel-based click reagent mix [1 μL RhN₃ (TAMRA azide (life technologies, T10182); 5 mM in DMSO), 1 μL fresh TCEP; 50 mM in ddH₂O, 3 μL TBTA ligand; 1.67 mM in 80% *t*-BuOH and 20% DMSO] and 1 μL 50 mM CuSO₄ were added and incubated for 1 h in the dark. SDS-PAGE was performed with 50 μL 2× Laemmli sample buffer as described in chapter 2.1.6.

2.3.4. Hemolytic Assay on agar plate

3 μL compound (100 mM) or DMSO and 3 μL diluted bacterial suspension (*S. aureus* NCTC8325 1:100 in B medium) were given on a sterile filter paper disk (5 mm diameter) on a blood agar plate (Columbia Sheep Blood Agar plate, PB5039A, Thermo Scientific). After incubation for 20 h at 37 °C, photos were taken with a LAS4000 scanner (GE Healthcare). Lighter area around the filter paper represents hemolytic activity.

2.3.5. Secretome Analysis

Growth and Precipitation

Bacteria were cultured under defined growth conditions according to chapter 2.2.1. for 20 h. Bacteria were transferred to 2 mL microcentrifuge tubes and centrifuged for 10 min at 6200×g at 4 °C. The supernatant was filtered (0.2 μm filter) in a 15 mL falcon tube, 10 mL -80 °C acetone (MS-grade) was added and proteins were precipitated over night at -20 °C.

The precipitated proteins were thawed on ice, pelletized (16900×g, 15 min, 4 °C) and supernatant was disposed. Falcon tubes were stored on ice during the following washing procedure: The proteins were washed two times with 1 mL cold methanol (−80 °C). Resuspension was achieved by sonication (15 sec at 10% intensity) and proteins were pelletized *via* centrifugation (16900×g, 10 min, 4 °C).

Reduction, Alkylation and Digest

Only MS grade water was used for the following procedures. After washing the pellet was resuspended in 200 µL denaturation buffer (7 M urea, 2 M thiourea in 20 mM HEPES buffer, pH 7.5) and vortexed. The mixture was transferred to a 1.5 mL microcentrifuge tube and centrifuged at max. speed for 5 min. 2 µL TCEP (500 mM in water) was added to the supernatant, vortexed shortly and incubated in a thermoshaker (600 rpm, 60 min, 37 °C). Then 2-iodoacetamide (IAA, 550 mM in 50 mM TEAB in water, 2 µL) was added, the tubes were mixed by vortexing shortly and incubated in a thermoshaker (600 rpm, 30 min, r.t., in the dark). Remaining IAA was quenched by the addition of DTT (500 mM in water, 4 µL). The tubes were shortly mixed by vortexing and incubated in a thermoshaker (600 rpm, 30 min, r.t.). LysC (0.5 µg/µL) was thawed on ice and 1 µL was added to each microcentrifuge tube, the tubes were shortly mixed by vortexing and incubated in a thermoshaker (600 rpm, 3 h, r.t., in the dark). TEAB solution (600 µL, 50 mM in water) and then trypsin (1.5 µL, 0.5 µg/µL in 50 mM acetic acid) were added to each tube with a short vortexing step after each addition. The microcentrifuge tubes were incubated in a thermoshaker (600 rpm, 17 h, 37 °C). The digest was stopped by adding 10 µL FA and vortexing.

Desalting

50 mg SepPak C18 columns (*Waters*) were equilibrated by gravity flow with 1 mL acetonitrile, 3×1 mL aqueous 0.1% TFA solution, 1 mL elution buffer (80% ACN, 0.5% FA) and 3×1 mL aqueous 0.1% TFA solution. Subsequently the samples were loaded by gravity flow, washed with 3×1 mL aqueous 0.1% TFA solution and 0.5 mL 0.5% FA solution. Peptides were eluted into new 2.0 mL Protein LoBind Eppendorf tubes, which was performed by the addition of 2×250 µL elution buffer (80% ACN, 0.5% FA) by gravity flow followed by 250 µL elution buffer by vacuum flow until all liquid was eluted from the column. The eluates were lyophilized.

MS/MS-preparation

Before MS measurement the samples were dissolved in 40 µL 1% FA by pipetting up and down, vortexing and sonication for 15 min (brief centrifugation after each step). 0.22 µm

centrifugal filter units (*Merck*) were equilibrated with 300 μ L 1% FA (centrifugation: 16200 \times g, 1 min, r.t.). Samples were filtered through the equilibrated filters (centrifugation: 16200 \times g, 2 min, r.t.)

MS/MS-measurement

Samples were analyzed *via* HPLC-MS/MS using an UltiMate 3000 nano HPLC system (Dionex) equipped with Acclaim C18 PepMap100 75 μ m ID \times 2 cm trap and Acclaim C18 PepMap RSLC, 75 μ m ID \times 50 cm separation columns coupled to Thermo Fischer LTQ Orbitrap Fusion (*Thermo Fisher Scientific Inc.*). Samples were loaded on the trap and washed for 10 min with 0.1% FA (at 5 μ L/min), then transferred to the analytical column and separated using a 112 min gradient from 4% to 35% ACN followed by 4 min at 80% ACN in 0.1% FA (at 200 nL/min flow rate). LTQ Orbitrap Fusion was operated in a 3 second top speed data dependent mode. Full scan acquisition was performed in the orbitrap at a resolution of 120000 and an ion target of 4e5 in a scan range of 300 – 1500 m/z. Monoisotopic precursor selection as well as dynamic exclusion for 60 sec were enabled. Precursors with charge states of 2 – 7 and intensities greater than 5e3 were selected for fragmentation. Isolation was performed in the quadrupole using a window of 1.6 m/z. Precursors were collected to a target of 1e4 for a maximum injection time of 35 ms with “inject ions for all available parallelizable time” enabled. Fragments were generated using higher-energy collisional dissociation (HCD) and detected in the ion trap at a rapid scan rate. Internal calibration was performed using the ion signal of fluoranthene cations (EASY-ETD/IC source).

Data Analysis

Peptide and protein identifications were performed using MaxQuant 1.6.0.1 software with Andromeda as search engine using following parameters: Carbamidomethylation of cysteines as fixed and oxidation of methionine as well as acetylation of N-termini as dynamic modifications, trypsin/P as the proteolytic enzyme, 4.5 ppm for precursor mass tolerance (main search ppm) and 0.5 Da for fragment mass tolerance (ITMS MS/MS tolerance). Searches were performed against the Uniprot database for *S. aureus* NCTC8325 (taxon identifier: 93061, downloaded on 16.02.2018). Quantification was performed using label-free quantification (LFQ). The match between runs (default settings) option was used. Identification was done with at least 2 unique peptides and quantification only with unique peptides.

Statistical analysis was performed with Perseus 1.6.0.0. LFQ ratios were $\log_2(x)$ transformed. $-\log_{10}(p\text{-values})$ were obtained by a two sample t -test over three biological replicates. Putative contaminants, reverse peptides and peptides only identified by site were deleted. Values were filtered for two in at least one group. Cut off lines were set at $-\log_{10}(p\text{-value})$ of 2 and at t -test difference of 2, for soluble fraction, and each 1 for insoluble fraction. p -values were corrected by permutation based FDR > 0.5.

2.3.6. Gel-based AfBPP in *S. aureus* lysate

Growth and Lysis

Bacteria were grown in a 500 mL Erlenmeyer flask with four baffles on the bottom. 125 mL B medium were inoculated with 1.25 mL overnight culture and bacteria were grown until they reached stationary phase, with an OD_{600} between 5.5 and 6.5. Cultures were collected in 50 mL falcon tubes and centrifuged at $6000\times g$ for 10 min at 4 °C. The supernatant was disposed and the pellet was washed with 40 mL PBS and stored overnight at -80 °C.

After the pellet was thawed on ice, it was resuspended in PBS to get a suspension with $OD_{600} = 40$ and lyzed *via* sonication (4×30 sec, 75% intensity), with cooling breaks in between. Lysates were centrifuged shortly and the supernatant was filtered (0.2 μm).

Labeling, Irradiation and Click Reaction

In a 96-well plate was given 0.5 μL compound (100, 50, 25, 10 mM stock concentrations in DMSO) or DMSO and 43 μL lysate was added to each well. For competition experiments both compounds were added simultaneously. After incubation for 1 h at r.t., the samples were irradiated under cooling 2×10 min with UV light (365 nm, *Philips* TL-D BLB 18 W), with shaking of the 96-well plate in between. To each well was added: 1 μL RhN_3 (TAMRA azide; 5 mM in DMSO), 1 μL fresh TCEP (50 mM in ddH_2O), 3 μL TBTA ligand (1.67 mM in 80% *t*-BuOH and 20% DMSO) and 1 μL CuSO_4 solution (50 mM in ddH_2O). The samples were mixed by pipetting up and down and incubated for 1 h at r.t. in the dark. SDS-PAGE was performed with 50 μL $2\times$ Laemmli sample buffer as described in chapter 2.1.5.

2.3.7. Western Blot Analysis

For western blot analysis, 5 μL marker (*Serva* Pink Color Protein Standard II) was used during SDS-PAGE. Before blotting, the gel was washed twice in blotting buffer (28 mM trizma, 39 mM glycine, 0.04% SDS, 20% MeOH) for 5 min. Gel and membrane (immunoblot PVDF membrane, *Bio-Rad*) were stacked between two filter papers (extra thick blot paper, *Bio-Rad*) in a Western Blot Transfer station (20 V, 1 h). The membrane was incubated

in 5% BSA in PBS-T (0.5% Tween 20 in PBS) solution at room temperature for 45 min, followed by 5 min washing in PBS-T. After incubation overnight with the primary antibody (SaClpP, *Abcam*, 1:5000 in 5% BSA in PBS-T) at 4 °C, the membrane was washed 3×10 min with PBS-T, incubated with the secondary antibody (goat anti-rabbit HRP, *Santa Cruz*, 1:10000 in 5% BSA in PBS-T) for 1 h at room temperature, and washed again 3×10 min with PBS-T, all under constant shaking. The membrane was then incubated with 2 mL of a freshly prepared ECL solution (1:1; ECL Prime Western Blotting Detection Reagent, *GE Healthcare*) for 3 min and chemiluminescence was measured with a LAS-4000 gel scanning station (*Fujifilm*).

2.3.8. Gel-based AfBPP in *S. aureus* intact cells

Growth, Labeling and Irradiation

Bacteria were grown in a 250 mL Erlenmeyer flask with four baffles on the bottom. 50 mL B medium were inoculated with 0.5 mL overnight culture and the bacteria were grown until they reached stationary phase, with an OD₆₀₀ between 5.5 and 6.5. Cultures were collected in a 50 mL falcon tube and centrifuged at 6000×g for 10 min at 4 °C. The supernatant was disposed and the pellet was washed with PBS and then resuspended in PBS to obtain a suspension with OD₆₀₀ = 40. To 198 µL of this suspension in a microcentrifuge tube, 2 µL of photoprobe (**235**, **266**, **288**, different concentrations in DMSO) or DMSO was added and the sample was briefly mixed by vortexing. After 1 h incubation at room temperature in the dark, the suspension was diluted with 800 µL PBS and transferred to a transparent 6-well plate and irradiated with UV light (365 nm, *Philips* TL-DBLB18W) under cooling for 14 min (if not defined differently), while the 6-well plate was shaken once after half of the time. The irradiated bacterial suspension was transferred to a 1.5 mL microcentrifuge tube and after centrifugation (6000×g, 10 min, 4 °C) the supernatant was removed and the pellets were stored overnight at -80 °C.

Lysis and Click Reaction

Pellets were resuspended in 200 µL PBS (4 °C) or 0.2% SDS in PBS and lysed *via* sonication (2×20 sec, 75% intensity, *Bandelin* Sonoplus). The lysate was centrifuged at 10000×g for 30 min at 4 °C or 14 °C, to separate the soluble from the insoluble fraction. The insoluble fraction was resuspended in 200 µL PBS (4 °C) or 0.4% SDS in PBS by sonication (10 sec, 10% intensity, *Bandelin* Sonoplus). 88 µL of each sample and each fraction were transferred to new 1.5 mL microcentrifuge tubes and treated with 10 µL gel-based AfBPP mix: 2 µL RhN₃ (TAMRA azide; 5 mM in DMSO), 2 µL freshly prepared TCEP (50 mM in ddH₂O),

6 μL TBTA ligand (1.67 mM in 80% *t*-BuOH and 20% DMSO) and 2 μL CuSO_4 (50 mM). The samples were mixed by vortexing and incubated for 1 h at room temperature in the dark. Samples were analyzed *via* SDS-PAGE (chapter 2.1.6.).

2.3.9. Gel-free AfBPP in *S. aureus* intact cells

Growth, Labeling and Irradiation

Bacteria were grown in a 250 mL Erlenmeyer flask with four baffles on the bottom. 50 mL BHB medium were inoculated with 0.5 mL overnight culture and the bacteria were grown until they reach stationary phase, with an OD_{600} between 6.5 and 7.5. Cultures were collected in a 50 mL falcon tube and centrifuged at $6000\times g$ for 10 min at 4 °C. The supernatant was disposed and the pellet was washed with PBS and then resuspended in PBS to get a suspension with $\text{OD}_{600} = 40$. To 990 μL of this suspension in a microcentrifuge tube 10 μL of photoprobe (**BH235**, **BH266**, **BH288**, different concentrations in DMSO) or DMSO was added and the tube was briefly mixed by vortexing. After 1 h incubation at room temperature in the dark, the suspension was diluted with 1 mL PBS and transferred into culture dishes (5.5 cm diameter) and irradiated with UV light (365 nm, *Philips* TL-DBLB18W) under cooling for 14 min, while the dishes were shaken shortly after 7 min. The irradiated bacterial suspension was transferred to 2 mL microcentrifuge tubes and after centrifugation ($6000\times g$, 10 min, 4 °C) the supernatant was removed, the pellets were washed with 1 mL PBS and were stored over night at -80 °C.

Lysis and Click Reaction

Pellets were resuspended in 1 mL PBS (4 °C), lysostaphin (5 μL , 10 mg/mL,) was added and shaken at 37 °C at 14000 rpm for 1 h. After the addition of SDS (20 μL 20% in PBS, final concentration 0.4%) the suspension was sonicated (10 sec, 20% intensity). The lysate was centrifuged at max. speed for 60 min at room temperature. The supernatant was used for the further workflow. Protein concentration was adjusted to 1.5 mg/mL after a BCA assay (chapter 2.1.5). In a 15 mL falcon tube, 500 μL of solution were treated with 43 μL click reagent mix: 3 μL biotin-PEG3- N_3 (*Jena Bioscience*, CLK-AZ104P4-100; 10 mM in DMSO), 10 μL TCEP (50 mM in ddH₂O), 30 μL TBTA ligand (1.667 mM in 80% *t*-BuOH and 20% DMSO). Resulting in final concentrations of: 233 μM biotin-PEG3- N_3 , 581 μM TCEP and 58.2 μM TBTA Ligand. The samples were mixed by vortexing, 10 μL CuSO_4 solution (50 mM in ddH₂O) were added to start the click reaction, the samples were mixed by vortexing again and incubated for 1 h at r.t. in the dark.

Precipitation and Enrichment

Subsequently 4 mL of cold acetone (-80°C , MS grade) were added and proteins were precipitated overnight at -20°C . The precipitated proteins were thawed on ice, pelletized ($16900\times g$, 15 min, 4°C) and the supernatant was disposed. Proteins were washed two times with 0.5 or 1 mL cold methanol (-80°C , MS grade). Resuspension was achieved by sonication (10 sec at 10% intensity) and proteins were pelletized *via* centrifugation ($16900\times g$, 10 min, 4°C). After the washing steps the supernatant was disposed and the pellet resuspended in 500 μL 0.2% or 0.4% SDS in PBS at r.t. by sonication (10 sec at 10% intensity).

50 μL avidin-agarose beads (*Sigma-Aldrich*) were prepared by washing three times with 1 mL 0.2% (w/v) SDS in PBS. All centrifugation steps were conducted at $400\times g$ for 2 min at room temperature. 500 μL protein solution was added to the washed avidin-agarose beads and incubated under continuous inverting (1 h, r.t.). Beads were washed three times with 1 mL 0.2% SDS in PBS and five times with 1 mL PBS.

Reduction, Alkylation and Digest

The beads were resuspended in 200 μL denaturation buffer (7 M urea, 2 M thiourea in 20 mM HEPES buffer, pH 7.5). TCEP (500 mM in MS-grade water, 2 μL) was added, the tubes were mixed by vortexing shortly and incubated in a thermoshaker (600 rpm, 60 min, 37°C). Then 2-iodoacetamide (IAA, 500 mM in 50 mM TEAB in MS-grade water, 2 μL) was added, the tubes were mixed by vortexing shortly and incubated in a thermoshaker (600 rpm, 30 min, r.t., in the dark). Remaining IAA was quenched by the addition of dithiothreitol (DTT, 500 mM in MS-grade water, 4 μL). The tubes were shortly mixed by vortexing and incubated in a thermoshaker (600 rpm, 30 min, r.t.). LysC (0.5 $\mu\text{g}/\mu\text{L}$) was thawed on ice and 1 μL was added to each microcentrifuge tube, the tubes were shortly mixed by vortexing and incubated in a thermoshaker (600 rpm, 2 h, r.t., in the dark). TEAB solution (600 μL , 50 mM in MS-grade water) and then trypsin (1.5 μL , 0.5 $\mu\text{g}/\mu\text{L}$ in 50 mM acetic acid) were added to each tube with a short vortexing step after each addition. The microcentrifuge tubes were incubated in a thermoshaker (600 rpm, 15 h, 37°C). The digest was stopped by adding 10 μL formic acid (FA) and vortexing. After centrifugation ($16616\times g$, 3 min, r.t.) the supernatant was transferred to a new Protein LoBind Eppendorf tube. Trifluoroacetic acid (TFA, 500 μL , aqueous 0.1% solution) was added to the beads and after vortexing and centrifugation ($16616\times g$, 3 min, r.t.) the supernatant was added to the supernatant collected before.

Desalting

50 mg SepPak C18 columns (*Waters*) were equilibrated by gravity flow with 1 mL acetonitrile, 1 mL elution buffer (80% ACN, 0.5% FA) and 3×1 mL aqueous 0.1% TFA solution. Subsequently the samples were loaded by gravity flow, washed with 3×1 mL aqueous 0.1% TFA solution and 0.5 mL aqueous 0.5% FA solution. Elution of proteins into new 2.0 mL Protein LoBind Eppendorf tubes was performed by the addition of 2×250 μ L elution buffer by gravity flow followed by 250 μ L elution buffer by vacuum flow until all liquid was eluted from the column. The eluates were lyophilized.

MS/MS-preparation

Before MS measurement the samples were dissolved in 30 μ L 1% FA by pipetting up and down, vortexing and sonication for 15 min (brief centrifugation after each step). 0.22 μ m centrifugal filter units (*Merck*) were equilibrated with 300 μ L 1% FA (16616×g, 1 min, r.t.) and samples were filtered through the equilibrated filters (centrifugation: 16200×g, 2 min, r.t.).

MS/MS measurement

Samples were analyzed *via* HPLC-MS/MS using an UltiMate 3000 nano HPLC system (*Dionex*) equipped with Acclaim C18 PepMap100 75 μ m ID × 2 cm trap and EASY-SPRAY RSLC C18 50 cm × 75 μ m separation columns coupled to Thermo Fischer Q Exactive Orbitrap (*Thermo Fisher Scientific Inc.*). Samples were loaded on the trap and washed for 7 min with 0.1% TFA (at 5 μ L/min), then transferred to the analytical column and separated using a 115 min gradient from 5% to 32% ACN followed by 10 min at 90% ACN in 0.1% FA (at 300 nL/min flow rate). Q Exactive Orbitrap was operated in a 3 second top speed data dependent mode. Full scan acquisition was performed in the orbitrap at a resolution of 140000 and an ion target of 3e6 in a scan range of 300–1500 m/z. Monoisotopic precursor selection as well as dynamic exclusion for 60 sec were enabled. Precursors with charge states not being one or unassigned with intensities greater than 1e3 were selected for fragmentation. Isolation was performed in the quadrupole using a window of 1.6 m/z. Precursors were collected to a target of 1e5 with a maximum injection time of 100 ms with “inject ions for all available parallelizable time” enabled. Fragments were generated using higher-energy collisional dissociation (HCD) and detected in the ion trap at a rapid scan rate. Internal calibration was performed using the ion signal of fluoranthene cations (EASY-ETD/IC source).

The mass spectrometry proteomics data have been deposited to the ProteomeXchange Consortium *via* the PRIDE partner repository with the dataset identifier PXD015244.^[193]

Data Analysis

Peptide and protein identifications were performed using MaxQuant 1.6.5.0 software with Andromeda as search engine using following parameters: Carbamidomethylation of cysteines as fixed and oxidation of methionine as well as acetylation of N-termini as dynamic modifications, trypsin as the proteolytic enzyme, 4.5 ppm for precursor mass tolerance (main search ppm) and 0.5 Da for fragment mass tolerance (ITMS MS/MS tolerance). Searches were performed against the Uniprot database for *S. aureus* NCTC8325 (taxon identifier: 93061, downloaded on 10.07.2018). Quantification was performed using label-free quantification (LFQ). The match between runs (default settings) option was used. Identification was done with at least 2 unique peptides and quantification only with unique peptides.

Statistical analysis was performed with Perseus 1.6.0.6. LFQ ratios were $\log_2(x)$ transformed. $-\log_{10}(p\text{-values})$ were obtained by a two sample *t*-test over three biological replicates. Putative contaminants, reverse peptides and peptides only identified by site were deleted. Values were filtered for three in at least one group. Cut off lines were set at $-\log_{10}(p\text{-value})$ of 1.3 and at *t*-test difference of 3. *p*- values were corrected by permutation based FDR > 0.5.

Bibliography

- [1] A. Jenkins, A. Diep, T. T. Mai, N. H. Vo, P. Warrener, J. Suzich, C. K. Stover, R. Sellman, *MBio* **2015**, *6*, 1–10.
- [2] H. F. L. Wertheim, D. C. Melles, M. C. Vos, W. Van Leeuwen, A. Van Belkum, H. A. Verbrugh, J. L. Nouwen, *Lancet Infect Dis.* **2005**, *5*, 751–762.
- [3] D. Balasubramanian, L. Harper, B. Shopsin, V. J. Torres, *Pathog. Dis.* **2017**, *75*, 1–13.
- [4] B. Wang, T. W. Muir, *Cell Chem. Biol.* **2016**, *23*, 214–224.
- [5] J. Kwiecinski, T. Jin, E. Josefsson, *Apmis* **2014**, *122*, 1240–1250.
- [6] A. Michel, F. Agerer, C. R. Hauck, M. Herrmann, J. Ullrich, J. Hacker, K. Ohlsen, *J. Bacteriol.* **2006**, *188*, 5783–5796.
- [7] L. D. Franklin, *N. Engl. J. Med.* **1998**, *339*, 520–532.
- [8] K. Surmann, M. Simon, P. Hildebrandt, H. Pförtner, S. Michalik, S. Stentzel, L. Steil, V. M. Dhople, J. Bernhardt, R. Schlüter, et al., *J. Proteomics* **2015**, *128*, 203–217.
- [9] R. J. Gordon, F. D. Lowy, *Clin. Infect. Dis.* **2008**, *46*, 350.
- [10] K. Chamoto, M. Al-Habsi, T. Honjo, *Springer Int. Publ.* **2017**, *410*, 75–97.
- [11] D. Frees, S. N. A. Qazi, P. J. Hill, H. Ingmer, *Mol. Microbiol.* **2003**, *48*, 1565–1578.
- [12] M. M. Dinges, P. M. Orwin, P. M. Schlievert, S. Biology, O. F. The, *Society* **2000**, *13*, 16–34.
- [13] R. N. S. Haddadin, S. Saleh, I. S. I. Al-Adham, T. E. J. Buultjens, P. J. Collier, *J. Appl. Microbiol.* **2010**, *108*, 1281–1291.
- [14] Z. Zheng, E. Mylonakis, B. Burgwyn Fuchs, Q. Liu, W. Kim, *Future Med. Chem.* **2018**, *10*, 1319–1331.
- [15] N. K. Archer, M. J. Mazaitis, J. William Costerton, J. G. Leid, M. E. Powers, M. E. Shirtliff, *Virulence* **2011**, *2*, 445–459.
- [16] C. M. Waters, B. L. Bassler, *Annu. Rev. Cell Dev. Biol.* **2005**, *21*, 319–346.
- [17] A. Shamir, *J. R. Soc. Med.* **2004**, *97*, 443–443.
- [18] M. Bigos, A. Deny, *Int. Rev. Allergol. Clin. Immunol.* **2008**, *14*, 101–109.
- [19] M. Albano, F. C. B. Alves, B. F. M. T. Andrade, L. N. Barbosa, A. F. M. Pereira, M. de L. R. de S. da Cunha, V. L. M. Rall, A. Fernandes Júnior, *Innov. Food Sci. Emerg. Technol.* **2016**, *38*, 83–90.

-
- [20] C. P. Harkins, B. Pichon, M. Doumith, J. Parkhill, H. Westh, A. Tomasz, H. de Lencastre, S. D. Bentley, A. M. Kearns, M. T. G. Holden, *Genome Biol.* **2017**, *18*, 1–11.
- [21] A. Venkatasubramaniam, T. Kanipakala, N. Ganjbaksh, R. Mehr, I. Mukherjee, S. Krishnan, T. Bae, M. Aman, R. Adhikari, *Toxins (Basel)*. **2018**, *10*, 377.
- [22] R Keijl Fukuda, *World Heal. Organ.* **2014**.
- [23] P. Baker, B. Cohen, J. Liu, E. Larson, *Epidemiol. Infect.* **2016**, *144*, 1014–1017.
- [24] D. L. F. Wong, “World Health Organization,” can be found under https://gateway.euro.who.int/en/indicators/amr_23-methicillin-resistant-staphylococcus-aureus-mrsa/, **2017**.
- [25] B. Windsor-Shellard, “Deaths involving MRSA : England and Wales, 1993 to 2016,” can be found under <https://www.ons.gov.uk/peoplepopulationandcommunity/birthsdeathsandmarriages/deaths/datasets/deathsinvolvingmrsaenglandandwales>, **2017**.
- [26] B. I. Duerden, *Eye* **2012**, *26*, 218–221.
- [27] P. Elstrøm, E. Astrup, K. Hegstad, Ø. Samuelsen, H. Enger, O. Kacelnik, *PLoS One* **2019**, *14*, 1–17.
- [28] F. Di Ruscio, J. V. Bjørnholt, T. M. Leegaard, A. E. F. Moen, B. F. De Blasio, *PLoS One* **2017**, *12*, 2006–2015.
- [29] B. D. Brooks, A. E. Brooks, *Adv. Drug Deliv. Rev.* **2014**, *78*, 14–27.
- [30] A. Fernandes, E. C. Balestrin, J. E. C. Betoni, R. De Oliveira Orsi, M. D. L. R. De Souza Da Cunha, A. C. Montelli, *Mem. Inst. Oswaldo Cruz* **2005**, *100*, 563–566.
- [31] S. E. Walsh, J.-Y. Maillard, A. D. Russell, C. E. Catrenich, D. L. Charbonneau, R. G. Bartolo, *J. Appl. Microbiol.* **2003**, *94*, 240–247.
- [32] C. T. Filgueiras, M. C. D. Vanetti, *Brazilian Arch. Biol. Technol.* **2006**, *49*, 405–409.
- [33] W. Li, H. Chen, Z. He, C. Han, S. Liu, Y. Li, *LWT - Food Sci. Technol.* **2015**, *62*, 39–47.
- [34] J. H. Lee, Y. G. Kim, J. G. Park, J. Lee, *Food Control* **2017**, *80*, 74–82.
- [35] C. Ngba Essebe, O. Visvikis, M. Fines-Guyon, A. Vergne, V. Cattoir, A. Lecoustumier, E. Lemichez, A. Sotto, J.-P. Lavigne, C. Dunyach-Remy, *Front. Cell. Infect. Microbiol.* **2017**, *7*, 1–11.
- [36] P. Recsei, B. Kreiswirth, M. O’Reilly, P. Schlievert, A. Gruss, R. P. Novick, *MGG Mol. Gen.*

- Genet.* **1986**, *202*, 58–61.
- [37] S. Bronner, H. Monteil, G. Prévost, *FEMS Microbiol. Rev.* **2004**, *28*, 183–200.
- [38] R. Singh, P. Ray, *Future Microbiol.* **2014**, *9*, 669–681.
- [39] J. M. Yarwood, P. M. Schlievert, *J. Clin. Invest.* **2003**, *112*, 1620–1625.
- [40] R. P. Novick, S. J. Projan, J. Kornblum, H. F. Ross, G. Ji, B. Kreiswirth, F. Vandenesch, S. Moghazeh, R. P. Novick, *MGG Mol. Gen. Genet.* **1995**, *248*, 446–458.
- [41] R. P. Novick, H. F. Ross, S. J. Projan, J. Kornblum, B. Kreiswirth, S. Moghazeh, *EMBO J.* **1993**, *12*, 3967–3975.
- [42] R. O. Nicholas, T. Li, D. Mcdevitt, A. Marra, S. Socoloski, P. L. Demarsh, D. R. Gentry, *Infect. Immun.* **1999**, *67*, 3667–3669.
- [43] S. P. Nair, M. Bischoff, M. M. Senn, B. Berger-Bächi, *Infect. Immun.* **2003**, *71*, 4167–4170.
- [44] M. J. Evans, B. F. Cravatt, *Chem. Rev.* **2006**, *106*, 3279–3301.
- [45] D. J. Lapinsky, *Bioorg. Med. Chem.* **2012**, *20*, 6237–6247.
- [46] P. P. Geurink, L. M. Prely, G. A. van der Marel, R. Bischoff, H. S. Overkleeft, *Top Curr Chem* **2012**, *324*, 85–113.
- [47] K. Lang, J. W. Chin, *Chem. Rev.* **2014**, *114*, 4764–4806.
- [48] H. Staudinger, J. Meyer, *Helv. Chim. Acta* **1919**, *2*, 635–646.
- [49] E. Saxon, C. R. Bertozzi, *Science (80-.)*. **2000**, *287*, 2007–2010.
- [50] V. V. Rostovtsev, L. G. Green, V. V. Fokin, K. B. Sharpless, *Angew. Chemie - Int. Ed.* **2002**, *41*, 2596–2599.
- [51] H. C. Kolb, K. B. Sharpless, *Drug Discov. Today* **2003**, *8*, 1128–1137.
- [52] K. E. Beatty, J. D. Fisk, B. P. Smart, Y. Y. Lu, J. Szychowski, M. J. Hangauer, J. M. Baskin, C. R. Bertozzi, D. A. Tirrell, *ChemBioChem* **2010**, *11*, 2092–2095.
- [53] D. L. Boger, *Chem. Rev.* **1986**, *86*, 781–793.
- [54] H. C. Kolb, M. G. Finn, K. B. Sharpless, *Angew. Chemie - Int. Ed.* **2001**, *40*, 2004–2021.
- [55] J. Eirich, J. L. Burkhardt, A. Ullrich, G. C. Rudolf, A. Vollmar, S. Zahler, U. Kazmaier, S. A. Sieber, *Mol. Biosyst.* **2012**, *8*, 2067–2075.
- [56] P. György, C. S. Rose, R. E. Eakin, E. E. Snell, J. Roger, *Science (80-.)*. **1941**, *93*, 477–478.

-
- [57] D. J. Lapinsky, D. S. Johnson, *Future Med. Chem.* **2015**, *7*, 2143–2171.
- [58] Y. Sadakane, Y. Hatanaka, *Anal. Sci.* **2006**, *22*, 209–218.
- [59] E. Smith, I. Collins, *Future Med. Chem.* **2015**, *7*, 159–183.
- [60] G. C. Terstappen, C. Schlüpen, R. Raggiaschi, G. Gaviraghi, *Nat. Rev. Drug Discov.* **2007**, *6*, 891–903.
- [61] L. Dubinsky, B. P. Krom, M. M. Meijler, *Bioorganic Med. Chem.* **2012**, *20*, 554–570.
- [62] P. Kleiner, W. Heydenreuter, M. Stahl, V. S. Korotkov, S. A. Sieber, *Angew. Chemie - Int. Ed.* **2017**, *56*, 1396–1401.
- [63] J. Das, *Chem. Rev.* **2011**, *111*, 4405–4417.
- [64] P. Kleiner, Insights into Phosphocrosslinker-Associated off-Target Protein Binding and Discovery of a Small Molecule Antibiotic Active against Multidrug-Resistant Gram-Positive Pathogens, Technische Universität München, **2018**.
- [65] M. Nitzan, P. Fechter, A. Peer, Y. Altuvia, D. Bronesky, F. Vandenesch, P. Romby, O. Biham, H. Margalit, *Nucleic Acids Res.* **2015**, *43*, 1357–1369.
- [66] J. Vomacka, V. S. Korotkov, B. Bauer, F. Weinandy, M. H. Kunzmann, J. Krysiak, O. Baron, T. Boettcher, K. Lorenz-Baath, S. A. Sieber, *Chem. - Eur. J.* **2016**, *22*, 1622–1630.
- [67] P. J. Boersema, R. Raijmakers, S. Lemeer, S. Mohammed, A. J. R. Heck, *Nat. Protoc.* **2009**, *4*, 484–494.
- [68] A. T. Giraud, A. Calzolari, A. A. Cataldi, C. Bogni, R. Nagel, *FEMS Microbiol. Lett.* **1999**, *180*, 117.
- [69] Y. Q. Xiong, J. Willard, M. R. Yeaman, A. L. Cheung, A. S. Bayer, *J. Infect. Dis.* **2006**, *194*, 1267–1275.
- [70] S. J. Peacock, T. J. Foster, B. J. Cameron, A. R. Berendt, *Microbiology* **1999**, *145*, 3477–3486.
- [71] M. Dalla Serra, M. Coraiola, G. Viero, M. Comai, C. Potrich, M. Ferreras, L. Baba-Moussa, D. A. Colin, G. Menestrina, S. Bhakdi, et al., *J. Chem. Inf. Model.* **2005**, *45*, 1539–1545.
- [72] B. R. Boles, A. R. Horswill, *PLoS Pathog.* **2008**, *4*, e1000052.
- [73] Q. Liu, X. Wang, J. Qin, S. Cheng, W.-S. Yeo, L. He, X. Ma, X. Liu, M. Li, T. Bae, *Front. Cell. Infect. Microbiol.* **2017**, *7*, 1–11.
- [74] W. C. Sung, D. Romo, *Org. Lett.* **2007**, *9*, 1537–1540.

- [75] J. Andersen, U. Madsen, F. Bjorkling, X. Liang, *Synlett* **2005**, 2209–2213.
- [76] J. Cox, M. Y. Hein, C. A. Lubner, I. Paron, N. Nagaraj, M. Mann, *Mol. Cell. Proteomics* **2014**, *13*, 2513–2526.
- [77] Z. Li, D. Boyd, M. Reindl, M. B. Goldberg, *J. Bacteriol.* **2014**, *196*, 367–377.
- [78] K. Xie, R. E. Dalbey, *Nat. Rev. Microbiol.* **2008**, *6*, 234.
- [79] S. R. Palmer, P. J. Crowley, M. W. Oli, M. Adam Ruelf, S. M. Michalek, L. Jeannine Brady, *Microbiol. (United Kingdom)* **2012**, *158*, 1702–1712.
- [80] A. Hasona, P. J. Crowley, C. M. Levesque, R. W. Mair, D. G. Cvitkovitch, A. S. Bleiweis, L. J. Brady, *Proc. Natl. Acad. Sci.* **2005**, *102*, 17466–17471.
- [81] M. H. Lin, J. C. Shu, H. Y. Huang, Y. C. Cheng, *PLoS One* **2012**, *7*, 3–9.
- [82] B. A. Frankel, M. Bentley, R. G. Kruger, D. G. McCafferty, *J. Am. Chem. Soc.* **2004**, *126*, 3404–3405.
- [83] S. K. Mazmanian, H. Ton-That, K. Su, O. Schneewind, *Proc. Natl. Acad. Sci.* **2002**, *99*, 2293–2298.
- [84] S. K. Mazmanian, G. Liu, E. R. Jensen, E. Lenoy, O. Schneewind, *Proc. Natl. Acad. Sci.* **2000**, *97*, 5510–5515.
- [85] L. Alksne, S. J. Projan, *Curr. Opin. Biotechnol.* **2000**, *11*, 625–636.
- [86] R. P. Novick, *Trends Microbiol.* **2000**, *8*, 148–151.
- [87] C. Opoku-Temeng, N. Dayal, J. Miller, H. O. Sintim, *RSC Adv.* **2017**, *7*, 8288–8294.
- [88] C. M. Gries, E. L. Bruger, D. E. Moormeier, T. D. Scherr, C. M. Waters, T. Kielian, *Infect. Immun.* **2016**, *84*, 3564–3574.
- [89] X. Peng, Y. Zhang, G. Bai, X. Zhou, H. Wu, *Mol. Microbiol.* **2016**, *99*, 945–959.
- [90] E. Culp, G. D. Wright, *J. Antibiot. (Tokyo)*. **2017**, *70*, 366–377.
- [91] W. N. Lipscomb, N. Sträter, *Chem. Rev.* **1996**, *96*, 2375–2434.
- [92] E. Proteases, S. Gottesman, M. R. Maurizi, S. Wickner, *Cell* **1997**, *91*, 435–438.
- [93] F. Ye, J. Li, C.-G. Yang, *Mol. Biosyst.* **2017**, *13*, 23–31.
- [94] I. T. Malik, H. Brötz-Oesterhelt, *Nat. Prod. Rep.* **2017**, *34*, 815–831.
- [95] A. Gribun, M. S. Kimber, R. Ching, R. Sprangers, K. M. Fiebig, W. A. Houry, *J. Biol. Chem.*

- 2005**, 280, 16185–16196.
- [96] F. Ye, J. Zhang, H. Liu, R. Hilgenfeld, R. Zhang, X. Kong, L. Li, J. Lu, X. Zhang, D. Li, et al., *J. Biol. Chem.* **2013**, 288, 17643–17653.
- [97] B. G. Lee, M. K. Kim, H. K. Song, *Mol. Cells* **2011**, 32, 589–595.
- [98] J. Zhang, F. Ye, L. Lan, H. Jiang, C. Luo, C.-G. Yang, *J. Biol. Chem.* **2011**, 286, 37590–37601.
- [99] M. S. Kimber, A. Y. H. Yu, M. Borg, E. Leung, H. S. Chan, W. A. Houry, *Structure* **2010**, 18, 798–808.
- [100] S. R. Geiger, T. Böttcher, S. A. Sieber, P. Cramer, *Angew. Chemie - Int. Ed.* **2011**, 50, 5749–5752.
- [101] D. Y. Kim, K. K. Kim, *J. Biol. Chem.* **2003**, 278, 50664–50670.
- [102] S. A. Joshi, G. L. Hersch, T. A. Baker, R. T. Sauer, *Nat. Struct. Mol. Biol.* **2004**, 11, 404–411.
- [103] M. C. Bewley, V. Graziano, K. Griffin, J. M. Flanagan, *J. Struct. Biol.* **2006**, 153, 113–128.
- [104] S. E. Glynn, A. Martin, A. R. Nager, T. A. Baker, R. T. Sauer, *Cell* **2009**, 139, 744–756.
- [105] S. G. Kang, M. N. Dimitrova, J. Ortega, A. Ginsburg, M. R. Maurizi, *J. Biol. Chem.* **2005**, 280, 35424–35432.
- [106] T. Akopian, O. Kandrор, R. M. Raju, M. UnniKrishnan, E. J. Rubin, A. L. Goldberg, *EMBO J.* **2012**, 31, 1529–1541.
- [107] E. Zeiler, N. Braun, T. Böttcher, A. Kastenmüller, S. Weinkauff, S. A. Sieber, *Angew. Chemie - Int. Ed.* **2011**, 50, 11001–11004.
- [108] D. Balogh, M. Dahmen, M. Stahl, M. Poreba, M. Gersch, M. Drag, S. A. Sieber, *Chem. Sci.* **2017**, 8, 1592–1600.
- [109] S. A. Goff, A. L. Goldberg, *Cell* **1985**, 41, 587–595.
- [110] G. Somero, *Annu. Rev. Physiol.* **1995**, 57, 43–68.
- [111] D. Frees, K. Savijoki, P. Varmanen, H. Ingmer, *Mol. Microbiol.* **2007**, 63, 1285–1295.
- [112] S. Bregenholt, F. Jaubert, O. Gaillot, P. Berche, J. P. Di Santo, *Infect. Immun.* **2001**, 69, 4938–4943.
- [113] M. W. Hackl, M. Lakemeyer, M. Dahmen, M. Glaser, A. Pahl, K. Lorenz-Baath, T. Menzel, S. Sievers, T. Böttcher, I. Antes, et al., *J. Am. Chem. Soc.* **2015**, 137, 8475–8483.
- [114] T. Böttcher, S. A. Sieber, *J. Am. Chem. Soc.* **2008**, 130, 14400–14401.

- [115] F. Weinandy, K. Lorenz-Baath, V. S. Korotkov, T. Böttcher, S. Sethi, T. Chakraborty, S. A. Sieber, *ChemMedChem* **2014**, *9*, 710–713.
- [116] H. Brötz-Oesterhelt, D. Beyer, H. P. Kroll, R. Endermann, C. Ladel, W. Schroeder, B. Hinzen, S. Raddatz, H. Paulsen, K. Henninger, et al., *Nat Med* **2005**, *11*, 1082–1087.
- [117] C. Walsh, *Nature* **2000**, *406*, 775–781.
- [118] G. Kaufman, *Nurs. Stand.* **2013**, *25*, 49–55.
- [119] K. H. Michel, R. E. Kastner, *A54556 Antibiotics*, **1985**.
- [120] B. Hinzen, S. Raddatz, H. Paulsen, T. Lampe, A. Schumacher, D. Habich, V. Hellwig, J. Benet-Buchholz, R. Endermann, H. Labischinski, et al., *ChemMedChem* **2006**, *1*, 689–693.
- [121] H. Koshino, H. Osada, T. Yano, J. Uzawa, K. Isono, *Tetrahedron Lett.* **1991**, *32*, 7707–7710.
- [122] J. D. Goodreid, J. Janetzko, J. P. Santa Maria, K. S. Wong, E. Leung, B. T. Eger, S. Bryson, E. F. Pai, S. D. Gray-Owen, S. Walker, et al., *J. Med. Chem.* **2016**, *59*, 624–646.
- [123] J. Kirstein, A. Hoffmann, H. Lilie, R. Schmidt, H. Rübsamen-Waigmann, H. Brötz-Oesterhelt, A. Mogk, K. Turgay, *EMBO Mol. Med.* **2009**, *1*, 37–49.
- [124] B.-G. Lee, E. Y. Park, K.-E. Lee, H. Jeon, K. H. Sung, H. Paulsen, H. Rübnsamen-Schaeff, H. Brötz-Oesterhelt, H. K. Song, *Nat Struct Mol Biol* **2010**, *17*, 471–478.
- [125] M. A. Sowole, J. A. Alexopoulos, Y.-Q. Cheng, J. Ortega, L. Konermann, *J. Mol. Biol.* **2013**, *425*, 4508–4519.
- [126] M. Gersch, K. Famulla, M. Dahmen, C. Göbl, I. Malik, K. Richter, V. S. Korotkov, P. Sass, H. Rübsamen-Schaeff, T. Madl, et al., *Nat Commun* **2015**, *6*, 6320.
- [127] P. Sass, M. Josten, K. Famulla, G. Schiffer, H.-G. Sahl, L. Hamoen, H. Brötz-Oesterhelt, *Proc. Natl. Acad. Sci.* **2011**, *108*, 17474–17479.
- [128] D. H. S. Li, Y. S. Chung, M. Gloyd, E. Joseph, R. Ghirlando, G. D. Wright, Y.-Q. Cheng, M. R. Maurizi, A. Guarné, J. Ortega, *Chem. Biol.* **2010**, *17*, 959–969.
- [129] T. Ni, F. Ye, X. Liu, J. Zhang, H. Liu, J. Li, Y. Zhang, Y. Sun, M. Wang, C. Luo, et al., *ACS Chem. Biol.* **2016**, *11*, 1964–1972.
- [130] J. Ollinger, T. O'Malley, E. A. Kesicki, J. Odingo, T. Parish, *J Bacteriol* **2012**, *194*, 663–668.
- [131] K. Famulla, P. Sass, I. Malik, T. Akopian, O. Kandror, M. Alber, B. Hinzen, H. Rübnsamen-Schaeff, R. Kalscheuer, A. L. Goldberg, et al., *Mol. Microbiol.* **2016**, *101*, 194–209.
- [132] D. W. Carney, K. R. Schmitz, J. V. Truong, R. T. Sauer, J. K. Sello, *J. Am. Chem. Soc.* **2014**,

- 136, 1922–1929.
- [133] M. Arvanitis, G. Li, D. D. Li, D. Cotnoir, L. Ganley-Leal, D. W. Carney, J. K. Sello, E. Mylonakis, *PLoS One* **2016**, *11*, 1–10.
- [134] F. von Nussbaum, M. Brands, B. Hinzen, S. Weigand, D. Häbich, *Angew. Chemie Int. Ed.* **2006**, *45*, 5072–5129.
- [135] M. T. Pstrągowski, M. Bujalska-Zadrozny, *Polish J. Microbiol.* **2015**, *64*, 85–92.
- [136] K. R. Schmitz, D. W. Carney, J. K. Sello, R. T. Sauer, *Proc. Natl. Acad. Sci.* **2014**, *111*, E4587–E4595.
- [137] B. P. Conlon, E. S. Nakayasu, L. E. Fleck, M. D. LaFleur, V. M. Isabella, K. Coleman, S. N. Leonard, R. D. Smith, J. N. Adkins, K. Lewis, *Nature* **2013**, *503*, 365–370.
- [138] D. W. Carney, C. L. Compton, K. R. Schmitz, J. P. Stevens, R. T. Sauer, J. K. Sello, *ChemBioChem* **2014**, *15*, 2216–2220.
- [139] E. Leung, A. Datti, M. Cossette, J. Goodreid, S. E. McCaw, M. Mah, A. Nakhamchik, K. Ogata, M. El Bakkouri, Y.-Q. Cheng, et al., *Chem. Biol.* **2011**, *18*, 1167–1178.
- [140] D. A. Dougan, *Chem. Biol.* **2011**, *18*, 1072–1074.
- [141] N. P. Lavey, J. A. Coker, E. A. Ruben, A. S. Duerfeldt, *J. Nat. Prod.* **2016**, *79*, 1193–1197.
- [142] U. Schmidt, K. Neumann, A. Schumacher, S. Weinbrenner, *Angew. Chemie Int. Ed. English* **1997**, *36*, 1110–1112.
- [143] J. D. Goodreid, E. da S. dos Santos, R. A. Batey, *Org. Lett.* **2015**, *17*, 2182–2185.
- [144] U. Schmidt, A. Lieberknecht, H. Griesser, J. Talbiersky, *J. Org. Chem.* **1982**, *47*, 3261–3264.
- [145] J. D. Goodreid, K. Wong, E. Leung, S. E. McCaw, S. D. Gray-Owen, A. Lough, W. A. Houry, R. A. Batey, *J. Nat. Prod.* **2014**, *77*, 2170–2181.
- [146] B. Hofbauer, Synthesis of Photo-Activated ADEP-Derivatives and Their Application for Target-Identification, Technische Universität München, **2015**.
- [147] T. Böttcher, S. A. Sieber, *ChemBioChem* **2009**, *10*, 663–666.
- [148] C. L. Compton, K. R. Schmitz, R. T. Sauer, J. K. Sello, *ACS Chem. Biol.* **2013**, *8*, 2669–2677.
- [149] C. Fetzer, V. S. Korotkov, R. Thänert, K. M. Lee, M. Neuenschwander, J. P. von Kries, E. Medina, S. A. Sieber, *Angew. Chemie* **2017**, *56*, 15746–15750.
- [150] P. Sehgal, C. Olsesn, J. V. Moeller, *Methods Mol. Biol.* **2016**, *1377*, 105–109.

- [151] I. T. Malik, H. Brötz-Oesterhelt, *Nat. Prod. Rep.* **2017**, *34*, 815–831.
- [152] T. Kroeger, B. Frieg, T. Zhang, F. K. Hansen, A. Marmann, P. Proksch, L. Nagel-Steger, G. Groth, S. H. J. Smits, H. Gohlke, *PLoS One* **2017**, *12*, 1–14.
- [153] M. Kohlstaedt, I. von der Hocht, F. Hilbers, Y. Thielmann, H. Michel, *Acta Crystallogr. Sect. D* **2015**, *71*, 1112–1122.
- [154] G. V. Semisotnov, N. A. Rodionova, O. I. Razgulyaev, V. N. Uversky, A. F. Gripas', R. I. Gilmanshin, *Biopolymers* **1991**, *31*, 119–128.
- [155] M. C. Lo, A. Aulabaugh, G. Jin, R. Cowling, J. Bard, M. Malamas, G. Ellestad, *Anal. Biochem.* **2004**, *332*, 153–159.
- [156] D. T. Gruszka, J. A. Wojdyla, R. J. Bingham, J. P. Turkenburg, I. W. Manfield, A. Steward, A. P. Leech, J. A. Geoghegan, T. J. Foster, J. Clarke, et al., *Proc. Natl. Acad. Sci. U. S. A.* **2012**, *109*, 7–9.
- [157] Y. Belyi, I. Rybolovlev, N. Polyakov, A. Chernikova, I. Tabakova, A. Gintsburg, *Open Microbiol. J.* **2018**, *12*, 94–106.
- [158] D. Subramanian, J. Natarajan, *Gene* **2015**, *574*, 149–162.
- [159] “UniProt,” can be found under <https://www.uniprot.org/uniprot/Q2FW51#function>, **2019**.
- [160] G. C. Winters, A. L. Mandel, J. R. Rich, B. J. Hedberg, T. H. H. Hsieh, E. M. J. Bourque, J. Babcook, *Cytotoxic and Anti-Mitotic Compounds, and Methods of Using the Same*, **2014**, WO 2014/144871 A1.
- [161] A. Isidro-Llobet, K. Hadje Georgiou, W. R. J. D. Galloway, E. Giacomini, M. R. Hansen, G. Mendez-Abt, Y. S. Tan, L. Carro, H. F. Sore, D. R. Spring, *Org. Biomol. Chem.* **2015**, *13*, 4570–4580.
- [162] E. D. Goddard-Borger, R. V. Stick, *Org. Lett.* **2007**, *9*, 3797–3800.
- [163] H. Gilman, J. E. Kirby, *Ames. Rec. trav. chim.* **1929**, *48*, 155.
- [164] J. F. Normant, *Synthesis (Stuttg.)*. **1972**, *2*, 63.
- [165] J. D. Goodreid, *Synthesis and Biological Evaluation of Antibacterial Small Molecule Activators of Caseinolytic Protease P and the Synthetic Utility of Metal Carboxylate Salts in Amidation Reactions with Amines*, University of Toronto, **2016**.
- [166] B. Van Der Meijden, J. A. Robinson, *Arkivoc* **2010**, *2011*, 130.
- [167] E. C. Griffith, R. E. Lee, “PDB protein data bank,” DOI 10.2210/pdb5VZ2/pdbcan be found

- under <https://www.rcsb.org/structure/5vz2>, **2017**.
- [168] T. Böttcher, S. A. Sieber, *Angew. Chemie Int. Ed.* **2008**, *47*, 4600–4603.
- [169] A. Cole, Z. Wang, E. Coyaud, V. Voisin, M. Gronda, Y. Jitkova, R. Mattson, R. Hurren, S. Babovic, N. Maclean, et al., *Cancer Cell* **2015**, *27*, 864–876.
- [170] M. G. Lei, R. K. Gupta, C. Y. Lee, *PLoS One* **2017**, *12*, 1–17.
- [171] J. Eirich, R. Orth, S. A. Sieber, *J. Am. Chem. Soc.* **2011**, *133*, 12144–12153.
- [172] D. C. Osipovitch, S. Therrien, K. E. Griswold, *Appl. Microbiol. Biotechnol.* **2015**, *99*, 6315–6326.
- [173] A. Resch, R. Rosenstein, C. Nerz, F. Go, *Society* **2005**, *71*, 2663–2676.
- [174] T. E. Benson, D. J. Filman, C. T. Walsh, J. M. Hogle, **1995**, *2*.
- [175] D. Szklarczyk, A. L. Gable, D. Lyon, A. Junge, S. Wyder, J. Huerta-Cepas, M. Simonovic, N. T. Doncheva, J. H. Morris, P. Bork, et al., *Nucleic Acids Res.* **2019**, *47*, D607–D613.
- [176] M. Artini, R. Papa, G. Barbato, G. L. Scoarughi, A. Cellini, P. Morazzoni, E. Bombardelli, L. Selan, *Bioorganic Med. Chem.* **2012**, *20*, 920–926.
- [177] J. Daiss, E. Schwarz, J. J. Varrone, J. Brodell, S. N. Bello-Irizarry, *Passive Immunization for Staphylococcus Infections*, **2015**, Wo 2015/089502.
- [178] T. Oshida, M. Sugai, H. Komatsuzawa, Y.-M. Hong, H. Suginaka, A. Tomasz, *Proc. Natl. Acad. Sci. USA* **1995**, *92*, 285.
- [179] L. A. Kirsebom, L. A. Isaksson, *Proc. Natl. Acad.* **1985**, *82*, 717–721.
- [180] A. Sonesson, K. Przybyszewska, S. Eriksson, M. Mörgelin, S. Kjellström, J. Davies, J. Potempa, A. Schmidtchen, *Sci. Rep.* **2017**, *7*, 1–12.
- [181] A. J. Laarman, G. Mijnheer, J. M. Mootz, W. J. M. Van Rooijen, M. Ruyken, C. L. Malone, E. C. Heezius, R. Ward, G. Milligan, J. A. G. Van Strijp, et al., *EMBO J.* **2012**, *31*, 3607–3619.
- [182] M. H. Lin, C. C. Li, J. C. Shu, H. W. Chu, C. C. Liu, C. C. Wu, *Proteomics* **2018**, *18*, 1–18.
- [183] P. Vijayalakshmi, P. Daisy, *J. Recept. Signal Transduct.* **2015**, *35*, 15–25.
- [184] S. Gul, R. Brown, E. May, M. Mazzulla, M. G. Smyth, C. Berry, A. Morby, D. J. Powell, *Biochem. J.* **2004**, *383*, 551–559.
- [185] B. Hofbauer, J. Vomacka, M. Stahl, V. S. Korotkov, M. C. Jennings, W. M. Wuest, S. A. Sieber, *Biochemistry* **2018**, *57*, 1814–1820.

- [186] M. Leybold, P. W. Wallace, M. Kljajic, M. Schittmayer, J. Pletz, C. Illaszewicz-Trattner, G. M. Guebitz, R. Birner-Gruenberger, R. Breinbauer, *Tetrahedron Lett.* **2015**, *56*, 5619–5622.
- [187] Y. Hayashi, T. Urushima, M. Shin, M. Shoji, *Tetrahedron* **2005**, *61*, 11393–11404.
- [188] M. Vellakkaran, M. M. S. Andappan, N. Kommu, *European J. Org. Chem.* **2012**, 4694–4698.
- [189] Y. Igarashi, K. Aoki, H. Nishimura, I. Morishita, K. Usui, **2012**, *60*, 1088–1091.
- [190] M. J. O'Donnell, J. Alsina, W. L. Scott, *Tetrahedron Lett.* **2003**, *44*, 8403–8406.
- [191] M. H. Wright, C. Fetzer, S. A. Sieber, *J. Am. Chem. Soc.* **2017**, *139*, 6152–6159.
- [192] C. Fetzer, Virulence Attenuation through Chemical and Genetic Manipulation of the Staphylococcus Aureus ClpXP Protease, Technische Universität München, **2018**.
- [193] J. A. Vizcaíno, A. Csordas, N. Del-Toro, J. A. Dianas, J. Griss, I. Lavidas, G. Mayer, Y. Perez-Riverol, F. Reisinger, T. Ternent, et al., *Nucleic Acids Res.* **2016**, *44*, D447–D456.
- [194] Y. Benjamini, Y. Hochberg, *J. R. Stat. Soc.* **1995**, *57*, 289–300.
- [195] D. W. Huang, B. T. Sherman, R. A. Lempicki, *Nat. Protoc.* **2009**, *4*, 44–57.
- [196] D. W. Huang, B. T. Sherman, R. A. Lempicki, *Nucleic Acids Res.* **2009**, *37*, 1–13.
- [197] M. Gersch, A. List, M. Groll, S. A. Sieber, *J. Biol. Chem.* **2012**, *287*, 9484–9494.
- [198] T. F. Gronauer, M. M. Mandl, M. Lakemeyer, M. W. Hackl, M. Meßner, V. S. Korotkov, J. Pachmayr, S. A. Sieber, *Chem. Commun.* **2018**, *54*, 9833–9836.
- [199] M. Stahl, V. S. Korotkov, D. Balogh, L. M. Kick, M. Gersch, A. Pahl, P. Kielkowski, K. Richter, S. Schneider, S. A. Sieber, *Angew. Chemie - Int. Ed.* **2018**, *57*, 14602–14607.
- [200] M. Gersch, R. Kolb, F. Alte, M. Groll, S. A. Sieber, *J. Am. Chem. Soc.* **2014**, *136*, 1360–1366.

List of Abbreviations

aa	amino acid
AAA proteins	ATPases Associated with diverse cellular Activities
AAD	<i>N</i> -acetylmuramoyl-L-alanine amidase domain-containing protein
ABPP	activity based protein profiling
ACN	acetonitrile
ACP	activator of self-compartmentalizing proteases
ADEP	acyldepsipeptide
A β BPP	affinity based protein profiling
Agr	accessory gene regulatory
AIP	auto-inducing peptide
AMD	<i>N</i> -acetylmuramoyl-L-alanine amidase domain
APCI	atmospheric pressure chemical ionization
ATET	anhydrotetracycline
ATF	D-alanine aminotransferase
a.u.	arbitrary units
BCA	bicinchoninic acid assay
Bn	benzyl
Boc	<i>tert</i> -butyloxycarbonyl
BSA	Bovine serum albumin
BTTA	2-(4-((bis((1-(<i>tert</i> -butyl)-1H-1,2,3-triazol-4-yl)methyl)amino)methyl)-1H-1,2,3-triazol-1-yl)acetic acid
calcd.	calculated
CAM	ceric ammonium molybdate

List of Abbreviations

ClpP	caseinolytic protease P
conc.	concentrated
CPS	capsular polysaccharide synthesis
d	doublet (NMR: multiplicity)
Da	Dalton
DAC	diadenylate cyclase
DCM	dichloromethane
dd	doublet of doublets (NMR: multiplicity)
ddH ₂ O	double-distilled water
Da	Dalton
DIPEA	diisopropylethylamine
DMAP	4-dimethylaminopyridine
DMEDA	1,2-Dimethylethylenediamine
DMF	dimethyl formamide
DMSO	dimethyl sulfoxide
DNA	desoxyribonucleic acid
DTT	dithiothreitol
EDC	1-ethyl-3-(3-dimethylaminopropyl)carbodiimide
EDTA	ethylenediaminetetraacetic acid
eq.	equivalent
ESI	electrospray ionization
<i>et al.</i>	<i>et alli</i>
EtOAc	ethyl acetate
EtOH	ethanol

FA	formic acid
FBS	fetal bovine serum
FDR	false discovery rate
FITC	fluorescein-5-isothiosyanate
GFP	green fluorescent protein
GO	gene ontology
h	hour
HATU	<i>O</i> -(7-Azabenzotriazol-1-yl)- <i>N,N,N',N'</i> -tetramethyluronium-hexafluorophosphat
HEPES	(4-(2-hydroxyethyl)-1-piperazineethanesulfonic acid)
Hla	<i>alpha</i> -hemolysin
HPLC	high pressure liquid chromatography
HR-MS	high resolution mass spectrometry
HTS	high throughput screen
Hz	Hertz
IAA	2-Iodoacetamide
int.	intensity
IPTG	Isopropyl- β -D-1-thiogalactopyranoside
<i>J</i>	coupling constant (Hz)
LC-MS	liquid chromatography mass spectrometry
LFQ	label free quantification
LHMDS	Lithium bis(trimethylsilyl)amide
LTQ	linear trap quadrupole
m	multiplet (NMR: multiplicity)
max.	maximal

List of Abbreviations

MIC	minimum inhibitory concentration
min	minute
NMR	nuclear magnetic resonance
MNBA	2-Methyl-6-nitrobenzoic anhydride
MRSA	methicillin resistant <i>S. aureus</i>
MS	mass spectrometry
MS/MS	tandem mass spectrometry
MSSA	methicillin sensitive <i>S. aureus</i>
MTT	3-(4,5-dimethylthiazol-2-yl)-2,5-diphenyltetrazolium bromide
MW	molecular weight
OD	optical density
ON	overnight
PBS	phosphate buffered saline
pip	pipecolic acid
PMA	phosphomolybdic acid
ppm	parts per million
QS	quorum sensing
RhN ₃	rhodamine azide
RNA	ribonuclein acid
Rot	repressor of toxins
r.t.	room temperature
s	singulet (NMR: multiplicity)
Sar	staphylococcal accessory response
SAR	structure activity relationship

SasG	<i>S. aureus</i> surface protein G
SDS	sodium dodecyl sulphate
SDS-PAGE	sodium dodecyl sulphate polyacrylamide gel electrophoresis
sec	second
SPPS	solid phase peptide synthesis
t	triplet (NMR: multiplicity)
TAMRA	Tetramethylrhodamine 5-Carboxamido-(6-Azidohexanyl)
TBS	<i>tert</i> -butyldimethylsilyl
TBTA	tris(benzyltriazolylmethyl)amine
TCEP	tris(2-carboxyethyl)phosphine
TCS	two-component system
TEAB	tetraethylammonium bromide
TFA	trifluoroacetic acid
TFL	trifunctional linker
THF	tetrahydrofurane
THPTA	Tris(3-hydroxypropyltriazolylmethyl)amin
TLC	thin layer chromatography
TMS	trimethylsilyl
TSA	thermal shift assay
TRIS	tris(hydroxymethyl)aminomethane
UV	ultraviolet
<i>virt.</i>	virtual
WB	western blot
wt	wild type

APPENDIX

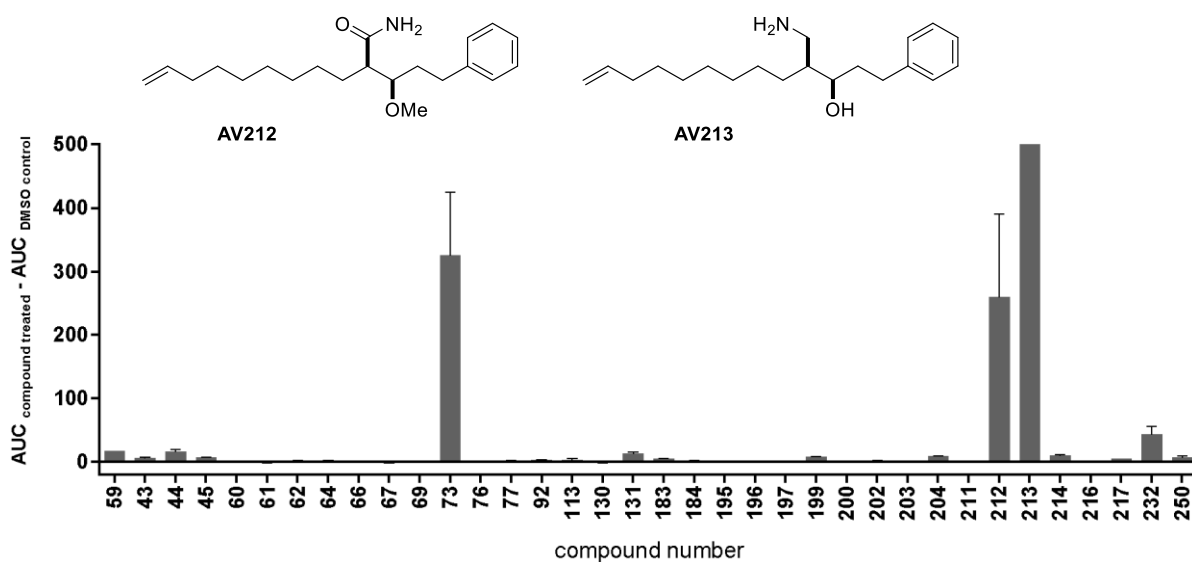
1. Additional Figures (Chapter II, III)

Figure A 1. A hemolysis assay screen of 35 compounds at a concentration of 50 μM was done in two technical replicates. AUC describes the readout parameter from the assay, the area under the curve (see methods for details). Structures of compounds AV212 and AV213.

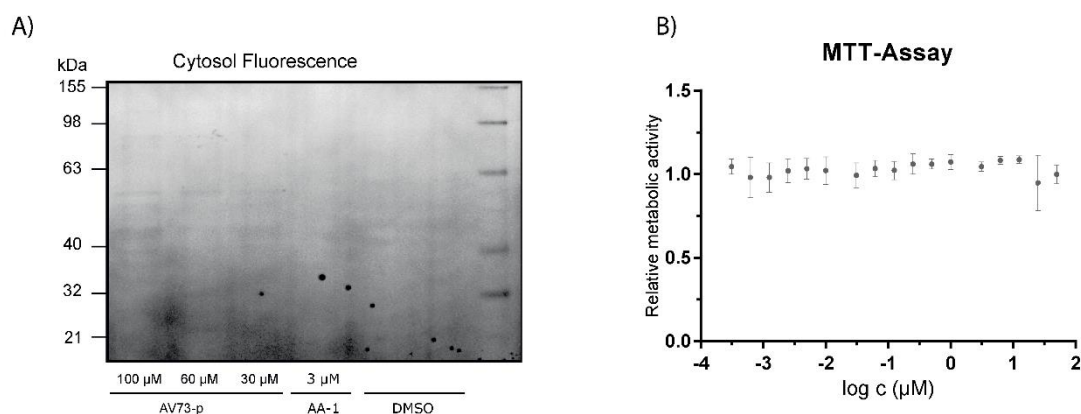
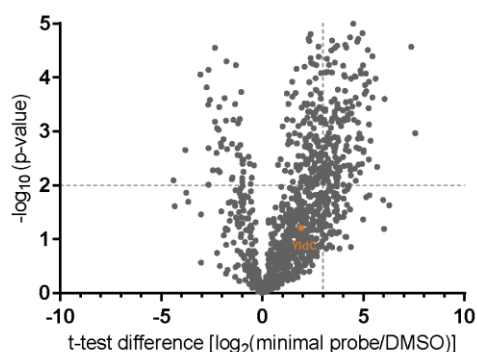
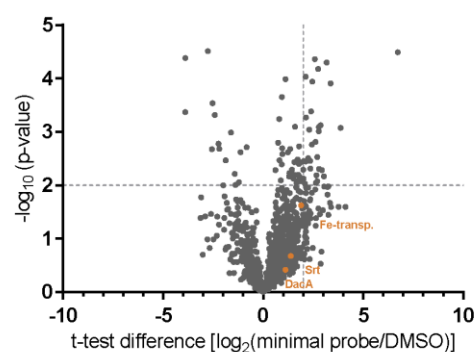


Figure A 2. A) Analytical labeling under hemolysis conditions with different concentrations of AV73-p, the minimalist aryl azide photoprobe AA-1 and a DMSO control. B) MTT-Assay: Cytotoxicity was tested with AV73 in HepG2 cells. No restriction of metabolic activity detected up to 50 μM . Experiment was performed in triplicates.

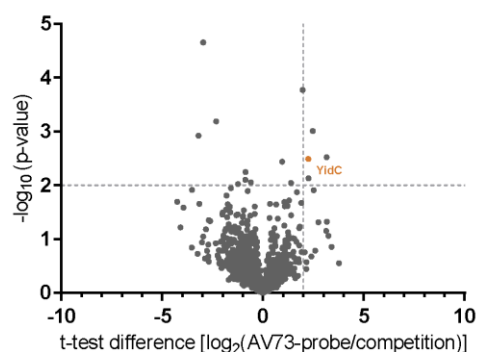
A) AfBPP: Background experiment, soluble fraction



B) AfBPP: Background experiment, insoluble fraction

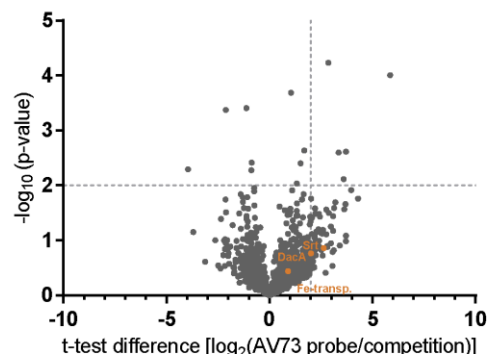


C) AfBPP: Competition experiment, soluble fraction



Ratio > 1.3	Uniprot IDs	Protein name
1,32	Q2FWP0	Uncharacterized leukocidin-like protein 1
1,36	Q2FV95	L-serine dehydratase, iron-sulfur-dependent, alpha subunit
1,36	Q2FWE0	Peptide chain release factor 1
2,72	Q2FWG4	Membrane protein insertase YidC

D) AfBPP: Competition experiment, insoluble fraction



Ratio > 1.3	Protein IDs	Protein name
1,32	Q2G2F8	ATP synthase subunit b
1,37	Q2G247	UPF0478 protein SAOUHSC_01855
1,41	Q2G2W5	Uncharacterized protein
1,44	Q2G0F6	Iron compound ABC transporter, putative, Fe-transp.
1,46	Q2G193	Uncharacterized protein
1,56	Q2FWA8	Lytic regulatory protein, putative
1,97	Q2FV99	Sortase, putative, Srt
2,21	Q2FW92	Diadenylate cyclase, DacA
2,36	Q2FVQ2	Uncharacterized lipoprotein SAOUHSC_02650
2,86	Q2FW64	Uncharacterized protein
2,99	Q2FXH8	Uncharacterized protein
3,48	Q2FWX4	Uncharacterized protein
85,39	Q2G257	Uncharacterized protein
>100	Q2FVN4	Uncharacterized protein
>100	Q2FWE1	Release factor glutamine methyltransferase

Figure A 3. AfBPP enrichment volcano plots of the minimal photoprobe **AA-1** vs. DMSO in the A) soluble and B) insoluble fraction. Targets discussed in the main part (cytosol: Q2FW4, membrane: Q2G0F6, Q2FV99, Q2FW92) are marked in orange. All experiments were performed in four biological replicates. Cut off lines were set at a minimum of \log_2 fold-change of 3 in A) and of 2 in B) and a minimum $-\log_{10}$ (p-value) of 2. Volcano plots of **AV73-p** vs. competition experiment in the C) soluble and D) insoluble fraction are shown. Targets discussed in the main part (cytosol: Q2FW4, membrane: Q2G0F6, Q2FV99, Q2FW92) are marked in orange. All experiments were performed in four biological replicates. Cut off lines were set at a minimum of \log_2 fold-change of 2 and a minimum $-\log_{10}$ (p-value) of 2. The ratio (AV73-p vs. competition) is shown in the tables below.

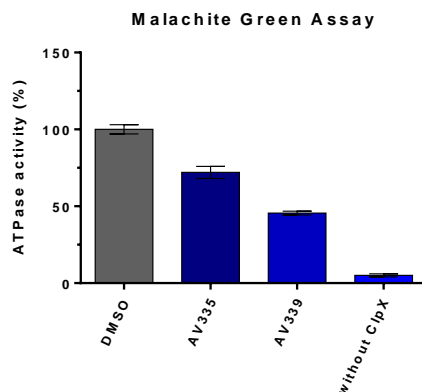


Figure A 4. Malachite green assay with compounds AV335 and AV339 (50 μ M). DMSO was used as a positive control, for the negative control the experiment was performed without ClpX. Activity was determined out of the initial slopes, and the DMSO control was set to a activity of 100%. Experiments were performed in triplicates.

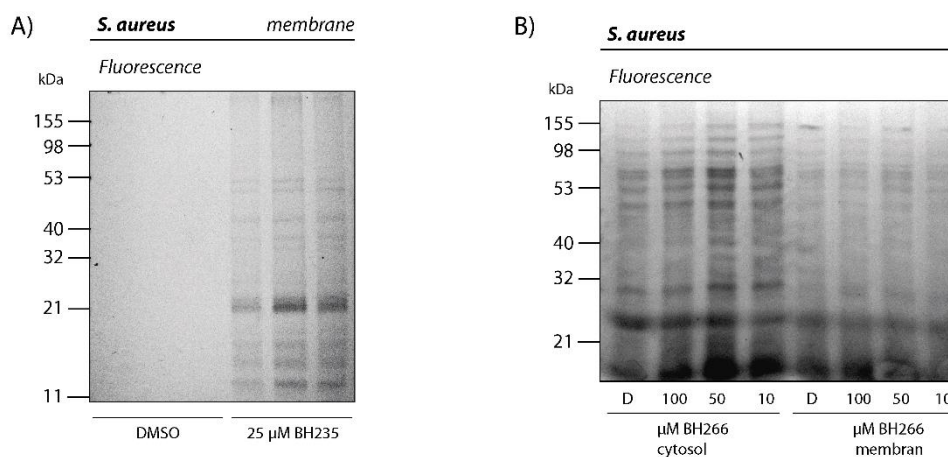


Figure A 5. A) Insoluble fraction after labeling with BH235 in *S. aureus* and after enrichment with a trifunctional linker. Bacteria were incubated for 1 h and irradiated for 14 min. B) Soluble and insoluble fraction of labeling experiment with BH266 in *S. aureus* with incubation for 1 h and irradiation for 40 min.

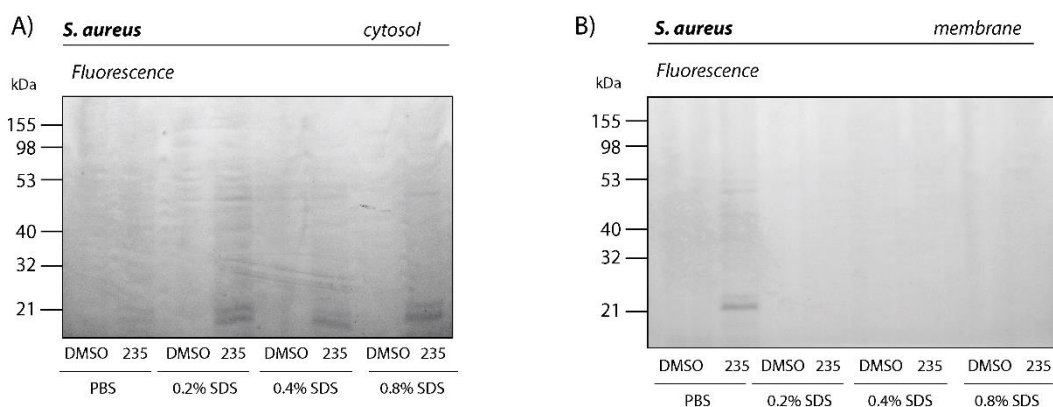


Figure A 6. A) Soluble and B) insoluble fraction of labeling with BH235 in *S. aureus*. Incubation time was 1h and different SDS concentrations for lysis were examined.

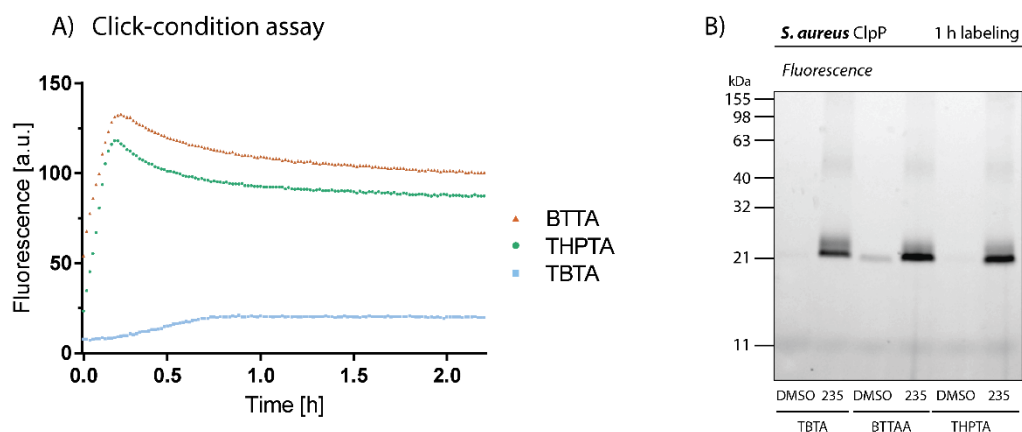


Figure A 7. Three different ligands were used in A) and B) to test for the best click conditions. A) Cumarine-azide was clicked to probe **BH235** and fluorescence was detected. Experiments were performed in triplicates. B) A β BPP was performed using **BH235** as probe with different click conditions, with same concentrations as tested in the click reaction assay.

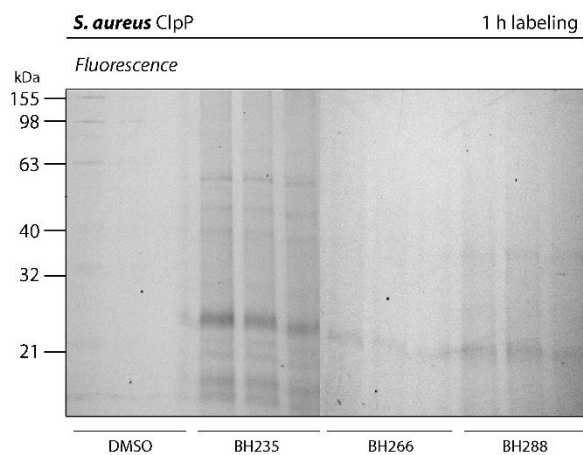


Figure A 8. MS-based A β BPP was performed with three different photoprobes and DMSO as negative control. A trifunctional linker was used, and enriched proteins were made visible *via* fluorescence. Bacteria were incubated for 1 h and irradiated for 14 min.

2. Stained Gels (Chapter III)

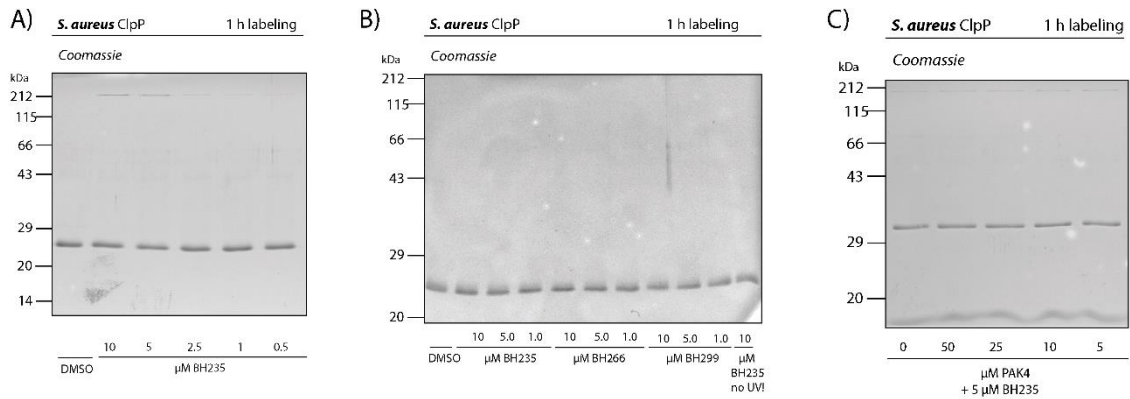


Figure A 9. Coomassie stained gels for figure 35.

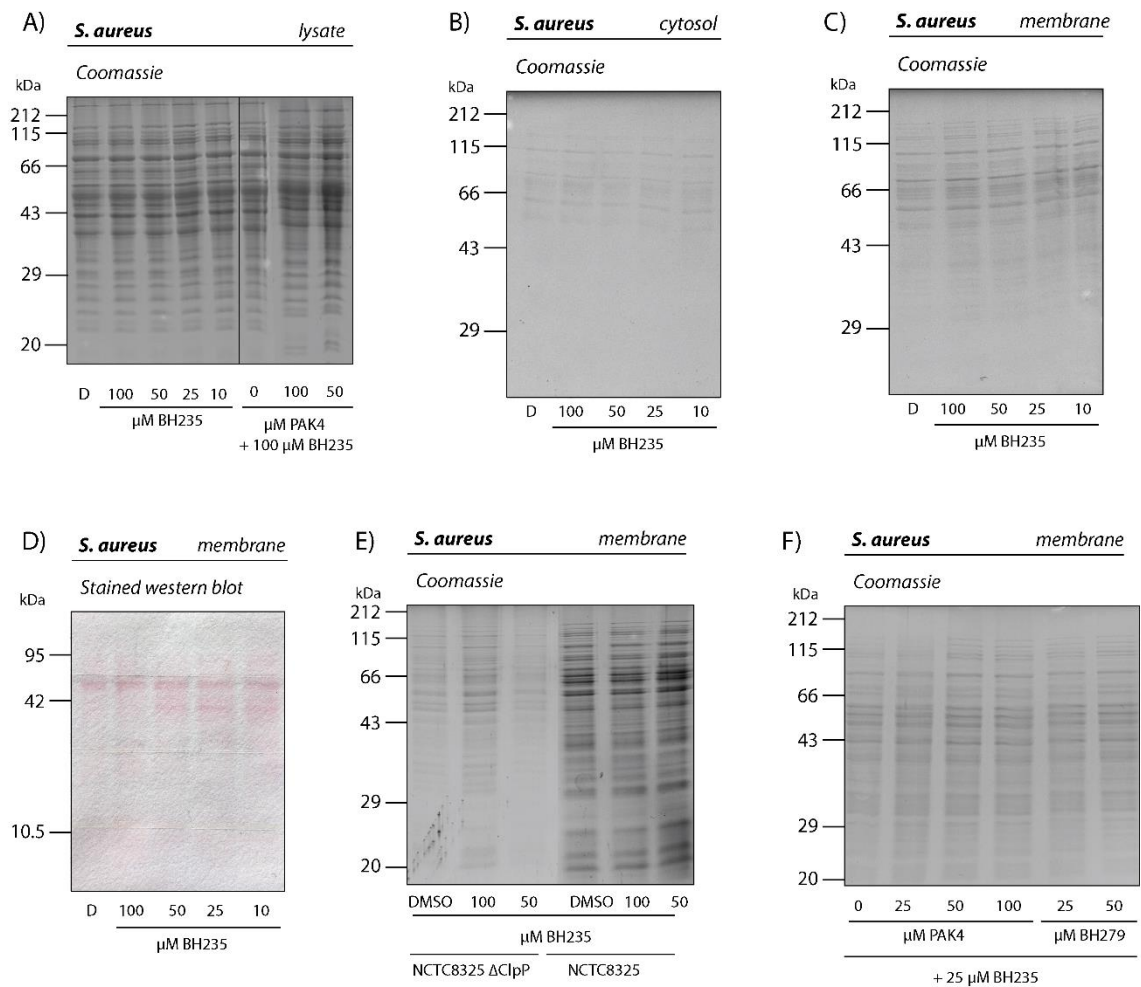


Figure A 10. Coomassie stained gels for A) labeling in lysate (Figure 36) and B) soluble and C) insoluble fraction of labeling *in situ* (Figure 37 A, B). D) Ponceau red stained western blot membrane for figure 37 C. E) Coomassie gel for labeling in wild type and $\Delta clpP$ strain (Figure 37 D). F) Coomassie gel for competitive labeling shown in figure 37 E.

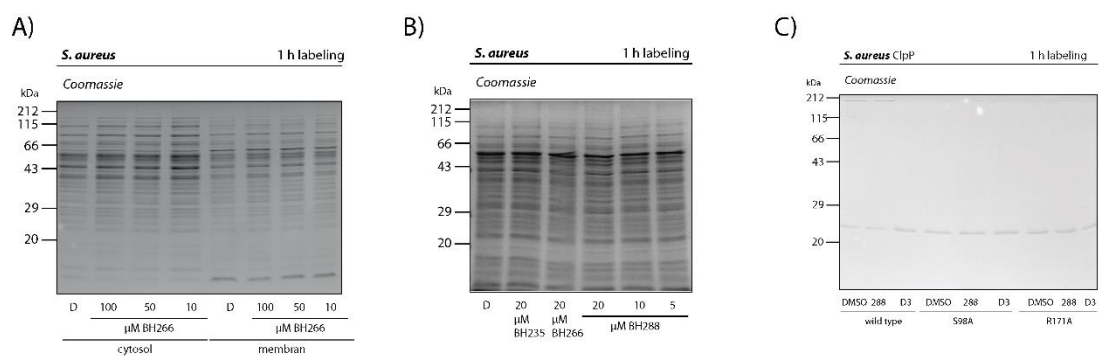


Figure A 11. Coomassie stained gels for A) **266** and B) **288** labeling in *S. aureus* intact cells and C) labeling in ClpP mutants (Figures 38, 39).

3. Tables

Table A 1. Functional protein annotation enrichment for extracellular proteins significantly down-regulated under hemolysis conditions. p-values were corrected with the method of Benjamini and Hochberg.^[194]

Category	Term	Count	%	Corr. p-value
UP_KEYWORDS	Secreted	7	46,7	6,1E-9
INTERPRO	Leukocidin/porin	5	33,3	2,6E-8
INTERPRO	Bi-component toxin, staphylococci	5	33,3	2,6E-8
GOTERM_BP_DIRECT	cytolysis in other organism	5	33,3	4,9E-8
UP_KEYWORDS	Signal	9	60,0	7,3E-7
UP_KEYWORDS	Hemolysis	4	26,7	9,9E-7
GOTERM_BP_DIRECT	hemolysis in other organism	4	26,7	2,8E-6
UP_KEYWORDS	Cytolysis	4	26,7	4,4E-6
UP_KEYWORDS	Toxin	4	26,7	4,4E-6
GOTERM_CC_DIRECT	extracellular region	6	40,0	3,4E-5
GOTERM_BP_DIRECT	pathogenesis	6	40,0	1,5E-4
INTERPRO	Extracellular fibrinogen binding protein, C-terminal	2	13,3	5,5E-2
GOTERM_CC_DIRECT	extracellular space	2	13,3	9,9E-3

Table A 2. Functional protein annotation enrichment for extracellular proteins significantly down-regulated under biofilm conditions. p-values were corrected with the method of Benjamini and Hochberg.^[194]

Category	Term	Count	%	Corr. p-value
UP_KEYWORDS	Secreted	8	66,7	9,9E-13
UP_KEYWORDS	Signal	10	83,3	5,7E-11
INTERPRO	Leukocidin/porin	5	41,7	4,0E-9
INTERPRO	Bi-component toxin, staphylococci	5	41,7	4,0E-9
GOTERM_BP_DIRECT	cytolysis in other organism	5	41,7	2,0E-9
GOTERM_CC_DIRECT	extracellular region	8	66,7	7,1E-9
UP_KEYWORDS	Hemolysis	4	33,3	2,0E-7
GOTERM_BP_DIRECT	hemolysis in other organism	4	33,3	2,2E-7
UP_KEYWORDS	Cytolysis	4	33,3	8,9E-7
UP_KEYWORDS	Toxin	4	33,3	8,9E-7
GOTERM_BP_DIRECT	pathogenesis	6	50,0	2,7E-6
GOTERM_MF_DIRECT	serine-type endopeptidase activity	2	16,7	8,8E-3
INTERPRO	Peptidase S1	2	16,7	6,2E-2
INTERPRO	Peptidase S1B, exfoliative toxin	2	16,7	5,0E-2
INTERPRO	Peptidase S1B, glutamyl endopeptidase I	2	16,7	5,0E-2
UP_KEYWORDS	Serine protease	2	16,7	3,7E-2
INTERPRO	Trypsin-like cysteine/serine peptidase domain	2	16,7	6,4E-2
UP_KEYWORDS	Virulence	2	16,7	1,4E-1
UP_KEYWORDS	Protease	2	16,7	1,5E-1

Table A 3. Proteins with the sortase SrtA motif (LPXTG). * Marked proteins do not have the motif at the C-terminus and are not relevant.

Uniprot ID	length [aa]	position	Name
Q2G015	927	890 - 894	Clumping factor A
Q2FUY2	877	838-842	Clumping factor B
P14738	1018	982-986	Fibronectin-binding protein A
Q2FZE9	350	313-317	Iron-regulated surface determinant protein A
Q2FZF0	645	610-614	Iron-regulated surface determinant protein B
Q2FXJ2	895	861-865	Iron-regulated surface determinant protein H
Q2FVX9*	164	79-83	Cyclic pyranopterin monophosphate synthase
Q2G2B2	1627	1595-1599	Surface protein G
Q2G0L5	994	958-962	Serine-aspartate repeat-containing protein C
Q2G0L4	1349	1312-1316	Serine-aspartate repeat-containing protein D
P02976	516	482-486	Immunoglobulin G-binding protein A
Q2FUW1	2271	2229-2233	Serine-rich adhesin for platelets
Q2FW62*	333	123-127	Zinc-type alcohol dehydrogenase-like protein
Q2FW95	2478	2440-2444	Uncharacterized protein
Q2FWH2	400	353-357	Uncharacterized protein
Q2FWN5*	435	28-32	Cation transport protein, putative
Q2FXH4	2186	2151-2155	Uncharacterized protein
Q2FZI4	268	254-258	Uncharacterized protein
Q2G1T5	917	881-885	Fibronectin binding protein B, putative
Q2G253	772	739-743	Uncharacterized protein

Table A 4. Most up and down regulated proteins of secretome analysis of *S. aureus* NCTC8325 with compound **CD10**. Sorted in decreasing t-test difference order. Cut off lines were set a minimum log₂ fold-change of 2 and a minimum log₁₀ (p-value) of 2.

t-test difference	-Log ₁₀ (p-value)	Protein ID	Protein Name
up regulated			
1,353	1,393	Q2FV52	Probable transglycosylase IsaA
1,955	1,666	Q2FVN6	Uncharacterized protein
1,053	1,512	Q2FW51	Truncated MHC class II analog protein
1,451	2,052	Q2FWB5	Uncharacterized protein
1,120	1,176	Q2FXM8	ATP-dependent 6-phosphofructokinase
1,214	1,005	Q2FXU4	Histidine-tRNA ligase
1,008	1,351	Q2G1F2	FMN-dependent NADH-azoreductase
1,010	1,458	Q2G2R8	Staphopain A
down regulated			
-2,047	1,853	Q2FX55	Conserved hypothetical phage protein
-1,661	1,330	Q2G0A1	Uncharacterized
-1,616	1,641	Q2G190	Uncharacterized

Appendix

Table A 5. Most up- and down-regulated proteins of secretome analysis of *S. aureus* NCTC8325 with compound **CD1**. Sorted in decreasing t-test difference order. Cut off lines were set a minimum \log_2 fold-change of 2 and a minimum \log_{10} (p-value) of 2.

t-test difference	$-\log_{10}$ (p-value)	Protein ID	Protein Name
up regulated			
2,471	3,206	Q2G188	ESAT-6 secretion accessory factor EsaA
2,289	3,117	Q2G190	Uncharacterized protein
2,223	2,424	Q2G2B2	Surface protein G
down regulated			
-2,099	2,636	Q2FVG3	Carboxylic ester hydrolase
-2,068	2,701	Q2FW81	Probable uridylyltransferase SAOUHSC_02423
-4,301	2,788	Q2FWD1	CTP synthase
-3,017	2,063	Q2FWZ2	Diacylglycerol kinase
-2,433	3,143	Q2FXA4	Ferrochelataase
-2,877	2,081	Q2FY01	Uncharacterized
-3,521	2,058	Q2FY08	Glycine-tRNA ligase
-2,361	2,021	Q2FY28	Uncharacterized
-3,848	2,132	Q2FYH6	Asparagine-tRNA ligase
-2,292	3,145	Q2FYS9	Aconitate hydratase
-3,584	3,286	Q2FZ62	Ribulose-phosphate 3-epimerase
-4,989	2,777	Q2FZ74	Dihydroorotase
-2,791	2,244	Q2FZR9	3-oxoacyl-[acyl-carrier-protein] synthase 2
-3,954	2,575	Q2FZV6	Probable cytosol aminopeptidase
-3,447	2,723	Q2FZW0	Uncharacterized
-2,555	2,205	Q2G115	Ribosome-binding ATPase YchF
-2,323	2,180	Q2G178	Uncharacterized
-2,183	2,477	Q2G1T6	UTP-glucose-1-phosphate uridylyltransferase
-2,031	2,117	Q2G200	UPF0738 protein SAOUHSC_00941
-3,368	2,129	Q2G276	Uncharacterized
-2,152	2,766	Q2G2A4	Dihydrolipoamide acetyltransferase component of pyruvate dehydrogenase complex
-3,991	3,136	Q2G2D7	Uncharacterized
-3,443	2,602	Q2G2W6	Uncharacterized

Table A 6. Soluble fraction of background binders with minimal aryl azide photoprobe. Experiments were performed in four biological replicates. All proteins with a \log_2 fold enrichment higher than 3 are listed in this table.

Protein IDs	$-\log_{10}$ (p-value)	\log_2 fold enrichment
AOA141HMF2	2,155	3,758
Q2FUQ3	3,512	3,718

Q2FUT9	4,072	4,899
Q2FV27	2,968	7,568
Q2FV95	4,746	4,352
Q2FVA5	3,141	3,149
Q2FVB4	2,370	3,136
Q2FVF9	2,309	4,589
Q2FVG8	3,216	3,076
Q2FVH5	2,870	3,381

Q2FVI4	2,189	3,733
Q2FVI6	3,336	4,402
Q2FVM2	2,908	3,220
Q2FVQ1	3,543	4,140
Q2FVQ5	3,239	4,070
Q2FVR4	2,412	3,069
Q2FVR9	3,924	5,279
Q2FVT1	3,390	3,994
Q2FVW8	2,771	3,344
Q2FVW9	6,674	4,838
Q2FVX8	3,165	4,739
Q2FVZ4	5,490	3,981
Q2FVZ5	2,117	3,713
Q2FW11	2,688	3,608
Q2FW14	2,853	3,183
Q2FW32	2,015	4,010
Q2FW38	2,184	4,387
Q2FW52	2,313	3,304
Q2FW75	2,822	3,770
Q2FW91	2,343	5,689
Q2FWA2	2,221	3,482
Q2FWC4	2,332	3,840
Q2FWD7	4,591	3,711
Q2FWE0	4,510	5,224
Q2FWE2	6,056	6,689
Q2FWE3	3,554	3,431
Q2FWE9	3,129	5,286
Q2FWH5	2,879	4,908
Q2FWX6	4,569	7,373
Q2FX22	3,599	3,571
Q2FX87	3,070	3,392
Q2FXF4	3,750	4,090
Q2FXF8	2,481	3,804
Q2FXH3	2,959	4,804
Q2FXH8	2,495	3,248
Q2FXI5	2,085	4,633
Q2FXI9	2,445	3,702
Q2FXJ6	4,394	5,451
Q2FXJ7	4,093	3,454
Q2FXM3	2,971	3,299
Q2FXP1	2,373	4,328
Q2FXQ3	2,255	3,747
Q2FXR7	4,558	4,160

Q2FXT5	3,696	5,074
Q2FXT7	4,822	4,959
Q2FXT8	3,431	5,259
Q2FXW4	3,420	4,200
Q2FXW6	2,708	3,541
Q2FY10	3,382	3,120
Q2FY17	4,684	3,446
Q2FY19	2,521	3,620
Q2FY21	4,022	4,575
Q2FY61	5,504	6,678
Q2FYG0	4,073	5,127
Q2FYG2	3,983	4,398
Q2FYK7	2,885	4,282
Q2FYL3	3,172	3,786
Q2FYS5	2,415	3,427
Q2FYV4	3,746	5,151
Q2FZ02	3,776	3,736
Q2FZ05	3,370	3,584
Q2FZ08	5,314	5,490
Q2FZ13	3,626	4,614
Q2FZ18	2,480	5,268
Q2FZ42	3,510	4,767
Q2FZ48	3,251	3,630
Q2FZ49	2,399	4,941
Q2FZ64	4,130	4,862
Q2FZ65	2,685	4,788
Q2FZ83	2,287	4,369
Q2FZ86	2,636	4,281
Q2FZA1	4,276	3,589
Q2FZF3	2,704	4,659
Q2FZJ5	4,015	4,091
Q2FZJ9	4,503	3,413
Q2FZK3	4,549	3,586
Q2FZN7	5,038	5,217
Q2FZQ5	2,662	4,132
Q2FZQ7	3,981	5,606
Q2FZV1	4,218	4,002
Q2FZW0	2,140	3,650
Q2FZX0	2,622	5,014
Q2FZY4	3,239	3,464
Q2FZY7	2,053	3,687
Q2FZZ2	4,095	3,143
Q2G033	7,296	3,821

Appendix

Q2G052	3,444	3,719
Q2G059	3,305	4,237
Q2G064	2,746	3,637
Q2G065	4,016	4,614
Q2G069	2,050	3,007
Q2G089	3,412	3,132
Q2G0B2	2,708	3,125
Q2G0D6	4,234	3,309
Q2G0E9	2,693	3,024
Q2G0F2	5,671	3,267
Q2G0F3	2,370	4,234
Q2G0L0	4,227	4,988
Q2G0M0	3,464	4,466
Q2G0M2	2,240	4,843
Q2G0P0	2,212	3,259
Q2G0Q7	4,348	3,200
Q2G0R6	2,897	3,572
Q2G0S7	2,345	3,636
Q2G0T4	2,774	3,262
Q2G0T5	2,276	3,835
Q2G0U0	3,096	3,903
Q2G0U2	2,575	3,125
Q2G0V7	3,215	4,537
Q2G0W9;Q2G0X1	5,057	3,418
Q2G0Z9	2,147	3,066
Q2G112	2,619	5,000
Q2G113	3,603	6,049
Q2G122	3,559	4,357
Q2G132	4,666	4,695
Q2G163	3,413	3,010
Q2G193	4,998	4,503
Q2G1A6	3,300	3,585
Q2G1A9	2,138	3,203
Q2G1B8	5,067	5,637
Q2G1G2	2,234	3,094
Q2G1G7	2,884	3,731
Q2G1I3	2,000	3,335
Q2G1J2	2,838	3,065
Q2G1N2	2,149	3,085
Q2G1N3	2,652	5,021
Q2G1P6	3,633	5,445
Q2G1U0	2,738	4,175
Q2G1U6	3,203	4,049

Q2G1V4	4,107	3,212
Q2G1Z5	3,224	4,244
Q2G236	2,526	3,994
Q2G239	2,868	4,744
Q2G254	2,853	4,211
Q2G258	2,377	3,271
Q2G268	2,080	3,248
Q2G270	5,447	6,063
Q2G280	2,828	5,358
Q2G282	4,716	4,755
Q2G2A1	2,257	3,330
Q2G2F8	2,327	3,129
Q2G2H3	2,626	3,572
Q2G2M7	4,606	4,101
Q2G2S6	2,384	4,766
Q2G2T9	3,207	3,846
Q2G2U6	3,191	3,438
Q2G2W5	4,048	4,065
Q2G2W8	3,430	3,783
Q9F0R1	2,358	4,035
Q9RFJ6	3,860	5,080

Table A 7. Insoluble fraction of background binders with minimal aryl azide photoprobe. Experiments were performed in four biological replicates. All proteins with a \log_2 fold enrichment higher than 3 are listed in this table.

Protein IDs	$-\log_{10}$ (p-value)	\log_2 fold enrichment
P52078	2,305	2,792
Q05615	2,315	2,358
Q2FUQ3	3,094	2,782
Q2FUS8	4,365	2,588
Q2FUT9	2,030	2,094
Q2FW22	2,764	2,434
Q2FW38	3,044	2,310
Q2FW64	2,049	2,640
Q2FW86	3,078	3,878
Q2FWD1	2,460	2,345
Q2FWM5	2,295	2,005
Q2FWX8	2,815	2,617
Q2FX98	4,035	2,128
Q2FXT5	2,532	2,709
Q2FXT7	2,128	2,013

Q2FXV3	2,190	2,662
Q2FYI9	2,511	2,249
Q2FYN4	2,170	3,034
Q2FZ15	3,387	2,396
Q2FZ54	3,015	2,787
Q2FZ65	3,273	2,140
Q2FZT6	2,457	2,034
Q2FZY7	4,179	2,747
Q2G0M2	3,129	2,876

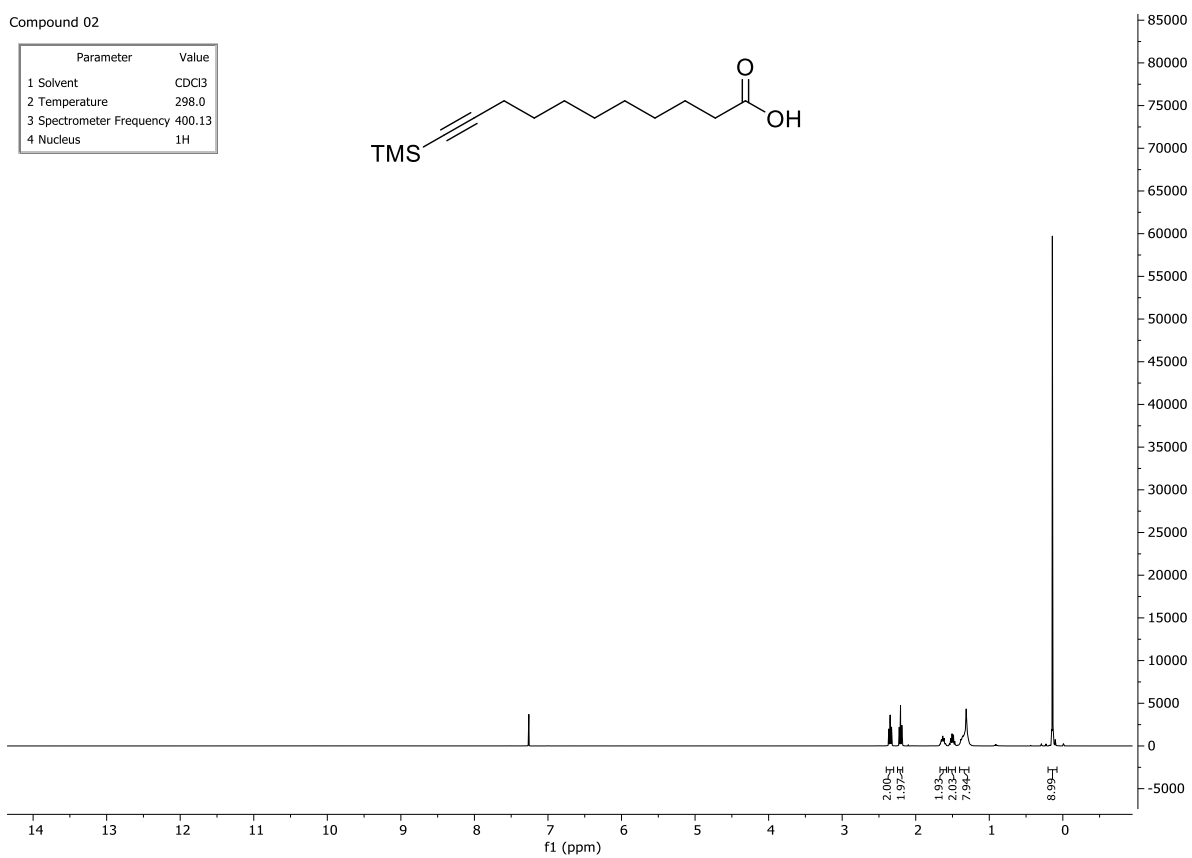
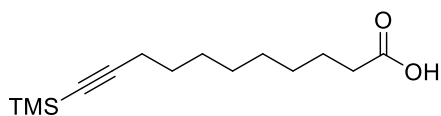
Q2G0S3	2,078	2,703
Q2G0V7	2,466	2,293
Q2G1K7	2,449	2,131
Q2G1U0	4,303	3,171
Q2G1Y5	3,944	2,461
Q2G1Y7	4,495	6,723
Q2G2S0	2,284	2,941
Q2G2W5	3,909	3,370

4. NMR Spectra

11-(trimethylsilyl)undec-10-ynoic acid (02)

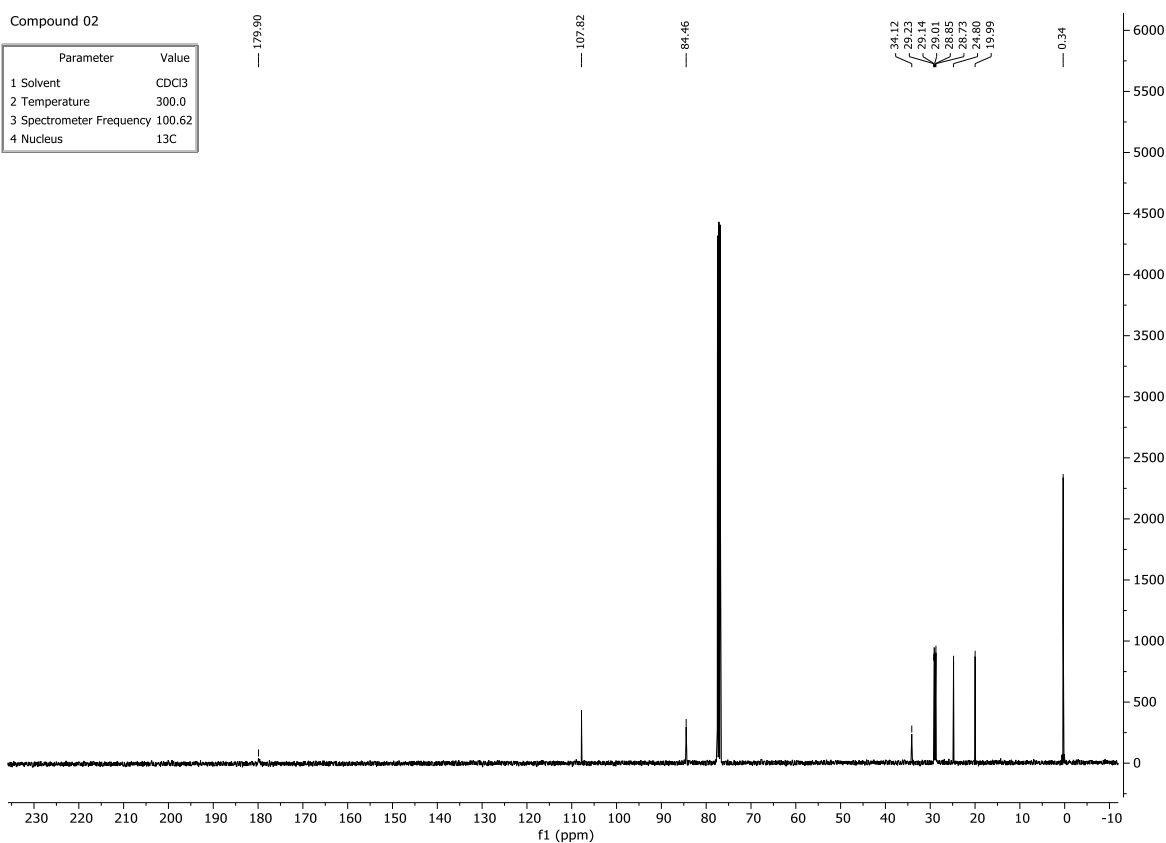
Compound 02

Parameter	Value
1 Solvent	CDCl ₃
2 Temperature	298.0
3 Spectrometer Frequency	400.13
4 Nucleus	¹ H



Compound 02

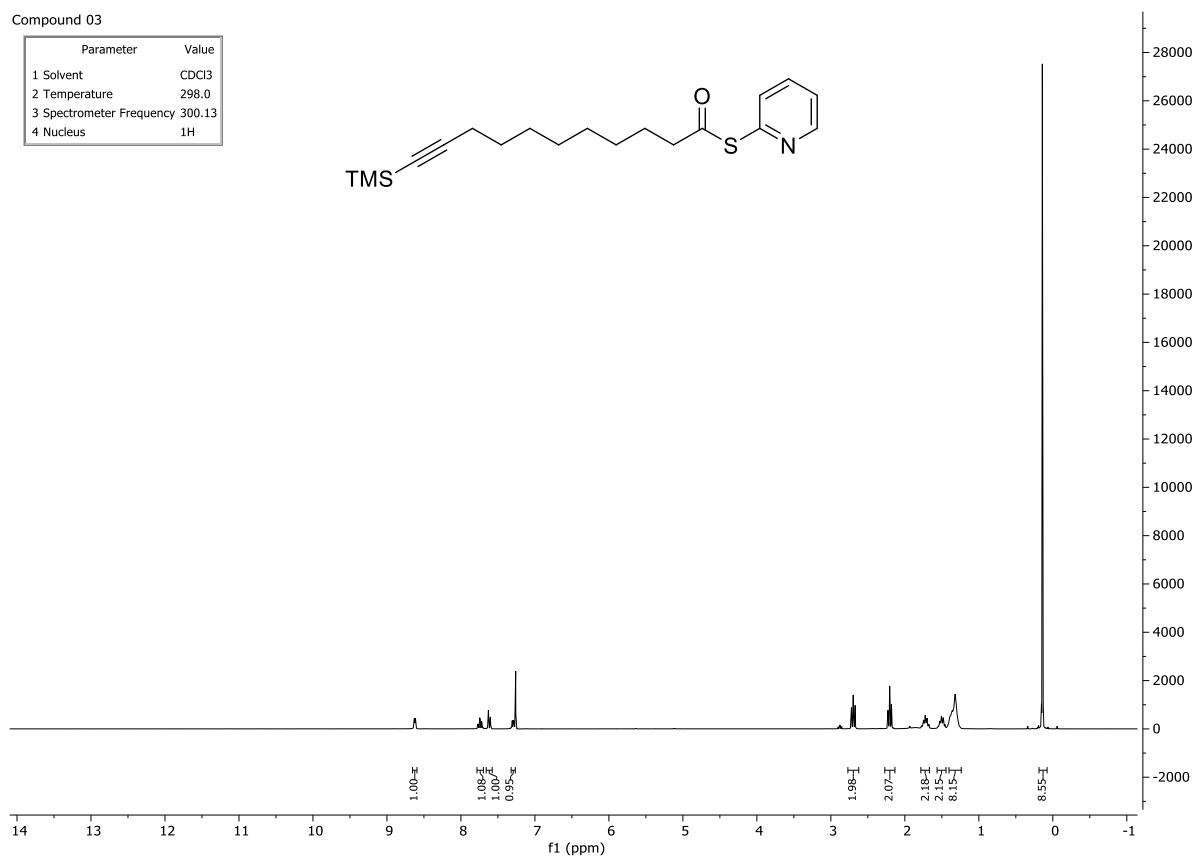
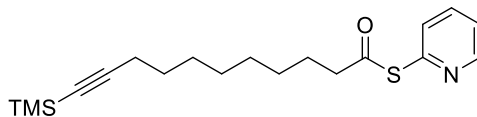
Parameter	Value
1 Solvent	CDCl ₃
2 Temperature	300.0
3 Spectrometer Frequency	100.62
4 Nucleus	¹³ C



S-(pyridin-2-yl) 11-(trimethylsilyl)undec-10-ynethioate (03)

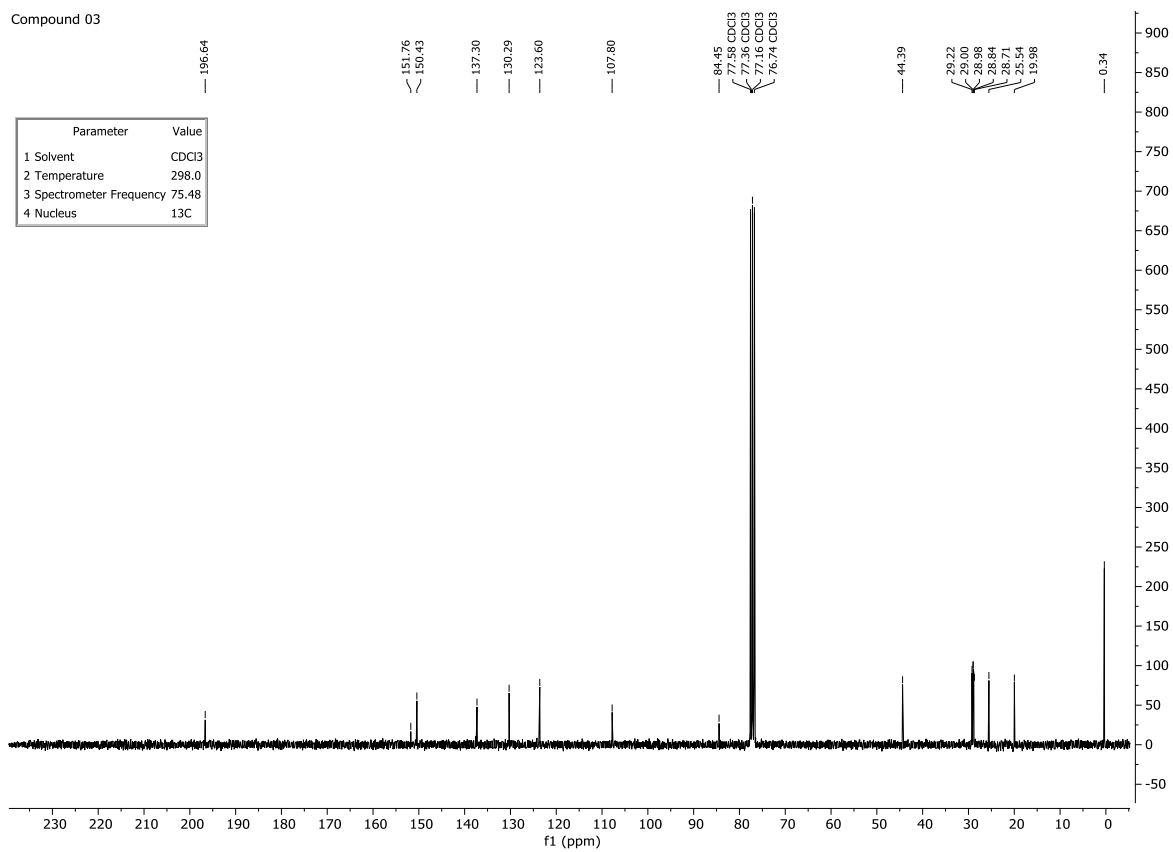
Compound 03

Parameter	Value
1 Solvent	CDCl ₃
2 Temperature	298.0
3 Spectrometer Frequency	300.13
4 Nucleus	¹ H



Compound 03

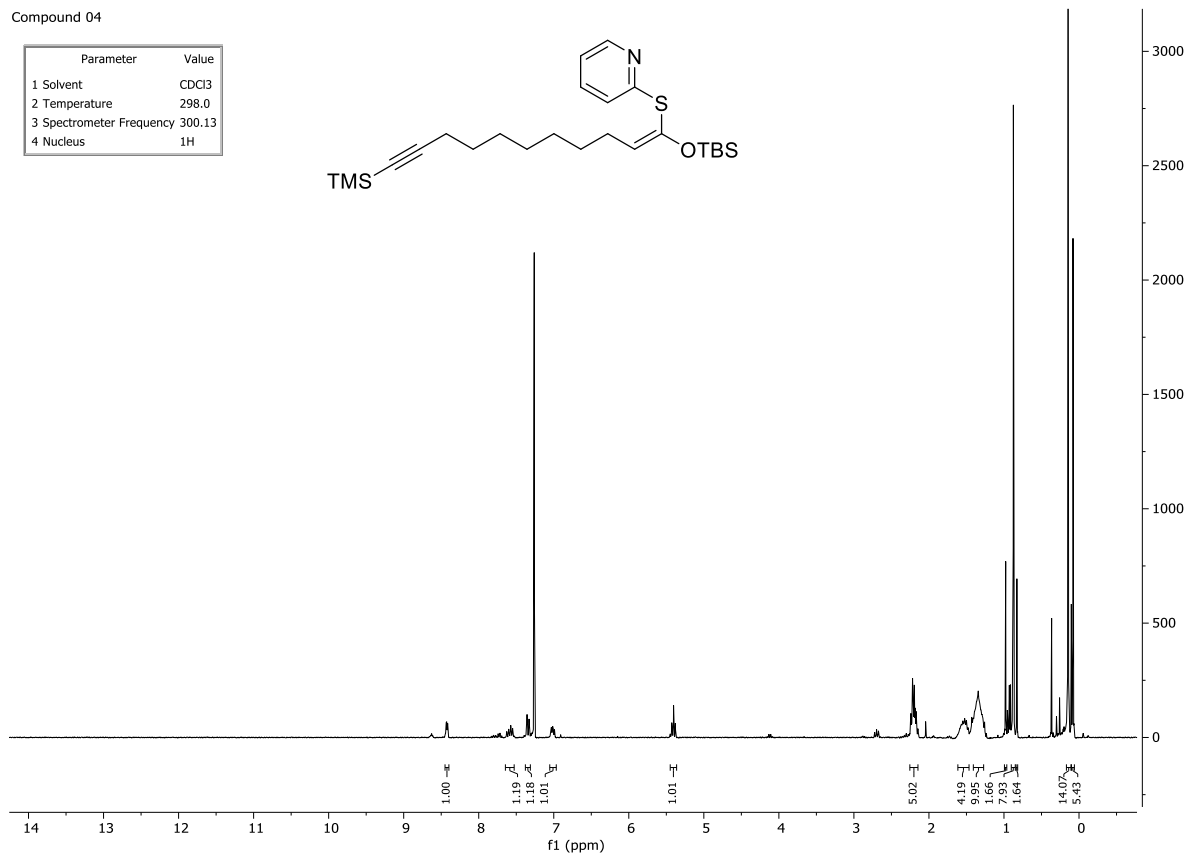
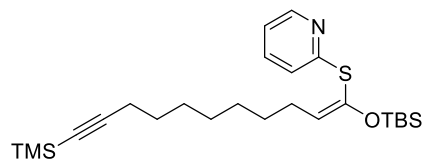
Parameter	Value
1 Solvent	CDCl ₃
2 Temperature	298.0
3 Spectrometer Frequency	75.48
4 Nucleus	¹³ C



(Z)-2-((1-((tert-butyldimethylsilyl)oxy)-11-(trimethylsilyl)undec-1-en-10-yn-1-yl)thio)pyridine (04)

Compound 04

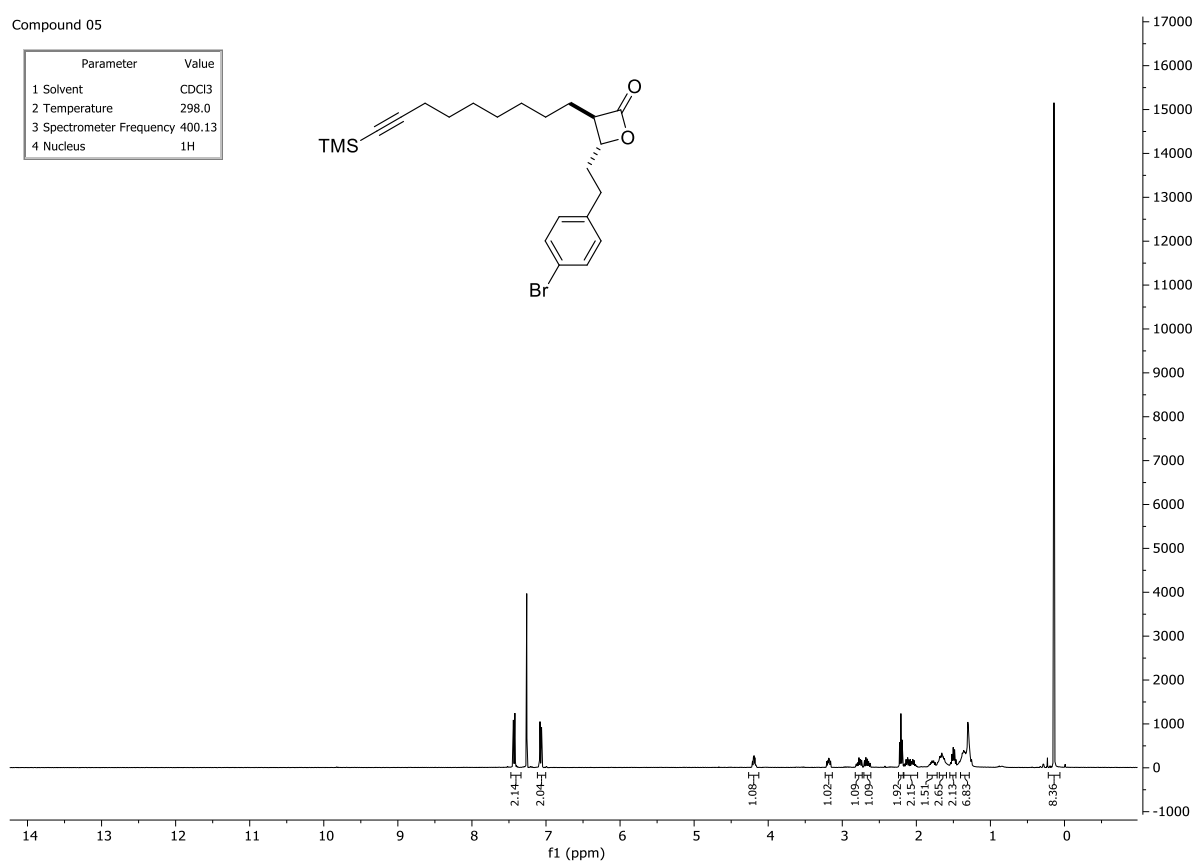
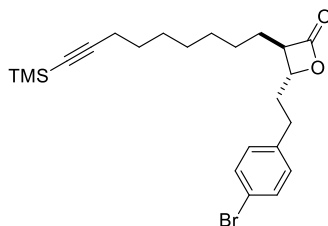
Parameter	Value
1 Solvent	CDCl3
2 Temperature	298.0
3 Spectrometer Frequency	300.13
4 Nucleus	¹ H



(3R,4R)-4-(4-bromophenethyl)-3-(9-(trimethylsilyl)non-8-yn-1-yl)oxetan-2-one (05)

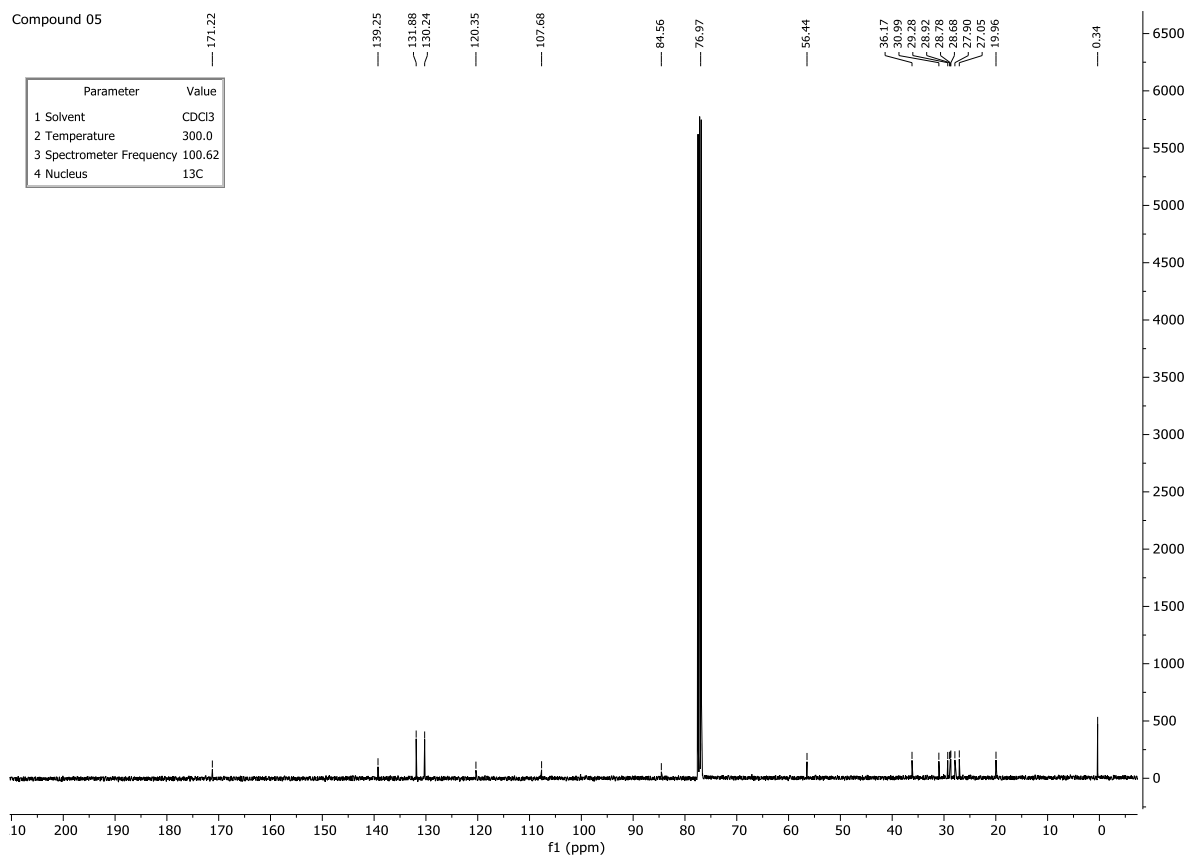
Compound 05

Parameter	Value
1 Solvent	CDCl ₃
2 Temperature	298.0
3 Spectrometer Frequency	400.13
4 Nucleus	¹ H



Compound 05

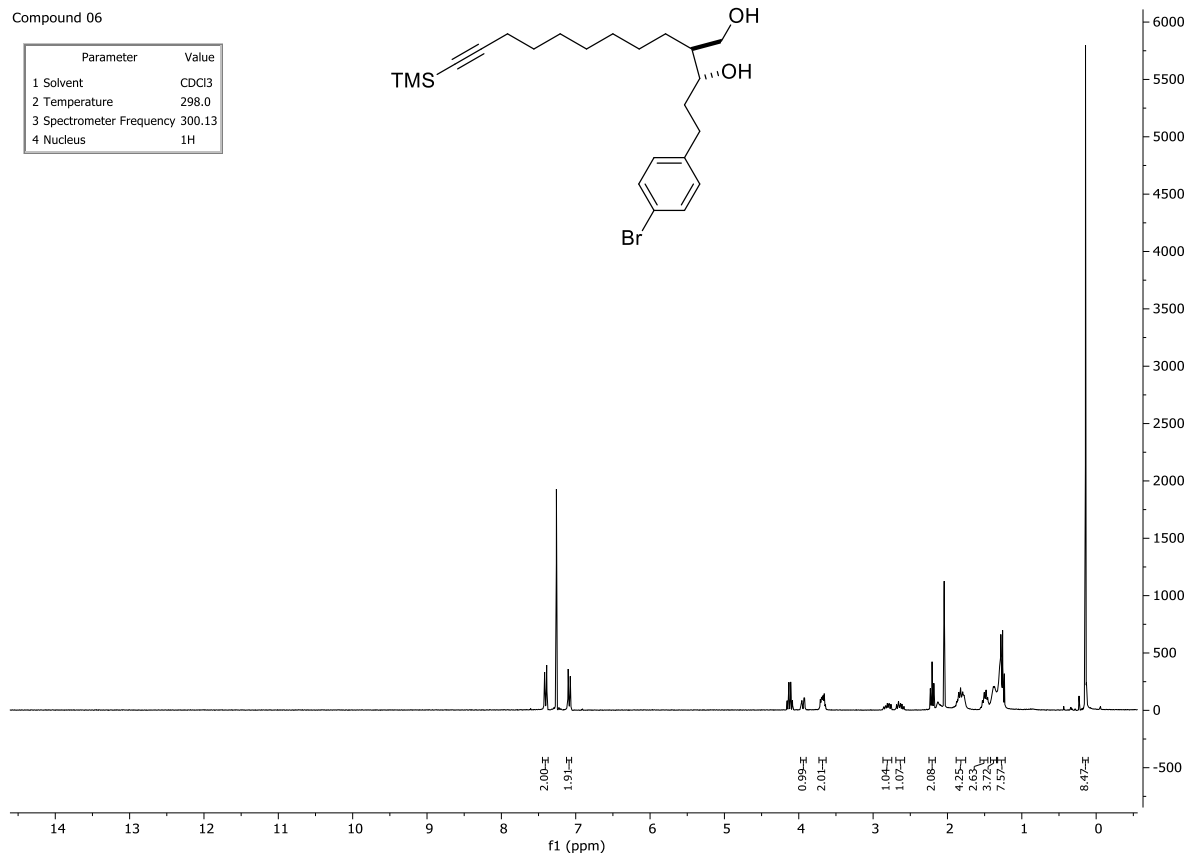
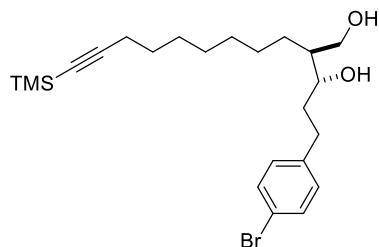
Parameter	Value
1 Solvent	CDCl ₃
2 Temperature	300.0
3 Spectrometer Frequency	100.62
4 Nucleus	¹³ C



(2S,3R)-5-(4-bromophenyl)-2-(9-(trimethylsilyl)non-8-yn-1-yl)pentane-1,3-diol (06)

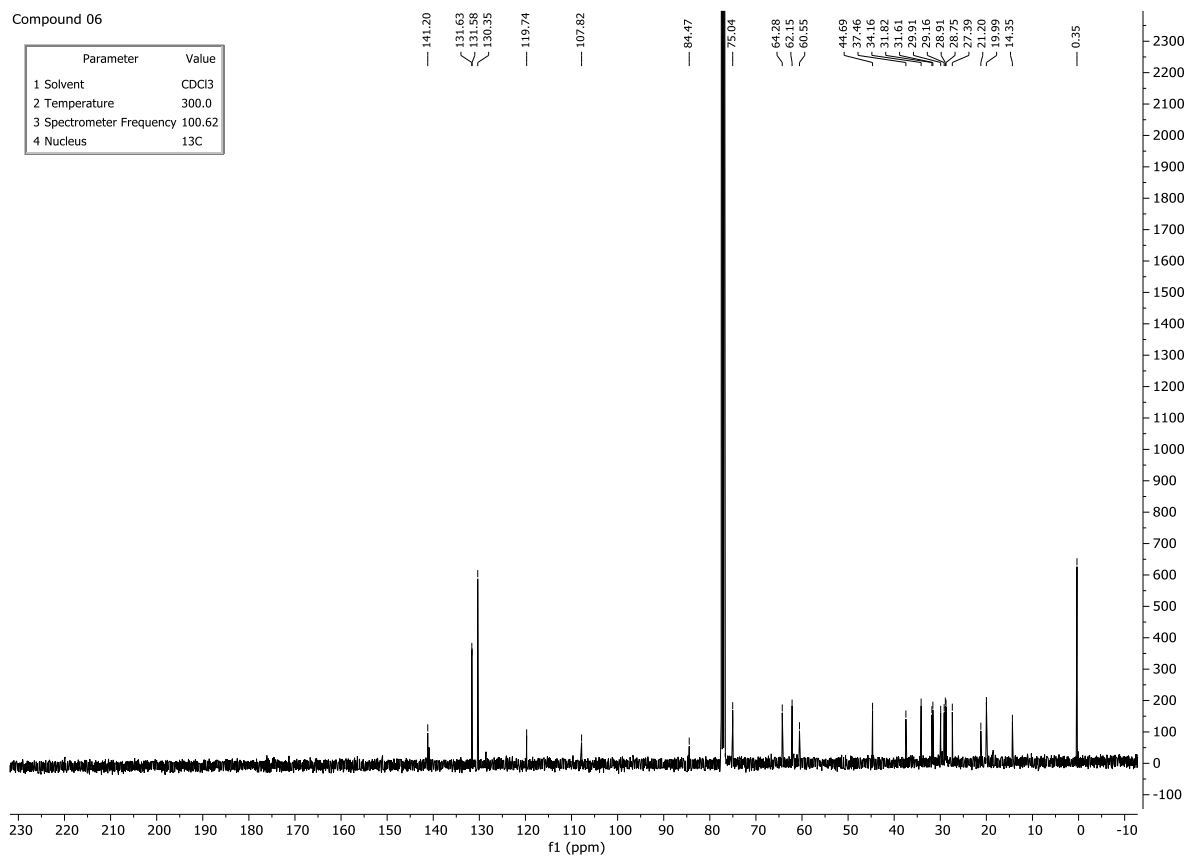
Compound 06

Parameter	Value
1 Solvent	CDCl ₃
2 Temperature	298.0
3 Spectrometer Frequency	300.13
4 Nucleus	¹ H



Compound 06

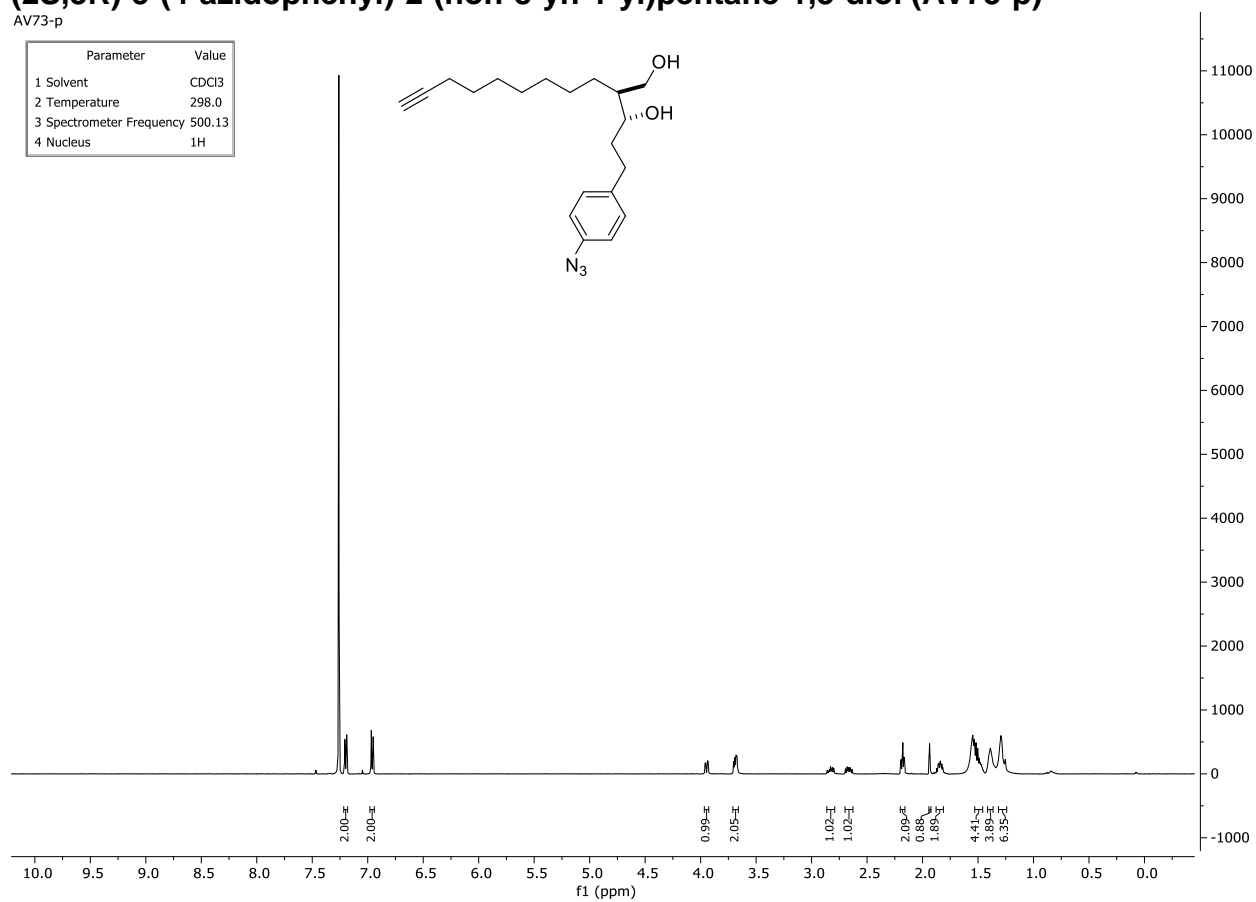
Parameter	Value
1 Solvent	CDCl ₃
2 Temperature	300.0
3 Spectrometer Frequency	100.62
4 Nucleus	¹³ C



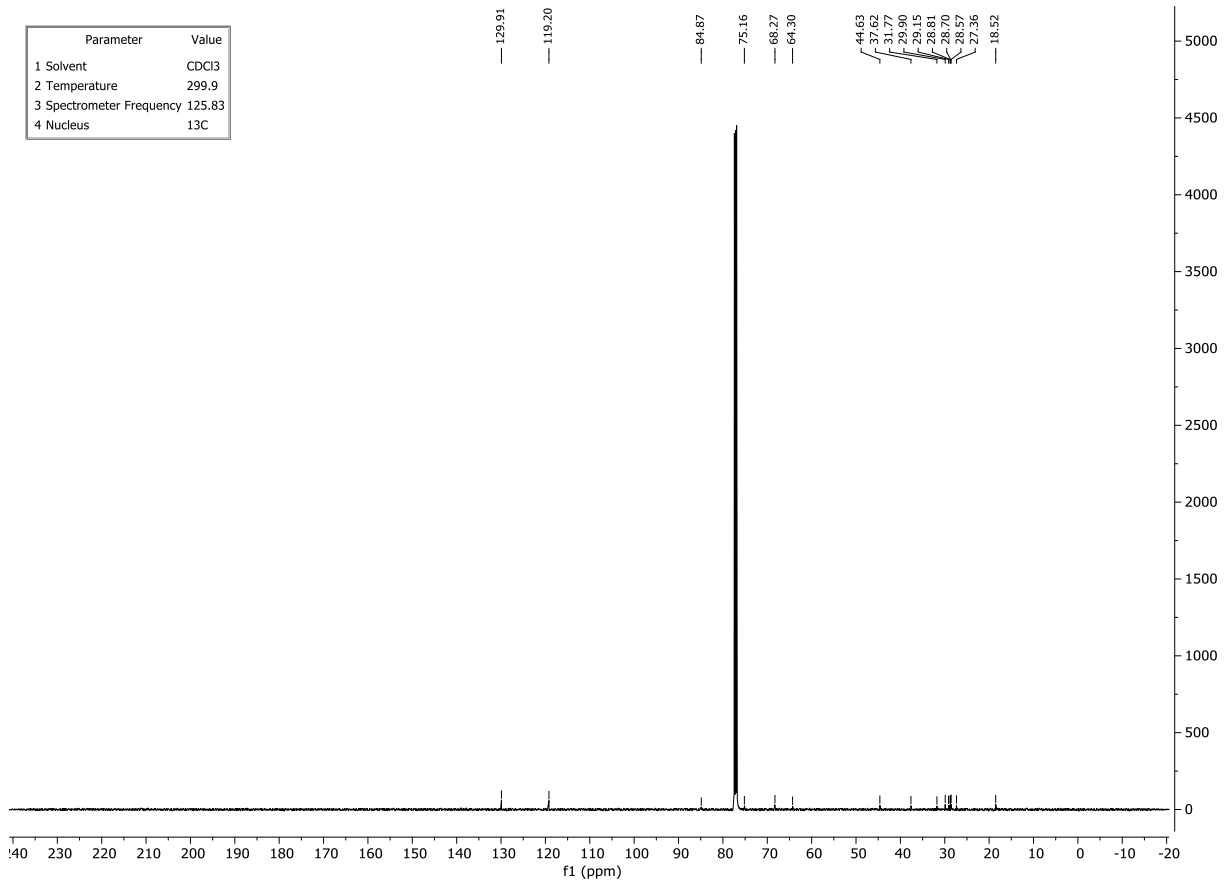
(2S,3R)-5-(4-azidophenyl)-2-(non-8-yn-1-yl)pentane-1,3-diol (AV73-p)

AV73-p

Parameter	Value
1 Solvent	CDCl ₃
2 Temperature	298.0
3 Spectrometer Frequency	500.13
4 Nucleus	¹ H



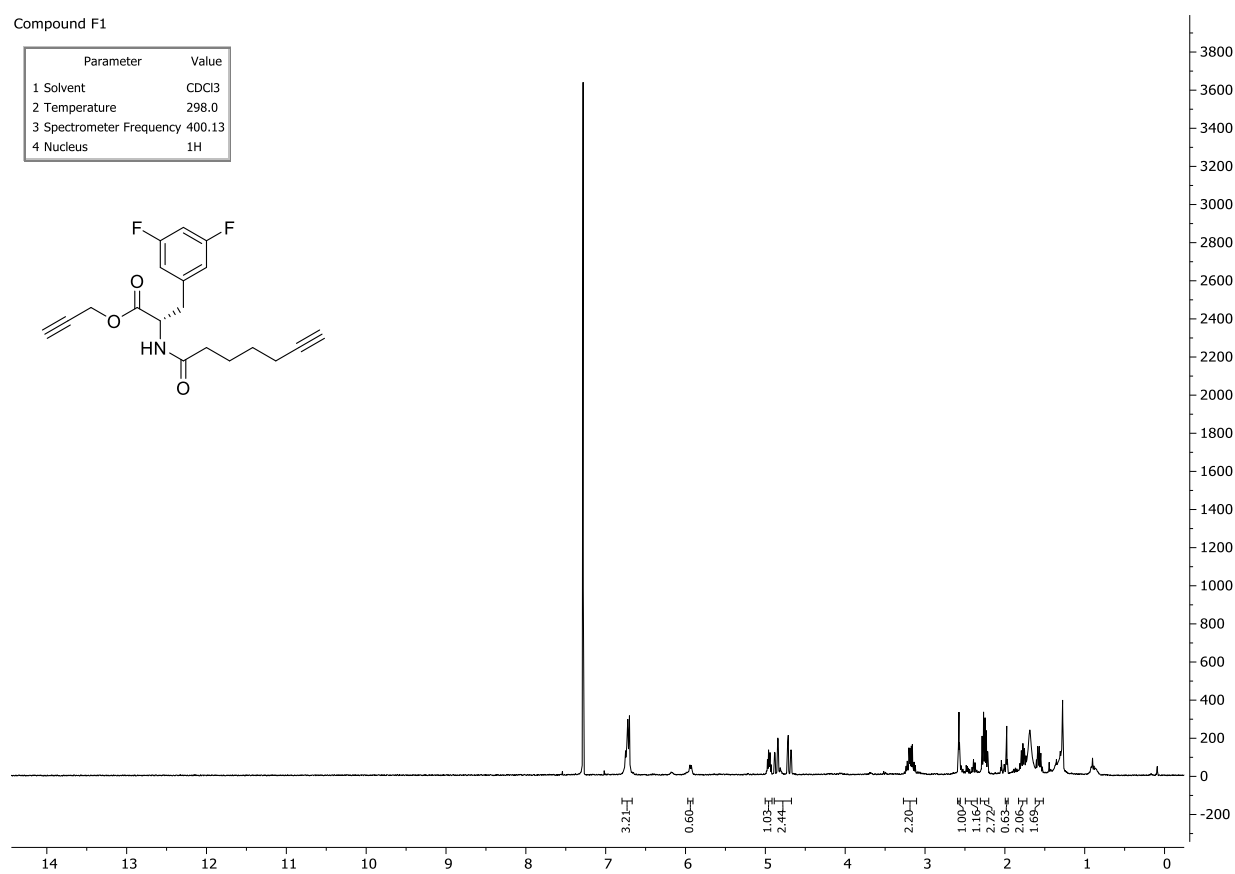
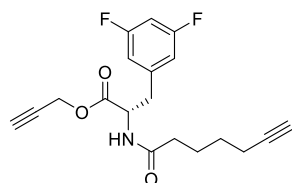
Appendix



Prop-2-yn-1-yl (S)-3-(3,5-difluorophenyl)-2-(hept-6-ynamido)propanoate (F1)

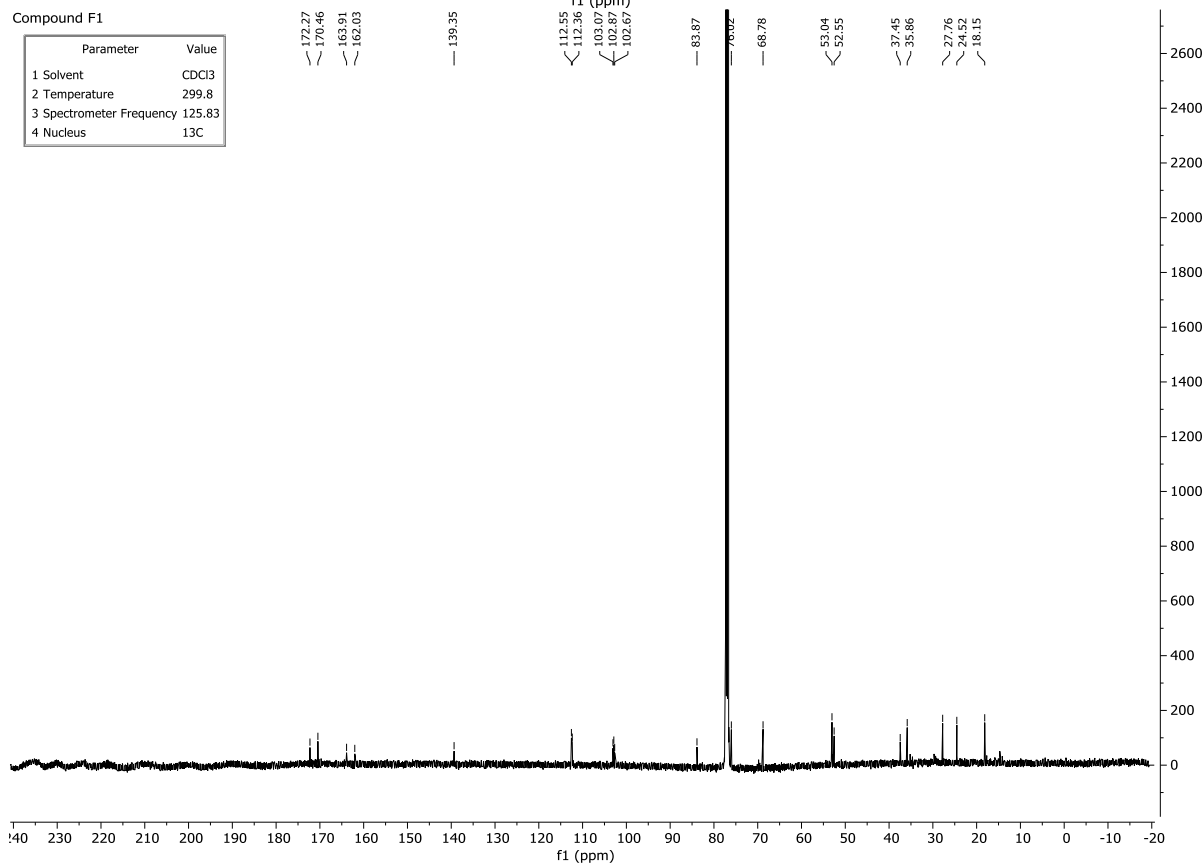
Compound F1

Parameter	Value
1 Solvent	CDCl ₃
2 Temperature	298.0
3 Spectrometer Frequency	400.13
4 Nucleus	¹ H



Compound F1

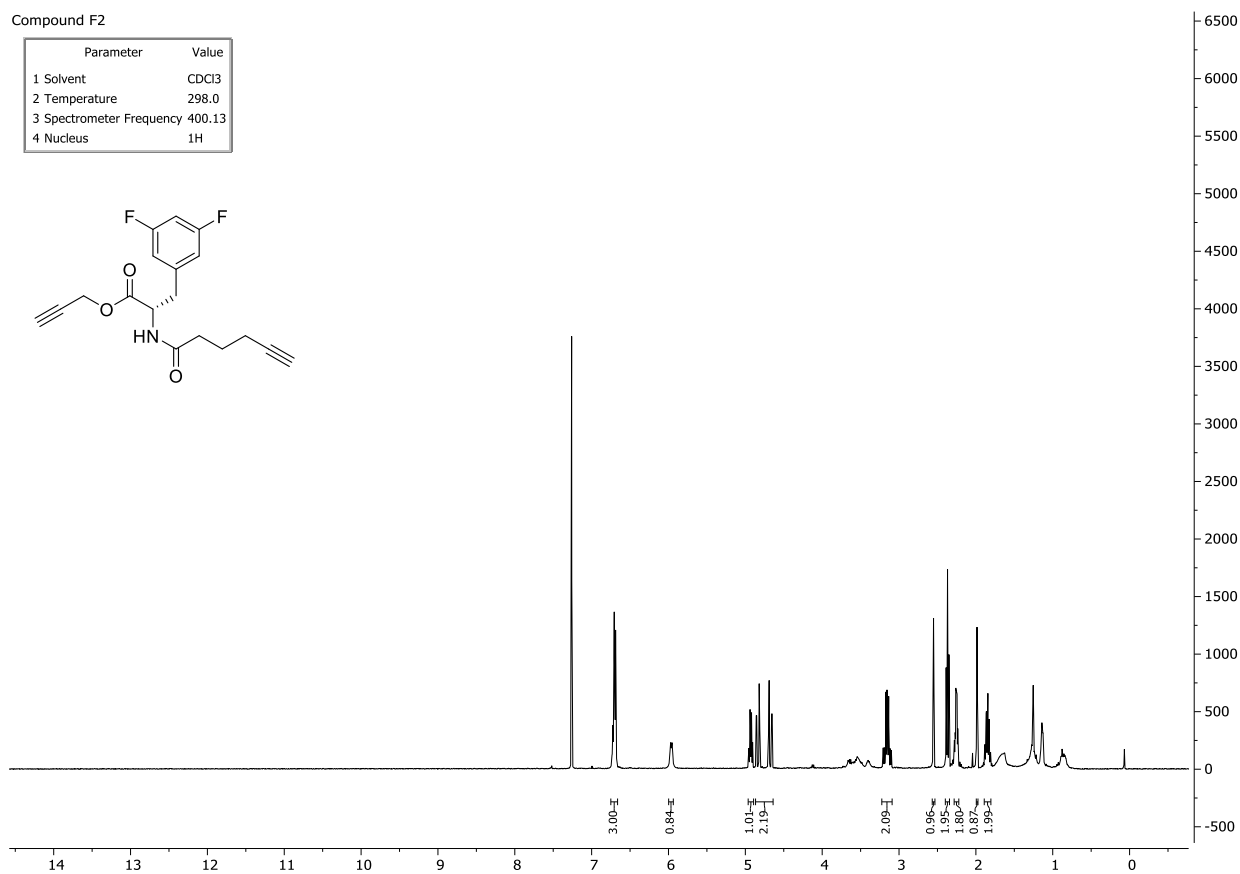
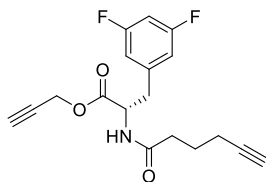
Parameter	Value
1 Solvent	CDCl ₃
2 Temperature	299.8
3 Spectrometer Frequency	125.83
4 Nucleus	¹³ C



Prop-2-yn-1-yl (S)-3-(3,5-difluorophenyl)-2-(hex-5-ynamido)propanoate (F2)

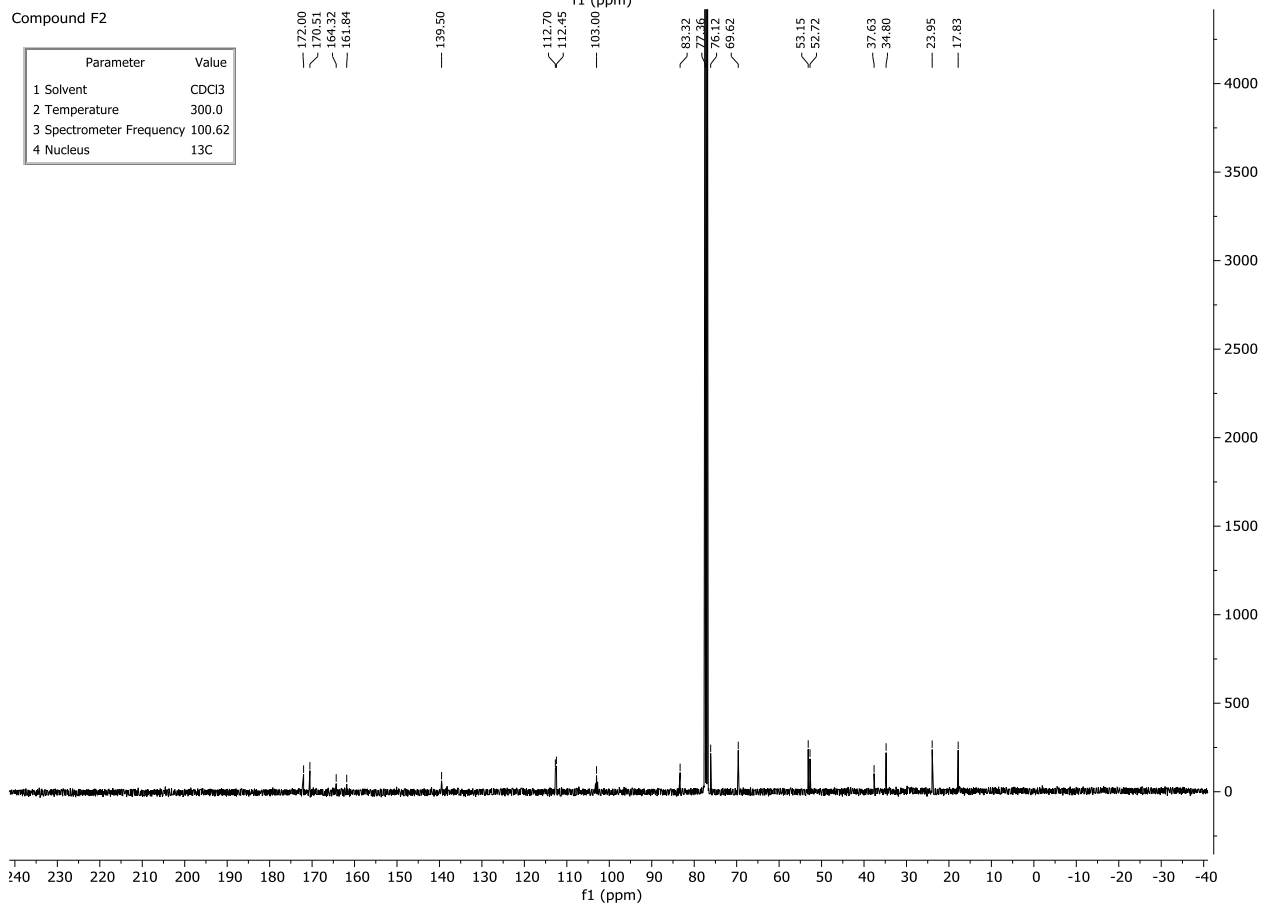
Compound F2

Parameter	Value
1 Solvent	CDCl ₃
2 Temperature	298.0
3 Spectrometer Frequency	400.13
4 Nucleus	¹ H



Compound F2

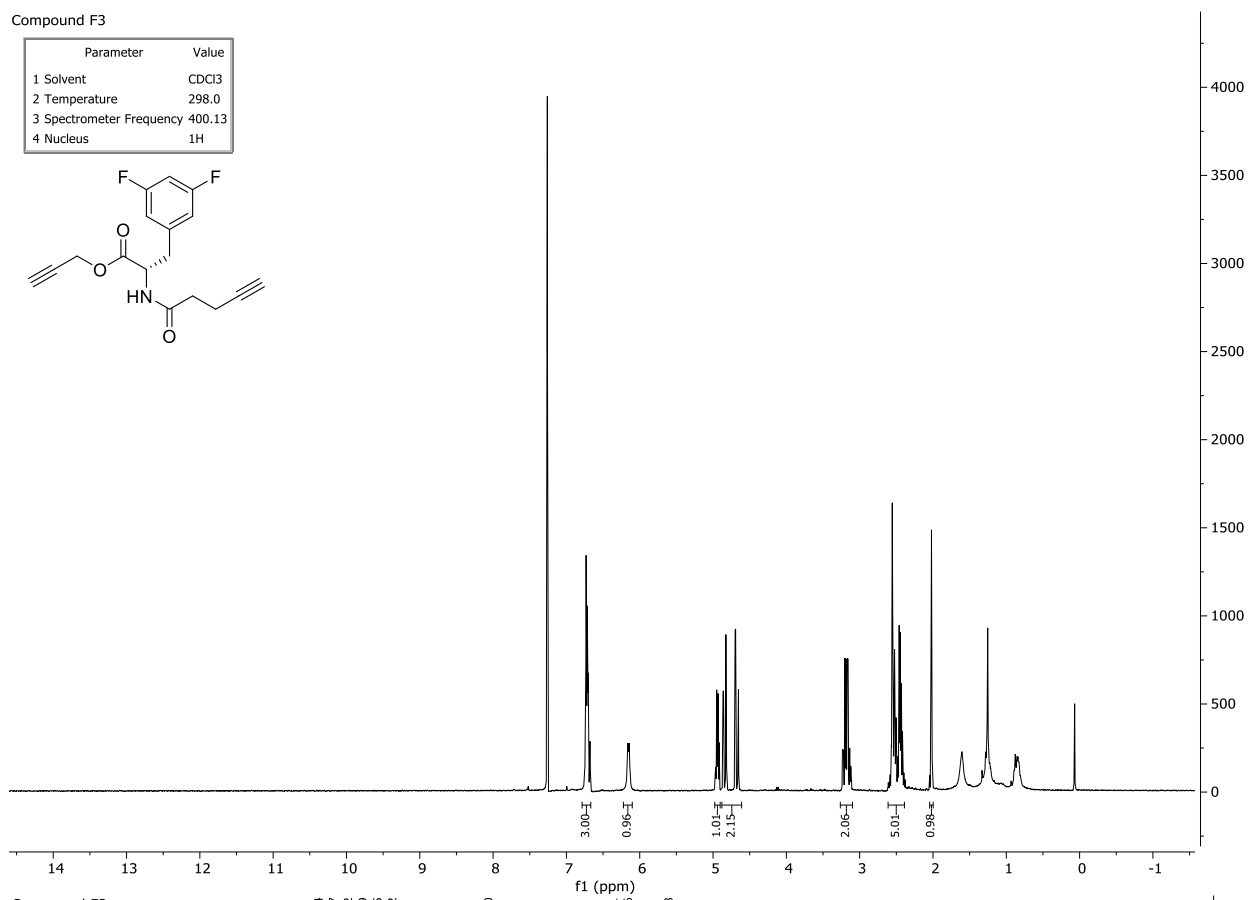
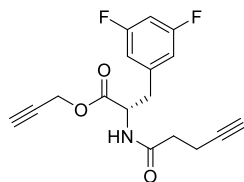
Parameter	Value
1 Solvent	CDCl ₃
2 Temperature	300.0
3 Spectrometer Frequency	100.62
4 Nucleus	¹³ C



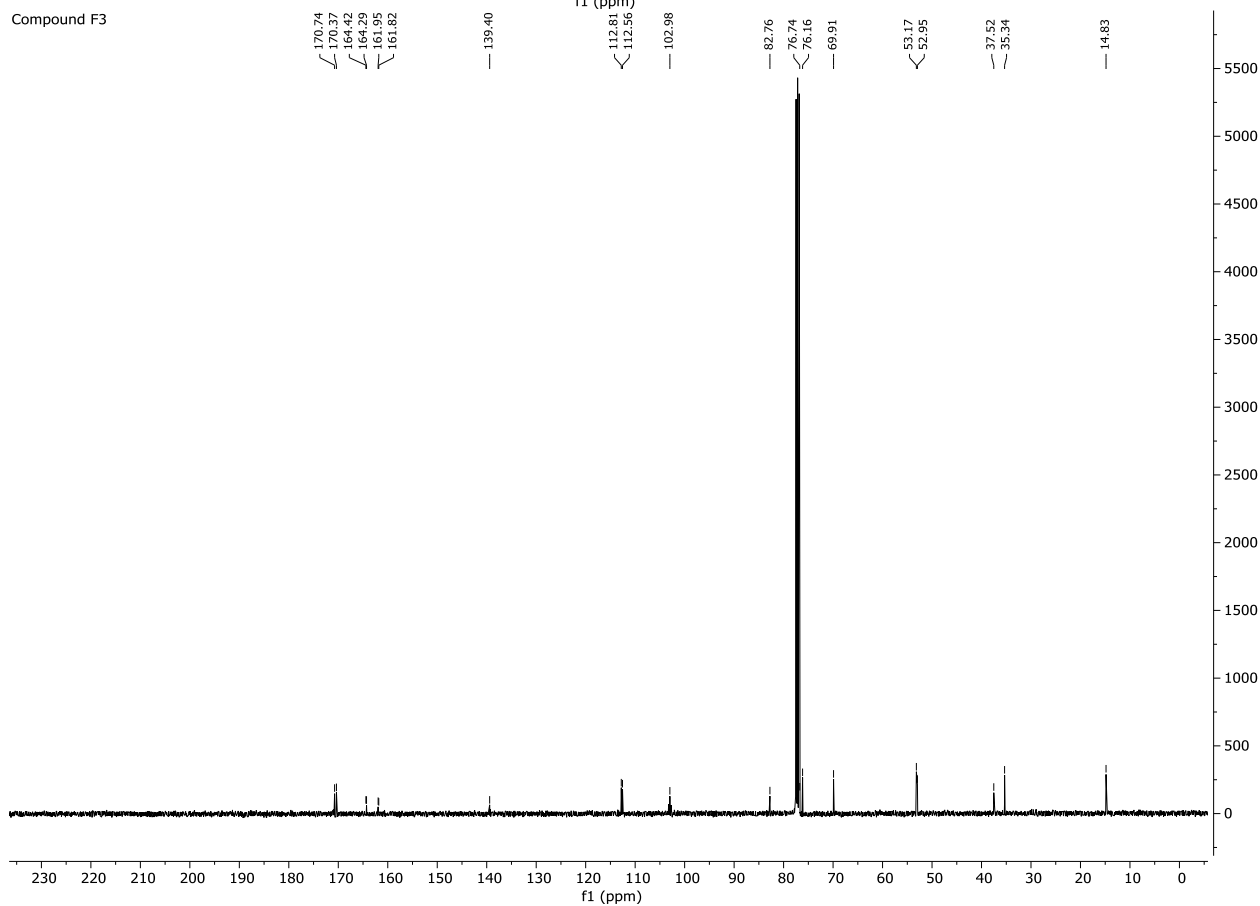
Prop-2-yn-1-yl (S)-3-(3,5-difluorophenyl)-2-(pent-4-ynamido)propanoate (F3)

Compound F3

Parameter	Value
1 Solvent	CDCl ₃
2 Temperature	298.0
3 Spectrometer Frequency	400.13
4 Nucleus	¹ H



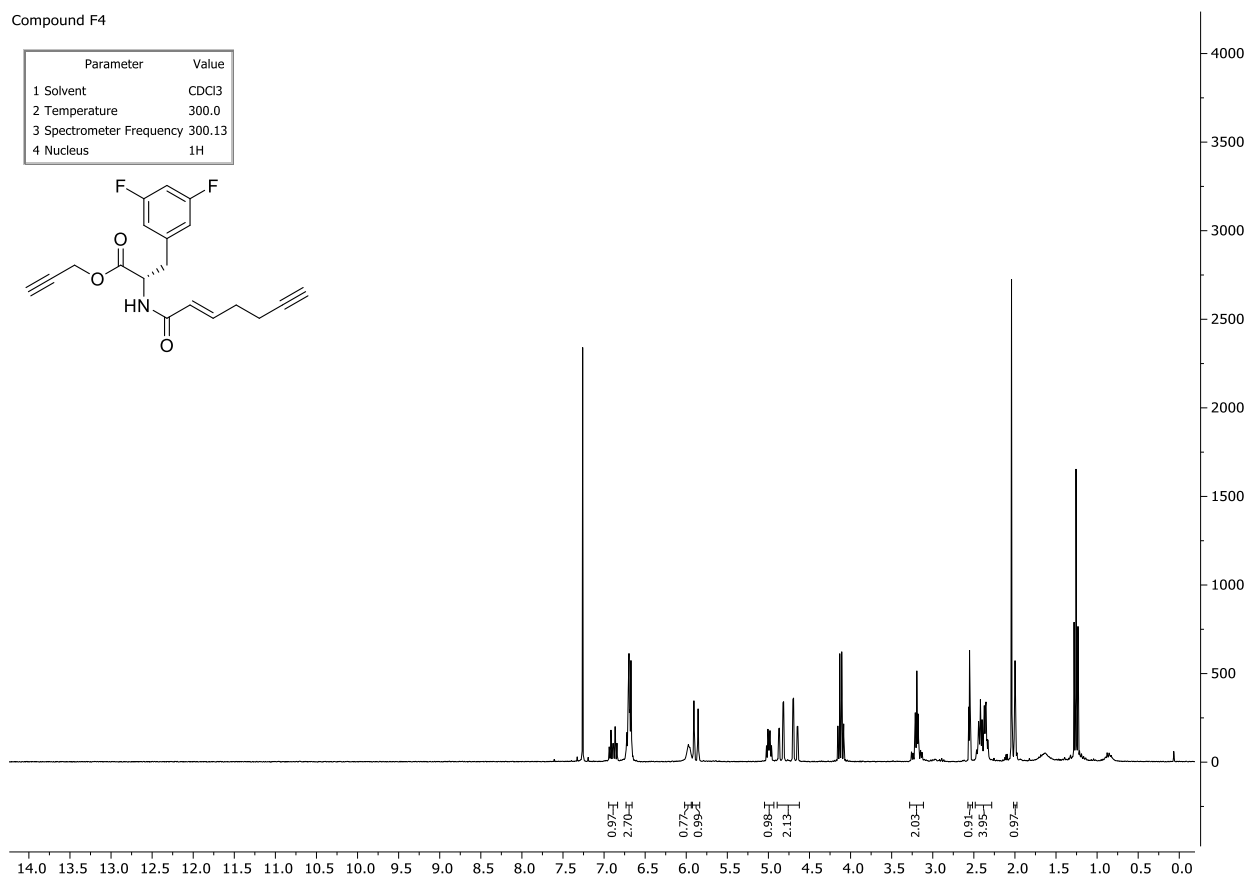
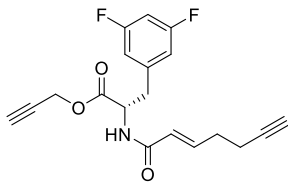
Compound F3



Prop-2-yn-1-yl (S,E)-3-(3,5-difluorophenyl)-2-(hept-2-en-6-ynamido)propanoate (F4)

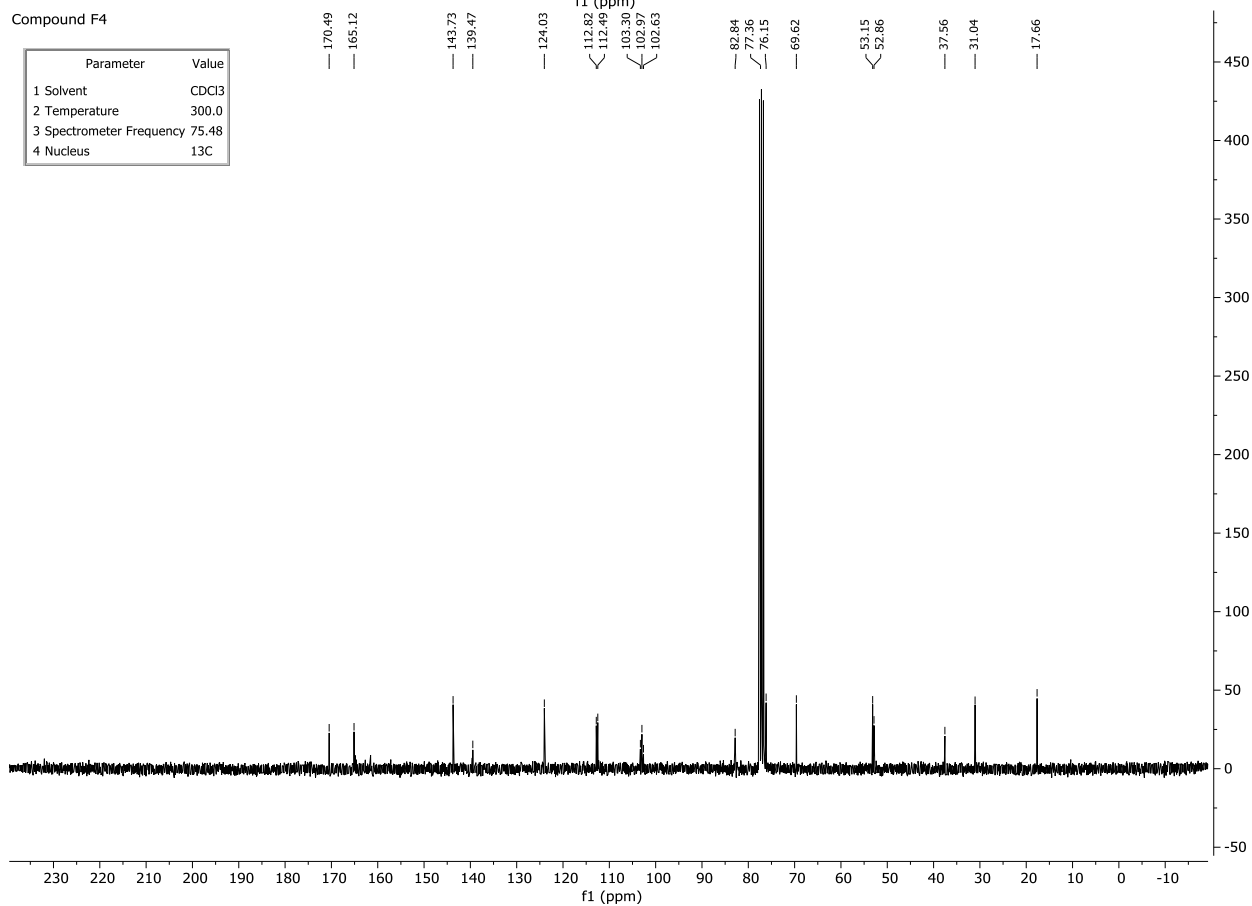
Compound F4

Parameter	Value
1 Solvent	CDCl ₃
2 Temperature	300.0
3 Spectrometer Frequency	300.13
4 Nucleus	¹ H



Compound F4

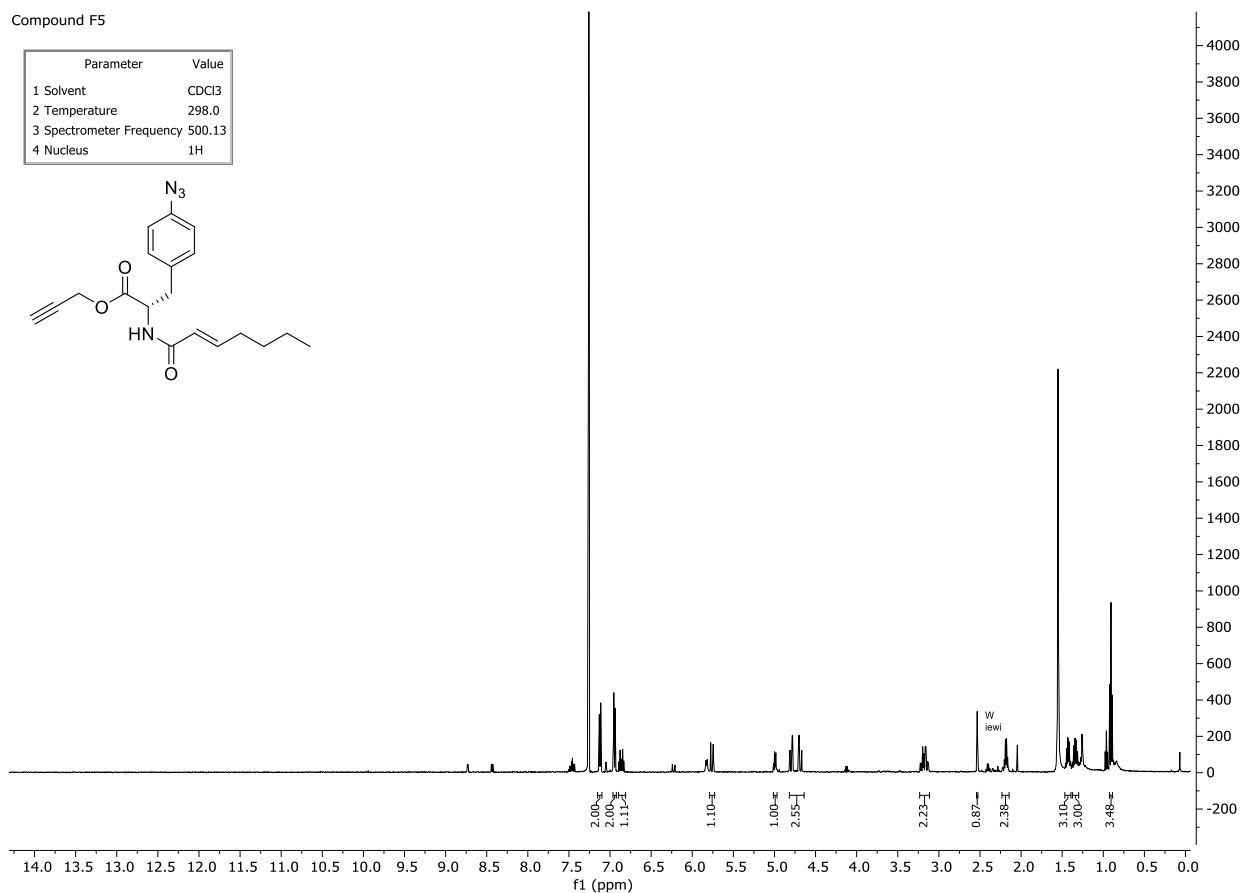
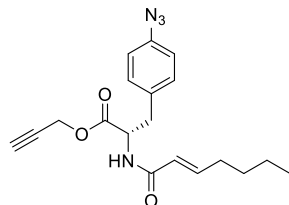
Parameter	Value
1 Solvent	CDCl ₃
2 Temperature	300.0
3 Spectrometer Frequency	75.48
4 Nucleus	¹³ C



Prop-2-yn-1-yl (S,E)-3-(4-azidophenyl)-2-(hept-2-enamido)propanoate (F5)

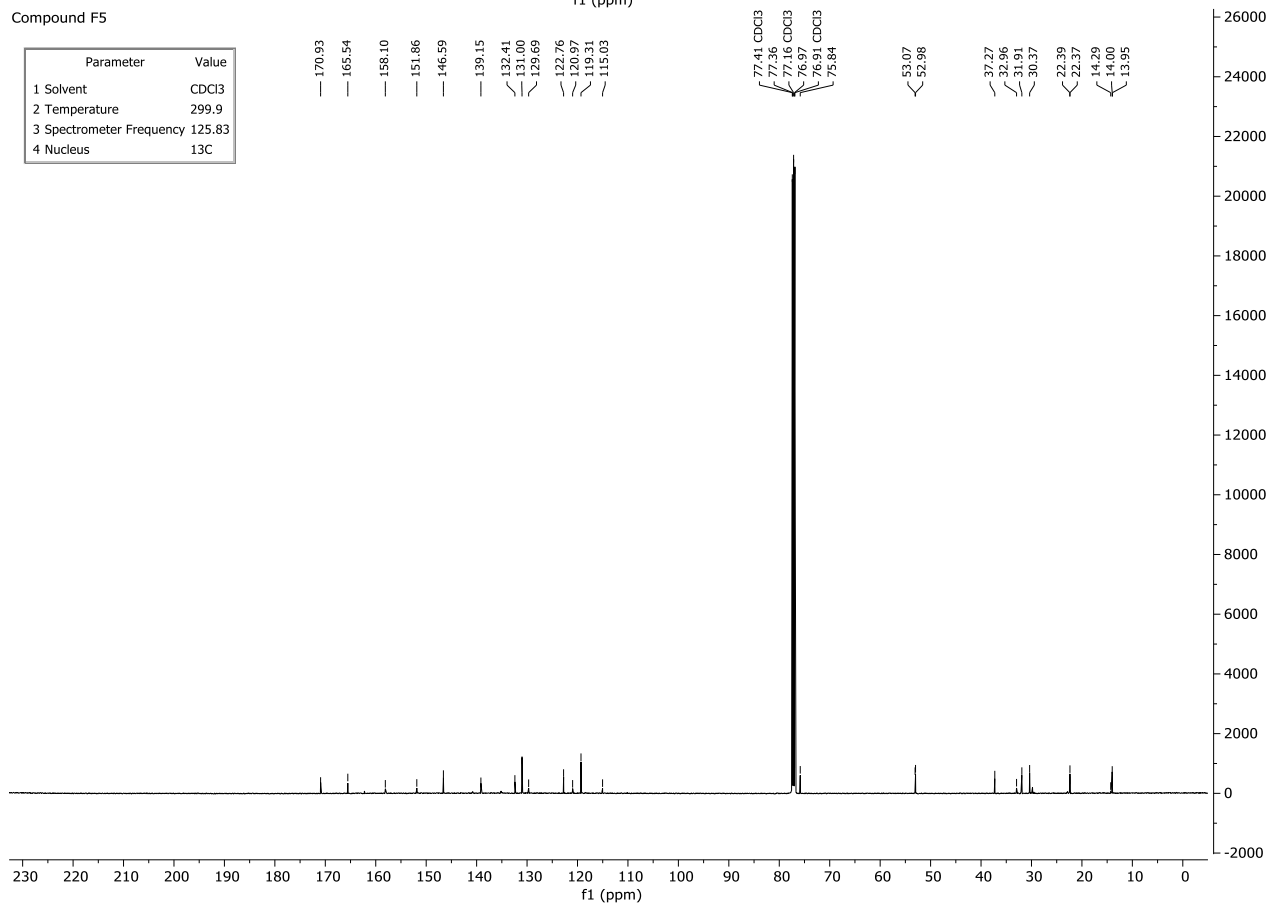
Compound F5

Parameter	Value
1 Solvent	CDCl ₃
2 Temperature	298.0
3 Spectrometer Frequency	500.13
4 Nucleus	¹ H



Compound F5

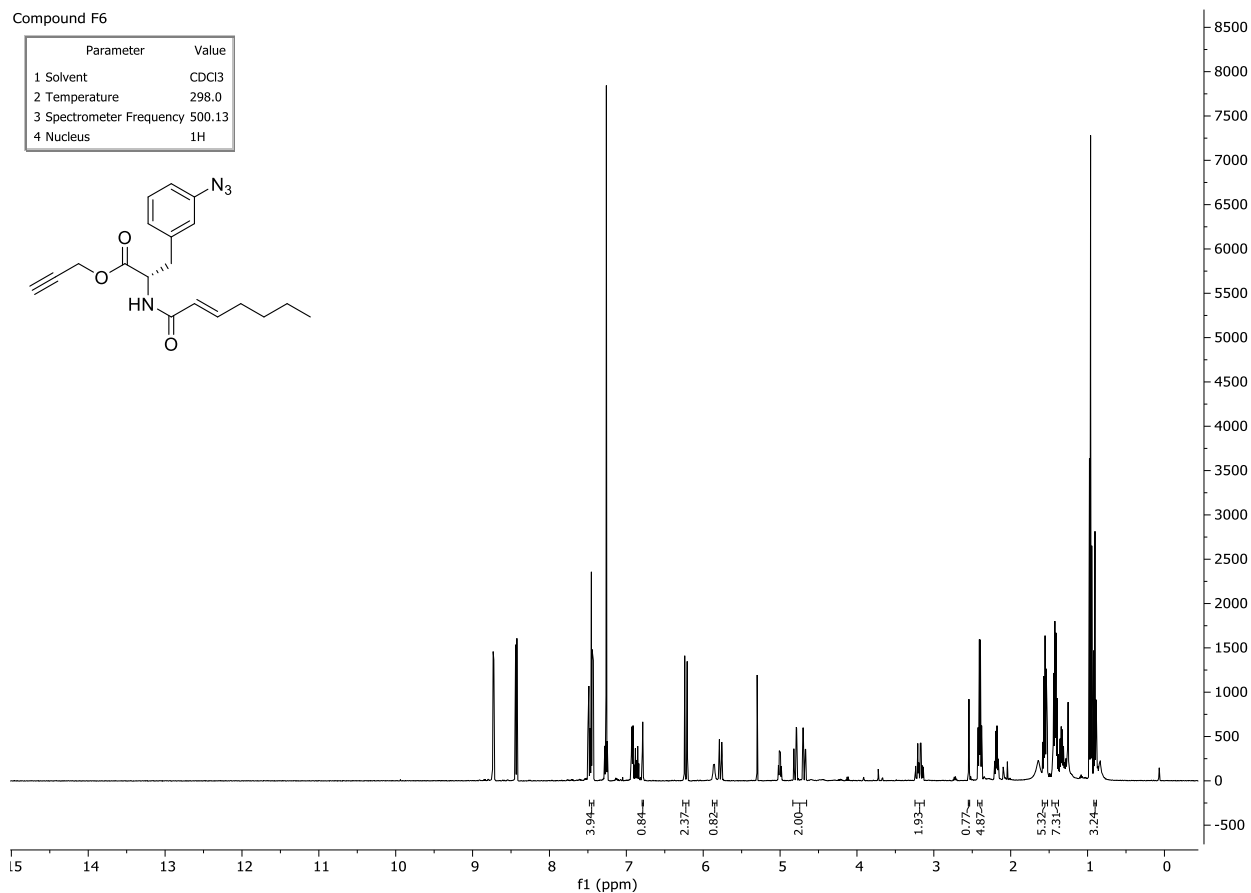
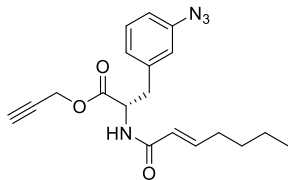
Parameter	Value
1 Solvent	CDCl ₃
2 Temperature	299.9
3 Spectrometer Frequency	125.83
4 Nucleus	¹³ C



Prop-2-yn-1-yl (S,E)-3-(3-azidophenyl)-2-(hept-2-enamido)propanoate (F6)

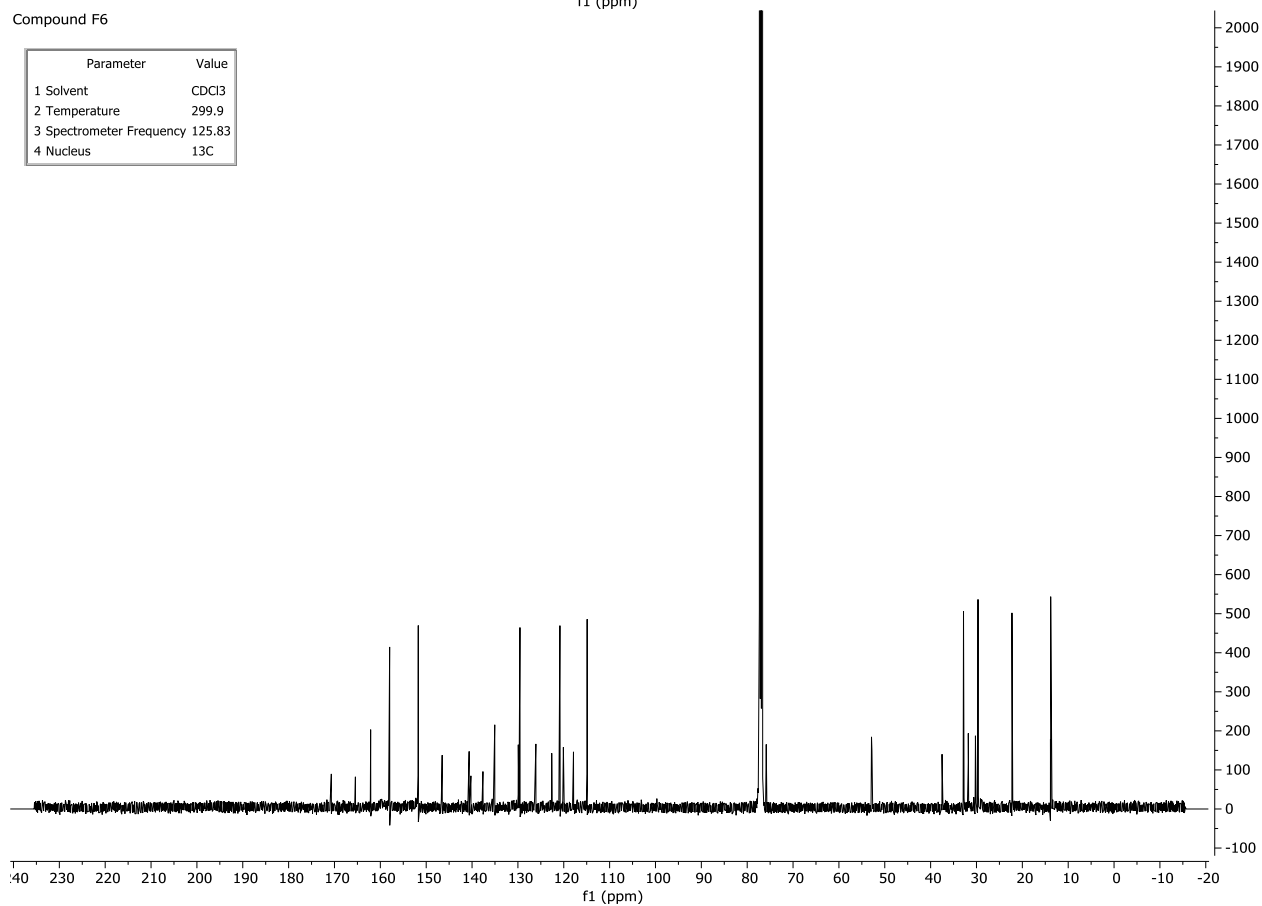
Compound F6

Parameter	Value
1 Solvent	CDCl ₃
2 Temperature	298.0
3 Spectrometer Frequency	500.13
4 Nucleus	¹ H



Compound F6

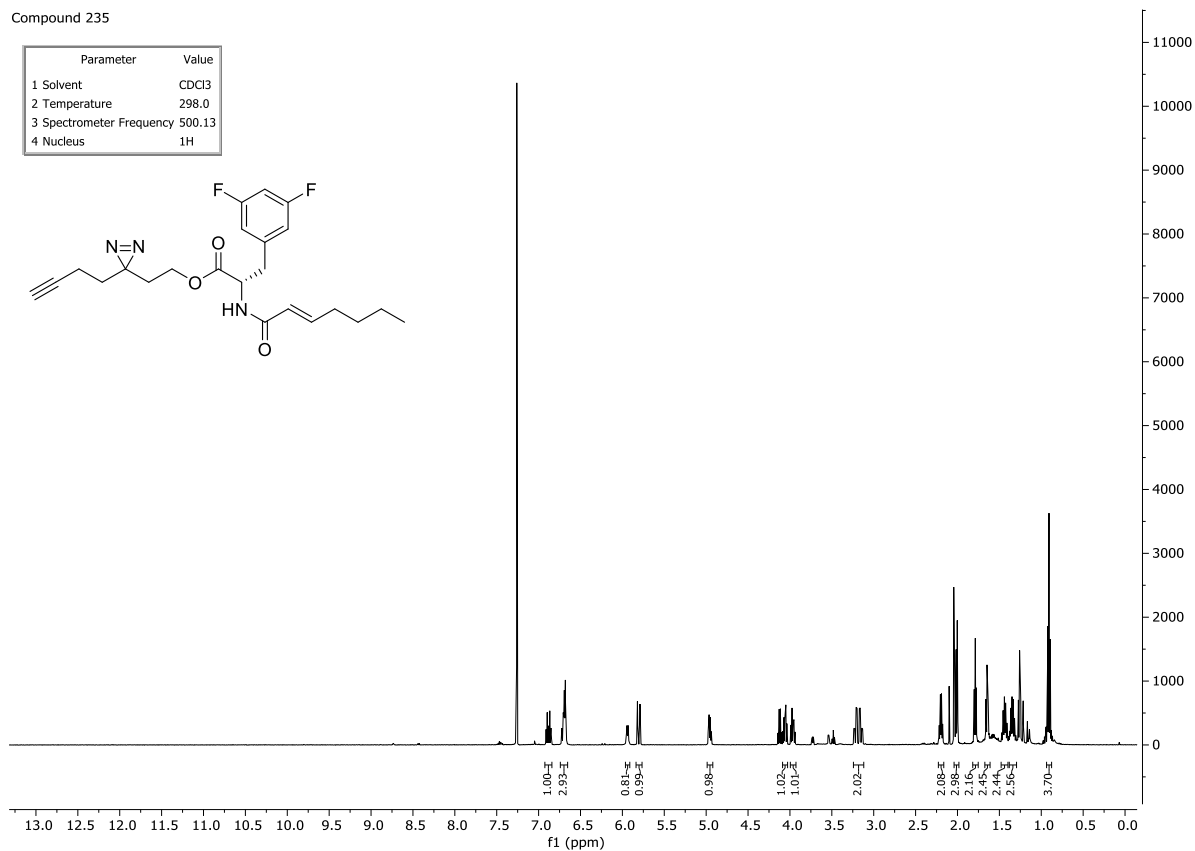
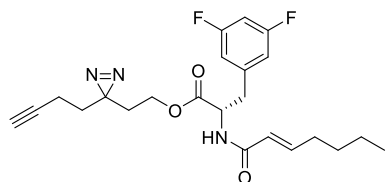
Parameter	Value
1 Solvent	CDCl ₃
2 Temperature	299.9
3 Spectrometer Frequency	125.83
4 Nucleus	¹³ C



2-(3-(but-3-yn-1-yl)-3H-diazirin-3-yl)ethyl(S,E)-3-(3,5-difluorophenyl)-2-(hept-2-enamido)propanoate (BH235)

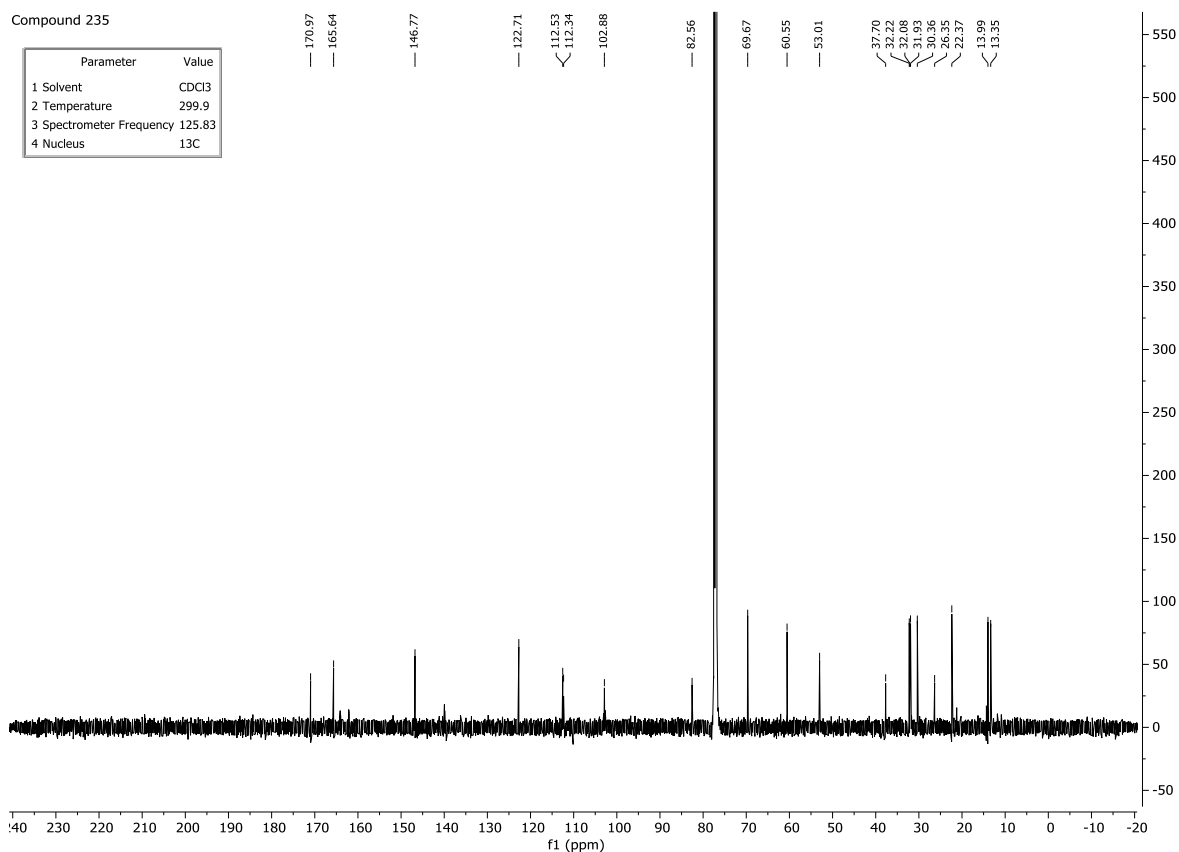
Compound 235

Parameter	Value
1 Solvent	CDCl ₃
2 Temperature	298.0
3 Spectrometer Frequency	500.13
4 Nucleus	¹ H



Compound 235

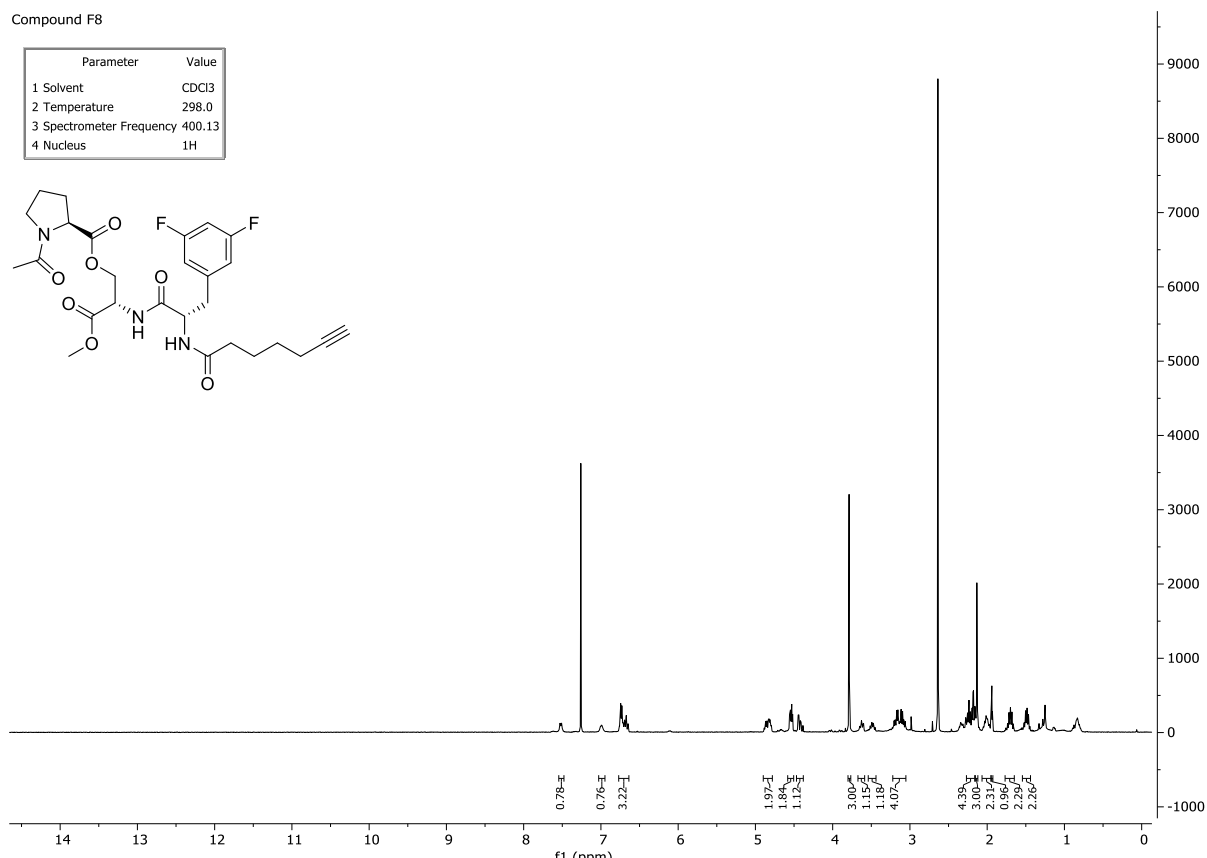
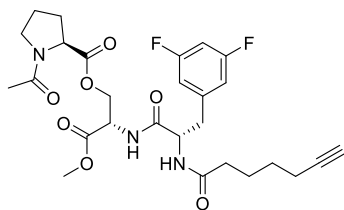
Parameter	Value
1 Solvent	CDCl ₃
2 Temperature	299.9
3 Spectrometer Frequency	125.83
4 Nucleus	¹³ C



(S)-2-((S)-3-(3,5-difluorophenyl)-2-(hept-6-ynamido)propanamido)-3-methoxy-3-oxopropyl acetyl-L-prolinate (F8)

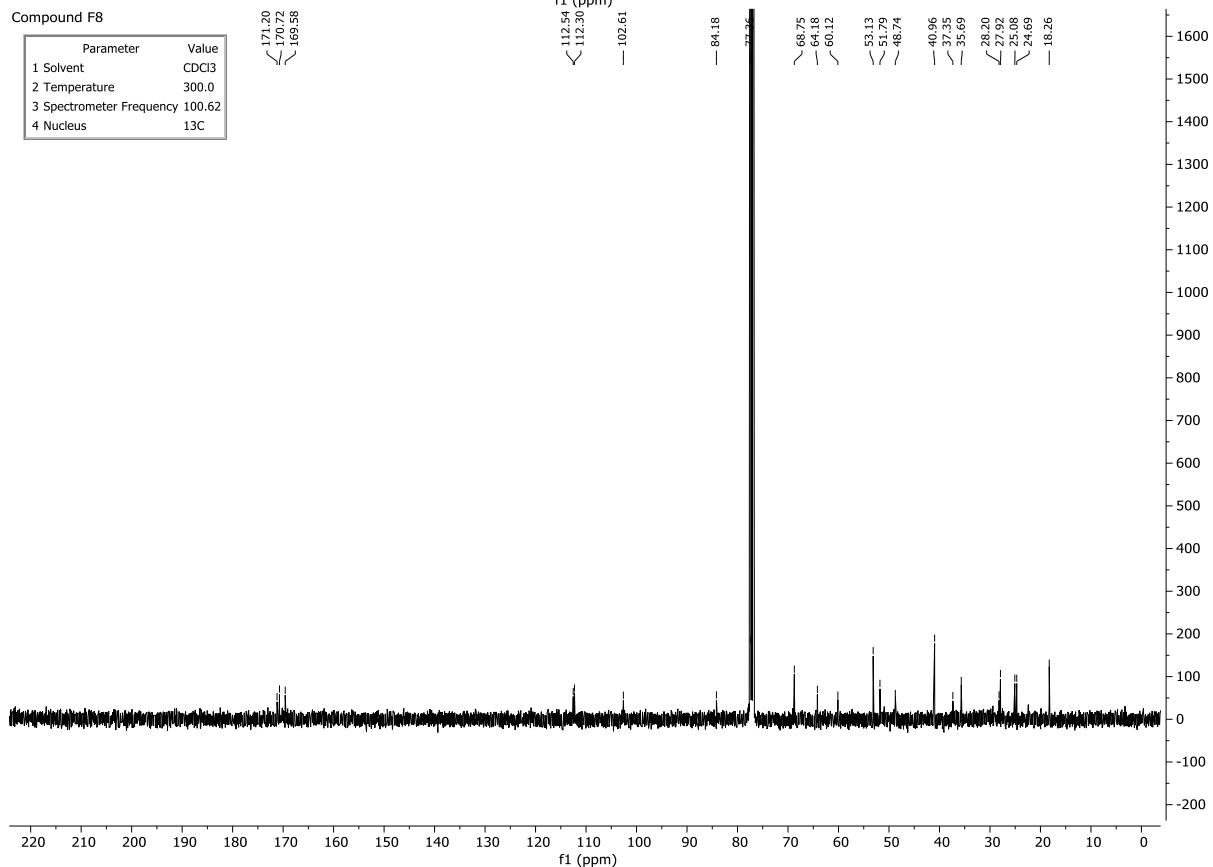
Compound F8

Parameter	Value
1 Solvent	CDCl ₃
2 Temperature	298.0
3 Spectrometer Frequency	400.13
4 Nucleus	¹ H



Compound F8

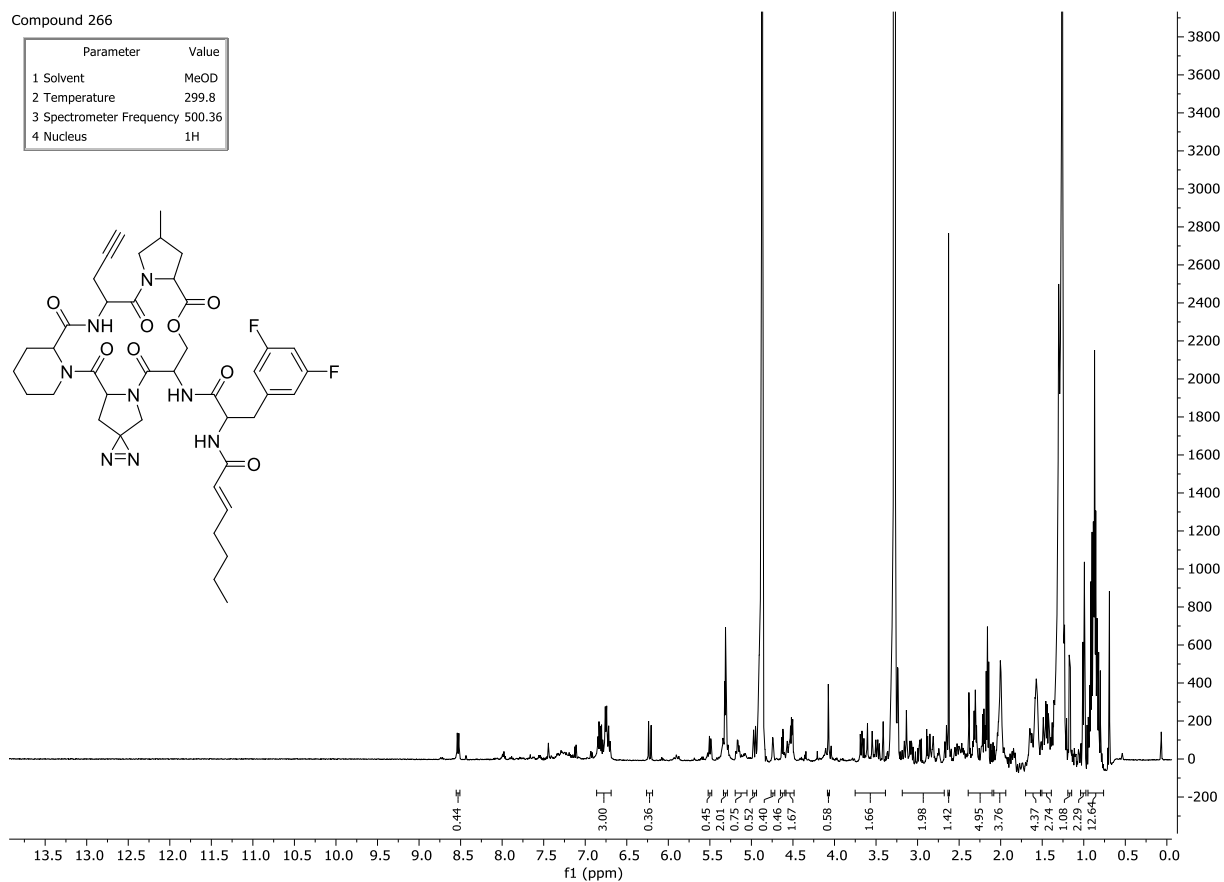
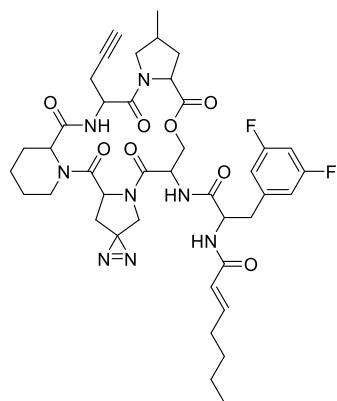
Parameter	Value
1 Solvent	CDCl ₃
2 Temperature	300.0
3 Spectrometer Frequency	100.62
4 Nucleus	¹³ C



ADEP-Probe BH266

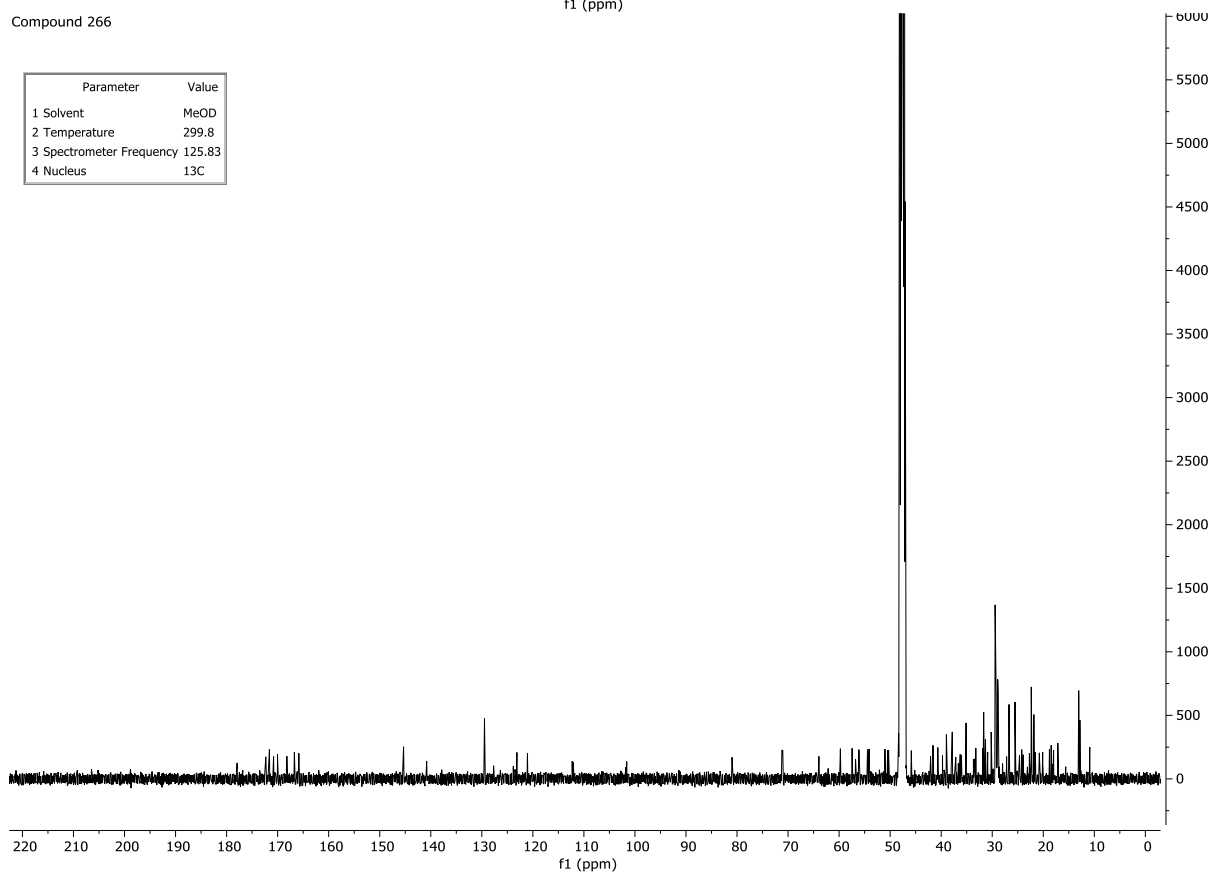
Compound 266

Parameter	Value
1 Solvent	MeOD
2 Temperature	299.8
3 Spectrometer Frequency	500.36
4 Nucleus	¹ H



Compound 266

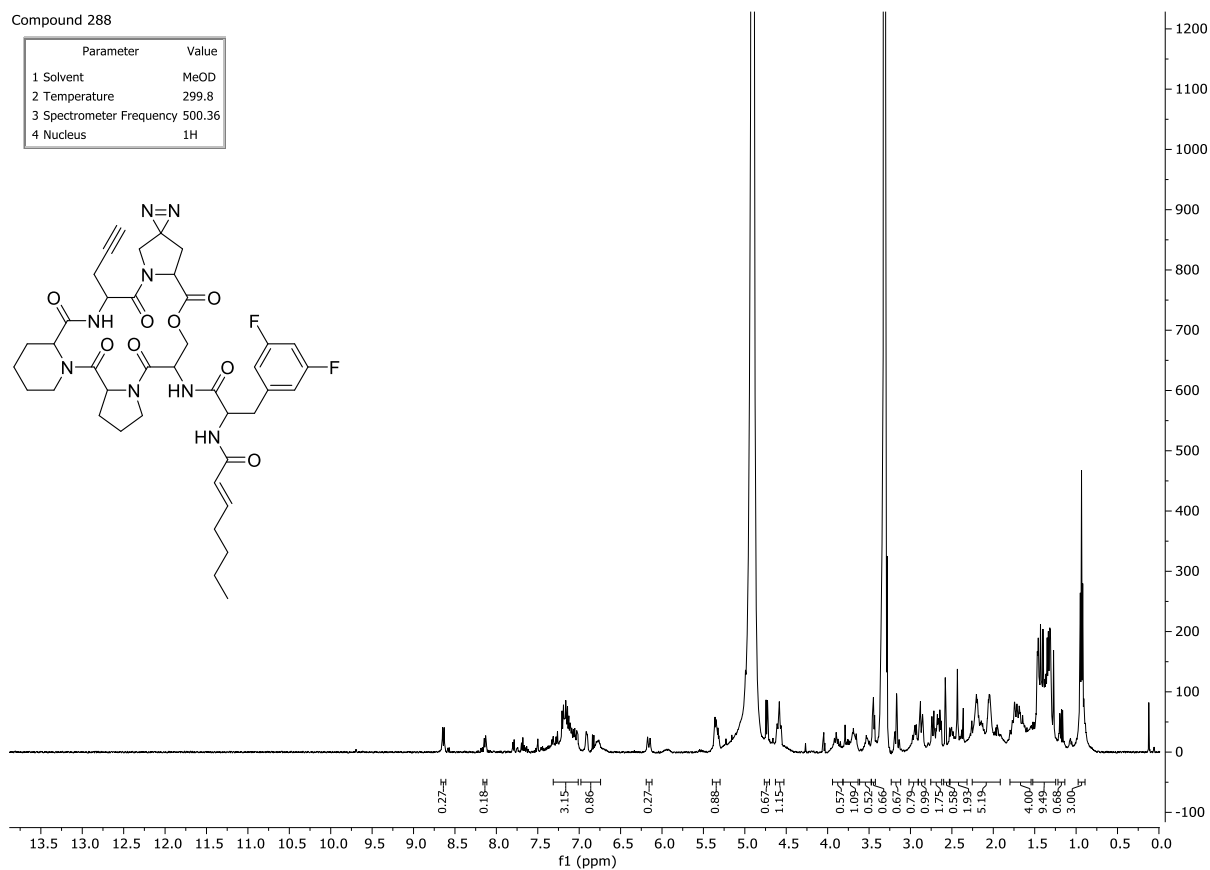
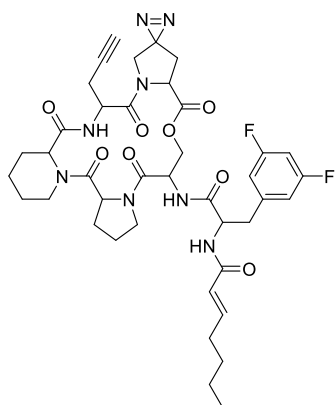
Parameter	Value
1 Solvent	MeOD
2 Temperature	299.8
3 Spectrometer Frequency	125.83
4 Nucleus	¹³ C



ADEP-Probe BH288

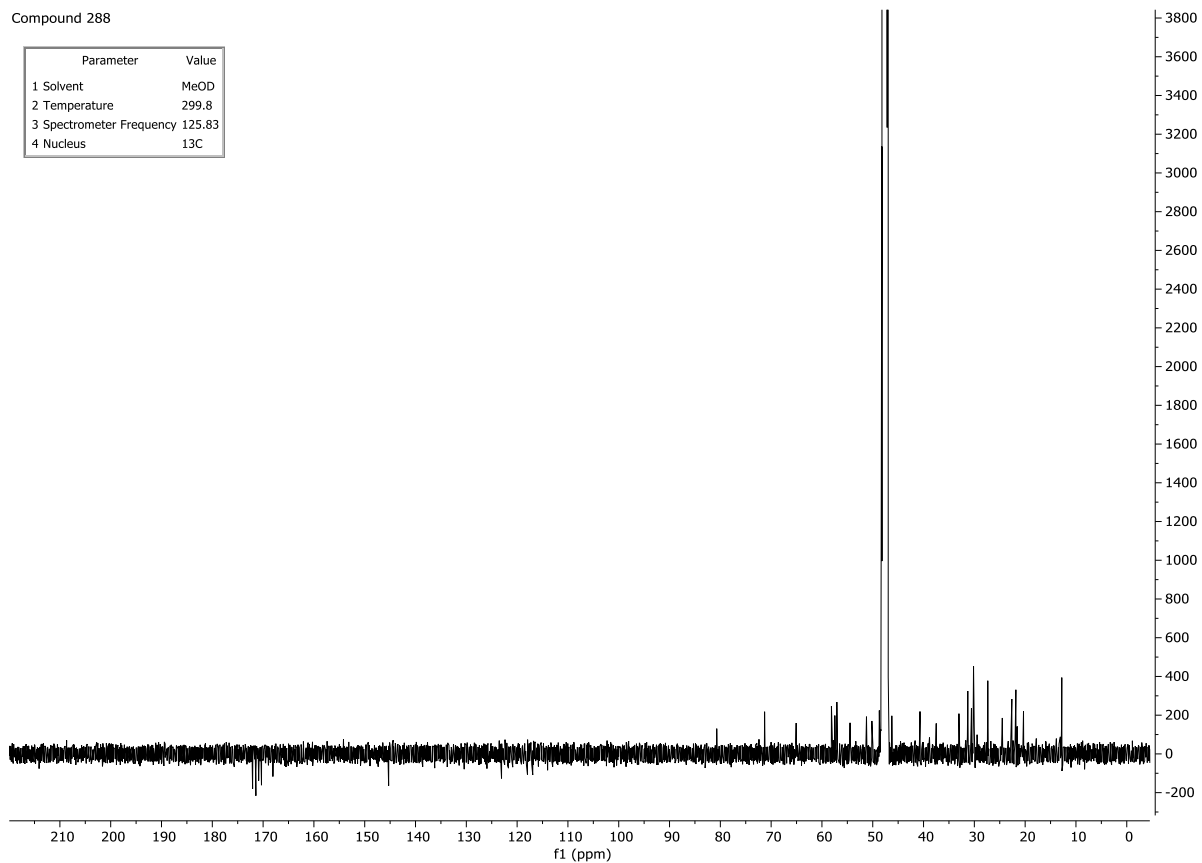
Compound 288

Parameter	Value
1 Solvent	MeOD
2 Temperature	299.8
3 Spectrometer Frequency	500.36
4 Nucleus	¹ H



Compound 288

Parameter	Value
1 Solvent	MeOD
2 Temperature	299.8
3 Spectrometer Frequency	125.83
4 Nucleus	¹³ C



Permissions

Reprinted with permission from *Biochemistry*, 2018 Mar 20; 57 (11): 1814-1820. Copyright 2018 American Chemical Society.

Reprinted with permission from Wiley. Original source: Eyermann, B., Meixner, M., Brötz-Oesterhelt, H., Antes, I. and Sieber, S. A. (2019), Acyldepsipeptide probes facilitate specific detection of caseinolytic protease P independent of its oligomeric and activity state. *ChemBioChem*. Accepted Author Manuscript. doi:10.1002/cbic.201900477